



CARBON NANOTUBES FOR ELECTROCHEMICAL (BIO)SENSING

By

Briza Pérez López

Thesis to opt for the PhD in Chemistry

Directors: Dr. Arben Merkoçi and Dr. Manel del Valle

Departament de Química, Facultat de Ciències
Universitat Autònoma de Barcelona

&

Nanobioelectronics and Biosensors Group,
Institut Català de Nanotecnologia

Bellaterra (Barcelona), Spain

May 2009

The present thesis titled “*Carbon nanotubes for electrochemical (bio)sensing*” has been performed at the laboratories of the Grup de Sensors i Biosensors del Departament de Química de la Universitat Autònoma de Barcelona and Nanobioelectronics and Biosensors Group at Institut Català de Nanotecnologia under the direction of Dr. Arben Merkoçi Hyka, ICREA Professor and Dr. Manel del Valle Zafra, UAB Titular d'universitat numerari.

Bellaterra, May 2009

Dr. Arben Merkoçi Hyka

Dr. Manel del Valle Zafra



Departament de Química,
Universitat Autònoma de Barcelona
Edifici C s/n. 08193 Bellaterra, España
Tel. +34 93 581 2118 Fax: +34 93 581 2379

The present PhD thesis was carried out thanks to the financial support provided by Universitat Autònoma de Barcelona through a PIF pre-doctoral scholarship and to the support of the following projects:

- Desarrollo de nuevas bionanoestructuras inteligentes para biosensores moleculares de interés medioambiental, Fundación Ramón Areces, XIII Concurso nacional para la adjudicación de ayudas a la investigación científica y técnica. (Project reference: Bionanosensores).
 - Development of novel nanomaterial based targeting approaches as emerging universal platforms with interest for biosensors. Grant by Ministerio de Ciencia e Innovación, Spain, (Project reference: MAT2008-03079).
 - Nanopartículas modificadas para análisis proteómico rápido basado en inmunoensayos con tecnologías de codificación electroquímica multiplex y lab-on-a-chip. Grant by Ministerio de Ciencia e Innovación, Spain, (Project reference: MEC, MAT2005-03553/)
 - Water Risk Management in Europe (WARMER). EU grant, (Project reference: FP6-034472-2005-IST-5).
-

Contents

Chapter 1	General introduction	1
	1.1. Nanotechnology and nanomaterials	3
	1.2. Carbon nanotubes	4
	1.3. Carbon nanotubes in electrochemical sensors and biosensors	11
	1.4. References	28
Chapter 2	Objectives	35
	Objectives	37
Chapter 3	Carbon nanotubes in sensing systems	39
	3.1. NADH detection	41
	3.2. Dopamine detection	57
	3.3. References	68
Chapter 4	Carbon nanotubes in biosensing systems	71
	4.1. Glucose detection	73
	4.2. Catechol detection	86
	4.3. References	95
Chapter 5	Global discussion, general conclusions and future	99
	5.1. Global discussion of results	101
	5.2. General conclusions	104
	5.3. Future perspectives	105
	5.4. References	106
Chapter 6	Publications	107
	1. B. Pérez , J. Sola, S. Alegret and A. Merkoçi. A carbon nanotube PVC based matrix modified with glutaraldehyde suitable for biosensor applications. <i>Electroanalysis</i> , 2008, 20 , 603.	
	2. G. Alarcón-Angeles, B. Pérez-López , M. Palomar-Pardave, M.T. Ramírez-Silva, S. Alegret and A. Merkoçi. Enhanced host–guest electrochemical recognition of dopamine using cyclodextrin in the presence of carbon nanotubes. <i>Carbon</i> , 2008, 46 , 898.	
	3. B. Pérez , M. del Valle, S. Alegret and A. Merkoçi. Carbon nanofiber vs. carbon microparticles as modifiers of glassy carbon and gold electrodes applied in electrochemical sensing of NADH. <i>Talanta</i> , 2007, 74 , 398.	
	4. Ü.A. Kirgoz, S. Timur, D. Odaci, B. Pérez , S. Alegret and A. Merkoçi. Carbon nanotube composite as novel platform for microbial biosensor. <i>Electroanalysis</i> , 2007, 19 (7-8), 893.	
	5. B. Pérez , M. Pumera, M. del Valle, A. Merkoçi and S. Alegret. Glucose Biosensor based on carbon nanotube epoxy composites. <i>J. Nanosci. Nanotechnol.</i> , 2005, 5 , 1694.	
	6. A. Merkoçi, M. Pumera, X. Llopis, B. Pérez , M. del Valle and S. Alegret. New materials for electrochemical sensing. VI. Carbon nanotubes. <i>Trends Anal. Chem.</i> , 2005, 24 , 826.	
	7. B. Pérez and A. Merkoçi. Application of carbon nanotubes in analytical chemistry. American Scientific Publishers, 2008, 2 , 337.	
Chapter 7	Annex	
	B. Pérez López and A. Merkoçi. Improvement of the electrochemical detection of catechol by the use of a carbon nanotube based biosensor. <i>Analyst</i> , 2009, 134 , 60.	

Abbreviations

AA	ascorbic acid
Ab-Ag-Ab	antibody-antigen-antibody
ADH	alcohol dehydrogenase
ALP	alkaline phosphatase
APTES	3-aminopropyltriethoxysilane
ATR	attenuated total reflectance
CD	cyclodextrin
CHIT	chitosan
CM	carbon materials
CME	chemically modified electrode
CMP	carbon microparticles
CNF	carbon nanofibers
CNTs	carbon nanotubes
CNTEC	carbon nanotube-epoxy composite
CNTPE	CNTs paste electrode
CP	carbon paste
CT	cholera toxin
CV	cyclic voltammetry
CVD	chemical vapor deposition
DA	dopamine
DDAB	didodecyldimethylammonium bromide
DET	direct electron transfer
ΔE	potential difference
DMF	dimethylformamide
DMSO	dimethyl sulphoxide
DNA	deoxyribonucleic acid
ds	double-stranded
EDS	energy dispersive X-ray spectroscopy
EIS	electrochemical impedance spectroscopy
E_{pa}/E_{pc}	anodic/cathodic peak potential
FAD	flavin adenine dinucleotide
FTIR	fourier transform infra-red
GA	glutaraldehyde
GC	glassy carbon
GCE	glassy carbon electrode
GEC	graphite-epoxy composite
GOx	glucose oxidase
GPa	gigapascal
GNp	gold nanoparticles
Hb	hemoglobin
HCG	human chorionic gonadotropin
HDV	hydrodynamic voltammogram
H₂O₂	hydrogen peroxide
HOPG	highly ordered pyrolytic graphite

HRP	horseradish peroxidase
IAs	immunoassays
ICN	Institut Català de Nanotecnologia
I_{pa}/I_{pc}	anodic/cathodic peak current
ISE	ion-selective electrodes
LbL	layer-by-layer
LC	liquid chromatography
LC/MS	liquid chromatography-mass spectrometry
LOD	limit of detection
MB	Meldola's blue
Mb	myoglobin
MWCNTs	multi-wall carbon nanotubes
NAD⁺/NADH	oxidized/reduced nicotinamide adenine dinucleotide
NiTsPc	tetrasulfonated metallophthalocyanine
PAMAM	polyamidoamine
PANI	polyaniline
PBS	phosphate buffer saline
PDMS	poly-(dimethylsiloxane)
PEG	polyethyleneglycol
Ppy	polypyrrole
PSA	specific antigen
PVA	poly(vinyl alcohol)
PVC	poly(vinylchloride)
r^2	correlation coefficient
RSD	relative standard deviation
SEM	scanning electron microscope
S/N	signal-to-noise
SPCE	screen printed carbon electrode
SWV	square-wave voltammetry
SWCNTs	single-wall carbon nanotubes
TB	toluidine blue
4-TBC	4- <i>tert</i> -butylcatechol
THF	tetrahydrofuran
Tpa	terapascal
Tyr	tyrosinase
UV-vis	ultraviolet-visible
WARMER	Water Risk Management in Europe

Abstract

The extraordinary mechanical properties and unique electrical properties of carbon nanotubes (CNTs) have stimulated extensive research activities across the world since their discovery by Sumio Iijima in 1991. The range of applications for CNTs is indeed wide ranging from nanoelectronics, with quantum wire interconnects and field emission devices to composites, chemical sensors and biosensors. The application of CNTs to design novel and improved (bio)sensors is the principal objective of this thesis. Different alternatives for CNTs integration into (bio)sensing systems have been developed and the results obtained including some previous theoretical introduction, the state of the art in the field, conclusions and future prospects are presented through the 7 chapters of this PhD thesis.

Chapter 1 is a general introduction on the state of the art of CNTs applications in (bio)sensing systems. It briefly describes also the synthesis, purification, functionalization and dispersion of CNTs followed by the reported applications in electrochemical sensors and (bio)sensors.

Chapter 2 introduces the objectives that have motivated this work.

Chapter 3 describes the study of the behaviour of CNTs to promote the electronic transference into electrochemical sensing systems. This chapter is related to sensors where there is not any biological molecule included in the sensing device. Modifications of conventional electrode surfaces and the responses toward β -nicotinamide adenine dinucleotide (NADH) and dopamine (DA) detection have been studied. The comparison of electrochemical efficiency between different carbon materials (i.e. carbon nanofibers and carbon microparticles) for NADH detection has been also studied.

CNTs biosensors based on the immobilization of enzymes (glucose oxidase (GOx) from *Aspergillus niger* and tyrosinase (Tyr) from mushroom) and cells (*Pseudomonas fluorescens*) on rigid and renewable biocomposites are discussed in details at *chapter 4*.

Chapter 5 summarizes and discusses the global results and conclusions related to this thesis giving at the same time the future perspectives of the research in this field. A book chapter and the articles already published upon the delivery of this thesis (*chapter 6*) and an article published later (*chapter 7*) are also included.

1

General introduction

Contents

1.1. Nanotechnology and nanomaterials	3
1.2. Carbon nanotubes	4
1.2.1. Structure and properties	5
1.2.2. Synthesis and purification	7
1.2.3. Functionalization and dispersion	8
1.2.4. General applications	11
1.3. Carbon nanotubes in electrochemical sensors and biosensors	11
1.3.1. Integration strategies	12
1.3.1.1. Modification of electrode surfaces	12
1.3.1.2. Pastes and composites	13
1.3.2. Applications in sensors	14
1.3.2.1. Detection of gases	14
1.3.2.2. Detection of metals	16
1.3.2.3. Detection of biomolecules	16
1.3.2.4. Detection of nanoparticles	19
1.3.3. Applications in biosensors	20
1.3.3.1. Enzyme based biosensors	21
1.3.3.2. Immunosensors	24
1.3.3.3. Genosensors	25
1.4. References	28

General introduction

1.1. Nanotechnology and nanomaterials

Nanotechnology, introduced almost half century ago, is one of the most active research areas with both novel science and useful applications that has been gradually establishing itself in the past two decades. The evolution of technology and instrumentation, as well as its related scientific areas such as physics and chemistry, are making the research on nanotechnology very attractive for many other areas.

It is generally known that the term nanotechnology was first used by Taniguchi in a paper, “On the Basic Concept of ‘nanotechnology’”, presented in 1974 to describe the manufacturing of products with tolerances less than 1 μ m.¹ However, the earliest impetus to the scientific and technological possibility of coaxing individual atomic and molecular building blocks into the making of useful materials, devices and applications was given by the Nobel prize-winning physicist Richard Feynman in a landmark lecture “There is Plenty of Room at the Bottom”, delivered at the American Physical Society (APS) in 1959. Feynman pointed out that “*The problems of chemistry and biology can be greatly helped if our ability to see what we are doing, and to do things on an atomic level, is ultimately developed— a development which I think can not be avoided.*”

Some years ago, nanotechnology applications seemed to be very distant. However, with the discovery of new nanomaterials with impressive properties that had never been seen before, nanoscience research got to increase notably and therefore nanotechnology applications and products have started to appear recently. Nevertheless, nanotechnology applications are beginning to come out and more research is needed to reach up to novel results and uses for these kinds of materials.²

Nanotechnology is considered to be the technology of the future; it is perhaps today’s most advanced manufacturing technology and has been called “extreme technology”, because of the theoretical limit of accuracy which is the size of a molecule or an atom.³

Of increasing interest in nanotechnology are the nanostructured materials, with dimensions, i.e. grain size, layer thickness or shapes, below 100 nm.³ The science and technology of nanoscale materials, devices, and their applications in functionally classified materials, molecular-electronics, nanocomputers, sensors, actuators and molecular machines, form the world of nanotechnology. The prefix “nano” corresponds to a basic unit on a length scale, meaning 10^{-9} meters, which is a hundred to a thousand times smaller than a typical biological cell or bacterium.⁴

The real progress in nanotechnology, however, has also been spurred by the discovery of atomically precise nanoscale materials such as fullerenes in the mid-1980s and carbon nanotubes (CNTs) in 1991.⁴ CNTs are undoubtedly one of the most interesting materials in the last twenty years. The outstanding properties that these materials possess have opened a new interesting research area in nanoscience and nanotechnology. In addition, new properties have been found and possible applications are frequently suggested for these materials.

Nowadays, the research in nanotubes covers different fields, being focused on the understanding and applications of these interesting materials. Other research field has been directed to basic science, with the target to modify structure and surface of CNTs. This later has allowed diversifying their properties and possible uses, opening new possibilities in chemistry, physics, engineering, medicine and materials science.²

1.2. Carbon nanotubes

The discovery in 1985 of buckminsterfullerene opened a new era for the carbon chemistry and novel materials. The Japanese Sumi Ijima discovered carbon nanotubes (CNTs) in 1991.⁵

From their discovery CNTs have generated great interest for various applications based on their field emission and electronic transport properties, their high mechanical strength, and their chemical properties.⁵ From this arises an increasing potential for the use of CNTs as field emission devices⁶, nanoscale transistors⁷, tips for scanning microscopy⁸ or components for composite materials.⁹

CNTs can be classified into single-wall carbon nanotubes (SWCNTs) and multi-wall carbon nanotubes (MWCNTs)¹⁰ (Figure 1.1). SWCNTs (Figure 1.1A) possess a cylindrical nanostructure formed by rolling up a single graphite sheet into a tube. SWCNTs can thus be considered as molecular wires with every atom on the surface.

MWCNTs (Figure 1.1B) comprise an array of such nanotubes that are concentrically nested like rings of a tree trunk.¹¹

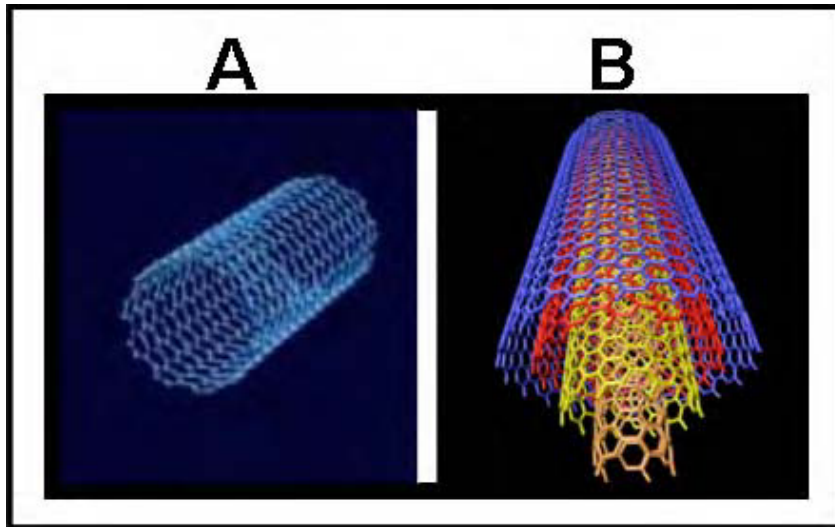


Figure 1.1. Schematic of an individual (A) SWCNTs and (B) MWCNTs.¹⁰

CNTs are one of the most commonly used building blocks in nanotechnology. With one hundred times the tensile strength of steel, thermal conductivity better than the purest diamond and electrical conductivity similar to copper but with the ability to carry much higher currents, CNTs seem to be a wonderful material.

1.2.1. Structure and properties

A SWCNT is formed when one single layer of graphite is wrapped onto itself and the resulting edge is joined. The structure of a SWCNT can be defined using a rolled-up vector r and a chiral angle θ (see Figure 1.2).^{12,13}

The rolled-up vector according to Equation (1.1) is a linear combination of base vectors a_1 and a_2 of the basic hexagon,

$$r = na_1 + ma_2 \quad \text{Equation (1.1)}$$

where m and n are integers. In Figure 1.2, the zone between the dashed lines is the area which is rolled up along an axis perpendicular to the rolled-up vector. Different types of nanotubes are defined by the values of m and n . Based on theoretical predictions¹⁴, SWCNTs can be either metallic or semiconducting, depending on their diameters and helical arrangement.

Whether a SWCNT is metallic or semiconducting, it is based on the band structure of a two-dimensional graphite sheet and periodic boundary conditions along the circumference direction. Considering the rolled-up vector, SWCNTs are metallic when $n - m = 3p$, where p is integer or semiconducting with all other n and m values. Figure 1.2 shows idealized images of defect-free SWCNTs (n,m) with open ends when they form metallic conducting structures: “armchair” state (10,10) or “zigzag” state (10,0) and a semiconducting structure: chiral state (10,5).

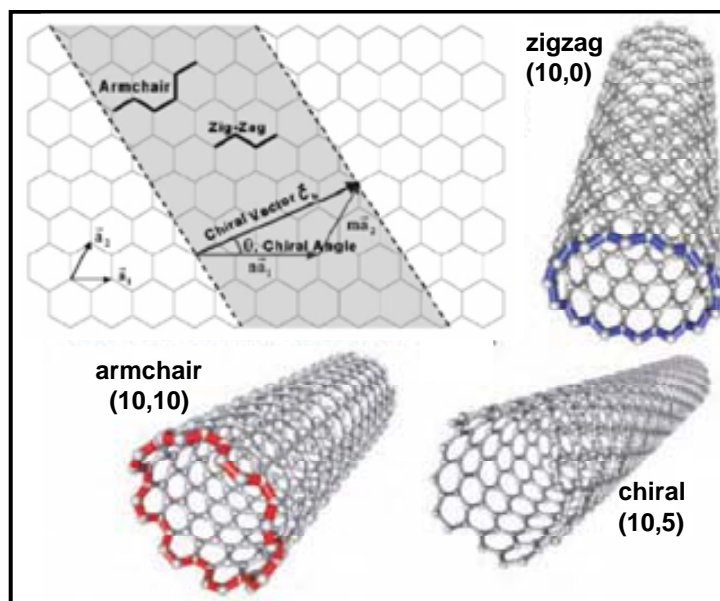


Figure 1.2. Schematic diagram showing how a hexagonal sheet of graphene is “rolled” to form a carbon nanotube.¹⁵ Idealized representation of defect-free SWCNTs (n,m) with open ends: a metallic conducting (10,10) tube (“armchair”); a semiconducting (10,5) tube (chiral); and a conducting (10,0) tube (“zigzag”).¹⁶

Some properties of CNTs are stated below.⁴

- **Electrical:** their structural parameters indicate how much the nanotube is twisted. CNTs can be highly conductive and hence can be metallic. Their conductivity has been shown to be a function of their chirality, the degree of twist as well as their diameter.¹⁷
- **Mechanical:** The small diameter of CNTs also has an important effect on the mechanical properties, compared with traditional micron-size graphitic fibres.¹⁸ Perhaps the most striking effect is the opportunity to associate high flexibility and high strength with high stiffness, an absent property in graphite fibres. These properties of CNTs open the way for a new generation of high

performance composites.¹⁹ The nanotube as a whole is very flexible because of the great length.⁴

- Chemical: high specific surface and σ - π rehybridization facilitate molecular adsorption, doping, and charge transfer on nanotubes, which, in turn, modulates electronic properties.
- Thermal and thermoelectric: nanotubes display very high thermal conductivity. Therefore, it is expected that nanotube reinforcements in polymeric materials may also significantly improve the thermal and thermo mechanical properties of these composites.¹⁷

1.2.2. Synthesis and purification

Three different methods are now well established to synthesize carbon nanotubes: arc-discharge, laser-ablation and chemical vapor deposition (CVD) (see Table 1.1).^{16,20}

However, in order to use carbon nanotubes in novel devices, it is necessary to produce these materials with a high crystallinity on an economically large scale. In this context, the catalytic CVD method is considered to be the optimum method for producing large amounts of CNTs, particularly with the floating-catalyst method.²¹ This technique is more controllable and cost efficient when compared with arc-discharge and other methods (for more details see reference 10).

Table 1.1. Summary and comparison of the most important synthesis procedures for CNTs. (Adapted from reference 16 and 20).

Synthesis method	Principle	SWCNTs or MWCNTs
Arc-discharge	Carbon atoms are generated through an electric arc-discharge at $T > 3000^\circ\text{C}$ between two electrodes. Nanotubes are formed in the presence of suitable catalyst metal particles (Fe, Co, or Ni).	Both
Laser-ablation	The laser-ablation process synthesizes CNT by irradiating a pulsed laser on a graphite rod containing catalysts heated to 1000°C or higher.	SWCNTs
Chemical Vapor Deposition (CVD)	Decomposition of a gaseous hydrocarbon source (ethylene or acetylene) is catalyzed by metal nanoparticles (Co or Fe) at high temperatures (500 - 1000°C). Carbon has a low solubility in these metals at high temperatures and thus the carbon will precipitate to form nanotubes.	Both

Extensive research has been dedicated to the purification of carbon nanotubes in order to remove foreign nanoparticles that modify the physico-chemical properties of carbon nanotubes.

Chemical methods have been applied to purify carbon nanotubes. SWCNTs purification developed by Smalley and co-workers²² consists of refluxing as-grown SWCNTs in nitric acid solutions. Subsequently, more-effective purification techniques have been developed with minor physical damage of the tubes.^{23,24,25} Other method reported by Martinez et al.²⁶ consists of a technique of high-temperature air oxidation in conjunction with microwave acid treatments that removes a high portion of metal particles in relatively short periods of time. The most effective methods to purify MWCNTs are high-temperature treatments in an inert atmosphere (graphitization or annealing) and removing structural defects (heptagons and heptagon–pentagon pairs) or impurities such as metallic compounds.²⁷

1.2.3. Functionalization and dispersion

For an important part of applications (i.e. biomedical applications or some kinds of biosensors) CNTs must be modified as a “soluble” product. Preparation of homogeneous dispersions of CNTs suitable for processing thin films and other applications is of great importance. Various methods can be used for this purpose (see typical examples in Figure 1.3 and for more details see reference 10).

End²⁸ and/or sidewall²⁹ functionalization, use of surfactants with sonication³⁰, polymer wrapping of nanotubes³¹⁻³³ and protonation by superacids³⁴ have been reported. Although these methods are quite successful, they are often related to the cutting of CNTs into smaller pieces (sonication and/or functionalization), thus partly losing the high aspect ratio.

To deal with the functionalization of CNTs, a distinction must be made between covalent and noncovalent functionalization. Covalent functionalization is based on direct covalent sidewall functionalization. It is associated with a change of hybridization from sp^2 to sp^3 and a simultaneous loss of conjugation. Functionalization takes advantage of chemical transformations from defect sites already present. Defect sites can be the open ends and holes in the sidewalls, terminated, for example, by carboxylic groups (Figure 1.4)³⁵, and pentagon and heptagon irregularities in the hexagon graphene

framework. Oxygenated sites, formed through oxidative purification, have also been considered as defects.³⁶

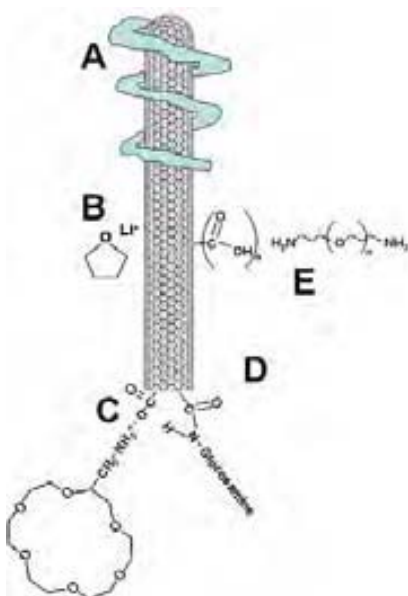


Figure 1.3. Schematic of typical CNTs solubilisation alternatives: (A) supramolecular wrapping with polymer; (B) CNTs-Li⁺ conducting polyelectrolyte; (C) with amino group of 2-aminomethyl-18-crown-6 ether; (D) by amide bonds with glucosamine; and, (E) by diamine-terminated oligomeric poly(ethylene glycol). For details see reference 10.

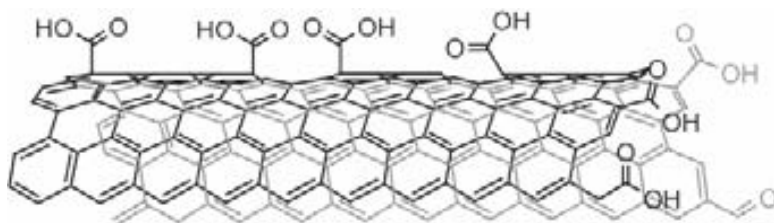


Figure 1.4. Scheme of carboxylation of CNTs, reflecting terminal and sidewall oxidation.³⁵

A non-covalent functionalization is mainly based on supramolecular complexation using various adsorption forces, such as Van der Waals and π -stacking interactions. All these functionalizations are exohedral derivatizations. A special case is the endohedral functionalization of CNTs, i.e. the filling of the tubes with atoms or small molecules (Figure 1.5).^{36,37}

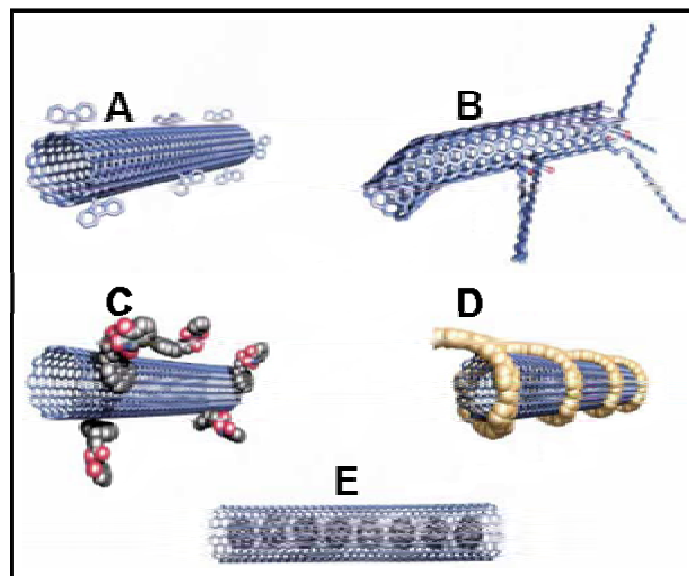


Figure 1.5. Functionalization possibilities for SWCNTs: A) covalent sidewall functionalization; B) defect-group functionalization; C) noncovalent exohedral functionalization with surfactants; D) noncovalent exohedral functionalization with polymers; and E) endohedral functionalization with, for example, C_{60} (see reference 36).

Kim et al.³⁸ provided an example of CNTs solubilisation. They developed a simple, efficient process for solubilizing CNTs with amylose in dimethyl sulphoxide– H_2O (DMSO– H_2O) mixture as well as in pure water. This process requires two important conditions, pre-sonication of CNTs in water and subsequent treatment of the fine CNTs dispersion with amylose in a specified DMSO– H_2O mixture, followed by a post-sonication. The best solvent composition was found to be 10–20% DMSO, in which amylose assumes an interrupted loose helix. The resulting colloidal solution was stable and exhibited no precipitation over several weeks.

To make nanotubes more easily dispersible, it is necessary to physically or chemically attach certain molecules (functional groups) to their smooth sidewalls without significantly changing the nanotubes' desirable properties.

CNTs functionalization by covalent modification was reported by Luong et al.³⁹ and MWCNTs were solubilized in a mixture of 3-aminopropyltriethoxysilane (APTES) and Nafion-perfluorinated ion-exchange resin and ethanol. Uniformly dispersed MWCNTs were obtained after 20 min sonication and used for sensor applications.

1.2.4. General applications

Carbon nanotubes have extraordinary electrical and thermal conductivity, and mechanical properties. They open an incredible range of applications in materials science, electronics, chemical processing, energy management, and many other fields.

CNTs are probably the best electron field-emitter. These extraordinary characteristics give CNTs potential in numerous applications including nanoelectronics, microscopy, nanoelectromechanical systems, and many more related to the development of high mechanical resistant materials for several industries and other applications; the scientific community is more motivated than ever to move beyond basic properties and explore the real issues associated with CNTs-based applications. Their focal point is as energy storage material: hydrogen storage, fuel cells and lithium battery; in composites for coating, filling and structural materials; as devices for molecular sensing and manipulation; in scanning probe microscopy; CNTs-based diodes and transistors; as field emission devices for X-ray instruments, in the development of chemical and physical sensors, biosensors and others applications.^{4,10}

Application of CNTs in different kinds of sensors and biosensors has been emerging in the last years. The application of CNTs in analytical science was lastly revised.⁴⁰ Several applications of CNTs in this field ranging from liquid chromatography (LC)⁴¹, stripping techniques⁴², and optical detections⁴³ have been overviewed. A detailed revision on the CNTs applications in electrochemical sensors and biosensors fields will be given in the following section.

1.3. Carbon nanotubes in electrochemical sensors and biosensors

Recent studies have demonstrated that CNTs exhibit strong electrocatalytic activity for a wide range of compounds, such as neurotransmitters^{44,45}, β -nicotinamide adenine dinucleotide (NADH)^{46,47}, hydrogen peroxide (H_2O_2)^{44,48}, ascorbic^{49,50} and uric acid⁴⁴, cytochrome c⁵¹, hydrazines⁵², hydrogen sulphide⁵³, amino acids⁵⁴ and deoxyribonucleic acid (DNA)⁵⁵ (details will be given in reference 56).

The high conductivity of CNTs in addition to the electrocatalytic activity encourages their use in electrochemical sensors and biosensors (the details are discussed in the reference 56).

One of the key issues when carbon nanotubes are used in electrochemical (bio)sensors is the way for to be integrated in the detection system.

1.3.1. Integration strategies

Several integration strategies have been described in details in reference 10. In the following part some of these strategies (ones used in this thesis or related to it) will be discussed.

1.3.1.1. Modification of electrode surfaces

Both non-oriented (random mixtures, Figure 1.6A left) and oriented (vertically aligned, Figure 1.6A right) CNTs have been used to modify several conventional electrode surfaces being the glassy carbon the most reported. For details see reference 10.

Oriented modifications

Li et al.⁵⁷ combined the micro- and nanolithography with catalytic CNTs growth techniques. A forest-like vertically aligned MWCNTs array was grown on Ni catalyst film by using plasma enhanced CVD. A dielectric encapsulation was then applied leaving only the very end of CNTs exposed to form inlaid nanoelectrode arrays. The electrical and electrochemical properties of this oriented MWCNTs array for small redox molecules have been characterized (by cyclic voltammetry (CV) and electrochemical impedance spectroscopy (EIS)), showing well-defined quasi reversible nanoelectrode behaviour and ultrasensitive detections. For details see reference 10.

Non-oriented modifications

CNTs have been used to modify the surface of a conventional glassy carbon electrode (GCE). The first use of CNTs was based on the modification of GCE with CNTs dispersed in sulphuric acid.⁴⁶ Prior to the surface modification, the glassy carbon electrode polished with alumina slurries and washed was cast with 10 μ L of a concentrated solution of CNTs in sulphuric acid (1 mg CNTs/ml). The coated electrode was dried at 200 °C for 3 h and it was ready to be used after a careful washing. The modification of GCE with CNTs was also done by using other three dispersing agents: dimethylformamide (DMF), concentrated nitric acid or a Nafion/water mixture.⁵⁸ In all

cases the CNTs were purified prior to use with nitric acid solution for 20 hours to ensure complete removal of metal catalysts from the CNTs. The CNTs casting solutions were dropped directly onto the glassy carbon surface and allowed to get dried. The electrode was then ready to be used. The authors found differences in the electrochemical reactivity between the CNTs modified electrodes and the control electrodes (glassy carbon treated in the same way but without CNTs). They attributed this difference to surface chemistries (primarily to defect densities) of the corresponding CNTs layers, associated with the different production and dispersion protocols. Another interesting conclusion regarding the differences in the electrocatalytic activities between electrodes modified with CNTs produced by arc or CVD method, is the independence of the casting mode. For details see reference 10.

Costa-García et al.^{59,60} have recently reported the modification of screen-printed carbon electrodes (SPCEs) with MWCNTs by depositing 4_μL of the MWCNT-COOH dispersion on the working electrode surface. The solution was left to dry at room temperature (20 °C) until its absolute evaporation. Finally, modified SPEs were carefully washed with DMF:H₂O (1:1) and dry under a nitrogen stream. In this way, they combined the advantages of the SPCEs with the excellent properties of the MWCNT for the detection of biomolecules.

1.3.1.2. Pastes and composites

Carbon paste (CP) and composite electrodes have been used in electrochemical sensors from several years. By analogy, similar matrices that involve CNTs have been lastly one of the focuses of research in the field of electrochemical sensors. CNTs inside the polymer matrix can be distributed either in randomly oriented (Figure 1.6B left) or vertical oriented (Figure 1.6B, right) way. Variety of binders, like mineral oil, teflon or epoxy resins, to produce CNTs pastes or composites, were reported being the rigid epoxy based CNTs composites less exploited. For details see reference 10.

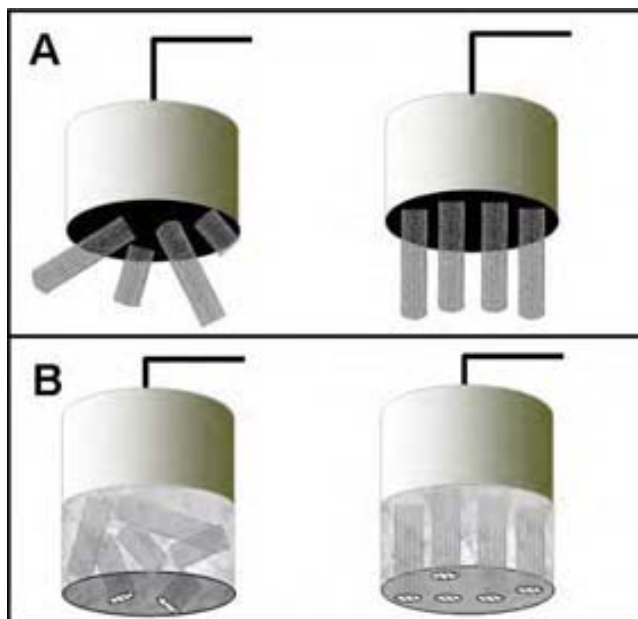


Figure 1.6. CNTs integration in electrochemical sensors. (A) electrode surface modifiers: non-oriented (left) and oriented (right) CNTs configuration; and (B) composites with non-oriented (left) and oriented (right) CNTs configuration (see reference 10).

1.3.2. Applications in sensors

Chemical sensors have become an increasingly attractive tool for monitoring noxious substances, for quality control and in medicinal and environmental chemistry. The tremendous importance of CNTs for sensors applications has led to wide research activities in this area. One of the advantages of these sensors is that they can be used as “one shot”-sensors that can be disposed after usage.

Some examples will be shown in summarized form in the following section (other examples are described in the reference 56).

1.3.2.1. Detection of gases

Gas sensor devices have attracted widespread attention in the past decades due to their potential applications in environmental pollution monitoring, flammable and toxic gas detection and food quality control.

The most important problem in gas sensors is their selectivity, i.e. the capability to provide different responses when they are exposed to different gaseous species. The efforts to improve the selectivity of gas sensors have also been focused on searching new sensing materials and more recently on using sensor arrays.⁶¹

CNTs-based gas sensors have received great attention beside other applications.⁶² Changes in the resistance of the CNTs layer have been used for detection of nitrogen dioxide⁶³, ammonia⁶⁴, hydrogen⁶¹, and inorganic vapor generally⁶⁵. Different interaction mechanisms between the analytes and CNTs as well as different modes of preparing CNTs based sensors have been reported. Various groups have explored the potential of CNTs for gas sensing, based on the electrical conductance change.

A novel antimony-carbon nanotube-tin oxide (Sb-CNTs-SnO₂) thin film using CNTs as growth guider and energy buffer was reported by J. Liu et al.⁶⁶ via the sol-gel method and ultrasonic dispersion technique, which could be potentially applied as a gas sensor for detecting indoor air pollutants emitted from building and decoration materials. Thin films were deposited on the 5 × 2 × 0.5 mm³ alumina (Al₂O₃) substrate with gold electrodes and ruthenium oxide (RuO₂) layer as heater for controlling the temperature. The results demonstrated that Sb-CNTs-SnO₂ thin film has higher sensitivity and shorter response time than the pure SnO₂ thin film and the Sb-SnO₂ thin film according to the gas sensing measurement. The possible mechanism of the better sensing performance has been primarily discussed from the aspects of growth guiding and energy buffering effects caused by CNTs. Furthermore, the electric field on the surface of Sb-CNTs-SnO₂ thin film is proposed as a rapid response to polar gases, e.g., formaldehyde, ammonia and toluene.

On the other hand, the polymers have been used to impart high sensitivity and selectivity in the gas electrodes.⁶⁷ Hyeok et al. fabricated a gas sensor from a nanocomposite by polymerizing pyrrole monomer with SWCNTs. Polypyrrole (Ppy) was prepared by a simple and straightforward in situ chemical polymerization of pyrrole mixed with SWCNTs, and the sensor electrodes were formed by spin-casting SWCNTs/Ppy onto pre-patterned electrodes. Ppy was uniformly coated on the wall of the SWCNTs to increase the specific surface area. The measured resistivity was greatly reduced due to the presence of the conductive SWCNTs network, whereas the specific surface area was increased about threefold. The sensitivity of the gas sensor fabricated with the SWCNTs/Ppy nanocomposite towards NO₂ gas as measured by a direct voltage divider at room temperature, was very high and similar to the one of the fabricated SWCNTs. The reported literature shows that CNTs are expected to be used as an economically viable material for use in gas detection. The successful utilization of

CNTs in gas sensors may open a new door for the development of novel nanostructured gas-sensing devices.

1.3.2.2. Detection of metals

Stripping analysis are the most sensitive electroanalytical techniques and highly suitable for the monitoring of toxic metals. Voltammetric stripping analysis has the capability of simultaneous multi-elements determination, and relatively cheaper instrumentation compared with spectroscopic techniques used for trace metal analysis. In addition, its low operating power makes them attractive as portable and compact instruments for onsite monitoring of trace metals.⁶⁸ The growing demand for reliable and real-time monitoring of trace metal contaminants in natural waters has prompted the development of new methods and appropriate sensors to perform *in situ* measurements.⁶⁹

In a recent study by Profumo et al.⁴² a CNTs chemically modified gold electrode (CNTs-CME) bearing SH groups has been developed for trace determination of As(III) and Bi(III) in natural and high-salinity waters. The preparation of this MWCNTs chemically modified electrode consisted of refluxing MWCNTs in SOCl_2 for 12 h. A solution of mercaptoethanol and of triethylamine in CH_2Cl_2 was added, and the mixture was refluxed for 24 h. The suspension was centrifuged and the solid repeatedly washed with methanol. The MWCNTs-CME was prepared by dipping the cleaned gold electrode in a sonicated suspension of 3 mg of derivatized nanotubes in 1 mL of DMSO for 48 h. It demonstrated to be effective for trace determination of As(III) and Bi(III) in acetic buffer.

1.3.2.3. Detection of biomolecules

NADH

A new kind of NADH sensor based on Meldola's blue (MB) functionalized carbon nanotubes nanocomposite film (MB/CNTs) modified glassy carbon electrode (GCE) has been reported.⁷⁰ MB could be firmly adsorbed on the surface of carbon nanotubes by non-covalent interactions without destroying the chemical and electronic structure of carbon nanotubes. Based on the results, a new NADH sensor was successfully established using the MB/CNTs/GCE. Under a lower operation potential of -0.1 V, NADH could be detected linearly up to a concentration of $500 \mu\text{M}$ with an extremely

low detection limit of 0.048 μM estimated at a signal-to-noise ratio of 3. The pattern developed using CNTs as catalyst supports to construct functionalized nanocomposite interface for oxidation of NADH suggested great potential applications in the designing of NADH sensors and a variety of NAD^+ -dependent dehydrogenase based biosensors, biofuel cells and bioelectronics.

Most of the CNTs based electrodes for NADH detection applications are based on physical adsorption of CNTs onto electrode surfaces, usually glassy carbon. However, it is important to note that CNTs have also been mixed with Teflon⁴⁸ or dispersed inside an epoxy resin.⁷¹

An example of carbon nanotube-epoxy composite (CNTEC) electrodes is reported by our group.⁷¹ CNTEC were constructed from two kinds of MWCNTs differing in the length (0.5–2 and 0.5–200 μm) mixed with epoxy resin. The behavior toward NADH of CNTEC electrodes prepared with different percentages of CNTs has been compared with that of graphite-epoxy composite (GEC) electrode. In all cases CNTEC electrodes provide better reversibility, peak shape, sensitivity and stability compared with GEC electrode. The obtained experimental results demonstrate remarkable electrochemical and mechanical behaviour of CNTs composites compared to graphite composites for electrochemical sensing of NADH (see Figure 3 in the reference 56).

CNTs electrodes allow highly sensitive, low-potential and stable amperometric sensing. Such ability of CNTs to promote the NADH electron-transfer reaction suggests great promise for dehydrogenases-based amperometric biosensors.

Dopamine

The interference due to the presence of ascorbic acid (AA) is one of the problems faced when dopamine (DA) is determined.⁷² AA has a similar oxidation potential and is usually present *in vivo* at concentrations 10 times higher than DA. Therefore, it is essential to establish simple and rapid methods for selective determination of DA in routine analysis. A conventional way is to coat the working electrode surface with an anionic film, such as Nafion, to protect the surface from the interference of the negatively charged.

A new layer-by-layer (LbL) nanostructured electroactive film to detect dopamine in the presence of ascorbic acid has been produced by Siqueira et al.⁷³. In this

study they have fabricated LbL films of polyamidoamine (PAMAM) incorporating MWCNTs (PAMAM-NT) alternated with nickel tetrasulfonated metallophthalocyanine (NiTsPc), in which the incorporation of CNTs enhanced the NiTsPc redox process and its electrocatalytic properties to detect dopamine.

The ability of the CNTs-incorporated films to distinguish between DA and AA was performed via CV using an electrolytic solution containing both AA and DA. Film growth was monitored by ultraviolet-visible (UV-vis) spectroscopy, which pointed to an exponential growth of the multilayers and cyclic voltammograms presented well-defined electroactivity with a redox pair at 0.86 and 0.87 V, reversibility, a charge-transfer controlled process, and high stability up to 100 cycles. The films were employed successfully in DA detection, with limits of detection and quantification of 10^{-7} and 10^{-6} mol·L⁻¹, respectively. Furthermore, films containing immobilized CNTs could distinguish between DA and its natural interferent (AA).

Ly et al.⁷⁴ presented a simply prepared sensor. They immobilized DNA onto the surface of a CNTs paste electrode (CNTPE). The CNTPE was prepared by mixing 40% CNTs and 40% DNA (double-stranded and prepared from calf thymus) with 20% mineral oil. The developed sensor was utilized to monitor DA ion concentration using the CV and square-wave (SW) stripping voltammetry methods. The detection limit obtained for DA (2.1×10^{-11} mol·L⁻¹) is very low compared to other common voltammetric methods. The relative standard deviation for the DA concentration of 0.05 µg·L⁻¹ was 0.02% (n =15) at the optimum conditions (see Figure 4 in the reference 56).

Other analytes

An interesting research in biological system using CNTs is the electrochemical study of hemoglobin (Hb). Didodecyldimethylammonium bromide (DDAB) film on the SWCNTs modified electrode was used to prepare the SWCNTs/DDAB film modified glassy carbon electrode.⁷⁵ This modified electrode was used to study the electrochemical behavior of Hb. Cyclic voltammetry of Hb showed two pairs of well-defined and nearly reversible peaks. The results obtained show that the electrochemical reaction of Hb on the SWCNTs/DDAB film modified electrode was controlled by absorption. The DDAB film lets the Hb maintain its suitable conformation and activity, which make an easy electron transfer between hemoglobin and SWCNTs modified electrode.

An interesting application includes the use of CNTs in the detection of blood cholesterol that it is of great clinical significance. Roy et al.⁷⁶ reported the fabrication of vertically aligned CNTs bioprobes on silicon substrates for enzymatic assay of cholesterol. The platform for the set of bioprobes was Si substrate (2 mm × 5 mm) on which a layer of SiO₂ (~300 nm thick) was grown by thermal oxidation. The substrate was then placed in a quartz tube CVD reactor, where MWCNTs were grown on the defined region (see figure 7A in reference 56). Due to its compatibility with the standard Si micro-fabrication technology, the proposed scheme has the potentiality to integrate an array of sensors for lab-on-a-chip systems. Other study was developed by Lia et al.⁷⁷. They have modified screen-printed carbon electrodes (on a polycarbonate substrate) with CNTs solution for the detection of total cholesterol. They verified that the presence of CNTs certainly causes an increase in the sensor signal as well as the signal to noise ratio.

Other interesting applications have been recently reported by Costa-García et al.^{59,60} They take advantages of the SPCEs and the excellent electroactivity of the MWCNTs for the detection of *p*-aminophenol and paracetamol in pharmaceutical compounds. They describe the enhanced electronic transfer properties of screen-printed electrodes modified with CNTs as electroanalytical tools being fast, cheap and simple devices.

1.3.2.4. Detection of nanoparticles

The remarkable properties of CNTs suggest also their use in developing (bio)sensing systems where nanoparticles have been involved. The simultaneous determination of the size and surface charge of individual acid-functionalized nanoparticles using a resistive-pulse counter based on a single 130-nm diameter pore defined by MWCNTs has been reported by Ito et al.⁴¹ A resistive-pulse *Coulter* counter based on a membrane containing a single MWCNTs channel was used to simultaneously determine the size and surface charge of carboxy-terminated polystyrene nanoparticles. The membrane was prepared from an epoxy section containing a MWCNTs channel mounted on a poly-(dimethylsiloxane) (PDMS) support structure. It was immobilized on a glass substrate (~12 × 12 mm) containing a cylindrical, sand-blasted hole (~2 mm diameter), as shown Figure 9 from reference 56.

Coulter particles counters have been used to count and analyze many different types of particles, ranging from biological cells to colloidal particles.⁷⁸ A typical *Coulter* counter consists of a single small pore (typically 5 μm -2 mm in diameter) that separates two electrolyte solutions. A constant potential is applied across the sensing pore, and the resulting ion current is continuously monitored. Transport of analyte particles through the pore results in an increase in the pore resistance, and the corresponding decrease in the ion current can be detected. The magnitude of the current decrease is correlative to the size of the analyte particles, and its duration is related to the residence time of the analyte in the pore. The number of such current pulses can be related to the analyte concentration. The principles governing this detection strategy predict that smaller sensing pores allow smaller particles detection. The width of the current pulses is a measure of the nanoparticle transport time, and it allows calculation of the electrokinetic surface charge. Different types of polystyrene nanoparticles having nearly the same size, but different electrokinetic surface charge, could be resolved on the basis of the difference in their transport time.

This new research shows a greatly improved signal-to-noise (S/N) ratio and better time resolution compared to their previous report of a MWCNTs based *Coulter* counter.⁷⁹ Accordingly, it is now possible to accurately measure the true height and width of pulse signals corresponding to transport of individual particles through a MWCNTs channel.

1.3.3. Applications in biosensors

Several studies on redox enzymes have promoted the electron transfer with electrodes in various ways.⁸⁰ In recent years, it has aroused great interest in modifying electrode surfaces on the molecular scale with novel nanomaterials for the direct electron transfer of redox enzymes and retention of bioactivity.⁸¹ This advantage has inspired research in coupling CNTs-based sensors with enzymes.¹⁰

Integration of biomaterials such as proteins, enzymes, antigens, antibodies or DNA with the CNTs essentially provides new hybrid systems that combine the conductive or semi-conductive properties of the CNTs with the recognition or catalytic properties of the biomaterials. Superior to other kinds of carbon-based materials, the internal cavities or external sides of CNTs walls provide the platform for the accommodation of the biomolecules. For example, in the following sections some

CNTs-based electrodes modified with enzymes will be described (more details in section 6.1 from reference 10).

1.3.3.1. Enzyme based biosensors

In the following part only applications related to three analytes (glucose, hydrogen peroxide and ethanol) are described. Some more applications can be read in the reference 10.

Glucose

Glucose is one of the most reported analyte detected via enzyme–CNTs electrodes. Several strategies have been used to immobilize the glucose oxidase (GOx) enzyme onto CNTs such as deposition onto crystalline gold nanoparticle modified MWCNTs electrode⁸², cross-linking in the matrix of chitosan⁸³, electropolymerization⁸⁴ etc.

A new amperometric glucose biosensor was constructed by Wang et al.⁸³ based on the immobilization of glucose oxidase (GOx) by cross-linking in the matrix of chitosan on a glassy carbon electrode modified by layer-by-layer assembled carbon nanotube (CNTs)/chitosan(CHIT)/gold nanoparticles (GNp) multi-layer films. With the increasing of CNTs/CHIT/GNp layers, the response current to H₂O₂ was changed regularly and the response current reached a maximum value when the number of CNTs/CHIT/GNp layers was 8. The assembling process of multi-layer films was simple to operate. The excellent electrocatalytic activity and special structure of the enzyme electrode resulted in good characteristics. The linear range was $6 \times 10^{-6} \sim 5 \times 10^{-3}$ M, with a detection limit of 3×10^{-6} M estimated at S/N ratio of 3, fast response time (less than 6 s). Moreover, it exhibited good reproducibility and stability.

Wang et al.⁸⁴ prepared a glucose biosensor based on CNTs as a dopant and GOx within an electropolymerized polypyrrole film. PPy/CNTs-GOx films were formed by using ‘oxidized’-CNTs as the sole charge-balancing anionic dopant. Such entrapment of the CNTs dopant does not compromise its electrocatalytic activity, facilitates a highly sensitive biosensing of glucose, and represents a simple and effective route for preparing amperometric enzyme electrodes. Details of the preparation, performance and advantages of the new PPy/CNT-GOx biosensor are given in the reference 83.

The possibility of direct electron-transfer between CNTs and GOx paves the way for the construction of a new generation of amperometric glucose biosensors. Such

electrical communication with GOx would obviate the need for a mediator and allow efficient transduction of the biorecognition event. The redox center of glucose oxidase, like those of most oxidoreductases, is electrically insulated by the protein shell. Because of this glycoprotein shell, the enzyme cannot be oxidized or reduced at the electrode at any potential. Guiseppi-Elie et al.⁸⁵ reported the direct electron transfer between SWCNTs and the redox active prosthetic group flavin adenine dinucleotide (FAD) of adsorbed GOx enzyme. Both FAD and GOx were found to spontaneously adsorb to unannealed CNTs that were cast onto glassy carbon electrodes (GCE). The peak current of the electroactive FAD at SWCNTs/GCE was almost 22 times larger than the one found at the bare GCE (see Figure 14 in the reference 56). This indicates a larger effective working electrode area of SWCNTs/GCE compared to GCE alone.

Hydrogen peroxide

The detection of hydrogen peroxide (H₂O₂) in environmental, industrial, chemical, food, and pharmaceutical fields is of great importance. Compared with other methods, such as titrimetry, spectrometry and chemiluminescence methods, the electrochemical techniques for the determination of H₂O₂ coupled with the intrinsic selectivity and sensitivity of enzymatic reactions are promising for the fabrication of simple and low-cost enzyme sensors.⁸⁶

A H₂O₂ biosensor was developed by Zhao et al.⁸⁷ based on the bioelectrochemistry of hemoglobin (Hb) at multi-wall carbon nanotubes (MWCNTs) noncovalently functionalized with biopolymers of sodium alginate (SA). The amperometric response of the biosensor varied linearly with the H₂O₂ concentration ranging from 40 to 200 μM, with a detection limit of 1.64×10^{-5} M (S/N = 3) and the good long-term stability.

Other example of a novel H₂O₂ biosensor has been fabricated by Liu and Hu⁸⁸ based on the direct electrochemistry and electrocatalysis of myoglobin (Mb) immobilized on silver nanoparticles and doped carbon nanotubes film by hybrid sol-gel techniques.

Another interesting research that involves the incorporation of CNTs for the detection of H₂O₂ is the fabrication of composites. As polyaniline (PANI) and CNTs are excellent materials for the construction of electrochemical sensors and biosensors, the combination of these two materials is also expected to be an excellent platform for

electrochemical sensing applications.⁸⁹ PANI has an excellent conductivity and electroactivity having special interest for applications in electrochemical biosensing systems.^{90,91}

Additionally, PANI can provide a suitable environment for the immobilization of biomolecules. PANI-modified electrodes have several advantages such as impressive signal amplification and elimination of electrode fouling. Compared with the biosensor without CNTs, the proposed biosensor exhibited enhanced stability and approximately eight-fold sensitivity.

A linear range from 0.2 to 19 μM for the detection of H_2O_2 was observed for the biosensor proposed by Luo et al.⁹², with a detection limit of 68 nM. The presence of CNTs in the PANI film could effectively increase the amount of immobilized horseradish peroxidase (HRP) and enhance the stability of the immobilized enzyme as well as the biosensor performance.⁵⁶

Ethanol

A rapid measurement of ethanol is very important in clinical, forensic as well as in food and beverages industry.⁹³ Many analytical methods such as titrations, colorimetric, spectrometric and chromatographic methods have been developed during past years for the determination of ethanol. The mentioned methods are precise and reliable, but require expensive instrumentation. Therefore, enzyme biosensor, a cost effective device, could be a perfect alternative to the detection of alcohol, using alcohol dehydrogenase (ADH) that catalyzes the oxidation of ethanol to acetaldehyde. An example of this development is the amperometric biosensor described by Santos et al.⁹⁴, based on co-immobilization of ADH and Meldola's Blue (MB) on MWCNTs by the cross-linking method using glutaraldehyde and agglutination with mineral oil. The efficiency of MB as an electron mediator on the electrode surface and CNTs as enzyme immobilization matrix was demonstrated.

Other example of amperometric ethanol biosensor was constructed by Tsai et al.⁹⁵ using ADH physically immobilized within poly(vinyl alcohol)–multi-wall carbon nanotube (PVA–MWCNTs) composite obtained by a freezing–thawing process. It comprises a MWCNTs conduit, a PVA binder, and an ADH function. The measurement of ethanol is based on the signal produced by NADH, the product of the enzymatic reaction.

The performance of the PVA–MWCNTs–ADH biocomposite modified glassy carbon electrode was evaluated by using CV and amperometry in the presence of NADH and in the presence of ethanol. The ethanol content in standard solutions was determined achieving a sensitivity of 196 nA mM^{-1} , a linear range up to 1.5 mM, and a response time of about 8 s were obtained. These characteristics allow its application for direct detection of ethanol in alcoholic beverages: beer, red wine, and spirit.

1.3.3.2. Immunosensors

Immunoassays (IAs) are analytical tests that use an antibody as very specific recognition element. The fabrication of immuno-CNTs assays via specific antibody-antigen interactions, may contribute to expand the detection scope of CNTs sensors.

The specific molecular recognition of antigens by antibodies, in formats where CNTs have been integrated, has been exploited to develop highly selective detection of proteins.⁹⁶ The IA has proven to be one of the most productive technology contributions to medicine and fundamental life science research in the twentieth century for both qualitative and quantitative analysis. A great number of research papers have appeared over the last years describing the development of novel IA strategies for detecting trace amounts of chemicals in environmental and food samples.

Li et al.⁹⁷ have developed a novel amperometric immunosensor for human chorionic gonadotropin (HCG) detection. It was fabricated incorporating toluidine blue (TB) and hemoglobin (Hb) on the multi-wall carbon nanotube (MWCNTs)–CHIT modified glassy carbon electrode, followed by electrostatic adsorption of a conducting gold nanoparticles (nanogold) film as sensing interface. The MWCNTs–CHIT matrix provided a congenial microenvironment for the immobilization of biomolecules and promoted the electron transfer to enhance the sensitivity of the immunosensor. Due to the strong electrocatalytic properties of Hb and MWCNTs toward H_2O_2 , it significantly amplified the current signal of the antigen–antibody reaction. The immobilized toluidine blue as an electron transfer mediator exhibited excellent electrochemical redox properties.

A sensitive method for the detection of cholera toxin (CT) (causative agent for diarrhea in humans) using an electrochemical immunosensor with liposomic magnification followed by adsorptive square-wave stripping voltammetry was described by Viswanathan et al.⁹⁸ The sensing interface consists of monoclonal antibody against

the B subunit of CT that is linked to poly(3,4-ethylenedioxythiophene) coated on Nafion-supported MWCNTs cast film on a glassy carbon electrode. The CT is detected by a “sandwich-type” assay on the electronic transducers, where the toxin is first bound to the anti-CT antibody and then to the GM1 liposomes encapsulated with an electroactive redox marker (potassium ferrocyanide). The GM1 electrochemical immunoassay can be an alternative method to enzyme-linked immunosorbent assay or other conventional assays for CT, taking advantage of sensitivity, speed and simplicity. MWCNTs were added into 1 mL of diluted Nafion solution, forming a black suspension. Prior the bare GCE was activated by mechanical polishing and by electrochemical treatment applying potentials of +1.5 and -0.2 V in 0.1 M H₂SO₄ for 5 and 3 s, respectively. The surface modification was preceded by casting few microliters of an aliquot of MWCNTs-Nafion solution. The solvent was allowed to evaporate at room temperature in the air. The immunosensing layers were fabricated on the modified electrode surface by immobilizing different concentrations of cholera toxin antibody during polymerization. The electrode was then treated with 0.5% PVA aqueous solution followed by rinsing with PBS and stored at 4 °C until use.

In the last years an immunosensor coupled to glassy carbon electrode (GCE) modified with MWCNTs (CNTs-GCE) integrated with microfluidic systems for rapid and sensitive quantification of prostate specific antigen (PSA) in human serum samples was reported by Panini et al.⁹⁹ Mouse monoclonal anti-PSA (5G6) antibodies were immobilized on a rotating disk. PSA in the serum sample is allowed to react immunologically with the immobilized anti-PSA and horseradish peroxidase (HRP) enzyme-labeled secondary antibodies specific to PSA. HRP, in the presence of H₂O₂ catalyzes the oxidation of 4-*tert*-butylcatechol (4-TBC), and the back electrochemical reduction was detected on CNTs-GCE at -0.15 V. The electrochemical detection can be done within 1 min and the total assay time was 30 min.

1.3.3.3. Genosensors

Biosensors based on nucleic acid interactions are called DNA biosensors or genosensors and represent a new and exciting area in (bio)analytical chemistry. The determination of nucleic acid sequences from humans, animals, bacteria and viruses is the departure point for solving different problems: investigations in food and water contamination caused by microorganisms, detection of genetic disorders, tissue matching, forensic

applications etc. DNA biosensor technologies are rapidly developed as an alternative to the classical gene assays, due to several advantages such as low cost, rapid analysis, simplicity and possibility of miniaturization.

The development of new transducing materials for DNA analysis, whose preparation is simple and suitable for mass fabrication, with a higher sensitivity and lower detection limits is a key issue in the research of electrochemical genosensing. Electrochemical genosensors are based on electrochemical transduction to detect the hybridization event. These devices can be exploited for monitoring sequence-specific hybridization events directly measuring the oxidation signal of DNA electroactive bases, DNA electroactive indicators forming complexes with DNA nitrogenous bases, or with the aid of oligonucleotides labelled with enzymes, dyes or nanoparticles.

The use of CNTs as a novel platform for DNA immobilization has recently attracted many researches. Aminated or carboxylated DNA oligonucleotides were covalently linked to the respective carboxylated or aminated SWCNTs multi-layer films through appropriate coupling chemistries. The resulting DNA functionalized SWCNTs multi-layer films exhibit excellent specificity and chemical stability under the conditions of DNA hybridization. This modified layer provides a via for the development of DNA hybridization sensors, where the exquisite binding specificity of biomolecular recognition is directly coupled to SWCNTs.¹⁰⁰

MWCNTs functionalized with a carboxylic acid group (MWCNTs–COOH) for covalent DNA immobilization and with a favorable performance for the rapid detection of specific hybridization were described by Cai et al.¹⁰¹ The hybridization reaction was followed by using daunomycin as an electroactive intercalator indicator (see Figure 1.7A). When hybridization occurs, daunomycin is intercalated in the DNA duplex and gives an increased electrochemical response compared to single-stranded DNA; the increase in the height of the daunomycin redox peak is used to detect the presence and the amount of the complementary sequence.

CNTs have a dual amplification role: recognition and transduction events. Therefore, they behave as carriers for enzyme tags and for accumulating the product of the enzymatic reaction. A new strategy for dramatically amplifying enzyme-linked electrical detection of proteins and DNA using CNTs as carrying enzymes has been developed by Wang et al.¹⁰². It consists of amplifying the electrical detection and producing an ultrasensitive bioelectronic detection of DNA hybridization. First, the alkaline phosphatase (ALP) enzyme tracer was immobilized on CNTs using 1-ethyl-3-

(3-dimethyl aminopropyl)carbodiimide as linker. After that, a capture of the ALP-loaded CNTs tags to the streptavidin-modified magnetic beads by a sandwich DNA hybridization (Figure 1.7B) or antibody-antigen-antibody (Ab-Ag-Ab) interaction is carried out. A similar loading effect has also been demonstrated earlier with quantum dots as electroactive labels for DNA hybridization detection¹⁰³ (Figure 1.7C).

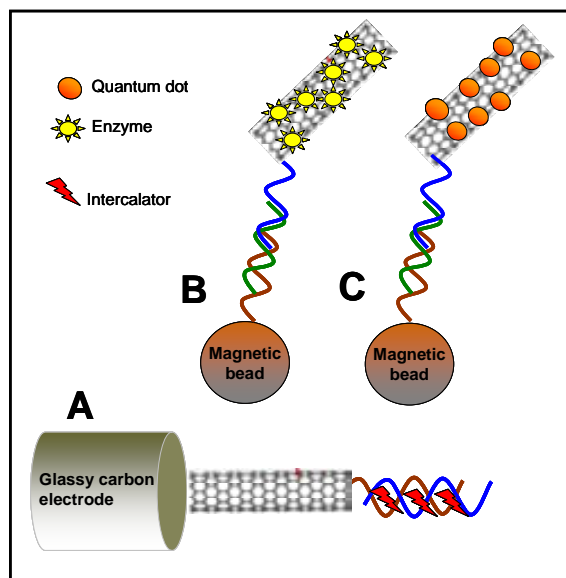


Figure 1.7. DNA detection via CNTs. (A) direct electron transfer via intercalator; (B) CNTs loaded with enzymes; and, (C) CNTs loaded with quantum dots (for more details see reference 10).

A novel electrochemical DNA-based biosensor for the detection of deep DNA damage has been designed by Galandova et al.¹⁰⁴ employing the bionanocomposite layer of MWCNTs in CHIT deposited on a screen-printed carbon electrode (SPCE). The biocomponent represented by double-stranded (ds) herring sperm DNA was immobilized on this composite using layer-by-layer coverage to form a robust film. A good correlation between the CV and electrochemical impedance spectroscopy (EIS) parameters has been found, confirming a strong effect of MWCNTs on the enhancement of the electroconductivity of the electrode surface and that of CHIT on the MWCNTs distribution at the electrode surface.

1.4. References

- ¹ N. Taniguchi, On the Basic Concept of Nanotechnology, 1974, Proc. ICPB Tokyo.
- ² V.B. King, Nanotechnology Research Advances, 2007, Nova Publishers ISBN 1600215254, 9781600215254, 187.
- ³ A.G. Mamalis, L.O.G. Vogtländer and A. Markopoulos, *Precision Eng.*, 2004, **28**, 16.
- ⁴ M. Meyyappan, Carbon Nanotubes: Science and Applications, 2005, CRC Press ISBN 0849321115, 9780849321115, 289.
- ⁵ S. Iijima, *Nature*, 1991, **56**, 354.
- ⁶ W.B. Choi, D.S. Chung, J.H. Kang, H.Y. Kim, Y.W. Jin, I.T. Han, Y.H. Lee, J.E. Jung, N.S. Lee, G.S. Park and J.M. Kim, *Appl. Phys. Lett.*, 1999, **75**, 3129.
- ⁷ S.J. Tans, A.R.M. Verschueren and C. Dekker, *Nature*, 1998, **393**, 49.
- ⁸ H. Dai, J.H. Hafner, A.G. Rinzler, D.T. Colbert and R.E. Smalley, *Nature*, 1996, **384**, 147.
- ⁹ M.S. Shaffer, X. Fan and A.-H. Windle, *Carbon*, 1998, **36**, 1603.
- ¹⁰ A. Merkoçi, M. Pumera, X. Llopis, B. Pérez, M. del Valle and S. Alegret, *Trends Anal. Chem.*, 2005, **24**, 826.
- ¹¹ A. Heller, *J. Phys. Chem. Res.*, 1992, **96**, 3579.
- ¹² S. Iijima, *Physica B+C*, 2002, **323**, 1.
- ¹³ V. N. Popov, *Mater. Sci. Eng., R*, 2004, **43**, 61.
- ¹⁴ T. Ando, H. Matsumura and T. Nakanishi, *Physica B+C*, 2002, **323**, 44.
- ¹⁵ M. Moniruzzaman and K.I. Winey, *Macromolecules*, 2006, **39** (16), 5194.
- ¹⁶ K. Balasubramanian and M. Burghard, *Small*, 2005, **1** (2), 180.
- ¹⁷ M. Foley, *Cheap Tubes Inc.*, 2006. <http://www.nanotech-now.com/Carbon-Nanotubes-101.htm>
- ¹⁸ M.S. Dresselhaus, G. Dresselhaus, K. Sugihara, I.L. Spain and H.A. Goldberg, Springer Series in Material Science 5, 1988, Springer-Verlag, Berlin, Heidelberg.
- ¹⁹ J.-P. Salvetat, J.-M. Bonard, N.H. Thomson, A.J. Kulik, L. Forró, W. Benoit and L. Zuppiroli, *Appl. Phys. A*, 1999, **69**, 255.
- ²⁰ E.C. Baddour and C. Briens, *Int. J. Chem. Reactor Eng.*, 2005 **3**:R3.

- ²¹ Endo, T. Hayashi, Y.A. Kim, M. Terrones and M.S. Dresselhaus, *Phil. Trans. R. Soc. Lond. A*, 2004, **362**, 2223.
- ²² J. Liu, A.G. Rinzler, H. Dai, J.H. Hafner, R.K. Bradley, P.J. Boul, A. Lu, T. Iverson, K. Shelimov, C.B. Huffman, F. Rodriguez-Macias, Y.S. Shon, T. R. Lee, D.T. Colbert and R.E. Smalley, *Sci.*, 1998, **280**, 1253.
- ²³ S. Bando, A.M. Rao, A. Thess and R.E. Smalley, *J. Phys. Chem. B*, 1997, **101**, 8839.
- ²⁴ A.G. Rinzler, J. Liu, H. Dai, P. Nikolaev, C.B. Huffman and F.J.R.-Macias, *Appl. Phys. A*, 1998, **67**, 29.
- ²⁵ A.C. Dillon, T. Gennett, K.M. Jones, J.L. Alleman, P.A. Parilla and M.J. Heben, *Adv. Mater.*, 1999, **11**, 1354.
- ²⁶ M.T. Martinez, M.A. Callejas, A.M. Benito, W.K. Maser, M. Cochet, J.M. Andres, J. Schreiber, O. Chauvet and J.L. Fierro, *Chem. Commun.*, 2002, 1000.
- ²⁷ R. Andrews, D. Jacques, D. Qian and E. C. Dickey, *Carbon*, 2001, **39**, 1681.
- ²⁸ J. Chen, M.A. Hamon, H. Hu, Y. Chen, A.M. Rao, P.C. Eklund and R.C. Haddon, *Sci.* 1998, **282**, 95.
- ²⁹ D. Tasis, N. Tagmatarchis, V. Georgakilas and M. Prato, *Chem. Eur. J.*, 2003, **9**, 4000.
- ³⁰ M.F. Islam, E. Rojas, D.M. Bergey, A.T. Johnson and A.G. Yodh, *Nano Lett.*, 2003, **3**, 269.
- ³¹ A. Star, J.F. Stoddart, D. Steuerman, M. Diehl, A. Boukai, E.W. Wong, X. Yang, S.W. Chung, H. Choi and J.R. Heath, *Angew. Chem. Int. Ed.*, 2001, **40**, 1721.
- ³² M.J. O'Connell, P. Boul, L.M. Ericson, C. Huffman, Y. Wang, E. Haroz, C. Kuper, J. Tour, K.D. Ausman and R.E. Smalley, *Chem. Phys. Lett.*, 2001, **342**, 265.
- ³³ J. Chen, H. Liu, W.A. Weimer, M.D. Halls, M.D.H. Waldeck and G.C. Walker, *J. Am. Chem. Soc.*, 2002, **124**, 9034.
- ³⁴ S. Ramesh, L.M. Ericson, V.A. Davis, R.K. Saini, C. Kittrell, M. Pasquali, W.E. Billups, W. Adams, R.H. Hauge and R.E. Smalley, *J. Phys. Chem. B*, 2004, **108**, 8794.
- ³⁵ A. Hirsch and O. Vostrowsky, *Top. Curr. Chem.*, 2005, **245**, 193.
- ³⁶ A. Hirsch, *Angew. Chem. Int. Ed.*, 2002, **41**, 1853.
- ³⁷ J.L. Bahr and J.M. Tour, *J. Mater. Chem.*, 2002, **12**, 1952.

- ³⁸ O.K. Kim, J. Je, J.W. Baldwin, S. Kooi, P.E. Pehrsson and L.J. Buckley, *J. Am. Chem. Soc.*, 2003, **125**, 4426.
- ³⁹ J.H.T. Luong, S. Hrapovic, D. Wang, F. Bensebaa and B. Simard, *Electroanalysis*, 2004, **16**, 132.
- ⁴⁰ A. Merkoçi, *Microchim. Acta.*, 2006, **152**, 157.
- ⁴¹ T. Ito, L. Sun and R.M. Crooks, *Anal. Chem.*, 2003, **75**, 2399.
- ⁴² A. Profumo, M. Fagnoni, D. Merli, E. Quartarone, S. Protti, D. Dondi, and A. Albini, *Anal. Chem.*, 2006, **78**, 4194.
- ⁴³ M. Penza, G. Cassano, P. Aversa, F. Antolini, A. Cusano, A. Cutolo, M. Giordano and L. Nicolais, *Appl. Phys. Lett.*, 2004, **85**, 2379.
- ⁴⁴ H. Luo, Z. Shi, N. Li, Z. Gu and Q. Zhuang, *Anal. Chem.*, 2001, **73**, 915.
- ⁴⁵ M.D. Rubianes and G.A. Rivas, *Electrochem. Commun.*, 2003, **5**, 689.
- ⁴⁶ M. Musameh, J. Wang, A. Merkoçi and Y. Lin, *Electrochem. Commun.*, 2002, **4**, 743.
- ⁴⁷ R.R. Moore, C.E. Banks and R.G. Compton, *Anal. Chem.*, 2004, **76**, 2677.
- ⁴⁸ J. Wang and M. Musameh, *Anal. Chem.*, 2003, **75**, 2075.
- ⁴⁹ J. Wang, M. Li, Z. Shi and N. Li, *Electroanal.*, 2002, **14**, 225.
- ⁵⁰ Z.H. Wang, J. Liu, Q.L. Liang, T.M. Wang and G. Luo, *Analyst*, 2002, **127**, 653.
- ⁵¹ J. Wang, M. Li, Z. Shi and N. Li, *Anal. Chem.*, 2002, **74**, 1993.
- ⁵² Y. Zhao, W.D. Zheng, H. Chen and Q.M. Luo, *Talanta*, 2002, **58**, 529.
- ⁵³ N. Lawrence, R.P. Deo and J. Wang, *Anal. Chim. Acta*, 2004, **517**, 131.
- ⁵⁴ J.X. Wang, M.X. Li, Z.J. Shi, N.Q. Li and Z.N. Gu, *Electroanal.*, 2004, **16**, 140.
- ⁵⁵ M.L. Pedano and G.A. Rivas, *Electrochem. Commun.*, 2004, **6**, 10.
- ⁵⁶ B. Pérez and A. Merkoçi, American Scientific Publishers, 2007, **2**, 337.
- ⁵⁷ J. Li, J.E. Koehne, A.M. Cassell, H. Chen, H. Tee Ng, Q. Ye, W. Fan, J. Han and M. Meyyappan, *Electroanalysis*, 2005, **17**, 15.
- ⁵⁸ N.S. Lawrence, R.P. Deo and J. Wang, *Electroanalysis*, 2005, **17**, 65.
- ⁵⁹ P.J. Lamas-Ardisana, P. Queipo, P. Fanjul-Bolado and A. Costa-García, *Anal. Chim. Acta*, 2008, **615**, 30.

- ⁶⁰ P. Fanjul-Boladoa, P.J. Lamas-Ardisanab, D. Hernández-Santosa and A. Costa-García, *Anal. Chim. Acta*, 2009, **638**, 133.
- ⁶¹ I. Sayago, E. Terrado, M. Aleixandre, M.C. Horrillo, M.J. Fernández, J. Lozano, E. Lafuente, W.K. Maser, A.M. Benito, M.T. Martínez, J. Gutiérrez and E. Muñoz, *Sens. Actuators B*, 2007, **122**, 75.
- ⁶² M. Trojanowicz, *Trends Anal. Chem.*, 2006, **25**, 5.
- ⁶³ C. Cantalini, L. Valentini, L. Lozzi, I. Armentano, J.M. Kenny and S. Santucci, *Sensor. Actuator B-Chem.*, 2003, **93**, 333.
- ⁶⁴ K.S. Ahn, J.H. Kim, K.N. Lee, C.O. Kim and J.P. Hong, *J. Korean Phys. Soc.*, 2004, **45**, 158.
- ⁶⁵ A. Modi, N. Koratkar, E. Lass, B. Wei, and P.M. Ajayan, *Nature*, 2003, **424**, 10.
- ⁶⁶ J. Liu, Z. Guo, F. Meng, Y. Jia and J. Liu, *J. Phys. Chem. C*, 2008, **112**, 6119.
- ⁶⁷ B.K. Hyeok, A. Seung, Y. Jeong, H.R. Hwang, and Y.H. Lee, *Adv. Mater.*, 2004, **16**, 12.
- ⁶⁸ M.A. Baldo, S. Daniele, I. Ciani, C. Bragato and J. Wang, *Electroanal.*, 2004, **5**, 6.
- ⁶⁹ M. Taillefert, G.W. Luther III and D.B. Nuzzio, *Electroanal.*, 2000, **12**, 401.
- ⁷⁰ L. Zhu, J. Zhai, R. Yang, C. Tian and L. Guo, *Biosens. Bioelectron.*, 2007, **22**, 2768.
- ⁷¹ M. Pumera, A. Merkoci and S. Alegret, *Sensor. Actuat. B-Chem.*, 2006, **113**, 617.
- ⁷² L. Falat and H.Y. Cheng, *Anal. Chem.*, 1982, **54**, 2108.
- ⁷³ J.R. Siqueira, L.H.S. Gasparotto, O.N. Oliveira, and V. Zucolotto, *J. Phys. Chem. C*, 2008, **112**, 9050.
- ⁷⁴ S.Y. Ly, *Bioelectrochem.*, 2005, **68**, 232.
- ⁷⁵ P. Yang, Q. Zhao, Z. Gu and Q. Zhuang, *Electroanal.*, 2004, **16**, 97.
- ⁷⁶ S. Roy, H. Vedala and W. Choi, *Nanotech.*, 2006, **17**, S14.
- ⁷⁷ G. Lia, J.M. Liao, G.Q. Hu, N.Z. Ma and P.J. Wu, *Biosens. Bioelectron.*, 2005, **20**, 2140.
- ⁷⁸ H. Bayley and C.R. Martin, *Chem. Rev.*, 2000, **100**, 2575.
- ⁷⁹ L. Sun and R.M. Crooks, *J. Am. Chem. Soc.*, 2000, **122**, 12340.

- ⁸⁰ X. Chen, C. Ruan, J. Kong, J. Deng, *Anal. Chim. Acta*, 2000, **412**, 89.
- ⁸¹ J. Liu, A. Chou, W. Rahmat, M.N. Paddon-Row and J.J. Gooding, *Electrochim. Acta*, 2005, **51**, 611.
- ⁸² R.B. Rakhi, K. Sethupathi and S. Ramaprabhu, *J. Phys. Chem. B*, 2009, **113** (10), 3190.
- ⁸³ Y. Wang, W. Wei, X. Liu and X. Zeng, *Mater. Sci. Eng. C*, 2009, **29**, 50.
- ⁸⁴ J. Wang and M. Musameh, *Anal. Chim. Acta*, 2005, **539**, 209.
- ⁸⁵ A. Guiseppi-Elie, C. Lei and R. Baughman, *Nanotech.*, 2002, **13**, 559.
- ⁸⁶ S.S. Razola, B.L. Ruiz, N.M. Diez, H.B. Mark and J.-M. Kauffmann, *Biosens. Bioelectron.*, 2002, **17**, 921.
- ⁸⁷ H.Y. Zhao, W. Zheng, Z.X. Meng, H.M. Zhou, X.X. Xu, Z. Li and Y.F. Zheng, *Biosens. Bioelectron.* 2009, in press.
- ⁸⁸ C.Y. Liu and J.M. Hu, *Biosens. Bioelectron.*, 2009, **24**, 2149.
- ⁸⁹ E. Granot, B. Basnar, Z. Cheglakov, E. Katz and I. Willner, *Electroanal.*, 2006, **18**, 26.
- ⁹⁰ E.I. Iwuoha, D.S. De Villaverde, N.P. García, M.R. Smyth and J.M. Pingarron, *Biosens. Bioelectron.*, 1997, **12**, 749.
- ⁹¹ A.N. Ivanov, L.V. Lukachova, G.A. Evtugyn, E.E. Karyakina, S.G. Kiseleva, H.C. Budnikov, A.V. Orlov, G.P. Karpacheva and A.A. Karyakin, *Bioelectroch.*, 2002, **55**, 75.
- ⁹² X. Luo, A.J. Killard, A. Morrin and M.R. Smyth, *Anal. Chim. Acta*, 2006, **575**, 39.
- ⁹³ L. Zhang, Z. Xu, X. Sun and S. Dong, *Biosens. Bioelectron.*, 2007, **22**, 1097.
- ⁹⁴ A.S. Santos, A.C. Pereira, N. Durán and L.T. Kubota, *Electrochim. Acta*, 2006, **52**, 215.
- ⁹⁵ Y.C. Tsai, J.-D. Huang and C.-C. Chiu, *Biosens. Bioelectron.*, 2007, **22**, 3051.
- ⁹⁶ E. Zacco, M.I. Pividori, and S. Alegret, *Anal. Chem.*, 2006, **78**, 1780.
- ⁹⁷ N. Li, R. Yuan, Y. Chai, S.C.H. An, *Bioprocess. Biosyst. Eng.*, 2008, **31**, 551.
- ⁹⁸ S. Viswanathan, L.C. Wu, M.R. Huang, and J.A.A. Ho, *Anal. Chem.*, 2006, **78**, 1115.
- ⁹⁹ N.V. Panini, G.A. Messina, E. Salinas, H. Fernández and J. Raba, *Biosens. Bioelectron.*, 2008, **23**, 1145.

¹⁰⁰ D.H. Jung, B.H. Kim, Y.K. Ko, M.S. Jung, S. Jung, S.Y. Lee and H.T. Jung, *Langmuir*, 2004, **20**, 8886.

¹⁰¹ H. Cai, X. Cao, Y. Jiang, P. He and Y. Fang, *Anal. Bioanal. Chem.*, 2003, **375**, 287.

¹⁰² J. Wang, G. Liu, M.R. Jan, *J. Am. Chem. Soc.*, 2004, **126**, 3010.

¹⁰³ J. Wang, G. Liu, M.R. Jan, Q. Zhu, *Electrochem. Comm.*, 2003, **5**, 1000.

¹⁰⁴ J. Galandova, G. Ziyatdinova and J. Labuda, *Anal. Sci.*, 2008, **24**, 711.

2

Objectives

CHAPTER 2

Objectives

The principal objective that raises this work consists of studying the electrocatalytic behaviour of carbon nanotubes (CNTs) and at the same time designing novel electrochemical (bio)sensors making use of different alternatives of CNTs integration into (bio)sensing systems, based on modifications of electrode surfaces with CNTs, or in the use of CNTs based (bio)composites. The work related to catechol detection was in line with the objectives of WARMER project, an FP6 European project that aims at developing an improved biosensor for phenolic compounds.

The detailed particular objectives are:

1. Evaluate the advantages of using CNTs as electrode modifiers in relation to the electrocatalytic properties beside the general analytical improvements achieved by the sensor. The evaluation of the ability of CNTs to promote the electron-transfer reaction would be the key point for the development of new amperometric biosensors.

- 1.1. Study the catalytic effects of CNTs integrated onto a conventional glassy carbon electrode with interest for β -nicotinamide adenine dinucleotide (NADH) detection.

- 1.2. Study a novel design for CNTs integration based on the use of poly(vinylchloride) (PVC) for CNTs dispersion as well as a matrix that ensures better mechanical/robustness properties of the sensor membrane. Additionally glutaraldehyde as a matrix linker with future promises for biosensors applications due to its ability for covalent binding of biological molecules will also be studied.

- 1.3. Evaluate and compare the CNTs efficiency for electrochemical oxidation of NADH. Compare them with other carbon materials (i.e. carbon nanofibers and

carbon microparticles) used as modifiers of conventional electrodes such as glassy carbon and gold.

1.4. Study the effect of CNTs in combination with cyclodextrin (CD) matrix to detect dopamine (DA) oxidation. As CD enhances the diffusion of DA through its cavities the objective is to study if the dispersed CNTs onto the electrode in presence of CD facilitate the DA recognition and the electron transfer.

1.5. Compare the modified electrode for DA detection with a glassy carbon electrode without modifications so as to verify the contribution of CD and CNTs in the improved electrochemical detection.

2. Evaluate a carbon nanotubes-epoxy composite (CNTEC) electrode that incorporates biological materials such as enzymes (glucose oxidase (GOx) from *Aspergillus niger* and tyrosinase (Tyr) from mushroom) and cells (*Pseudomonas fluorescens*) as well as compare the modified electrodes with conventional graphite epoxy composite electrodes.

2.1. Develop a CNTs biosensor based on a rigid and renewable carbon nanotube (CNTs) biocomposite based on the immobilization of GOx through physical entrapment inside an epoxy resin matrix. Evaluate if the use of CNTs as the conductive part of the composite ensures better incorporation of enzyme into the epoxy matrix and a faster electron transfer rates between the enzyme and the transducer.

2.2. Develop a microbial biosensor based on a carbon-nanotube epoxy composite (CNTEC) platform used to immobilize cells (*Pseudomonas fluorescens*) via the use of gelatin and cross-linking with glutaraldehyde.

2.3. Construct and characterize an amperometric biosensor based on tyrosinase integrated within a carbon nanotube epoxy composite electrode. Evaluation of the electrochemical response toward catechol as a model phenolic compound. This has been carried out as part of the WARMER project, an FP6 European project that aims at developing an automatic analyzer for phenolic compounds and heavy metals in sea water.

3

Carbon nanotubes in sensing systems

Contents

3.1. NADH detection	41
3.1.1. Sensing with electrodes modified with CNTs dispersed in a (Poly)vinylchloride matrix	43
3.1.1.1. Experimental	43
3.1.1.2. Results and discussion	45
3.1.1.3. Conclusions	52
3.1.2. Sensing with electrodes modified with carbon microparticles and nanofibers	53
3.1.2.1. Results and discussion	53
3.1.2.2. Conclusions	57
3.2. Dopamine detection	57
3.2.1. Experimental	59
3.2.2. Results and discussion	60
3.2.3. Conclusions	67
3.3. References	68

Carbon nanotubes in sensing systems

Application and integration of CNTs to chemical sensors (that do not use biological molecules as receptors) are described in this chapter, and refer to the analysis of NADH and dopamine.

3.1. NADH detection

β -nicotinamide adenine dinucleotide (NADH) is involved as a cofactor in hundreds of enzymatic reactions of NAD^+/NADH -dependent dehydrogenases. The electrochemical oxidation of NADH has thus been the subject of numerous studies related to the development of amperometric biosensors.^{1,2} Problems inherent to anodic detection are the large overvoltage encountered for NADH oxidation at ordinary electrodes³ and surface fouling associated with the accumulation of reaction products.⁴ For these reasons, considerable efforts have been devoted for identifying new electrode materials which reduce the overpotential for NADH oxidation and minimize surface passivation effects⁵ (see figure 3.1).

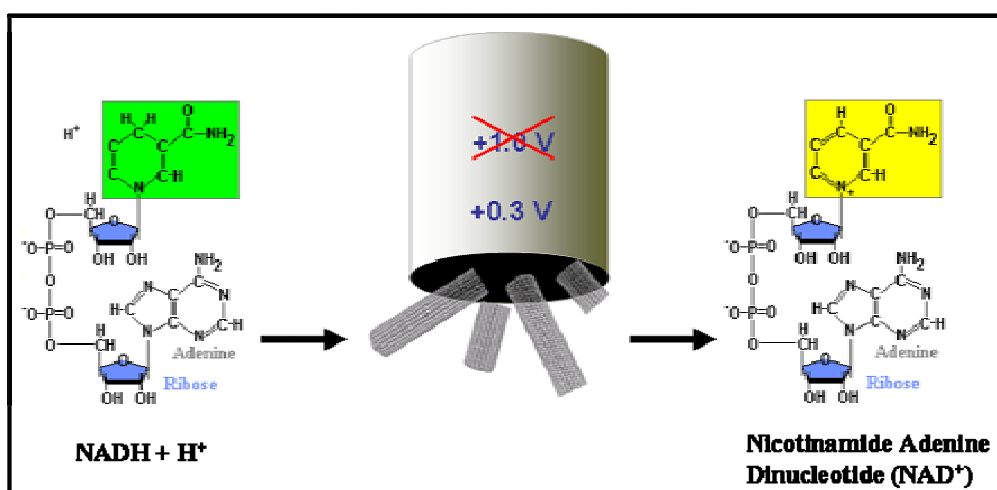


Figure 3.1. Representation of catalytic oxidation of NADH at CNTs modified glassy carbon electrode. Surface casting of a glassy carbon electrode with concentrated sulfuric acid dispersion of CNTs has been performed (see reference 5).

Recent studies have demonstrated that CNTs exhibits strong electrocatalytic activity for a wide range of compounds, such as neurotransmitters⁶, NADH^{5,7}, hydrogen peroxide^{6,9}, ascorbic^{6,10}, and uric acid⁶, cytochrome¹¹, hydrazines¹², hydrogen sulfide¹³, amino acids¹⁴ and DNA.¹⁵ It has been suggested that electrocatalytic properties are originated from the ends of CNTs.⁷

Gorski et al.¹⁶ reported an electrochemical sensing platform based on the integration of redox mediators and CNTs in a polymeric matrix. To demonstrate the concept, a redox mediator, Azure dye (AZU), was covalently attached to polysaccharide chains of chitosan (CHIT) and dispersed with CNTs to form composite films for the amperometric determination of NADH. The incorporation of CNTs into CHIT-AZU matrix facilitated the AZU-mediated electrooxidation of NADH. In particular, CNTs decreased the overpotential for the mediated process by an extra 0.30 V and amplified the NADH current by ca. 35 times (at -0.10 V) while reducing the response time from ca. 70 s for CHIT-AZU to ca. 5 s for CHIT-AZU/CNTs films.

F. Valentini et al.¹⁷ studied the oxidation of NADH at a glassy carbon (GC) electrode modified by electropolymerization of poly(1,2-diaminobenzene) (1,2-DAB) in the presence of CNTs¹⁸. The NADH amperometric response of the conducting nanotubule-modified GC electrode showed a peak at 0.63 V with a sensitivity of 99 nA/mM, and an operational stability of 2 days.

Two alternative sensor designs for NADH detection have been studied and the obtained results are presented in the following sections. Both designs are based in the modification of conventional electrodes. In the first design (section 3.1.1), a (Poly)vinylchloride (PVC) matrix to disperse CNTs so as to ensure a better mechanical/robustness properties of the sensor membrane has been used. Additionally, glutaraldehyde as a matrix linker with great future promises for biosensors applications due to its ability for covalent binding of biological molecules has also been employed. In the second design (section 3.1.2), have used carbon nanofibers (CNF) with the idea of looking at improved properties of CNF modified electrodes for NADH detection. A simple physical adsorption of CNF onto conventional electrodes has been used.

The ability of CNTs to promote the NADH electron-transfer reaction with a great promise for dehydrogenases-based amperometric biosensors will be shown for both cases (for more details see published articles^{19,20}).

3.1.1. Sensing with electrodes modified with CNTs dispersed in a (Poly)vinylchloride matrix

It is well known the use of poly(vinylchloride) (PVC) as an inert matrix for electrochemical sensors. Its application to build membranes for ion-selective electrodes (ISE) has shown several advantages. PVC ensures a well dispersion of ion-recognition sites and at the same time give robustness to the ISE membrane in addition to novel opportunities to be applied in several forms and shapes due to the flexibility of its structure.²¹

The electrochemical study of a glassy carbon (GC) electrode modified with a polymeric matrix based in MWCNTs mixed with tetrahydrofuran (THF), PVC and finally incubated in a glutaraldehyde (GA) solution (MWCNTs+THF+PVC+GA/GC (MWCNTs-TPG/GC)) will be presented in the following sections for NADH detection.

The used CNTs matrix promotes better the electron transfer of NADH minimizing the fouling effect. The obtained results show remarkable electrochemical and mechanical advantages of MWCNTs-TPG/GC electrode compared to bare glassy carbon electrode with a great promise for future amperometric biosensors applications.

3.1.1.1. Experimental

Materials and reagents

Multi-wall carbon nanotubes (CNTs-200: length, 0.5–200 μm ; o.d., 30–50 nm; wall thickness, 12–18 nm; produced by chemical vapor deposition method) were supplied by Aldrich (Stenheim, Germany). The CNTs were purified in HNO_3 to remove impurities such as amorphous carbon, graphite particles, and metal catalysts. Further purification was accomplished by stirring the CNTs in 2 M nitric acid (Panreac, Spain; <http://www.panreac.es>) at 25 $^\circ\text{C}$ for 24 h. NADH reduced form, tetrahydrofuran (THF), poly(vinyl chloride) (PVC), glutaraldehyde (GA) solution (50% aqueous solution), potassium dihydrogenphosphate and potassium hydrogenphosphate were obtained from Sigma. The working solutions (NADH) were prepared daily by dilution in 0.1 M phosphate buffer at pH 7.0 with ultra pure water from a Millipore-MilliQ system.

Instruments

The SEM images were conducted using a Hitachi S-3200N scanning electron microscope (SEM), equipped with secondary electron detector, backscatter electron detector. The samples were placed on an aluminium stub covered with a carbon adhesive tab (Electron Microscopy Sciences). IR measurements were performed with a Fourier Transform Infra-Red (FTIR) spectrophotometer (BRUKER, TENSILE model 27) equipped with an Attenuated Total Reflectance (ATR) experimental configuration (SPECAC, model MKII Golden Gate). The samples (in solid form) were prepared in the same way as in the preparation of the modified electrodes.

Cyclic voltammetry (CV) and chronoamperometry experiments were performed using an electrochemical analyzer Autolab 20 (Eco Chemie, The Netherlands) and an LC-4C amperometric detector (BAS) connected to a personal computer with GPES software.

The measurements were carried out with a typical cell of 10 mL at room temperature (25 °C), using a three electrodes configuration. A platinum and an Ag/AgCl electrodes were used as counter and reference electrode, respectively. Unmodified and modified GC electrodes using a MWCNTs+THF+PVC+GA matrix (MWCNTs-TPG/GC) were used as working electrodes. MWCNTs-TPG/GC electrode was prepared in our laboratory according to the procedure described below. A magnetic stirrer provided the convective transport during the amperometric measurements.

Preparation and modification of GC electrode surface

CNTs were purified prior to use by a 2 M nitric acid solution. The GC electrode (3 mm in diameter, CH Instrument) was first polished with alumina paper (polishing strips 301044-001, Orion, Spain) and then washed with THF and water (5:5 v/v).

A polymeric matrix of MWCNTs+THF+PVC was prepared via dispersing 1.4 mg MWCNTs and 4 mg PVC into a 750 μ L of THF by ultrasonication agitation for about 10 min. The GC electrode was coated with 4 μ L of the MWCNTs+THF+PVC matrix and finally incubated during 30 seconds in a GA solution, washed with few redistilled water and dried at 40 °C for about 30 min obtaining a MWCNTs-TPG film onto the GC electrode surface. After the modification, the surface of the MWCNTs-TPG/GC was washed carefully with double distilled water.

Electrochemical measurements

Cyclic voltammetry (CV) and chronoamperometry studies were performed using an electrochemical analyzer Autolab 20 (Eco Chemie, The Netherlands). A platinum (Pt) wire and an Ag/AgCl electrode were used as counter and reference electrode, respectively, and the MWCNTs-TPG/GC was used as the working electrode. The amperometric responses to NADH were measured in aliquots of 10 mL of a 0.1 M phosphate buffer solution pH 7.0 where various additions of NADH were then applied onto the reaction cell. The applied potential to the working electrode for NADH determination was +0.70 V for MWCNTs-TPG/GC electrode. The background current was allowed to decay to a constant level before aliquots of NADH sample were added to the stirred buffer solution.

3.1.1.2. Results and Discussion

A detailed description of the obtained results is given in the published article¹⁹. In brief, the results are described and discussed in the following sections.

Characterization of MWCNTs dispersed in different systems

Before application into a biosensor system the CNTs must be first modified so as to be transformed to a soluble product. The preparation of homogeneous dispersions of CNTs suitable for processing into thin films or for other applications is of a great importance. Various methods have been used for this purpose. They often indicate cutting the CNTs into smaller pieces (after sonication) or changing the CNTs chemistry (after functionalization), thus partly losing sometimes the electrochemical properties of CNTs. The use of polymers for wrapping of carbon nanotubes²²⁻²⁴ is another simpler alternative.

Tetrahydrofuran and its mixture with poly(vinylchloride) were firstly used to solubilize the MWCNTs. Figure 3.2 (A, B) shows images of the prepared suspensions. While both the above solutions seemed to have a well homogenized distribution a 'flocculate' like aspect was observed in the case of the use of the THF mixed with PVC and a GA solution (see Figure 3.2C). Moreover the above suspension seemed to better adhere onto the electrode surface.

The MWCNTs suspension prepared in the three different mediums were characterized using scanning electron microscopy (SEM), and in addition the above samples were analyzed by using the IR spectroscopy.

Figure 3.2 (lower images) displays the SEM images of MWCNTs in: A) tetrahydrofuran; B) THF mixed with poly(vinylchloride) and C) THF mixed with PVC and a glutaraldehyde solution. The MWCNTs are clearly visualized in the case of THF (see Figure 3.2A). In difference from the previous 3.2A image the MWCNTs in the figure 3.2B are now 'loaded' with small aggregates of the PVC. The PVC seems to be attached onto the MWCNTs ensuring by this way a well homogenization of the whole mixture. Figure 3.2C is the SEM of a similar mixture as 3.2B but in the presence of glutaraldehyde. The comparison of Figure 3.2B with Figure 3.2C reveals (additionally to the upper solution image) that some chemical interactions might have occurred between MWCNTs, PVC and GA. The former, functionalized with carboxylic groups (MWCNTs-COOH), might have formed hydrogen bonds (through OH groups) with both, GA and PVC. The hydrogen bonds formed around the nanotubes (case of THF+PVC+GA) seem to have filled the empty voids between individual carbon nanotubes and PVC, thus achieving a better entrapment of MWCNTs-COOH within the THF+PVC+GA matrix compared to the THF+PVC one.

Furthermore, the surface of the GC electrode modified with THF+PVC+GA mixture seemed to be better covered/modified, ensuring a more compact layer and apparently with a higher retention capacity than the one without GA.



Figure 3.2. Upper part: Images of the MWCNTs in THF (A), THF+PVC (B), and in THF+PVC+GA solution (C). Lower part: SEM images of the same solutions as in the upper images. The same acceleration voltage (15 kV) and resolution are used. Others experimental details as explained in the text.

The results obtained by SEM images are further supported by the corresponding ATR-IR spectra (see Figure 3.3) of GC electrodes modified with MWCNTs-COOH in THF (A), THF mixed with PVC (B), and THF mixed with PVC and a GA solution (C). The appearance of peaks at 1730 cm^{-1} corresponding to C=O stretching of carboxylic groups, and at 3300 cm^{-1} corresponding to stretching of hydroxyl groups (Figure 3.3A) clearly indicates that -COOH groups are present on the surface of MWCNTs. While the IR spectrum of Figure 3.3B shows new signals at 1425, 1330, 1255, 955, and 690 [$\nu(\text{C-Cl})$] cm^{-1} corresponding to the PVC matrix, $\nu(\text{O-H})$ and $\nu(\text{C=O})$ are shown very broadened, absorbing from 2750 down to 2570 cm^{-1} , and around 1650 respectively, both being downshifted compared to their corresponding values in absence of PVC (spectrum 3.3A). This can be associated to MWCNTs-COO-H...Cl(PVC) hydrogen bonding probably promoting the wrapping of carbon nanotubes by the PVC matrix (Figure 3.3B).

The spectrum of Figure 3.3C, closely resembling that of 3.3B, indicates that upon incubation in GA CNTs are still forming CNTs-COO-H...Cl hydrogen bonds with PVC. However, the additional band at 1730 cm^{-1} in 3.3C can be assigned to the presence in the matrix of GA molecules with a free carbonyl group at one end, but with their second carbonyl at the other end involved in CNTs-COO-H...O=C(GA) hydrogen bonding interactions. This would contribute, together with $\nu(\text{C=O})$ of CNTs-COOH (spectrum 3.3B), to the broad and downshifted band around 1650 cm^{-1} in spectrum 3.3C. Therefore, once glutaraldehyde is introduced into the matrix (CNTs+PVC), it seems to compete with PVC for the same OH groups of CNTs but probably without a total displacement of the previously attached PVC. This phenomenon is still unclear and needs further studies but, according to our ATR-IR results, might have likely occurred due to intermolecular hydrogen bonds, as reported in the case of polyethyleneglycol (PEG)/chitosan (CS) where a cross-linked blend is formed.²³

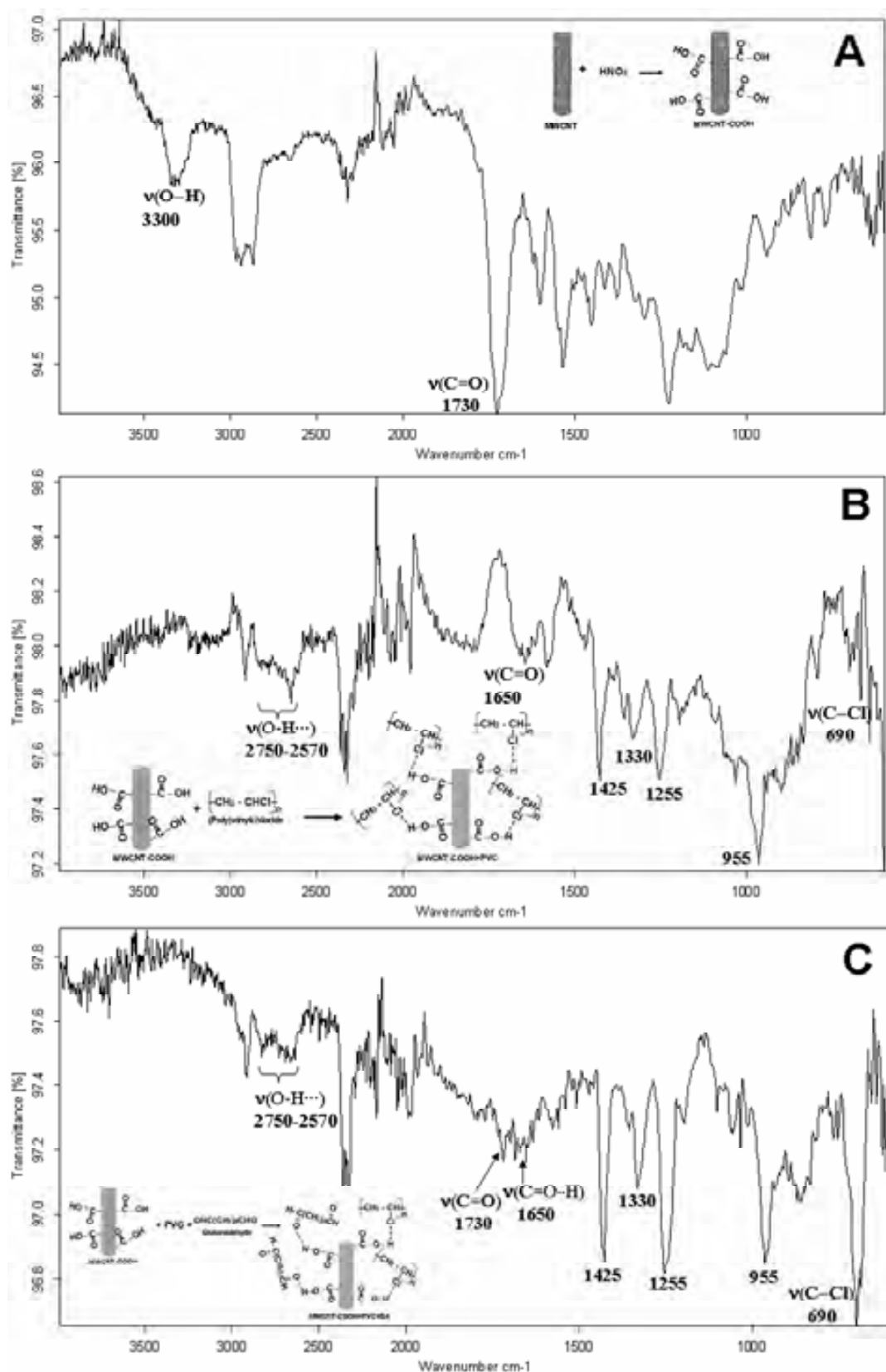


Figure 3.3. ATR-IR spectra of GC electrodes modified with MWCNTs-COOH in THF (A), THF+PVC (B), and of this latter incubated in a glutaraldehyde aqueous solution (C). Inset: Scheme proposed to approach interactions in the system (see text). Absorptions between 2000 and 2400 cm^{-1} correspond to atmospheric CO_2 .

The presence of PVC and GA would of course provoke an opposite effect on the sensor response. Nevertheless, a compromise between the advantages of having a binding matrix (PVC for mechanical / stability improvements and glutaraldehyde for future crosslinking with enzymes) and the risks of blocking of CNTs ends / extremes exists. The results in the coming section will show that part of the CNTs ends should have been still available and probably responsible for the observed improvements.

The composition of the MWCNTs-TPG matrix has been optimized and the values reported (as given in section 3.1.1.1 Preparation and modification of GC electrode surface) have been chosen as a compromise between the CNTs solubility in THF and the corresponding current responses (for more details see published article¹⁹).

Electrochemical behavior

Cyclic voltammetry of NADH at GC electrode

Figure 3.4 shows the CVs of a 0.1 M phosphate buffer pH 7 (blank solution) using a bare (a), a MWCNTs+THF+PVC+GA modified (MWCNTs-TPG) (b), and a MWCNTs+THF+PVC modified (c) GC electrode at 100 mV/s, at room temperature (25 °C), using a three electrode configuration as it is described previously, as well as the corresponding CVs at the unmodified (a'), MWCNTs-TPG modified (b'), and MWCNTs+THF+PVC (c') GC electrode for a 5 mM NADH solution using the same experimental conditions. Irreversible oxidation processes of NADH for the three electrodes are observed. A significant current coming from NADH oxidation at the MWCNTs-TPG/GC starts to be generated at +0.5 V with a peak at around +0.7 V. This represents a negative shift of the oxidation potential of around +0.15 V with respect to bare GC electrode (a'). Moreover a higher current (around 5 μ A higher) for the MWCNTs-TPG modified electrode compared to the bare electrode can be observed.

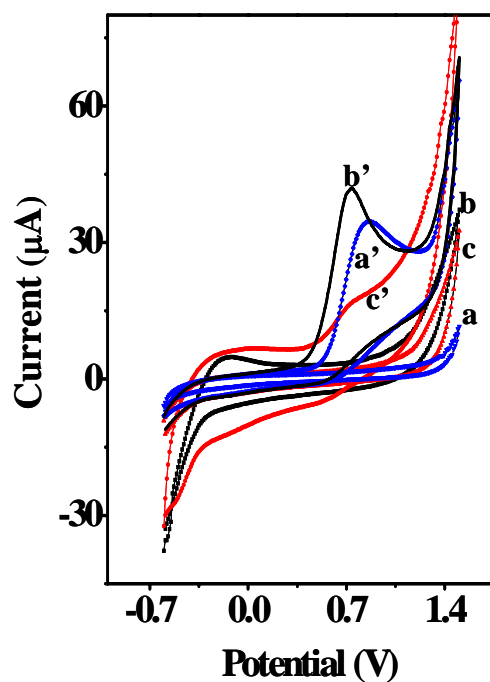


Figure 3.4. Cyclic voltammograms (CV) of 0.1 M phosphate buffer pH 7 using a bare (a) a MWCNTs+THF+PVC+GA modified (b), and a MWCNTs+THF+PVC modified (c) GC electrode. The CV responses (a' for bare, b' and c' for the modified electrodes) toward a 5 mM NADH solution are also shown using the same electrodes. The scan rate was 100 mV/s and potential range from -0.6 to +1.5 V. The composition of the modifying solution was: 1.4 mg MWCNTs, 4.0 mg PVC, 750 mL THF and GA solution. Other experimental details are explained in the text.

Catalytic activity of the MWCNTs-TPG/GC electrode

Evaluate the catalytic activity of the MWCNTs-TPG/GC electrode toward NADH oxidation is of considerable interest. Direct oxidation of NADH is the most common electrochemical approach to NADH detection. However, the electrochemical methods possess some drawbacks due to the high overpotential, interfering side reactions, and electrode fouling. Thus, in the last decade, various strategies have been used to modify electrodes for minimizing these problems.^{25,26} In the case of MWCNTs-TPG/GC, as it was already reported, there is a catalytic effect on the oxidation of NADH, making a higher sensitive detection of this compound compared to the bare GC electrode (for more details see Figure 4 in the published article¹⁹).

Amperometric detection of NADH at modified electrode

The current response toward NADH was studied on the way of two concentrations: for responses to lower NADH concentrations (0.1 mM NADH) at three different potentials: +0.5 V (a), +0.6 V (b), and +0.7 V (c) in 0.1 M phosphate buffer pH 7 (see Figure 5 in the published article¹⁹) and responses to higher NADH concentrations (1.0 mM NADH). In brief, the results are described and discussed only for responses to higher NADH concentrations in the following section:

Responses to higher NADH concentrations

Figure 3.5 shows that MWCNTs-TPG/GC electrode offers substantially higher signal compared to bare electrode using a working potential of +0.70 V. The sensitivity of the modified GC electrode for NADH determination, found to be approximately 2 times larger than for the bare electrode, is clearly visualized.

In the calibration curves (insets) the plots of current vs. NADH concentration have a linear range from 1.0 to 10 mM for both the bare (a) and the modified (b) GC electrode. The correlation coefficients were 0.999 (both a and b) and the corresponding detection limits of 0.088 mM and 0.085 mM, respectively. The corresponding calibration plots show sensitivities of 5 $\mu\text{A mM}^{-1}\text{cm}^{-2}$ for bare electrode and 13 $\mu\text{A mM}^{-1}\text{cm}^{-2}$ for MWCNTs-TPG/GC electrode. In addition, for the MWCNTs-TPG/GC electrode, a set of 3 different amperometric measurements for 1 mM NADH with a single electrode yielded a relative standard deviation of 5%, indicating a good repeatability of the measurements. However, for the unmodified GC electrode the relative standard deviation (RSD) is of 14% which might also be related with a possible fouling of the bare GC electrode.

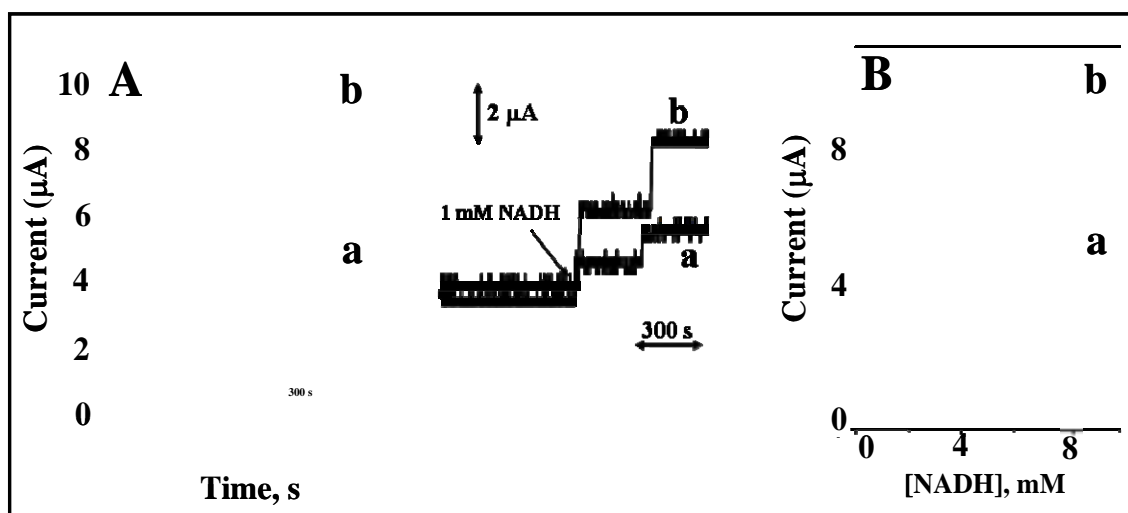


Figure 3.5. Current–time recordings from amperometric experiments (A) and calibration plots obtained for successive additions of 1 mM NADH in 0.1 M phosphate buffer pH 7 (B) and at unmodified (a) and at modified (b) GC electrode. Working potential: +0.7 V. The stability of the response (as zoom of the left recordings) is shown for each electrode used. Experimental conditions as in Figure 3.3.

Stability test

The response stability was checked during each step of the amperometric response of 1 mM NADH at MWCNTs-TPG/GC electrode at operating potential of +0.7 V. The right steps are a zoom of the two current time responses (see Figure 3.5) showing the stability of the MWCNTs-TPG/GC electrode toward NADH over around 20 seconds of response time. It can be observed that the current obviously increases after the addition of NADH maintaining then a steady state response thereafter.

3.1.1.3. Conclusions

This work demonstrates that the modification of GC electrode with a mixture of MWCNTs+PVC+THF+GA represents an interesting alternative for NADH based amperometric biosensors. MWCNTs-TPG/GC electrode shows higher detection sensitivity (approximately 2 times) compared to the bare GC electrode; promotes electronic transference and facilitates the amperometric determination of NADH starting at a potential +0.40 V. In addition, it reports a standard deviation of 5%, indicating a good repeatability of the measurements. The potential shift gained due to the use of a polymeric matrix with MWCNTs will bring advantages providing relatively lower working potentials in future biosensor applications.

This novel MWCNTs/PVC/GA matrix might have future interesting applications in connection to enzyme immobilization by cross-linking and the glutaraldehyde within the matrix. Moreover, this MWCNTs/PVC/GA system may avoid the use of redox mediators that beside their advantages foul the electrode surface. Further, it is quite homogenous, ensures good adhesion onto the GC electrode surface and is simple to be applied.

3.1.2. Sensing with electrodes modified with carbon microparticles and nanofibers

Carbon nanofibers (CNF)²⁰ have been lastly shown to be another attractive form of carbon materials (CM) beside CNTs with interest for electrochemical sensors. In general carbon microparticles (CMPs), CNTs and CNFs have shown significant improvements in the development of novel sensors and biosensors.²⁷⁻³¹ The high-surface area of CMs may also lead to new signal transduction processes^{32,33} and to increased sensitivity in sensing applications.³⁴⁻³⁶ These CMs are used as doping materials for electrochemical sensors.

The efficiency of CNFs and CMPs (employed either before or after acidic treatments) as modifiers of conventional electrodes (glassy carbon (GC) and gold (Au) electrodes) used for NADH detection is also studied and the results will be presented in following sections.

3.1.2.1. Results and discussion

A detailed description of the experimental part including the obtained results related to the application of the different CMs (CMP & CNF) for NADH detection is given in the published article²⁰. In the following section only few of the most important results are summarized.

Electrochemical study of electrode surfaces

The electrochemical properties of the CMs were examined using cyclic voltammetry (CV). The fast and reliable detection of NADH at low potential is particularly important. The electrochemical signal transduction ability of CMs and their possible application in biosensor systems were evaluated by measuring the response of GC and Au electrodes modified with treated and untreated CMPs and CNFs. However in this section the results obtained for only the GC electrodes are shown. Those obtained for Au

electrodes, where the same conditions as for GC electrodes were applied, can be seen in the published article.²⁰

Figure 3.6 shows the cyclic voltammograms of bare GC electrode and GC electrodes modified with untreated (A) and treated (B) CNFs. The same CVs for the GC electrodes modified with untreated (C) and treated (D) CMPs are also shown. A phosphate buffer saline (PBS) pH 7.0 containing 2.5 mM NADH and a scan rate of 100 mVs⁻¹ during a potential range from -0.6 to 1.2 V have been used in all cases. All the CVs clearly show the NADH oxidation peaks comparing to PBS buffer. The peak currents for NADH oxidation are of a similar magnitude for each CM independently of being treated or not.

GC electrodes utilized as substrate for deposition of carbon material films display a significantly different response compared to the gold electrodes (see Figure 4 of published article²⁰). The sensitivity toward NADH oxidation, in the case of electrodes modified with CMPs is higher with GC electrode (see Figure 3.6C and D) than with Au electrode (see Figure 4C and D of published article²⁰) (note the differences in scale). Higher electrochemical responses, in both electrodes (GC and Au), have been observed for modifications using CNFs. The peak current (84.69 μ A at +0.352 V) for the NADH oxidation for modified GC with untreated CNF was shifted with a $\Delta E = +0.393$ V respect to bare GC electrode.

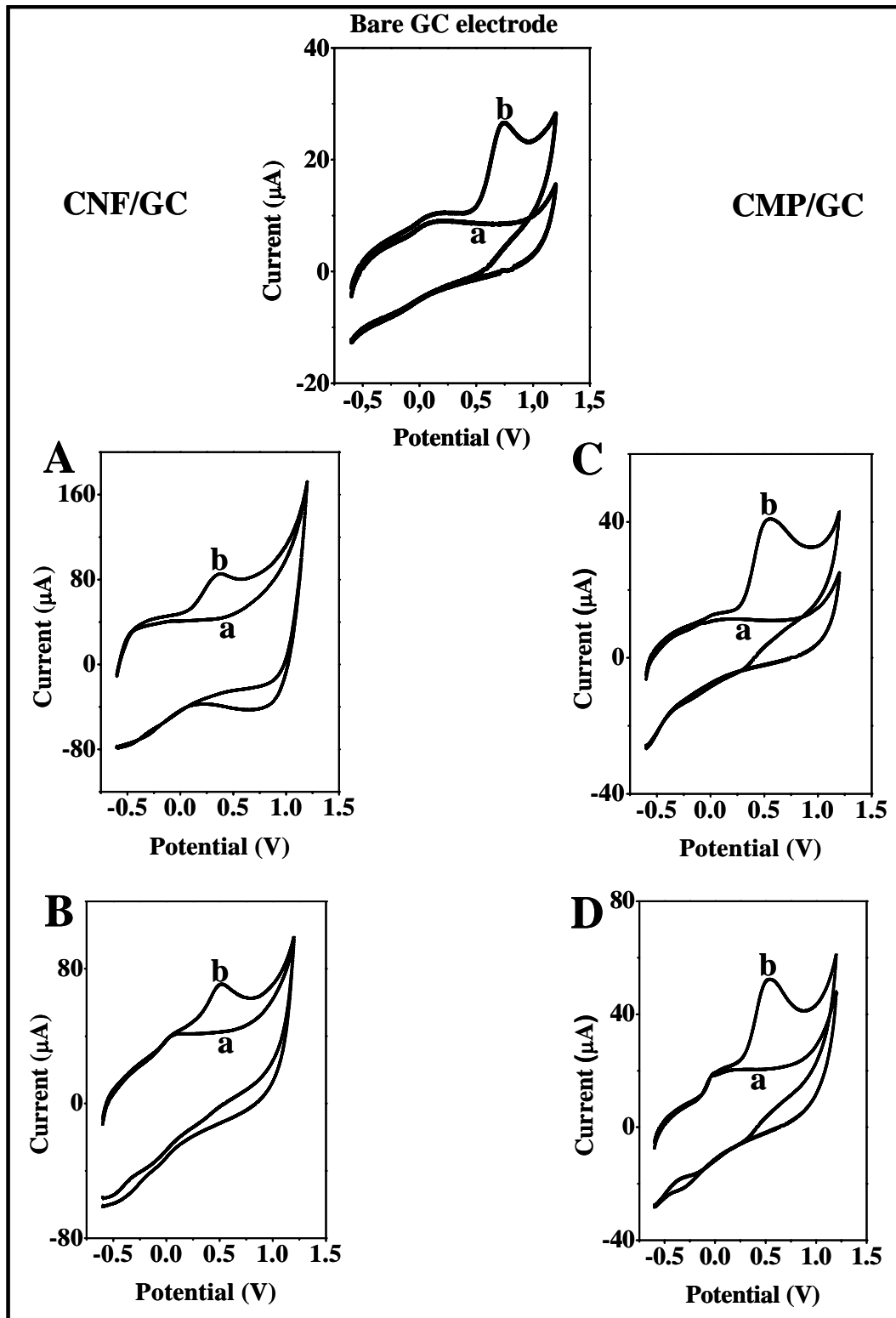


Figure 3.6. Cyclic voltammograms (CV) for a 0.1M phosphate buffer pH 7 (a) using: a bare GC electrode (upper CVs) and GC electrodes modified with untreated CNFs (A), treated CNFs (B), untreated CMPs (C), and treated (D) CMPs. The CV responses toward a 2.5 mM NADH solution (b) (at the same pH) are also shown using the same electrodes. The scan rate was 100 mV/s and potential range from -0.6 to 1.2 V. The composition of the modifying solution for all the cases was 0.7 mg carbon material and 700 μ L DMF, respectively. Other experimental details as explained in the text.

Comparing both electrodes used (Au and GC), the sensitivity based on the current observed increases from untreated to treated CMPs and from treated to untreated CNFs (Figure 4 (see published article²⁰) and Figure 3.6). From the obtained results, it can be concluded that the modifications with CNF brings to the electrodes higher sensitivity to the oxidation of NADH and therefore the electrochemical properties are more favorable comparing to modifications with CMPs.

Table 3.1 summarizes all the values (potential and currents) discussed previously for each electrode and the corresponding modifications. The shown differences can be attributed to the different structural forms of the carbon materials used. Carbon nanofibers (see Figure 3 in published article²⁰) provide a very high-surface area and, consequently, a very high number of binding sites for NADH. This high density of binding sites may increase sensitivity in the same manner as in porous materials.³⁷ Generally, electron transfer may be easier at samples containing a higher proportion of binding sites, producing a faster electron transfer.

The principal reasons for different “electrocatalytic” properties of carbon materials on different substrates toward different analytes are still unclear and are under investigation. A possible explanation of such effects is the different contact resistances of carbon materials (CMPs and CNFs) with the GC and Au electrode surfaces.³⁸

Table 3.1. Summary of responses toward a solution of NADH 2.5 mM at 0.1M phosphate buffer pH 7 obtained by two different electrode transducers (GC and Au) modified with carbon nanofibers (CNFs)+dimethylformamide (DMF) and graphite+DMF.

Transducer Modifier		Glassy carbon (GC)			Gold (Au)		
		I _p (μ A)	E _o (V)	Δ E (V)	I _p (μ A)	E _o (V)	Δ E (V)
Graphite	untreated	40.91	0.538	0.207	18.21	0.517	0.186
	treated	52.42	0.535	0.210	21.04	0.505	0.198
Carbon nanofibers	untreated	84.69	0.352	0.393	83.32	0.349	0.353
	treated	71.28	0.505	0.240	25.58	0.520	0.183

I_p: the peak of the NADH oxidation current; E_o: NADH oxidation potential; Δ E: shift of the oxidation potentials between bare and modified electrodes.

3.1.2.2. Conclusions

CNFs modifications show in most of the cases (except treated CNF at Au electrode) lower overpotentials and higher oxidation currents for the detection of NADH comparing to modifications performed with CMPs. The shown ability of untreated CNF to promote the electron transfer between NADH and the electrode surface suggest an attractive electrocatalytic nanomaterial for development of new amperometric biosensors. In addition to the attractive electrocatalytic properties the solubility of CNF in DMF better facilitates its manipulation for future biosensing applications.

A detailed evaluation between CNF and CNTs based modifications that will take into consideration the formed carboxylic groups in both nanomaterials, between other differences (as possible responsible of catalytic effect) will be object of another work in the future. This comparison will also help to explain better the electrocatalytic effect of CNTs itself which has been the focus of our work.

3.2. Dopamine detection

Since its discovery in the 1950s, dopamine (DA) has been of interest to neuroscientists and chemists as an important neurotransmitter in the mammalian central nervous system.³⁹ It can cause Parkinson's disease and other similar diseases. Thus, various commonly usable analytical methods for dopamine and its analogs have been developed in the past. Some examples of these methods are the rapid liquid chromatography/tandem mass spectrometry (LC-MS/MS), the chromatography method and the capillary electrophoresis mass spectrometry. Although all these methods are very sensitive they require sophisticated and temperature control systems for separation followed by spectrophotometric or electric detection systems. Recently, there has been an increasing demand for more sensitive and simpler analytical methods. Square-wave voltammetry techniques are very useful and popular for trace analysis since these techniques are compact, efficient, and sensitive.⁴⁰ Various voltammetry techniques, depending on the working electrode material, have been found to have a low detection limit required for neurotransmitter DA analysis. Wu and Hu⁴¹ studied the electrochemical behaviour for DA by using a glassy carbon electrode (GCE) modified with a homogeneous and stable suspension of MWCNTs with Nafion. MWCNTs-

Nafion modified GCE not only improves the redox peak currents but also makes the redox reaction of DA more reversible.⁴²

The combination of CNTs electrocatalytic activity with the known advantages of other compounds seems to be a very important alternative for new electroanalytical challenges. Molecules as cyclodextrin (CD) are used to stabilize, dissolve, retain and liberate in a controlled way a large number of organic or inorganic chemicals through the formation of inclusion complexes. Moreover, CD has been studied with different compounds as recognition agent and to study the adsorption phenomena related to electrode interactions.

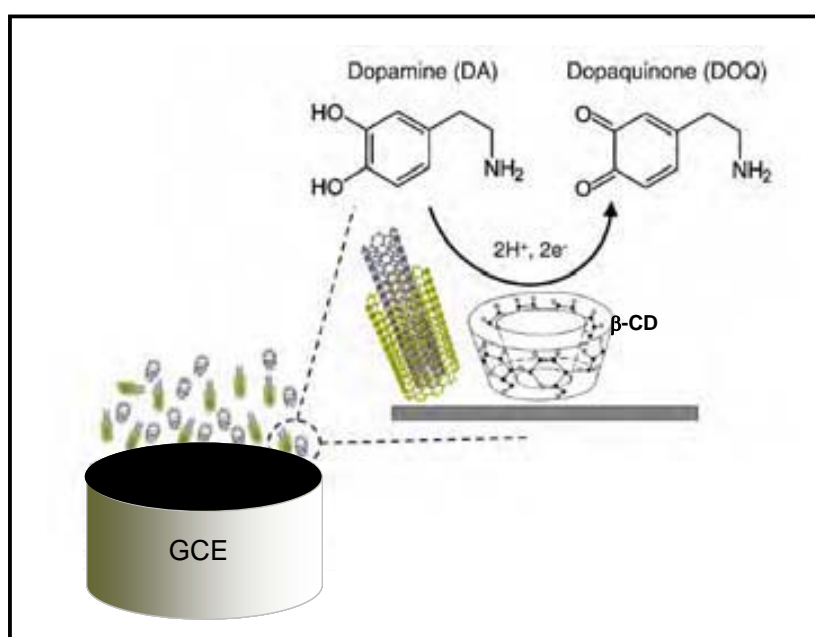


Figure 3.7. Schematic (not in scale) of the electrochemical sensor modified with the MWCNTs/ β -CD matrix. The dopamine oxidation reaction is also shown.

Taking into consideration the electrochemical properties of CNTs as well as the reported properties of CD, a novel strategy for DA detection, based on the simultaneous modification of a glassy carbon electrode with a novel MWCNTs/ β -CD matrix (see schematic representation in Figure 3.7), will be described in the following sections. The chemical recognition of DA by the use of CD is combined with the added advantage of a faster electron transfer process due to the CNTs present at the electrode interface. In this study the DA oxidation in the surface of the electrode is enhanced by its diffusion through the CD cavities and the easy contact with the dispersed MWCNTs that facilitate the electron transfer. The operability of this system is compared with the DA detection

using glassy carbon electrode without modifications so as to verify the contribution of CD and MWCNTs in the electrochemical detection (for more details see published article⁴³).

3.2.1. Experimental

Reagents

All reagents were of analytical grade: the dopamine (DA) and β -cyclodextrin (β -CD) used were from Sigma, while the KH_2PO_4 and K_2HPO_4 were from Fluka. The multi-wall carbon nanotubes (MWCNTs) (0.5–200 μm) were from Aldrich (Stenheim, Germany) and contains 95% MWCNTs. All solutions were prepared with deionized water type 1 with 18.2 MX resistivity, free from organic matter, obtained from a US Filter PURE-LAB Plus UV, deaerated with nitrogen and freshly prepared prior to each determination.

Equipment

The electrochemical studies were carried out using a conventional three-electrode cell with Pt as counter electrode and Ag/AgCl as reference. Glassy carbon electrodes (GCE) (from CH Instrument, Texas, USA) modified or not with MWCNTs-CD were used as working electrodes. All electrochemical measurements, such as cyclic voltammetry and amperometry were carried out with the aid of an electrochemical analyzer Autolab 20 and a PC for experimental parameter control and data acquisition. All measurements were conducted under the presence of a nitrogen atmosphere at a 25 ± 1 °C temperature. The scanning electronic microscopy images from the MWCNTs-CD films were obtained with the aid of a Hitachi S-3200N SEM.

Electrode modification with MWCNTs- β -CD film

In order to eliminate metal impurities the carbon nanotubes were dispersed in 2 M nitric acid solution during 24 h at 25 °C, and washed afterwards with deionized water to neutrality and finally dried in accordance with the procedure described in the reference 29.

The MWCNTs were checked by scanning electron microscopy JEOL JSM-6300 (SEM, JEOL LTD, Tokyo, Japan) with microanalysis equipped by an X-ray energy

dispersive spectrometer (EDS) (Link ISIS-200, England) in order to evaluate the amount of impurities (remained from their synthesis) before and after washings with HNO₃.

A quantity of 1mg of MWCNTs was ultrasound-dissolved then in 1mL of β -CD at 10%. Ten microliters of this solution were introduced over the GCE, the surface of which have been previously prepared by applying the polishing procedures recommended (CH Instrument, Texas, USA). The electrode was left during 30 min to be dried at 60 °C and after that washed carefully with small portion of deionized water before used. The modified electrode was kept at room temperature when it was not used.

3.2.2. Results and discussion

A detailed description of the obtained results is given in the published article⁴³. In brief, the results are described and discussed in the following sections:

Purification of MWCNTs

The study by SEM and the corresponding microanalysis show that the traces of iron (Fe), nickel (Ni) and potassium (K) from 0.5%, 1.6% and 1.5% were decreased to 0.1%, 0.9% and 0.4% after treatment with nitric acid as described in section 3.2.1 Electrode modification with MWCNTs- β -CD film.

Characterization of materials by SEM

Figure 3.8 shows the SEM images of MWCNTs, β -CD and MWCNTs/ β -CD deposited over an aluminium stub covered with a carbon adhesive tab (Electron Microscopy Sciences). It is possible to observe the tube morphology of MWCNTs (A) and the small sheets/layers of β -CD (B). The MWCNTs/ β -CD agglomerates (C) is also shown. The β -CD sheets, not observed now, should have been covered by CNTs due to electrostatic interactions.³⁹

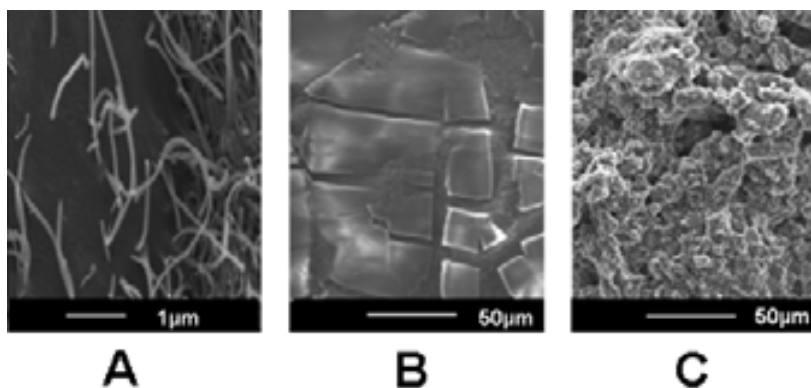


Figure 3.8. SEM images of A) MWCNTs, B) β -CD and C) MWCNTs/ β -CD.

The immobilization capability of CNTs is combined with the β -CD adsorption property, a well known phenomena occurring onto carbon.⁴⁴ Additionally, the host-guest interaction ability of CD is combined now with its facility to disperse MWCNTs that additionally enhance the electrochemical detection of DA.

The DA oxidation in the surface of the electrode is enhanced by its diffusion through the β -CD cavities and easy contact with the dispersed MWCNTs that facilitate the electron transfer. Its electrochemical behavior was evaluated by measuring the response of GC electrode surface modified with CNTs and β -cyclodextrin film (GCE/MWCNTs/ β -CD). These results were compared with those obtained by unmodified GCE (detailed results given at the published article⁴³) using the same conditions. In the following sections the results will be shown only for GCE/MWCNTs/ β -CD.

Voltammetric behaviour and pH effect

Figure 3.9 (A&B) shows the voltammograms recorded for 0.1 mM DA in phosphate buffer at pH values of 3.4 and 7.4, respectively, using a potential scan rate of $0.1 \text{ V}\cdot\text{s}^{-1}$. The potential differences between E_{pa} and E_{pc} , for the GCE/MWCNTs/ β -CD are $\Delta E_{\text{p}} = 83\text{mV}$ at pH 3.4 and $\Delta E_{\text{p}} = 63\text{mV}$ at pH 7.4. This means that the MWCNTs/ β -CD surface film deposited onto the GCE electrode surface increases the electron transfer process compared to the bare GCE. The ratio of the currents was $I_{\text{a}}/I_{\text{c}} = 0.75$ and 1 at pH 3.4 and pH 7.4, respectively. Furthermore, it is relevant to underline that the current increases 10 times as compared to GCE (see Figure 3 at published article⁴³) and that the behaviour as a function of pH appeared to be maintained; that is, in pH 7.4 the E_{pa} value appears at more negative potentials. The significant increase of the current for the GCE/MWCNTs/ β -CD compared to the bare GCE is probably due to the increase of the electrostatic interaction between DA and CD modified electrode. Nevertheless the current increase might also be caused by the electron transfer enhancement due to the presence of MWCNTs to the surface of which might be adsorbed the CD by Van der Waals forces.⁴⁵

A drastic enhancement of the voltammetric background current at the GCE/MWCNTs/ β -CD (see Figure 3.9) compared to the GCE (see Figure 3 in the published article⁴³) was also observed. This large background current should be caused

by the complex impedance of the modified electrode/electrolyte interface compared to the non-modified electrode.

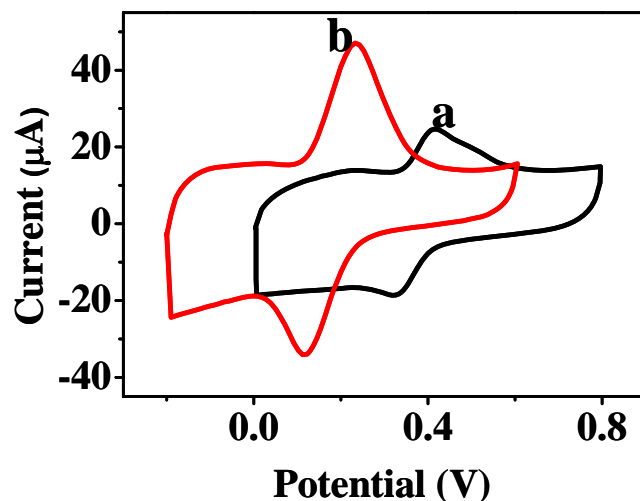


Figure 3.9. Cyclic voltammograms (CV) of 0.1 mM DA at (a) pH 3.4 and (b) pH 7.4, in 0.01 M phosphate buffer with a potential scan rate of $0.1 \text{ V}\cdot\text{s}^{-1}$. Working electrode: GCE/MWCNTs/ β -CD.

Table 3.2. Values obtained for the anodic (E_{pa}) and cathodic (E_{pc}) peak potentials, the anodic peak current (I_{pa}) and the potential difference between the anodic and cathodic peaks (ΔE), using cyclic voltammetry of the 0.1mM DA solution at pH 3.4 and pH 7.4 in 0.01M phosphate buffer, with GCE/MWCNTs/ β -CD.

pH	Working electrode	E_{pa}/mV	E_{pc}/mV	$\Delta E/\text{mV}$	$I_{pa}/\mu\text{A}$	I_{pc}/I_{pa}
3.4	GCE	495.0	233.0	262.0	3.5	0.98
	GCE/MWCNTs/ β -CD	417.0	336.0	83.0	15.7	0.75
7.4	GCE	253.0	102.0	151.0	8.6	0.78
	GCE/MWCNTs/ β -CD	185.0	122.0	63.0	17.5	0.54

Effect of the scan rate

Figure 3.10 shows the DA voltammograms for GCE/MWCNTs/ β -CD at different scan rates at pH 3.4 (see Figure 3.10A) and 7.4 (see Figure 3.10B), respectively; the E_{pa} and E_{pc} values change slightly while the scan rate increase. When the rate increased 10 times, the ΔE values for pH 3.4 and 7.4 were 60 mV and 90 mV and the current ratios between the peaks were 0.7 and 0.4, respectively. These results demonstrate that the oxidation process of DA at the GCE/MWCNTs/ β -CD can be considered quasi-reversible.

The peak current increased linearly with the scan rate's root and the corresponding linear equation is $i(\mu\text{A}) = 8.623v^{1/2} + 0.354$ with a linear correlation coefficient of 0.997 at pH 3.4. In the case of pH 7.4 the corresponding linear equation is $i(\mu\text{A}) = 6.95v^{1/2} + 8.315$ with a linear correlation coefficient of 0.995. Therefore, the oxidation process of DA at the GCE/MWCNTs/ β -CD is diffusion controlled in both values of pH.

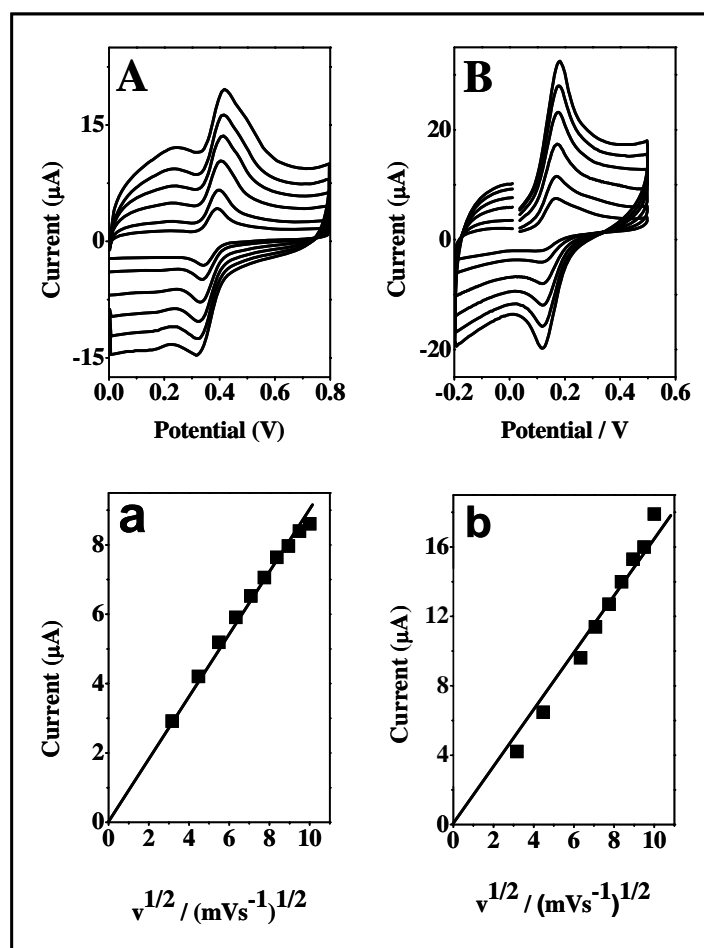


Figure 3.10. Cyclic voltammograms of DA 0.1mM in 0.01 M phosphate buffer at (A) pH 3.4 and (B) pH 7.4, at different potential scan rates: 0.01, 0.02, 0.04, 0.06, 0.08, 0.09 and 0.1 $\text{V}\cdot\text{s}^{-1}$. Corresponding calibration plots of anodic current as a function of scan rate at (a) pH 3.4 and (b) pH 7.4. Working electrode: GCE/MWCNTs- β -CD.

Hydrodynamic voltammetry was carried out to enable selection of the working potentials for the amperometric detection of DA. Figure 3.11 shows the current values attained when the potential is varied from -0.2 V to 0.6 V. The curves obtained show that the GCE/MWCNTs/ β -CD responds to DA's oxidation at potentials higher than 0.2 V when the pH is 7.4, whereas at pH 3.4 oxidation occurs at potentials higher than 0.3 V while the current signal increases rapidly between 0.1 and 0.2 V. Further, it is shown

that the response with GCE/MWCNTs/ β -CD is greater at pH 7.4 compared to that observed at pH 3.4; this allows the amperometric determination of dopamine at lower potentials. These potentials are consistent with those obtained via CV. Therefore, the working potentials to be applied for the detection of DA should be 0.5 and 0.3 V for pH 3.4 and 7.4, respectively, lower in the case of pH 3.4 compared to the bare GCE (for more details see the published article⁴³).

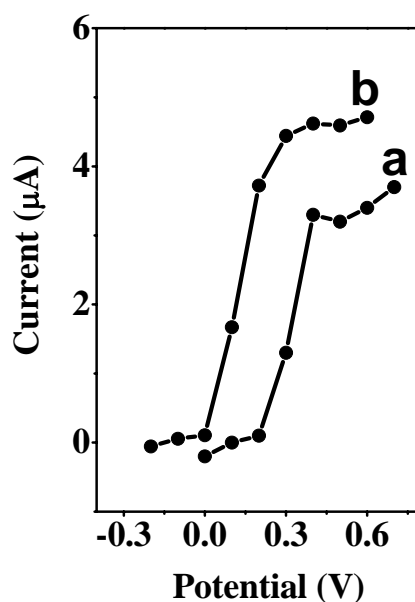


Figure 3.11. Hydrodynamic voltammograms of 0.1 mM DA with GCE/MWCNTs- β -CD at (a) pH 3.4 and (b) pH 7.4 in 0.1 mM phosphate buffer.

Amperometric detection of DA using the GCE/MWCNTs/ β -CD

The amperometric responses to DA obtained with the GCE/MWCNTs/ β -CD for pH 7.4 and 3.4 are compared in Figure 3.12; the current response shows that the oxidation current (I_{pa}) at pH 3.4 is directly proportional to the DA concentration within the range from 0.02 to 0.1 mM. The linear equation describing the behaviour is $j(\mu\text{A}/\text{cm}^2) = 117.91[\text{DA}] + 2529$, with a correlation coefficient of 0.995. At pH 7.4 the current response for the oxidation (I_{pa}) of DA is directly proportional for a concentration range from 0.01 to 0.08 mM. The linear equation describing this behaviour is $j(\mu\text{A}/\text{cm}^2) = 116.63[\text{DA}] + 0.8024$, with a correlation coefficient (r^2) of 0.990. However, in the concentration range below 0.03 mM, the linear correlation coefficient improves attaining the value of 0.999. The linear equation describing the behaviour is $j(\mu\text{A}/\text{cm}^2) = 145.25[\text{DA}] + 0.3546$, for pH 7.4 that means that the sensibility of the

GCE/MWCNTs/ β -CD is better at pH 7.4 (see Table 3.3 for comparison data with the bare GCE (for more details see published article⁴³)).

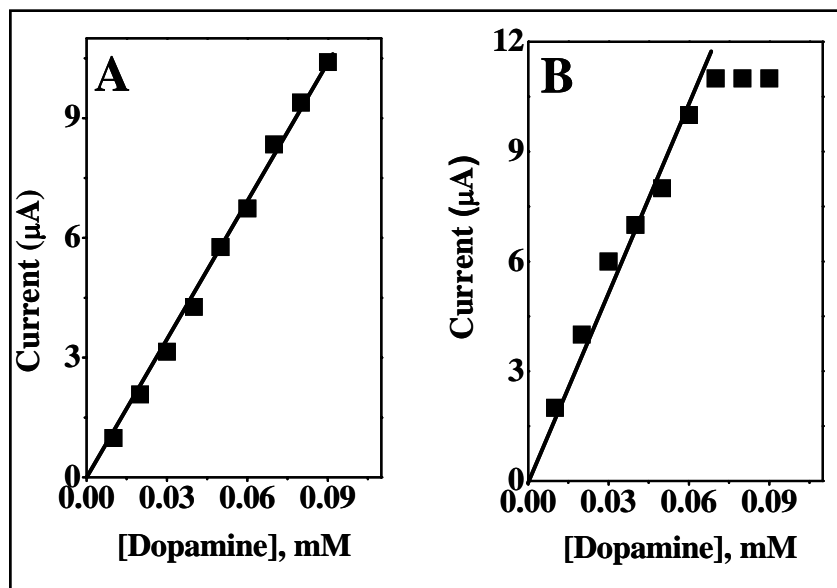


Figure 3.12. Amperometric calibration plots obtained with GCE/MWCNTs/ β -CD at (A) pH 3.4 and 0.5 V as working potential and (B) pH 7.4 and 0.3 V as working potential for successive additions of 0.01 mM DA, in 0.01 M phosphate buffer.

Table 3.3. Parameters obtained from the amperometric detection in 0.1mM DA at pH 3.4 and pH 7.4 in 0.01M phosphate buffer, using CV with the electrodes: GCE, GCE/MWCNTs/ β -CD.

pH	E_{pa} (mV)	Working electrode	Sensitivity (μ A/mM)	r^2	Concentration range (μ M)	Detection limit (μ M)
3.4	500	GCE	35.14	0.993	0-40	—
		GCE/MWCNTs/ β -CD	117.91	0.995	20-100	—
7.4	300	GCE	22.2	0.915	0-40	25
		GCE/MWCNTs/ β -CD	116.63 145.25	0.990 0.999	0-80 0-30	6.7

Selectivity in dopamine sensing

The analysis of DA is normally affected by the presence of other electroactive species especially ascorbic acid (AA) present in physiological fluid. Therefore we investigated

the DA sensing in the presence of AA. The study of AA interference was performed by using the non-modified GCE as well as the MWCNTs/ β -CD/GCE.

Cyclic voltammograms of a 0.1 mM DA, 0.8 mM AA and 0.8 mM DA + AA (1:8) solutions were performed first by using a GCE without any modification. The results obtained are shown at Figure 3.13. The oxidation peak potential (E_{pa}) of the 0.8 mM AA appears at $E_{pa} = 504$ mV while for 0.1 mM DA the $E_{pa} = 273$ mV. The CV of DA in the presence of AA at a molar ratio AA/DA of 8:1 shows a unique peak at $E_{pa} = 431$ mV. The results obtained show that the presence of AA makes DA detection impossible, using a non-modified GC electrode.

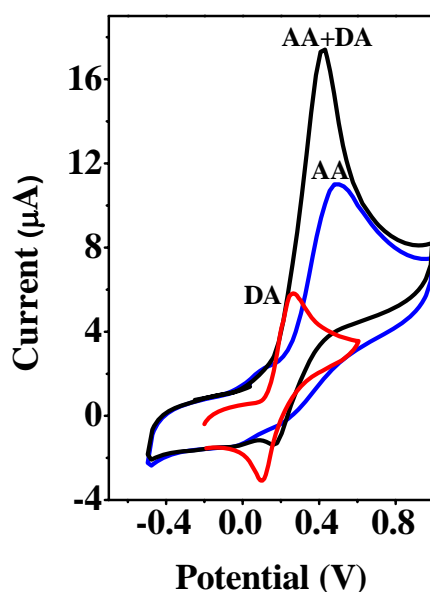


Figure 3.13. Cyclic voltammograms of DA (0.1 mM), AA (0.8 mM) and a mixture of DA + AA solutions at concentration of 0.8 mM (1:8) in PBS 0.01 M and pH 7.4 using a GCE without modification.

The detection of DA in the presence of AA 0.8 mM pH 7.4 was analyzed by CV (see Figure 3.14A), the signal located around 0.1 V is the corresponding to ascorbic acid, the signal of the dopamine is observed at a potential of 0.3 V, the height and amplitude of the peak corresponding to DA increases proportionally with the concentration.

Figure 3.14B shows the behaviour of the current peak vs. concentration of DA. It is possible to observe that the response is proportional to the DA concentration in the interval of concentration of 0–0.5 mM, the linear equation in this interval of concentration is $i(\mu\text{A}) = 451.29[\text{DA}] + 0.53$ the coefficient of linear correlation is of 0.992.

The limit of detection (LOD) for the MWCNTs/ β -CD modified electrode is 37 μ M DA (calculated as the 3σ from the calibration curve obtained by plotting the DA oxidation peak at the concentration range from 0 to 0.5 mM in the presence of AA).

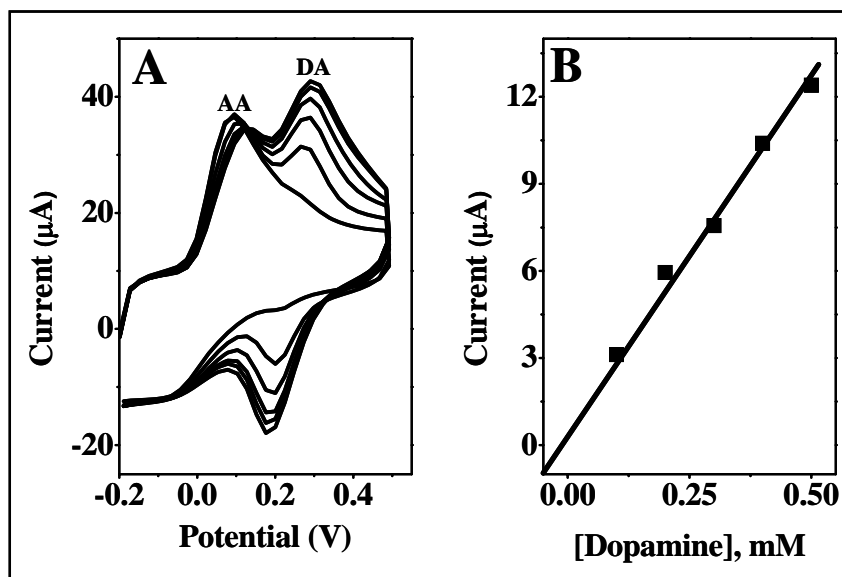


Figure 3.14. (A) Cyclic voltammetry of AA 0.8 mM and CVs obtained after 10 consecutive additions of a 0.01 mM DA solution, (B) calibration plot for successive additions of 0.01mM DA in 0.01 M phosphate buffer. Working electrode: GCE/MWCNTs/ β -CD.

3.2.3. Conclusions

A novel strategy to selectively detect dopamine (DA) using a doubly-modified glassy carbon electrode (GCE) using β -cyclodextrin (β -CD) as molecular receptor and multi-wall carbon nanotubes (MWCNTs) as enhancer of electron transfer is presented.

The guest DA molecule inside the immobilized β -CD host acts as a mediator that ensures a better electrical contact between the GCE and the bulk DA solution. Moreover, the MWCNTs adjacent to the β -CD enhance the electron transfer improving the overall electrochemical response of the DA detection system.

The proposed β -CD/MWCNTs/GCE increases the rate of electron transfer of dopamine that is corroborated by the oxidation potential shift toward more negative potentials and the fact that the DA redox process is more reversible. The DA response improves comparing to other reported systems. The developed matrix, which is applied as a modified electrode improves also the selectivity toward AA. The response of the developed system toward DA in the presence of higher concentrations of ascorbic acid shows no alterations.

3.3. References

- ¹ M.J. Lobo, A.J. Miranda and P. Tunon, *Electroanalysis*, 1997, **9**, 191.
- ² L. Gorton and E. Dominguez, *Rev. Mol. Biotechnol.*, 2002, **82**, 371.
- ³ W. Blaedel and R. Jenkins, *Anal. Chem.*, 1975, **47**, 1337.
- ⁴ J. Wang, L. Angnes and T. Martinez, *Bioelectrochem. Bioenerg.*, 1992, **29**, 215.
- ⁵ M. Musameh, J. Wang, A. Merkoci and Y. Lin, *Electrochem. Commun.*, 2002, **4**, 746.
- ⁶ H. Luo, Z. Shi, N. Li, Z. Gu and Q. Zhuang, *Anal. Chem.*, 2001, **73**, 915.
- ⁷ R.R. Moore, C.E. Banks and R.G. Compton, *Anal. Chem.*, 2004, **76**, 2677.
- ⁸ J. Wang and M. Musameh, *Anal. Chem.*, 2003, **75**, 2075.
- ⁹ S. Hrapovic, Y. Lui, K.B. Male and J.H. Luong, *Anal. Chem.*, 2004, **76**, 1083.
- ¹⁰ Z.H. Wang, J. Liu, Q.L. Liang, T.M. Wang and G.Luo, *Analyst*, 2002, **127**, 653.
- ¹¹ J. Wang, M. Li, Z. Shi and N. Li, *Anal. Chem.*, 2002, **74**, 1993.
- ¹² Y. Zhao, W.D. Zhang, H. Chen and Q.M. Luo, *Talanta*, 2002, **58**, 529.
- ¹³ N. Lawrence, R.P. Deo and J.Wang, *Anal. Chim. Acta*, 2004, **517**, 131.
- ¹⁴ J.X. Wang, M.X. Li, Z.J. Shi, N.Q.Li and Z.N. Gu, *Electroanalysis*, 2004, **16**, 140.
- ¹⁵ M.L. Pedano and G.A. Rivas, *Electrochem. Commun.*, 2004, **6**, 10.
- ¹⁶ M. Zhang and W. Gorski, *Anal. Chem.*, 2005, **77**, 3960.
- ¹⁷ F. Valentini, A. Salis, A. Curulli and G. Palleschi, *Anal. Chem.*, 2004, **76**, 3244.
- ¹⁸ M. Badea, A. Curulli and G. Palleschi, *Biosens. Bioelectron.*, 2003, **18**, 689.
- ¹⁹ B. Pérez, J. Sola, S. Alegret and A. Merkoçi, *Electroanalysis*, 2008, **20**, 603.
- ²⁰ B. Pérez, M. del Valle, S. Alegret and A. Merkoçi, *Talanta*, 2007, **74**, 398.
- ²¹ S. Alegret and A. Merkoçi (Eds), *Electrochemical Sensor Analysis*, 2007, **49**, Comprehensive Analytical Chemistry, Elsevier B.V.
- ²² A. Star, J.F. Stoddart, D. Steuerman, M. Diehl, A. Boukai, E.W. Wong, X. Yang, S.W. Chung, H. Choi and J.R. Heath, *Angew. Chem. Int. Ed.*, 2001, **40**, 1721.
- ²³ W.H. Jiang and S.J. Han, *J. Polym. Sci., Part B: Polym. Phys.*, 1998, **36**, 1275.

- ²⁴ M. In het Panhuis and V.N. Paunov, *Chem. Commun.*, 2005, 1726.
- ²⁵ C.X. Cai, X. Ju and H.Y. Chen, *Anal. Chim. Acta*, 1995, **310**, 145.
- ²⁶ L. Gorton, G. Bremle, E. Csöregi, G. Jönsson-Pettersson and B. Persson, *Anal. Chim. Acta*, 1991, **249**, 43.
- ²⁷ Ü.A. Kirgoz, S. Timur, D. Odaci, B. Pérez, S. Alegret and A. Merkoçi, *Electroanalysis*, 2007, 19, 893.
- ²⁸ S. Alegret, A. Merkoçi, M.I. Pividori and M. del Valle, Chapter Encyclopedia of Sensors, in: A.G. Craig, C.D. Elizabeth, V.P. Michael (Eds.), The Pennsylvania State University, University Park. USA. Forwarded by Prof. R.A. Marcus, Nobel Prize Laureate, 2006, **3**, 23. <http://www.aspbs.com/eos/>.
- ²⁹ B. Pérez, M. Pumera, M. del Valle, A. Merkoçi and S. Alegret, *J. Nanosci. Nanotechnol.*, 2005, **5**, 1694.
- ³⁰ S. Alegret, A. Merkoçi and S. Alegret (Eds.), *Integrated Analytical Systems*, Elsevier, Amsterdam, 2003, 377, ISBN: 0-444-51037-0 (NL).
- ³¹ A. Merkoçi, M. Pumera, X. Llopis, B. Pérez, M. del Valle and S. Alegret, *Trends Anal. Chem.*, 2005, **24**, 826.
- ³² K.-P.S. Dancil, D.P. Greiner and M.J. Sailor, *J. Am. Chem. Soc.*, 1999, **121**, 7925.
- ³³ J.M. Buriak, *Chem. Commun.*, 1999, 1051.
- ³⁴ L.A. DeLouise and B.L. Miller, *Anal. Chem.*, 2004, **76** (23), 6915.
- ³⁵ J. Wang, Q. Chen, C.L. Renschler and C. White, *Anal. Chem.*, 1994, **66**, 1988.
- ³⁶ C. Lei, Y. Shin, J. Liu and E. Ackerman, *J. Am. Chem. Soc.*, 2002, **124**, 11242.
- ³⁷ S.E. Baker, K.-Y. Tse, E. Hindin, B.M. Nichols, T.L. Clare and R.J. Hamers, *Chem. Mater.* 2005, **17**, 4971.
- ³⁸ M. Pumera, A. Merkoçi and S. Alegret, *Electrophoresis*, 2007, **28**, 1274.
- ³⁹ D.R. Shankaran, K. Iimura and T. Kato, *Sensor. Actuat. B-Chem.*, 2003, **94**, 73.
- ⁴⁰ S.Y. Ly, *Bioelectrochem.*, 2005, **68**, 232.
- ⁴¹ K. Wu and S.Hu, *Microchim. Acta*, 2004, **144**(1–3), 131.
- ⁴² P.J. Britto, K.S.V. Santhanam and P.M. Ajayan, *Bioelectrochem. Bioeng.*, 1996, **41**(1), 121.

⁴³ G. Alarcón-Angeles, B. Pérez-López, M. Palomar-Pardave, M.T. Ramírez-Silva, S. Alegret and A. Merkoçi, *Carbon*, 2008, **46**, 898.

⁴⁴ I. Abe, T. Fukuhara, N. Kawasaki, M. Hitomi and Y. Kera, *J. Colloid Interface Sci.* 2000, **229**, 615.

⁴⁵ G. Chambers, C. Carroll, G.F. Farrell, A.B. Dalton, M. McNamara, M. In het Panhuis and H. J. Byrne, *Nano Lett.*, 2003, **3**(6), 843.

4

Carbon nanotubes in (bio)sensing systems

Contents

4.1. Glucose detection	73
4.1.1. Glucose oxidase based biosensor	74
4.1.1.1. Experimental	75
4.1.1.2. Results and discussion	77
4.1.1.3. Conclusions	80
4.1.2. Cell (<i>Pseudomonas fluorescens</i>) based biosensor	81
4.1.2.1. Results and discussion	81
4.1.2.2. Conclusions	85
4.2. Catechol detection	86
4.2.1. Experimental	87
4.2.2. Results and discussion	89
4.2.3. Conclusions	93
4.3. References	95

Carbon nanotubes in biosensing systems

This chapter summarizes the application and integration CNTs to chemical sensors that use biological molecules as receptors. The electrochemical detection for glucose and catechol are described in the following sections:

4.1. Glucose detection

For the treatment and control of diabetes, the amount of blood glucose has to be monitored. For this reason, the glucose biosensor is the most extensively studied among the different types of enzyme-based biosensors.^{1,2} A lot of efforts are still being done with the idea to further improve the performance of this biosensor. Improvements of its selectivity toward interferences as well as the sensitivity have been the focuses of the researches with interests in application ranges from clinical to food industry etc.

Two alternative biosensor designs for glucose detection have been studied and the obtained results are presented in the following sections. Both designs are based in carbon nanotubes-epoxy composite (CNTEC) electrodes incorporating biological material, such as enzymes (glucose oxidase (GOx) from *Aspergillus niger*) and cells (*Pseudomonas fluorescens*). In the first design (section 4.1.1) GOx from *Aspergillus* which has two tightly bound flavine adenine dinucleotide (FAD) cofactors has been used.³ It catalyzes the electron transfer from glucose to oxygen accompanying the production of gluconolactone and hydrogen peroxide.¹ The second design (section 4.1.2) developed in collaboration with Ülkü Anik's research group represents a microbial biosensor that can specifically recognize glucose intimately connected or integrated within a transducer, using *Pseudomonas fluorescens* as a biological sensing element onto the surface electrode. In this way, glucose may be measured by using the assimilation capacity of the microorganism as an index of the respiration activity or of the metabolic activity.⁴ The major application of microbial biosensors is in the environmental field.^{5,6}

In the following sections, the effect of CNTs to promote electron transfer in both designs of biosensors will be shown (for more details see published articles^{7,8}). Figure 4.1. shows the schematic diagram of an enzyme-based CNTs biosensor.

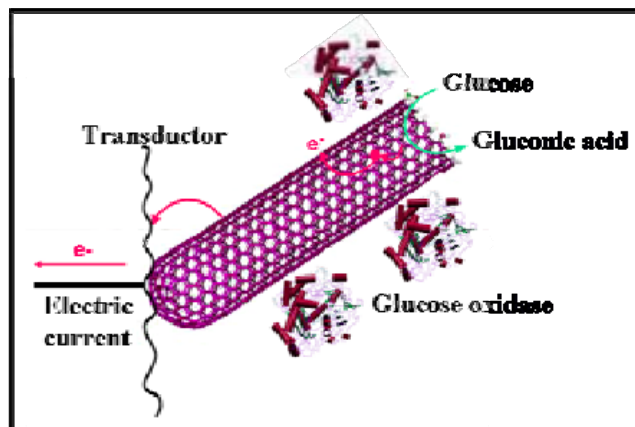


Figure 4.1. Schematic diagram of a carbon nanotube biosensor. The enzyme immobilization allows the direct electron transfer from the enzyme active site to electrochemical transducer. (Adapted from reference 9)

4.1.1. Glucose oxidase based biosensor

Glucose oxidase (GOx) has been extensively used to monitor the blood glucose levels in diabetics for its catalytic ability to glucose. But for the active site of GOx, FAD, being deeply embedded within a protective protein shell, the realizing of the direct electron transfer (DET) for GOx is extremely difficult. A variety of attempts have been done in order to improve the communication between active site and electrode.^{10,11}

The effective immobilization of GOx is one of the key features for successful application of amperometric biosensors. These biosensors combine the bioselectivity of redox enzymes with the inherent sensitivity of amperometric transductions, and have proven to be very useful for the quantification of glucose. Hence, it is pertinent to explore and develop a simple and reliable method to integrate CNTs with enzymes. Many methods such as GOx incorporation into carbon paste and the use of self-assembled monolayers, cross-linking, physical adsorption, and nafion have been employed to immobilize GOx. GOx has been immobilized onto CNTs via polypyrrole^{12,13} or even through CNTs inks.¹⁴ However, some of these methods are relatively complicated, require unattractive reagents, and have led to biosensors with stability problems.¹⁵ In this section will be developed for glucose determination a multi-wall carbon nanotubes (MWCNTs) biosensor based on the GOx immobilization through

physical entrapment inside an epoxy resin matrix, forming a rigid and renewable sensing surface. The corresponding results will be shown in the following sections.

4.1.1.1. Experimental

Reagents

Glucose oxidase (GOx, type VII, *Aspergillus niger* (EC 1.1.3.4), 200,000 U per gram of solid, Catalog No. G-2133) and β -D-(+) glucose were purchased from Sigma. The multi-walled carbon nanotubes powders (0.5–200 μ m) (MWCNTs), were purchased from Aldrich (Stenheim, Germany) with ~95% purity. Further purification was accomplished by stirring the carbon nanotubes in 2 M nitric acid (Panreac, Spain) at 25 °C for 24 hours, according to the procedure described earlier.¹⁶ Graphite powder (particle size 50 μ m) was obtained from BDH, U.K. Epoxy resin Epotek H77 A and hardener Epotek H77 B were received from Epoxy Technology. The working solutions (β -D-(+) glucose) were prepared daily by dilution in 0.1 M phosphate buffer at pH 7.0 with ultra pure water from a Millipore-MilliQ system.

Apparatus

The amperometric measurements were performed with an LC-4C amperometric detector (BAS). Electrochemical experiments were carried out with a typical cell of 10 mL, room temperature (25 °C) and using a three electrodes configuration. A platinum and Ag/AgCl electrodes were used as counter and reference electrode, respectively. A magnetic stirrer provided the convective transport during the amperometric measurements. The SEM images were conducted using a Hitachi S-3200N scanning electron microscope (SEM).

Procedures

Construction of the glucose biosensor

Carbon nanotube-epoxy composite (CNTEC) electrodes were prepared by mixing manually (using a spatula) multi-walled carbon nanotubes (MWCNTs) with epoxy resin Epotek H77 A and hardener Epotek H77 B in the ratio 20:3 (80.0% w/w). Graphite-epoxy composite (GEC) electrodes (blank electrodes) were prepared in a similar way by mixing graphite powder with Epoxy resin Epotek H77 A and hardener Epotek H77 B in

the ratio 20:3 as described previously.^{17,18} CNTEC and GEC electrodes containing the GOx enzyme (GOx-CNTEC and GOx-GEC; see schematic presentation in Figure 4.2) were prepared by mixing carbon nanotubes powder or graphite (18.0% w/w) with GOx (2.0% w/w), followed by the incorporation of Epoxy resin (80.0% w/w) and mixing for 30 minutes to ensure an homogeneous biocomposite paste; this paste was then introduced in a PVC tube containing an electrical connection through a copper disk and wire. The conducting biocomposite was cured at 40 °C for one week. Prior being used the hardened electrode surface was polished with different abrasive papers of decreasing grain size, ending with alumina paper (polishing strips 301044-001, Orion, Spain).

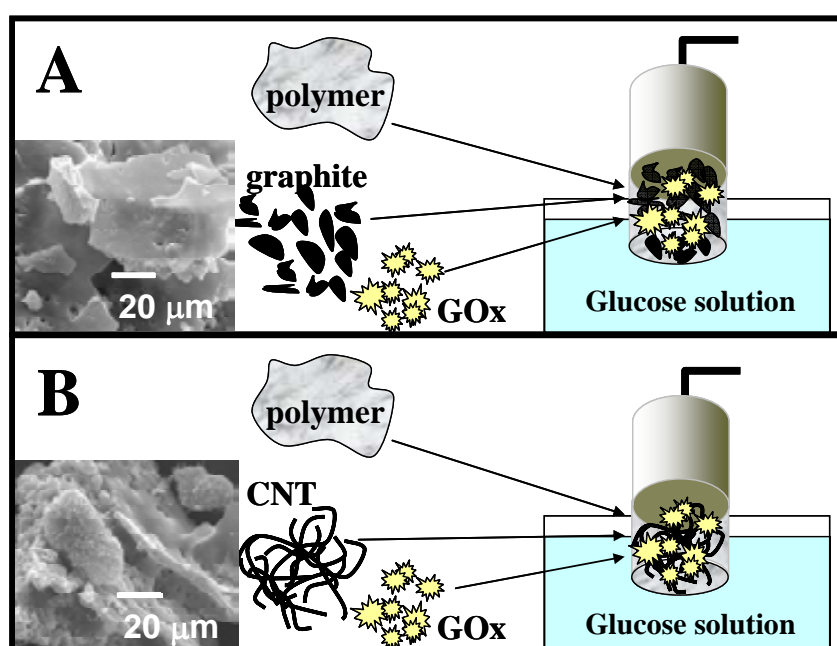


Figure 4.2. Schematic of the glucose biosensors based on GEC (A) and CNTEC (B). Shown, the left side, are also the SEM images of the dried mixtures of glucose oxidase with graphite (A) and CNTs (B) before mixing with the epoxy polymer to form GEC and CNTEC pastes. A better entrapment of GOx inside the sponge like structure of the CNTs bundles compared to graphite particle is clearly visualized in the SEM images. Electrodes composition: Carbon, 18% (w/w); GOx, 2% (w/w); epoxy, 80% (w/w).

Amperometric determination of glucose

The steady state amperometric response to glucose was measured in aliquots of 10 mL of buffer solution with differing additions of glucose applied then onto the reaction cell. The measurements were carried out in a 0.1 M phosphate buffer solution pH 7.0, employed as supporting electrolyte. The applied potential to the working electrode for glucose determination was +0.55 V and +0.90 V for GOx-CNTEC and GOx-GEC

electrodes respectively. The background current was allowed to decay to a constant level before aliquots of glucose sample were added to the stirred buffer solution.

4.1.1.2. Results and discussion

A detailed description of the obtained results and scanning electron microscopy (SEM) images of the biosensor surfaces are given in the published article⁷. In brief, the electrochemical results are described and discussed in the following sections. These results will be compared with a conventional GEC biosensor.

Amperometric detections

Electrocatalytic properties of the glucose biosensor

For developing oxidase-based biosensors the detection of hydrogen peroxide is of considerable interest. It is widely known that the electrooxidation and electroreduction of hydrogen peroxide at different carbonaceous materials (glassy carbon, graphite paste, graphite, carbon fiber, glassy carbon paste, carbon screen-printed electrodes), require elevated overvoltages. In the case of CNTEC, as it was already reported there is an important catalytic effect both on the reduction and oxidation of hydrogen peroxide, making a high sensitive detection of this compound possible. Figure 4.3 compares hydrodynamic voltammograms for a 4 mM glucose solution at GOx-GEC (a) and at GOx-CNTEC (b) electrodes. The oxidation current for the hydrogen peroxide enzymatically generated by glucose oxidase incorporated into the epoxy composite matrix starts at potential +0.55 V at GOx-CNTEC, while at GOx-GEC electrode it starts at +0.90 V. A potential shift of around $\Delta E = 0.35$ V is clearly observed. Moreover, at GOx-CNTEC the signal increases around 90% (note the different current scales at Figure 4.3) indicating larger glucose signal when the GOx-CNTEC electrode was employed. CNTs significantly promote the electron transfer between hydrogen peroxide and GOx-CNTEC facilitates the low potential amperometric determination of glucose.

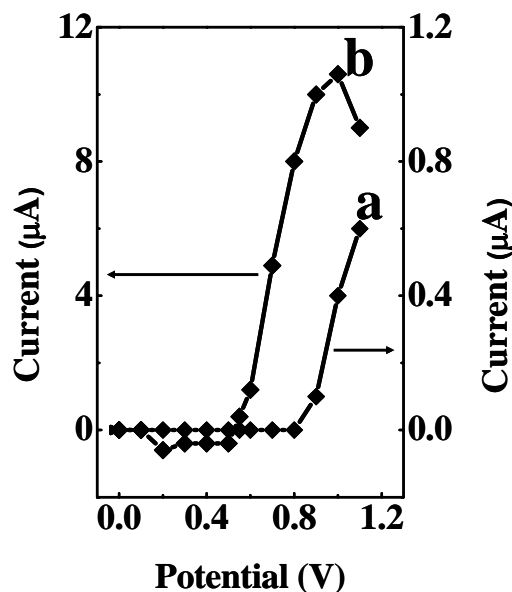


Figure 4.3. Hydrodynamic voltammogram for 4 mM glucose for GOx-GEC (a) and at GOx-CNTEC (b) in 0.1 M phosphate buffer pH 7.0. Electrodes composition: as described in the Figure 4.2.

Calibration of glucose biosensor

The amperometric responses of GOx-GEC and GOx-CNTEC electrodes to glucose are compared in Figure 4.4. The steps correspond to the responses of GOx-GEC (a) and GOx-CNTEC (b) for successive additions of 0.5 mM glucose in 0.1 M pH 7.0 phosphate buffer solution and using operating potentials of +0.90 V (A) and +0.55 V (B). The resulting calibration plots (insets) are also shown. It can be observed that GOx-CNTEC electrodes offers substantially higher signals for both operating potentials (+0.55 and +0.90 V) compared to GOx-GEC electrode.

The electrocatalytic activity of carbon nanotubes is even more pronounced from comparison of the response at +0.55 V, where the conventional GOx-GEC electrode is not responding (see Figure 4.4B, curve a). The sensitivity of detection at an applied potential of +0.90 V for glucose determination, based on the amount of hydrogen peroxide produced by enzyme reaction, was found to be more than 6 times larger than that when an applied potential +0.55 V was employed. As expected from the hydrodynamic voltammogram (HDV) (Figure 4.3), higher sensitivity is observed at +0.90 V (note the different scales). In Figure 4.4A the plot of current vs. glucose concentration was linear over a wide concentration range of 0.5–4.5 mM for GOx-CNTEC electrode (A, b), had a correlation coefficient of 0.999, a linear concentration range of GOx-GEC (A, a), the electrode was 0.5–2.5 mM, a correlation coefficient of

0.999 (in this range), and detection limits of 0.09 mM and 0.10 mM respectively. The corresponding calibration plots show sensitivities of $0.10 \mu\text{A}\cdot\text{mM}^{-1}$ for GOx-GEC electrode and $3.21 \mu\text{A}\cdot\text{mM}^{-1}$ for GOx-CNTEC electrode.

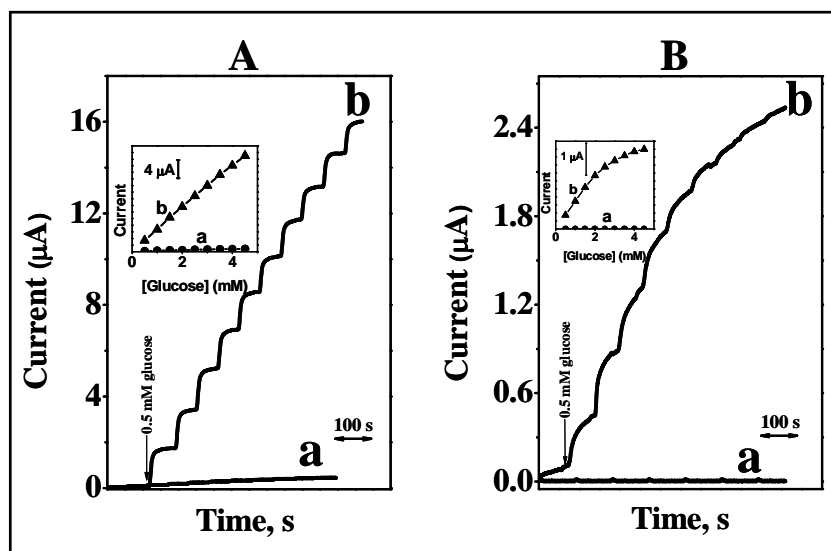


Figure 4.4. Current-time recordings obtained from amperometric experiments at GOx-GEC (a) and at GOx-CNTEC (b) for successive additions of 0.5 mM glucose. Working potential: (A) +0.90 V and (B) +0.55 V in 0.1 M phosphate buffer pH 7.0. The insets show the corresponding calibration plots. Electrodes composition: as described in the Figure 4.2.

Stability measurements

The functioning principle of the glucose biosensor is based on the amperometric detection of H_2O_2 , which is generated during the course of the enzyme-catalyzed oxidation of glucose by dissolved oxygen. In this work, amperometric measurements were carried out in 0.1 M phosphate buffer solution pH 7.0 under magnetic stirring. Figure 4.5 presents the stability of the response for 4 mM glucose at the GOx-CNTEC electrode at operating potential of +0.90 V. It can be observed that the current increases obviously after the addition of glucose maintaining then a steady state response thereafter. Additionally, a response time of about 30 seconds can be observed from Figure 4.5.

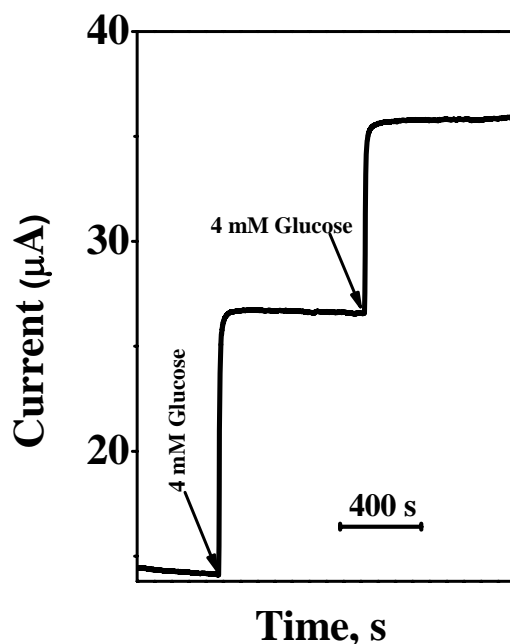


Figure 4.5. Stability of the response of the GOx-CNTEC biosensor to additions of 4 mM glucose. Conditions: +0.9 V in 0.1 M phosphate buffer solution pH 7.0. Electrodes composition: as described in the Figure 4.2.

4.1.1.3. Conclusions

A biosensor for glucose detection based on immobilization of glucose oxidase within a rigid carbon nanotube epoxy composite matrix was demonstrated. The results presented above reveal the ability of CNTEC to promote the electron transfer between the glucose oxidase and the hydrogen peroxide produced by the enzymatic reaction. The observed results were rationalized by the following explanations: (i) The CNTs dispersed in the epoxy resin ensure an electrical contact with GOx better than the graphite particles do. This is due to the sponge-like structure of the CNTs that probably achieves improved electrical contacts with GOx. (ii) The CNTs structure ensures better microelectrode arrays compared to graphite particles. This may also enhance the signal to noise ratio that has also been reported for graphite based composites.¹⁶ The CNTs biocomposite based biosensor exhibited excellent sensitivity and stability for the determination of glucose. Moreover, it is simple, it has a fast and reproducible response, and low cost. Nevertheless a future interdisciplinary research, which is under exploitation in our laboratory, could lead to a new generation of electrochemical biosensors based on robust biosensor with better electron transfer including for other enzymes.

4.1.2. Cell (*Pseudomonas fluorescens*) based biosensor

In this second glucose biosensor design the CNTs are incorporated firstly into an epoxy polymer, forming an epoxy composite hybrid material used as transducer. *Pseudomonas fluorescens* cell as biological material was introduced via a gelatin membrane and was then cross-linked with glutaraldehyde.

Pseudomonas fluorescens is an aerobic, gram-negative bacterium which use organic compounds as their only source of carbon and energy and has shown to be an interesting model to study the biochemical impact of environmental stress on cellular metabolism.¹⁹

The characterization and optimization of the biosensor were performed by using glucose as a substrate. Amperometric measurements were based on the respiratory activity of the cells which means, in the presence of glucose, oxygen consumption due to the metabolic pathway of the *P. fluorescens* was followed by means of a potentiostat. In order to investigate the contribution of CNTs on the microbial biosensor response, obtained results under the optimum conditions were compared with a conventional graphite epoxy composite electrode (GECE) modified with bacterial cells. Following these studies, following sections contain the most important results obtained with a carbon nanotube epoxy composite (CNTEC) modified with bacterial cells for future applications as a microbial biosensor.

4.1.2.1. Results and discussion

A detailed description on the experimental part including the obtained results related to the carbon nanotube composite as novel platform for microbial biosensor for glucose detection is given in the published article⁸. In the following section are only summarized some of the most important results.

Optimization of experimental parameters

Effect of pH

According to the optimization studies the effect of pH on the electrode response was investigated by using phosphate buffer systems (50 mM) between pH 6.0 – 8.2 for 2.0

mM glucose. The response current of the electrode to glucose increases significantly from pH 6.5 to 7.5, and then a sharp decrease is obtained at pH values higher than 7.5 (see Figure 2 in the published article⁸). As a result pH 7.5 was chosen as optimum pH and used for further studies.

Effect of temperature

The amperometric response of the microbial electrode to 2.0 mM glucose was measured at different temperatures varying from 25 to 42 °C, the results are shown in Figure 3 (see published article⁸). As best current value was observed at 35 °C, further experiments were conducted at this temperature.

Effect of cell amount

For this purpose 12.5 μL , 25 μL , and 37.5 μL of bacterial cell which have the same cell titer were used to prepare three immobilization mixtures. To investigate the effect of cell amount three separate calibration graphs were obtained by using each amount. The highest responses were obtained with 25 μL cell amount. As the cell activity of 12.5 μL was inadequate and 37.5 μL bacterial cells caused diffusion problem to the substrate, both amounts have tended to decrease the resulting signal. Further experiments were conducted by using 25 μL cell amounts (see Figure 4.6).

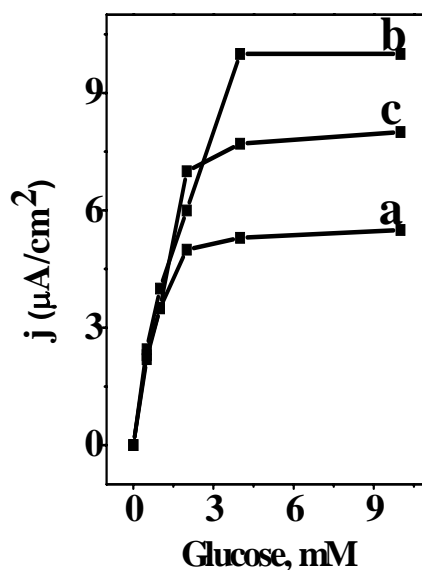


Figure 4.6. Effect of cell amount (12.5 μL (a), 25 μL (b), 37.5 μL (c)) on the electrode response in phosphate buffer (50 mM at pH 7.5, 30 °C, -700mV).

Stability

The stability of cell based biosensor was investigated at working conditions (30 °C in phosphate buffer, pH 7.5) by using 2 mM glucose and a 13% decrease of activity is observed after 4 hours (data not shown). During this period approximately 16 measurements have been made and it could be possible to make more measurements in a longer time period. Moreover, to be sure of the life time of bacterial cells in bioactive layer and to obtain reproducible results, the sensors including daily inoculated cells were prepared freshly for each day and utilized through the experiments.

Effect of working potential

The effect of working potential was searched by measuring the amperometric responses of two types of microbial electrode based on CNTEC and GECE to 2.0 mM glucose at different potentials vs. Ag/AgCl between -550 and -800 mV. As it was mentioned before, the measurement was based on the respiratory activity of the cells. At lower potentials (between -550 and -650 mV), CNTEC showed almost 1.5 fold higher biosensor response value than traditional GECE that was in agreement with the fact that CNTs promote electron-transfer reactions at low potentials. However, maximum currents were obtained at -700 and -750 mV for both systems (see Figure 4.7) and for this reason -700 mV was chosen as the operating potential for further experiments.

At the previous section, glucose biosensor was fabricated by dispersing MWCNTs inside the epoxy resin⁷ and as a result, lower detection potential (+0.55 V) than for GOx-GECE (+0.90 V; difference $\Delta E = +0.35$ V) was obtained.

Due to loss of metabolic activity of microbial cell, it is inappropriate to disperse bacterial cell into composite materials like epoxy. For this reason they were immobilized onto the electrode surface by means of gelatin membrane.²⁰ Both gelatin membrane and the structure of bacterial cell membrane act like a diffusion barrier for electron transfer and tend to slow down the reaction kinetics. Though better current values were observed with CNTEC, in our opinion, due to these complex mechanisms, significant lower values can not be obtained in terms of operating potential. The effect of CNTs on electron transfer kinetics at microbial systems will be under investigation with the help of monomeric and polymeric mediators.

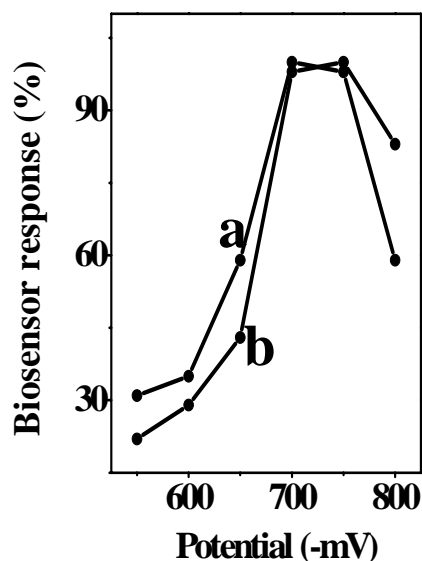


Figure 4.7. Effect of working potential on the electrode response in phosphate buffer (50 mM at pH 7.5, 30 °C). CNTEC electrodes modified with bacterial cells (a) and GEC electrodes modified with bacterial cells (b).

Analytical characteristics

CNTEC electrode provides linear relationship between biosensor response (y) and substrate concentration (x) in the range of 0.5–4.0 mM glucose under the response times of 100 s with the equation of $y = 2.1x + 1.67$ ($R^2 = 0.995$, y in mM, x in $\mu\text{A}/\text{cm}^2$). At higher concentrations, standard curve showed a deviation from linearity. On the other hand, with GECE the same linearity was obtained while the equation of linear graph was estimated as $y = 0.795x + 0.897$ with $R^2 = 0.983$ (y in mM, x in $\mu\text{A}/\text{cm}^2$) respectively.

Besides, it was observed that CNTEC possess higher current values (2 to 3 folds) compared to GECE. This can be attributed to unique properties of CNTs that promote the electronic transference.^{21,22} Though the electrocatalytic properties of the CNTs have not been completely explained yet, it was suggested that the open ends of the nanotubes might be responsible from this attractive behavior.¹⁸ The repeatability of the biosensor was tested for 2 mM of glucose ($n=7$) and the standard deviation (SD) and variation coefficient (cv) were calculated as ± 0.06 mM and 2.7%, respectively.

Moreover, the substrate specificities of proposed biosensor to different utilizable substrates (galactose, mannose, phenol, ethanol and methanol) were also tested and given in Table 1 (see published article⁸). No signal was obtained for phenol as well as

methanol and ethanol. Since non adapted bacterial cell were used, they did not metabolize phenol and alcohols as expected.

4.1.2.2. Conclusions

CNTEC microbial biosensor was characterized for glucose detection and compared with conventional GECE based microbial biosensor. As the electron transfer mechanism in the case of bacterial cells is more complicated than as it is for enzymes, lower operating potential could not be obtained with CNTEC based microbial biosensor. Although the immobilization method used in this work provides mild conditions in terms of protecting microbial activity the usage of gelatin membrane for immobilization procedure rather than dispersing the cells into the epoxy¹⁸ might have affected the global response mechanism. On the other hand, higher current values (2 to 3 folds) were observed with CNTEC microbial biosensor when compared with GECE based microbial biosensor.

Microbial biosensors are a good alternative to monitor some global parameters such as bioavailability and toxicity which cannot be probed with molecular recognition or chemical analysis since complex reactions including bacterial metabolic pathways.¹⁹ In view of the direct relevance of bioavailability and toxicity to the presence of pollutants, many of the efforts at the development of whole-cell biosensors were directed towards environmental applications. The microbial cell used in this work is well known phenol-degrading bacteria. However, adaptation process is required before using this kind of microbial cells as specific degrader organisms. Adaptation process may be operationally defined as an increase in the ability of a microbial community to degrade a chemical after prolonged exposure to the material. This phenomena could be due to the several alterations in structure and function of microbial species such as induction or depression of enzymes, genetic change etc.²³ It could also be possible to use the same bacteria, as the one used in the present study, after an adaptation process to obtain microbial sensors for the environmental monitoring of other analytes.^{24,25}

4.2. Catechol detection

Over the last decade, the biosensors for environmental surveillance became more prevalent in literature with the emphasis to phenol determination and control.²⁶ Phenols are compounds of large scale production that cause ecologically undesirable effects.²⁷ Most phenols exhibit different toxicities and their determination is very important for evaluating the total toxicity of an environmental sample. For that reason new alternative biosensor designs for phenolic compounds are being developed and investigated. Rigid conducting carbon nanotubes-polymer based composites are reported. The nature of these materials makes them modifiable, permitting the incorporation of a great number of biological materials that can be immobilised by blending them with these composites to form new biocomposite materials.²⁸

The use of carbon nanotubes (CNTs) has become relevant due to their excellent conductivity including the improvement of electron transfer between the enzymes and the electrode surfaces²⁹ and at the same time provides a very good matrix for enzyme immobilization.³⁰ On the other hand, the biosensors based on nanostructured compounds^{7,18} have demonstrated to be simple in preparation and offer a great promise for developing amperometric biosensors. Figure 4.8 shows the schematic representation of the electrochemical detection of catechol by the use of a carbon nanotube based biosensor.

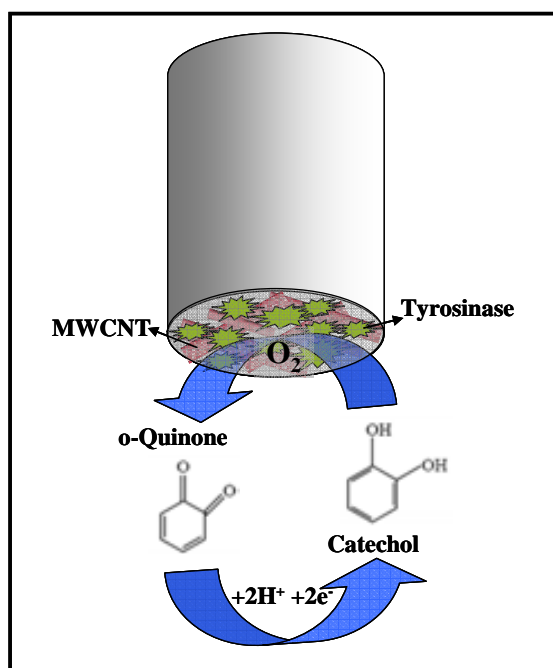


Figure 4.8. Schematic representation of the reaction of catechol with tyrosinase.

Many biosensors have been developed using the catalytic activity of the redox enzymes for phenol determination such as tyrosinase, peroxidase, laccase³¹ using different electrode materials, flow systems and sample pre-treatment techniques.

Tyrosinase, also known as polyphenol oxidase, is a copper monooxygenase that catalyzes the oxidation of catechols to the corresponding *o*-quinones.³²⁻³⁴ The liberated quinone species can be further electrochemically reduced to phenolic substances at low potential in the absence of mediators.^{35,36} Electrochemical reduction of quinones is incomplete. This is because quinones are highly unstable in water and they easily polymerize to polyaromatic compounds.³⁷ In spite of this problem, sensors based on this approach have been reported using graphite electrodes and graphite-epoxy based composite electrodes.^{38,39}

Tyrosinase-based bioelectrodes^{40,41} have been reported; however, one of the most important analytical problems that appear in the case of tyrosinase-modified electrodes is their low operational stability, especially for detecting *o*-diphenols.^{42,43} This can be due to the fact that the enzyme is lost in the surrounding environment (especially when physical methods are used for enzyme immobilization), or due to its inactivation by the radical species that appear during the biocatalytic oxidation.⁴⁴ Thus, it is of great significance to develop new approaches to detect phenol derivatives with high sensitivity. The main features of a biocomposite based on CNTs and tyrosinase for catechol detection will be described in the following sections and its potential for the construction of an amperometric biosensor will also be discussed.

4.2.1. Experimental

Reagents and solutions

Tyrosinase from mushroom (Tyr, 2034 U per mg, Catalog No. 93898), catechol, potassium dihydrogen phosphate and potassium hydrogen phosphate were purchased from Sigma. Epoxy resin Epotek H77 A, hardener Epotek H77 B were received from Epoxy Technology. The multi-walled carbon nanotubes powder (0.5-200 μm) (MWCNTs), were purchased from Aldrich. The CNTs were purified in HNO_3 to remove impurities such as amorphous carbon, graphite particles and metal catalysts. Further purification was accomplished by stirring the CNTs in 2 M nitric acid at 25°C for 24 h.

Graphite powder (particle size 50 μm) was obtained from BDH, U.K. The alumina paper (polishing strips 301044-001), was obtained from Orion, Spain.

The standard catechol solutions were prepared daily by dilution in 0.1M phosphate buffer at pH 6.5 with ultra pure water from a Millipore-MilliQ system.

Apparatus and electrodes

Cyclic voltammetry (CV) and chronoamperometry experiments were performed using an electrochemical analyzer Autolab 20 (Eco Chemie, The Netherlands) and an LC-4C amperometric detector (BAS) connected to a personal computer with GPES software.

The measurements were performed in 10 mL of a 0.1 M phosphate buffer solution (PBS) pH 6.5 without deoxidizing, at room temperature (25 °C) using three electrodes based configuration. Platinum and Ag/AgCl electrodes were used as counter and reference electrode, respectively. The tyrosinase biosensor based on carbon nanotubes epoxy-composite (CNTEC-Tyr) and the tyrosinase biosensor based on a graphite epoxy-composite (GECE-Tyr) were used as working electrodes.

Procedures

Tyrosinase biosensor preparation

The carbon nanotube-epoxy biocomposite (CNTEC-Tyr) and graphite epoxy-biocomposite (GECE-Tyr) electrodes were prepared by mixing manually during 30 minutes the tyrosinase (Tyr) (2.0% w/w), Epoxy resin (80.0% w/w) and carbon nanotubes or graphite powder (18.0% w/w), respectively (Figure 4.8); the prepared biocomposite paste was then introduced into a PVC tube containing an electrical connector completed by using a copper disk and wire. The biocomposite was cured at 40 °C for one week. Before measurements, the cured biosensor surface was polished with different abrasive papers of decreasing grain size, ending in alumina paper. The biosensors (CNTEC-Tyr and GECE-Tyr) were kept in refrigerator while not being used.

Electrochemical measurements

Electrochemical experiments were carried out with a typical 10 mL cell, at room temperature (25°C) and using the three electrodes configuration. A magnetic stirrer provided the convective transport during the amperometric measurements.

Cyclic voltammetry using modified electrodes (CNTEC-Tyr and GECE-Tyr) were performed in 0.02 mM catechol solution. The response of catechol was measured in 10 mL of a 0.1 M phosphate buffer solution (PBS) pH 6.5. The potential range used for catechol determination was -0.4 to +0.8 V for CNTEC-Tyr and GECE-Tyr. The surface coverage (Γ) of CNTEC-Tyr and GECE-Tyr was estimated from the area of the cyclic voltammetric peaks corresponding to the oxidation of catechol. According to the equation $\Gamma = Q/nFA$,⁴⁵ where Q is the area of the catechol oxidation peak, n is the number of electrons involved in the oxidation, F is the Faraday's constant, and A is the area of the electrode ($A=0.2827 \text{ cm}^2$), Γ was found to be of $2.1 \times 10^{-8} \text{ mol/cm}^2$ for GECE-Tyr and of $2.7 \times 10^{-8} \text{ mol/cm}^2$ for CNTEC-Tyr.

The steady state amperometric response to catechol was measured in aliquots of 10 mL of buffer solution with different additions of catechol added into the reaction cell. The measurements were carried out in a 0.1 M phosphate buffer solution pH 6.5, used as supporting electrolyte. The applied potential to the working electrode for catechol determination was -0.2 V using CNTEC-Tyr and GECE-Tyr electrodes respectively. The background current was allowed to decay to a constant level before aliquots of phenolic compounds sample were added to the stirred buffer solution.

4.2.2. Results and discussion

A detailed description of the obtained results is given in the published article⁴⁶. In brief, the results are described and discussed in the following sections. The results of biosensor based on CNTs epoxy composite (CNTEC-Tyr) will be compared with a tyrosinase biosensor based on a graphite epoxy-composite (GECE-Tyr).

Effect of scan rate

Figures 4.9A and 4.10A illustrate the influence of the potential scan rate ν on the cyclic voltammograms of GECE-Tyr and CNTEC-Tyr electrodes in 0.2 mM catechol solution (at 10, 20, 30, 40, 50, 60, 70, 80, 90, 100 mV/s, scanning potential range: -0.5 to 0.8 V)

in 0.1 M phosphate buffer pH 6.5. It can be observed that the scan rate affects the position of the oxidation and reduction peaks.

Inspection of the curves reveals that an increase in the scan rates, ν , increases the current of the oxidation of catechol and shifts the anodic peak potential (E_{pa}) toward more positive potentials as the rate increased, whereas the cathodic peak potential (E_{pc}) shifts toward more negative potentials. The differences of these potential shifts for CNTEC-Tyr are 104 mV and 131 mV, respectively.

The influence of sweep rate ν ($\nu^{1/2}$) on anodic peak current (I_{pa}) is shown in Figure 4.9B for GECE-Tyr and Figure 4.10B for CNTEC-Tyr respectively. Further analysis of the results indicate that the anodic peak current increases linearly with the square root of the rate, and the corresponding linear equation is $i(\mu\text{A}) = 26.038 \nu^{1/2} - 62.46$ with a linear correlation coefficient of 0.9902 for GECE-Tyr and for CNTEC-Tyr the corresponding linear equation is $i(\mu\text{A}) = 34.369\nu^{1/2} - 100.794$ with a linear correlation coefficient of 0.9889, both cases at pH = 6.5. The relation between I_{pa} and $\nu^{1/2}$ indicates that the anodic dissolution process within the potential range of peak (Figure 4.9B and 4.10B) is a diffusion controlled process.

The difference between the E_{pa} and the E_{pc} , for the GECE-Tyr is $\Delta E_p = 214$ mV and for the CNTEC-Tyr is $\Delta E_p = 206$ mV, both obtained at a potential scan rate of 100 $\text{mV}\cdot\text{s}^{-1}$, and the current ratio between the peaks (I_a/I_c) is 0.98 and 1.14, respectively. These results demonstrate that the oxidation process of catechol in both electrodes can be considered quasi-reversible.

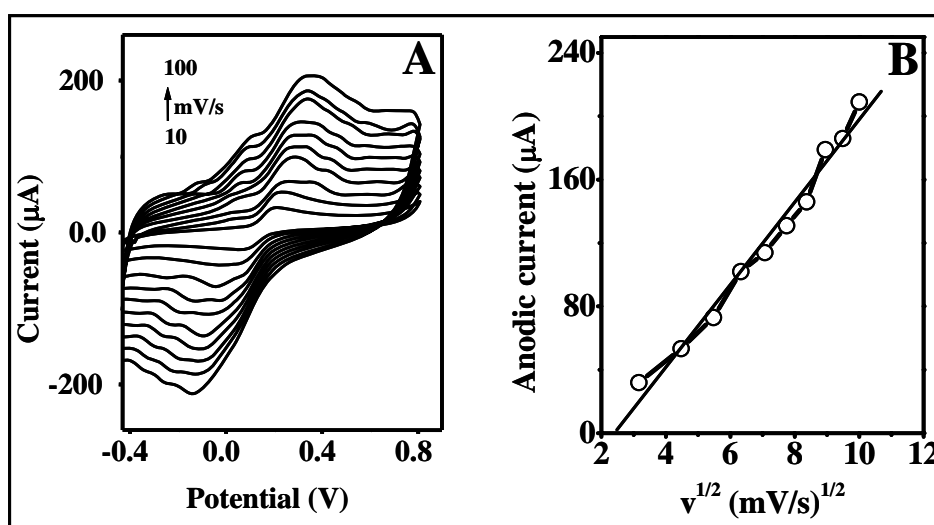


Figure 4.9. (A) Cyclic voltammograms of GECE-Tyr electrode in 0.2 mM catechol solution (at 10, 20, 30, 40, 50, 60, 70, 80, 90, 100 mV/s , scanning potential range: -0.5 to 0.8 V); (B) plots of anodic peak currents versus the square root of scan rate.

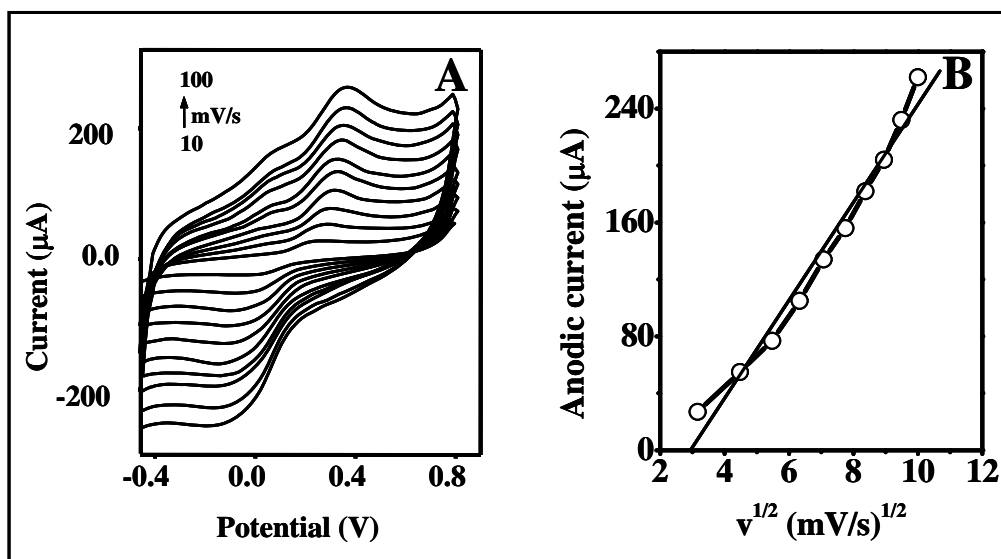


Figure 4.10. (A) Cyclic voltammograms of CNTEC-Tyr electrode in 0.2 mM catechol solution (at 10, 20, 30, 40, 50, 60, 70, 80, 90, 100 mV/s, scanning potential range: -0.5 to 0.8 V); (B) plots of anodic peak currents versus the square root of scan rate.

Amperometric behaviour of tyrosinase biosensor

The hydrodynamic voltammogram (HDV) data are very important for selecting the operating potential for amperometric measurements. In the case of CNTEC-Tyr, as it was already reported, there is an important catalytic effect on the reduction of *o*-quinone and oxidation of catechol, making it possible for high sensitive detection of phenolic compounds. Figure 4.11 compares hydrodynamic voltammograms for 0.025 mM catechol for GECE-Tyrosinase (a) and at CNTEC-Tyrosinase (b) in 0.1M phosphate buffer pH 6.5. The reduction current for the *o*-quinone enzymatically generated starts at potential -0.2 V at CNTEC-Tyr and GECE-Tyr. At CNTEC-Tyr the signal increases around 80% at the potential of -0.2 V (observe the different current scales at Figure 4.11) indicating that the sensitivity largely increases as consequence of the type of material.

Therefore, carbon nanotubes promote in a very efficient way the electron transfer between *o*-quinone and CNTEC-Tyr. This electrocatalytic activity facilitates low-potential amperometric determination of catechol.

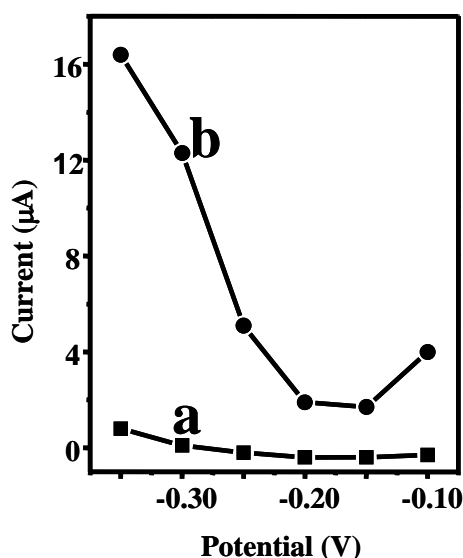


Figure 4.11. Hydrodynamic voltammogram for 0.025 mM catechol for GECE-Tyr (a) and at CNTEC-Tyr (b) in 0.1 M phosphate buffer pH 6.5.

Biosensor response toward catechol

The amperometric responses for the determination of catechol on GECE-Tyr (a) and CNTEC-Tyr (b) electrodes at the scan rate of $100 \text{ mV}\cdot\text{s}^{-1}$ are compared in Figure 4.12. It shows well-defined responses for each successive addition of 0.02 mM catechol at the graphite-epoxy-Tyr composite (GECE-Tyr) (a) and carbon nanotube-epoxy composite (CNTEC-Tyr) (b) electrodes using operating potential of -0.2 V in 0.1M phosphate buffer solution pH 6.5, with their respective calibration plots (insets). The CNTEC-Tyr electrode offers substantially larger signals reflecting the electrocatalytic properties of carbon nanotubes. The sensitivity of detection for catechol determination at an applied potential of -0.2 V is based on the amount of *o*-quinone produced by enzymatic reaction between catechol and tyrosinase. It was of $46 \text{ }\mu\text{A}/\text{mM cm}^2$ for GECE-Tyr and of $294 \text{ }\mu\text{A}/\text{mM cm}^2$ for CNTEC-Tyr with a current intensity 90% higher than GECE-Tyr (note the different scales) (Figure 4.12). Nevertheless, the repeatability of the method was obtained in one day by the same analyst using the same reagent solutions demonstrating to be better for GECE-Tyr than for CNTEC-Tyr with a $\text{RSD} = 5\%$ ($n = 3$) and $\text{RSD} = 8\%$ ($n = 3$), respectively. The plots of current vs catechol concentration were linear for a concentration range of 0.0–0.15 mM at CNTEC-Tyr and GECE-Tyr electrodes (inset calibration plots (4.12a and 4.12b) with a correlation coefficient of 0.990 and 0.996, respectively.

The highest current response for CNTEC-Tyr due to the distinctive properties of CNTs, especially, the biocompatibility and ability to facilitate electron transfer make them suitable candidates for immobilization of biomolecules and biosensor applications.^{47,48} A variety of enzymes by using CNTs as molecule wires to facilitate the electron transfer of enzyme with electrode have been employed in the relatively new field of enzyme-based nanotube sensors.⁴⁹

The stability of the CNTEC-Tyr and GECE-Tyr electrodes is very important during the chronoamperometric experiments. It was studied using the same conditions as afore mentioned. For each different addition of 0.02 mM catechol solution a response time of about 20 s was observed and thereafter a good stability is maintained at GECE-Tyr during 5 minutes and a better current increase with CNTEC-Tyr, operating at a potential of -0.2 V, the electrodes being stable for more than 24 h (results not shown).

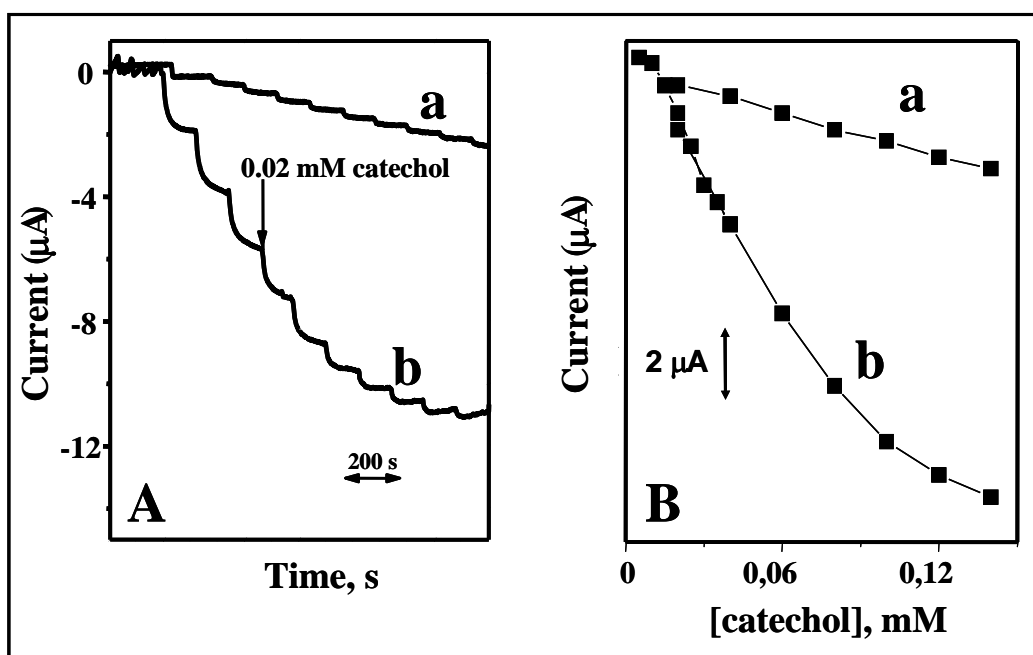


Figure 4.12. Current-time recordings obtained from amperometric experiments (A) and the corresponding calibration plot (B) at GECE-Tyr (a) and at CNTEC-Tyr (b) for successive additions of 0.02 mM catechol, respectively. Working potential: -0.2 V in 0.1 M phosphate buffer pH 6.5. The inset shows the corresponding calibration plot.

4.2.3. Conclusions

The obtained results described above illustrate an attractive construction of a renewable biosensor for the catechol detection. Tyrosinase maintains its enzymatic properties in the composite matrix; furthermore, the sensing surface can be renewed by a simple

polishing procedure resulting in a fresh surface. Various additives may be incorporated into the biocomposite matrix to enhance further the analytical performance.

One of the outstanding features of these conducting biomaterials is their rigidity. The proximity of the redox centres of tyrosinase and the carbon nanotubes on the sensing surface favours the transfer of electrons between electroactive species. Composites electrodes modified with carbon nanotubes show improved electrochemical properties offering important advantages: i) CNTEC-Tyr exhibits better electronic properties than GECE-Tyr due to the promotion in a very efficient way of electron transfer between *o*-quinone and CNTEC-Tyr electrode; ii) CNTEC-Tyr shows a detection limit (0.01 mM) almost half of that obtained by GECE-Tyr; iii) The CNTs biocomposite offers the possibility for electrode surface renewing forming a new active layer; and lastly iv) The CNTEC-Tyr and GECE-Tyr amperometric biosensors are very attractive for mass fabrication so as to obtain low cost biosensors.

4.3. References

- ¹ R.B. Rakhi, K. Sethupathi and S. Ramaprabhu, *J. Phys. Chem. B.*, 2009, in press.
- ² S.H. Lim, J. Wei, J. Lin, Q. Li and J.K. You, *Biosens. Bioelectron.* 2005, **20**, 2341.
- ³ H.J. Hecht, H.M. Kalisz, J. Hendle, R.D. Schmid and D. Schomburg, *J. Mol. Biol.* 1993, **229**, 153.
- ⁴ K. Riedel, *Enzyme and Microbial Biosensors: Techniques and Protocols Part II* (Eds: A. Mulchandani, K. R. Rogers), Humana Press, Totowa, NJ 1998, 199.
- ⁵ S.F. D'Souza, *Appl. Biochem. Biotechnol.*, 2001, **96**, 225.
- ⁶ J. Liu and B. Mattiasson, *Water Res.*, 2002, **36**, 3786.
- ⁷ B. Pérez, M. Pumera, M. del Valle, A. Merkoçi and S. Alegret, *J. Nanosci. Nanotechnol.*, 2005, **5**, 1694.
- ⁸ Ü.A. Kirgoz, S. Timur, D. Odaci, B. Pérez, S. Alegret and A. Merkoçi, *Electroanalysis*, 2007, **19** (7-8), 893.
- ⁹ S. Sotiropoulou and N.A. Chaniotakis, *Anal. Bioanal. Chem.*, 2003, **375**, 103.
- ¹⁰ Y. Liu, M. Wang, F. Zhao, Z. Xu and S. Dong, *Biosens. Bioelectron.*, 2005, **21**, 984.
- ¹¹ A. Guiseppi-Elie, C. Lei and R. Baughman, *Nanotech.*, 2002, **13**, 559.
- ¹² M. Gao, L. Dai, and G. Wallace, *Synth. Met.*, 2003, **137**, 1393.
- ¹³ K.P. Loh, S.L. Zhao and W.D. Zhang, *Diamond Rel. Mater.*, 2004, **13**, 1075.
- ¹⁴ J. Wang and M. Musameh, *Analyst.*, 2004, **129**, 1.
- ¹⁵ A. Salimi, R. Compton and R. Hallaj, *Anal. Biochem.*, 2004, **333** (1), 49.
- ¹⁶ S. Alegret and A. Merkoçi, *Integrated Analytical Systems*, edited by S. Alegret, Amsterdam, 2003, Elsevier, 377.
- ¹⁷ M. Pumera, M. Aldavert, C. Mills, A. Merkoçi and S. Alegret, *Electrochim. Acta*, 2005, **50**, 3702.
- ¹⁸ M. Pumera, A. Merkoçi and S. Alegret, *Sens. Actuators B*, 2006, **113**, 617.
- ¹⁹ V.D. Appanna and R.D. Hamel, *Dev. Microbiol.*, 1999, **3**, 615.
- ²⁰ S. Timur, N. Pazarlioglu, R. Pilloton and A. Telefoncu, *Talanta*, 2003, **61**, 87.
- ²¹ A. Merkoçi, M. Pumera, X. Llopis, B. Perez, M. del Valle and S. Alegret, *Trends Anal. Chem.*, 2005, **24**, 826.

- ²² E. Banks and R. Compton, *Analyst*, 2006, **131**, 15.
- ²³ R.J. Shimp and F.K. Pfaender, *Appl. Environ. Microbiol.*, 1987, **53**, 1496.
- ²⁴ J.C. Philp, S. Balmand, E. Hajto, M.J. Bailey, S. Wiles, A.S. Whiteley, A.K. Lilley, J. Hajto and S.A. Dunbar, *Anal. Chim. Acta*, 2003, **487**, 61.
- ²⁵ S. Belkin, *Curr. Opin. Microbiol.*, 2003, **6**, 206.
- ²⁶ K.R. Rogers, *Biosens. Bioelectron.*, 1995, **10**, 533.
- ²⁷ J. Kulys and R. Vidziunaite, *Biosens. Bioelectron.*, 2003, **18**, 319.
- ²⁸ F. Cèspeles and S. Alegret, *Trends Anal. Chem.*, 2000, **19** (4), 276.
- ²⁹ A. Merkoçi, *Microchim. Acta.*, 2006, **152**, 157.
- ³⁰ B. Pérez, J. Sola, S. Alegret and A. Merkoçi, *Electroanalysis*, 2008, **20** (6), 603.
- ³¹ N. Durán and E. Esposito, *Appl. Catal. B Environ.*, 2000, **28**, 83.
- ³² E.I. Solomon, U.M. Sundaram and T.E. Machonkin, *Chem. Rev.*, 1996, **96**, 2563.
- ³³ H. Decker and F. Tucek, *Trends Biochem. Sci.*, 2000, **25**, 392.
- ³⁴ E.J. Land, C.A. Ramsden and P.A. Riley, *Acc. Chem. Res.*, 2003, **36**, 300.
- ³⁵ T. Toyata, S.S. Kuan and G.G. Guilbault, *Anal. Chem.*, 1985, **57**, 1925.
- ³⁶ A. Ghindilis, V. Gavrilova and A. Yaropolov, *Biosens. Bioelectron.*, 1992, **7**, 127.
- ³⁷ N.H. Horowitz, M. Fling and G. Horn, *Methods Enzymol.* Academic Press, New York, 1970, 120.
- ³⁸ F. Ortega, E. Domínguez, G.J.-Pettersson and L. Gorton, *J. Biotechnol.*, 1993, **31**, 289.
- ³⁹ P. Önnérjörd, J. Emnéus, G.M.-Varga and L. Gorton, *Biosens. Bioelectron.*, 1995, **10**, 607.
- ⁴⁰ E.S. Forzani, G.A. Rivas and V.M. Solís, *J. Electroanal. Chem.*, 1999, **461**, 174.
- ⁴¹ E.S. Forzani, V.M. Solís and E.J. Calvo, *Anal. Chem.*, 2000, **72**, 5300.
- ⁴² A.I. Yaropolov, A.N. Kharybin, J. Emnéus, G.M.-Varga and L. Gorton, *Anal. Chim. Acta.*, 1995, **308**, 137.
- ⁴³ F. Ortega, E. Domínguez, E. Burestedt, J. Emnéus, L. Gorton and G. M.-Varga, *J. Chromatogr.*, 1994, **A675**, 65.

- ⁴⁴ C. Nistor and J. Emnéus, *Waste Manage.*, 1999, **19**, 147
- ⁴⁵ A.J Bard and L. R. Faulkner, *Electrochemical Methods*, Wiley, New York, 2001.
- ⁴⁶ B. Pérez López and A. Merkoçi, *Analyst*, 2009, **134**, 60.
- ⁴⁷ M. Shim, N.W.S. Kam, R.J. Chen, Y. Li and H. Dai, *Nano Lett.*, 2002, **2**, 285.
- ⁴⁸ E. Katz and I. Willner, *Chem. Phys. Chem.*, 2004, **5**, 1084.
- ⁴⁹ Y. Liu, X. Qu, H. Guo, H. Chen, B. Liu and S. Dong, *Biosens. Bioelectron.*, 2006, **21**, 2195.

5

Global discussion, general conclusions and future perspectives

Contents

5.1. Global discussion of results	101
5.2. General conclusions	104
5.3. Future perspectives	105
5.4. References	106

Global discussion, general conclusions and future perspectives

5.1. Global discussion of results

Several sensors and biosensors designs that integrate carbon nanotubes with the electrochemical transducers via several other compounds (binding matrix, biological molecules etc.) have been studied. The glassy carbon (GC) electrode modified with a polymeric matrix, based in a MWCNTs mixed with tetrahydrofuran (THF), PVC and finally incubated in a glutaraldehyde (GA) solution (MWCNTs+THF+PVC+GA/GC (MWCNTs-TPG/GC)), has demonstrated to be an interesting alternative for amperometric sensing of β -nicotinamide adenine dinucleotide (NADH). MWCNTs-TPG/GC sensor has showed a higher detection sensitivity (approximately 2 times) compared to the bare GC electrode; promotes electronic transference and facilitates the amperometric determination of NADH starting at a potential +0.40 V. In addition, reports a standard deviation of 5%, indicating a good repeatability of the measurements. The potential shift gained due to the use of a polymeric matrix with MWCNTs brings advantages providing relatively lower working potentials in future biosensor applications. The proposed matrix can be easily coupled in the future to suitable dehydrogenases enzymes by means of a crosslinking with biomolecules (i.e. enzymes) that can be easily performed using glutaraldehyde.

Modifications of conventional electrodes with carbon nanofibers (CNFs) have showed in most cases (except treated CNF at gold electrode) lower overpotentials and higher oxidation currents for the detection of NADH comparing to modifications performed with carbon microparticles (CMPs) or graphite. The shown ability of untreated CNF to promote the electron transfer between NADH and the electrode surface suggests an attractive electrocatalytic nanomaterial for development of new amperometric biosensors. In addition to the attractive electrocatalytic properties, the solubility of CNF in dimethylformamide (DMF) facilitates its manipulation for future biosensing applications.

From the dopamine (DA) oxidation has been concluded that the β -cyclodextrin/MWCNTs/glassy carbon electrode (β -CD/MWCNTs/GCE) exhibits highly electrocatalytic activity. The modified electrode provides a higher selectivity in voltammetric measurements of DA. The verification of this enhanced response of the MWCNTs in the presence of β -CD may point out the way toward the use of other supramolecules for the chemical manipulation and processing of MWCNTs for sensor applications. As a result, it is essential to achieve a true understanding of the response enhancement as well as of the nature of such interactions linked with the unique properties of MWCNTs in the presence of a molecular host like β -CD. The use of a combination of host-guest electrostatic interactions with an electron enhancer is a novel aspect allowing a more rational design of analytical strategies that could find application in neuroscience. Studies in this direction are currently underway.

A biosensor for glucose detection based on immobilization of glucose oxidase (GOx) within a rigid carbon nanotube epoxy composite (CNTEC) matrix has been evaluated and the results reveal the ability of CNTEC to promote the electron transfer between the glucose oxidase and the hydrogen peroxide produced by the enzymatic reaction. The reported results were rationalized by the following explanations: (i) The CNTs dispersed in the epoxy resin ensure an electrical contact with GOx better than the graphite particles. This is due to the sponge-like structure of the CNTs that probably achieves improved electrical contacts with GOx. (ii) The CNTs structure ensures better microelectrode arrays compared to graphite particles. This may also enhance the signal to noise ratio that has also been reported for graphite based composites. The CNTs biocomposite based biosensor exhibited excellent sensitivity and stability for the determination of glucose. Moreover, it is simple, it has a fast and reproducible response, and low cost. Nevertheless a future interdisciplinary research, which is under exploitation in our laboratory, could lead to a new generation of electrochemical biosensors based on robust biosensor with better electron transfer including for other enzymes.

Carbon nanotube epoxy composite (CNTEC) electrodes have been developed, characterized and compared with graphite-epoxy composite (GEC) electrodes prepared from the same epoxy resin. According to the obtained results, the CNTEC electrode has shown an improved electrochemistry for glucose. It is also stated that the resulting CNTEC electrode might offer a great promise for biosensing by incorporating other

biomolecules. On the other hand, the modification of conventional GECE with bacterial cells result to be more complicated than for enzymes. Lower operating potential could not be obtained with CNTEC based microbial biosensor. Although the immobilization method used in this modification provides mild conditions in terms of protecting microbial activity the usage of gelatine membrane for immobilization procedure rather than dispersing the cells into the epoxy might have affected the overall response mechanism. On the other hand, higher current values (2 to 3 folds) were observed with CNTEC microbial biosensor when compared with GECE based microbial biosensor. Design of CNTs based arrays might also be promising as a good platform for the bacteria and such arrays can serve for high-throughput screening of chemicals and drugs. Utility of different immobilization matrices, as well as electron transfer mediators to overcome the possible diffusion problems and to get more efficient biosensor systems are under investigation.

The results corresponding to catechol detection have illustrated an attractive construction of renewable biosensors. Tyrosinase maintains its enzymatic properties in the composite matrix; furthermore, the sensing surface can be renewed by a simple polishing procedure resulting in a fresh surface. Various additives may be incorporated into the biocomposite matrix to enhance the analytical performance further. One of the outstanding features of these conducting biomaterials is their rigidity. The proximity of the redox centres of tyrosinase and the carbon nanotubes on the sensing surface favours the transfer of electrons between electroactive species. Composite electrodes modified with CNTs show improved electrochemical properties offering important advantages: i) CNTEC-Tyr exhibit better electronic properties than GECE-Tyr due to the promotion in a very efficient way of electron transfer between o-quinone and CNTEC-Tyr electrode; ii) CNTEC-Tyr shows a detection limit (0.01 mM) almost half of that obtained by GECE-Tyr; iii) CNTs biocomposite offers the possibility for electrode surface renewing forming a new active layer; and lastly iv) The CNTEC-Tyr and GECE-Tyr amperometric biosensors are very attractive for mass fabrication so as to obtain low cost biosensors.

5.2. General conclusions

Several possible applications of CNTs, with emphasis on material science-based applications with interest for sensor design have been described. Remarks are made to the electrochemical applications of CNTs.

The main message is that the unique structure, topology and dimensions along with electrochemical properties make the CNTs an interesting material which can be suitable for a variety of sensors designs. The remarkable physical properties of CNTs create a host of application possibilities. Some of these are based on the novel electronic and mechanical behaviour of CNTs.

Various are the advantages that CNTs bring to the electrochemical sensor designs. Perhaps the most attractive feature of CNTs enzyme based biosensor found up to date is an improved operational stability. Nevertheless, to assess the feasibility and advantages of using CNTs in designing (bio)sensors issues such as how the CNTs are produced and dispersed, the surface chemistry and morphology, effective surface area and presence of metal impurities need to be examined thoroughly and resolved.

The reported works up to date are trying to put in evidence the electrochemical activity of CNTs based electrochemical sensors, including potential shifts compared to the corresponding non-modified sensors. Most of the authors coincide in the fact that the presence of oxidants such as strong acids can open the ends of CNTs or introduce defects in their sidewalls.¹ An acid treatment (purification) also introduces oxygen-containing surface groups (e.g., carboxyl or quinone), which are believed to improve electrocatalytic properties of CNTs. The extent to which different factors affect the electrochemical behaviour depends on the mechanism of the particular redox system. In contrary with this widespread opinion, Musameh et al.² demonstrates that introduction of oxygen functionalities at the end of the caps or the walls does not enhance the electrocatalytic ability of CNTs. Future careful examination of CNTs oxidation phenomena is needed. Compton recently demonstrated evidence that electrocatalytic properties of MWCNTs originate from their ends.^{3,4} He showed that the MWCNTs show the similar electrocatalytic effect as edge planes of highly ordered pyrolytic graphite (HOPG) and carbon powder, while fullerene (fullerene “ball-like” molecule does not contain any “open edges”) modified electrodes showed behaviour similar to basal plane HOPG electrode. This discovery is coherent with Wang’s explanation of

electrocatalytical effect of CNTs and his description of electrochemical activation of MWCNTs.²

5.3. Future perspectives

The exploitation of CNTs in the design of electrochemical (bio)sensors is still in its beginnings. Future efforts should aim at better understanding the structural-electrochemical reactivity of CNTs-modified electrodes and the factors that govern the electron-transfer kinetics of these attractive devices so as to avoid precipitated conclusions in attributing electrocatalytic properties to nanotubes without conducting the appropriate control experiments. It was shown that in some cases the electrocatalytic effect of carbon powder is similar to effect of carbon nanotubes^{3,4} while in other cases there is a huge difference between carbon powder and carbon nanotubes.^{5,6}

The future applications of the developed CNTs based (bio)sensors require further developments in the following directions:

- a) Improve the electrochemical response (sensitivity, detection limit, stability etc.) toward catechol as well as to other phenolic compounds with interest within WARMER project, an FP6 European Project that aims at developing an automatic analyzer of phenolic compounds and heavy metals using electrochemical techniques. This work is now under development by other members of the research group at Institut Català de Nanotecnologia (ICN).
- b) Development of CNTs based screen-printed sensors. These devices will offer several advantages such as cost efficiency, miniaturization beside improvements of the reproducibility. Novel alternatives for dispersing CNTs into other polymeric matrixes and solvents to develop novel CNTs-inks with interest for screen-printing technology of CNTs based conducting electrodes will be studied.
- c) Application of the developed devices in a lab-on-a-chip system to evaluate the electrochemical response so as to improve the sensitivity and operational stability using a minimum volume of sample for future applications in medicine and environmental studies.

5.4. References

- ¹ C.N. Rao, B.C. Satishkumar, A. Govindaraj and M. Nath, *Chem. Phys. Chem.*, 2001, **2**, 78.
- ² M. Musameh, N.S. Lawrence and J. Wang, *Electrochem. Comm.*, 2005, **7**, 14.
- ³ R.R. Moore, C.E. Banks and R.G. Compton, *Anal. Chem.*, 2004, **76**, 2677.
- ⁴ C.E. Banks, R.R. Moore, T.J. Davies and R.G. Compton, *Chem. Commun.*, 2004, **16**, 1804.
- ⁵ J. Wang and M. Musameh, *Anal. Chem.*, 2003, **75**, 2075.
- ⁶ M. Pumera, A. Merkoçi and S. Alegret, *Trends Anal. Chem.*, 2006, **25**, 219.

6

Publications

- 1) **B. Pérez**, J. Sola, S. Alegret and A. Merkoçi. A carbon nanotube PVC based matrix modified with glutaraldehyde suitable for biosensor applications. *Electroanalysis*, 2008, **20**, 603.
- 2) G. Alarcón-Angeles, **B. Pérez-López**, M. Palomar-Pardave, M.T. Ramírez-Silva, S. Alegret and A. Merkoçi. Enhanced host-guest electrochemical recognition of dopamine using cyclodextrin in the presence of carbon nanotubes. *Carbon*, 2008, **46**, 898.
- 3) **B. Pérez**, M. del Valle, S. Alegret and A. Merkoçi. Carbon nanofiber vs. carbon microparticles as modifiers of glassy carbon and gold electrodes applied in electrochemical sensing of NADH. *Talanta*, 2007, **74**, 398.
- 4) Ü.A. Kirgoz, S. Timur, D. Odaci, **B. Pérez**, S. Alegret and A. Merkoçi. Carbon nanotube composite as novel platform for microbial biosensor. *Electroanalysis*, 2007, **19** (7-8), 893.
- 5) **B. Pérez**, M. Pumera, M. del Valle, A. Merkoçi and S. Alegret. Glucose Biosensor based on carbon nanotube epoxy composites. *J. Nanosci. Nanotechnol.*, 2005, **5**, 1694.
- 6) A. Merkoçi, M. Pumera, X. Llopis, **B. Pérez**, M. del Valle and S. Alegret. New materials for electrochemical sensing. VI. Carbon nanotubes. *Trends Anal. Chem.*, 2005, **24**, 826.
- 7) **B. Pérez** and A. Merkoçi. Application of carbon nanotubes in analytical chemistry. American Scientific Publishers, 2008, **2**, 337.

A carbon nanotube PVC based matrix modified with glutaraldehyde suitable for biosensor applications

B. Pérez, J. Sola, S. Alegret and A. Merkoçi

Electroanalysis

2008, **20**, 603-610



Full Paper

A Carbon Nanotube PVC Based Matrix Modified with Glutaraldehyde Suitable for Biosensor Applications

Briza Pérez-López,^{a,b} Joan Sola,^c Salvador Alegret,^b Arben Merkoçi^{a,b,*}

^a Nanobioelectronics & Biosensors Group, Institut Català de Nanotecnologia, Universitat Autònoma de Barcelona 08193 Bellaterra, Catalonia, Spain

^b Grup de Sensors & Biosensors, Departament de Química, Universitat Autònoma de Barcelona, 08193 Bellaterra, Catalonia, Spain

^c Àrea de Química Inorgànica, Departament de Química, Universitat Autònoma de Barcelona, 08193 Bellaterra, Catalonia, Spain

*e-mail: arben.merkoci.icn@uab.es

Received: July 28, 2007

Accepted: November 5, 2007

Abstract

Carbon nanotubes (CNTs) are offering a great promise for developing electrochemical sensors. Distinctive properties of CNTs such as a high surface area, ability to accumulate analyte, minimization of surface fouling and electrocatalytic activity are very attractive for electrochemical sensing. The electrochemical study of a glassy carbon (GC) electrode coated with a matrix based in multiwall carbon nanotubes (MWCNTs), tetrahydrofuran (THF) mixed with poly(vinyl chloride) (PVC) and with a glutaraldehyde (GA) solution (MWCNTs-TPG/GC), for β -Nicotinamide adenine dinucleotide (NADH) detection is discussed in this work using cyclic voltammetry (CV) and chronoamperometry. The used CNTs matrix promotes better the electron transfer of NADH minimizing the fouling effect. The obtained results show remarkable electrochemical and mechanical advantages of MWCNTs-TPG/GC electrode compared to bare glassy carbon electrode with a great promise for future amperometric biosensors applications.

Keywords: Multiwall carbon nanotubes, Glassy carbon electrode, NADH, Polymeric matrix, Electrochemical sensing

DOI: 10.1002/elan.200704119

1. Introduction

The rapid development of new nanomaterials and nanotechnologies has provided many new opportunities for electroanalysis. In particular the unique properties of carbon nanotubes (CNTs) make them extremely attractive for the fabrication of chemical sensors, in general and electrochemical sensors particularly [1].

Recent studies have demonstrated that CNTs exhibits strong electrocatalytic activity for a wide range of compounds, such as neurotransmitters [2], NADH [3, 4], hydrogen peroxide [2, 5, 6], ascorbic [2, 7], and uric acid [2], cytochrome c [8], hydrazines [9], hydrogen sulfide [10], amino acids [11] and DNA [12]. It has been suggested that electrocatalytic properties originate from the ends of CNTs [4].

The study of the oxidation of β -nicotinamide adenine dinucleotide (NADH), a cofactor in NAD^+/NADH -dependent dehydrogenases, has been the subject of numerous studies related to the development of amperometric biosensors. The most important problems to anodic detection are the large overvoltage encountered for NADH oxidation at ordinary electrodes and surface fouling associated with the accumulation of reaction products [13]. For the above reasons significant efforts have been dedicated for identifying new electrode materials that will reduce the overpotential for NADH oxidation and minimize surface passivation effects [3]. Highly sensitive, low-potential and stable

amperometric sensing have been expecting for CNTs based electrodes. Such ability of CNTs to promote the NADH electron-transfer reaction suggests great promise for dehydrogenases-based amperometric biosensors.

The catalytic oxidation of NADH and highly stable amperometric NADH response at glassy carbon electrodes modified with CNTs coatings (dispersed in a solution of concentrated sulfuric acid) have been reported [14]. The CNTs-coating offers a marked (490 mV) decrease in the overvoltage for the NADH oxidation and eliminates surface fouling effects.

Gorski et al. [15] reported an electrochemical sensing platform based on the integration of redox mediators and CNTs in a polymeric matrix. To demonstrate the concept, a redox mediator, Azure dye (AZU), was covalently attached to polysaccharide chains of chitosan (CHIT) and dispersed with CNTs to form composite films for the amperometric determination of NADH. The incorporation of CNTs into CHIT-AZU matrix facilitated the AZU-mediated electrooxidation of NADH. In particular, CNTs decreased the overpotential for the mediated process by an extra 0.30 V and amplified the NADH current by ca. 35 times (at -0.10 V) while reducing the response time from ca. 70 s for CHIT-AZU to ca. 5 s for CHIT-AZU/CNTs films.

Although most of the CNTs based electrodes for NADH detection applications are based on physical adsorption of CNTs onto electrode surfaces usually glassy carbon, how-

ever, it is important to note that CNTs have been also mixed with Teflon [16] or dispersed inside the epoxy resin. This last one, a carbon nanotube-epoxy composite (CNTEC) electrode is reported by our group [17]. CNTEC were constructed from two kinds of MWCNTs differing in the length (0.5–2 and 0.5–200 μm) mixed with epoxy resin. The behavior toward NADH of CNTEC electrodes prepared with different percentages of CNTs has been compared with that of graphite-epoxy composite (GEC) electrode. In all cases CNTEC electrodes provide better reversibility, peak shape, sensitivity and stability compared with GEC electrode. The obtained experimental results demonstrate remarkable electrochemical and mechanical advantages of CNTs composites compared to graphite composites for electrochemical sensing of NADH.

Cyclic voltammetry studies of a sensor based on modification of basal plane pyrolytic graphite (BPPG) electrode with phenothiazine dyes (Toluidine blue (TB) or Azure C) and CNTs for NADH detection have been reported [18]. The results presented that the adsorbed phenothiazine dyes onto the CNTs had a considerable effect upon the redox behavior of NADH achieving oxidative peak potential at lower potentials.

F. Valentini et al. [19] studied the oxidation of NADH at a GC electrode modified by electropolymerization of poly(1,2-diaminobenzene) (1,2-DAB) in the presence of CNTs [20]. The NADH amperometric response of the conducting nanotubule-modified GC electrode showed a peak at 0.63 V with a sensitivity of 99 nA/mM, and an operational stability of 2 days.

Another alternative for the integration of CNTs onto a glassy carbon electrode with interest for NADH detection will be reported. It is based on the use of PVC as a novel matrix for CNTs dispersion as well as to ensure better mechanical/robustness properties of the sensor membrane compared to the use of a CNT layer only. Additionally glutaraldehyde as a matrix linker with great future promises for biosensors applications due to its ability for covalent binding of biological molecules is used. The ability of CNTs to promote the NADH electron-transfer reaction with a great promise for dehydrogenases-based amperometric biosensors will be shown.

2. Experimental

2.1. Materials and Reagents

Multiwall carbon nanotubes (CNT-200: length, 0.5–200 μm ; o.d., 30–50 nm; wall thickness, 12–18 nm; produced by chemical vapor deposition method) were supplied by Aldrich (Stenheim, Germany). The CNTs were purified in HNO_3 to remove impurities such as amorphous carbon, graphite particles, and metal catalysts. Further purification was accomplished by stirring the CNTs in 2 M nitric acid (PanReac, Spain; <http://www.panreac.es>) at 25 °C for 24 h. β -Nicotinamide adenine dinucleotide reduced form (NADH), tetrahydrofuran (THF), poly(vinyl chloride) (PVC), gluta-

raldehyde (GA) solution (50% aqueous solution) and potassium dihydrogenphosphate and potassium hydrogenphosphate were obtained from Sigma. The working solutions (NADH) were prepared daily by dilution in 0.1 M phosphate buffer at pH 7.0 with ultra pure water from a Millipore-MilliQ system.

2.2. Instruments

The SEM images were conducted using a Hitachi S-3200N scanning electron microscope (SEM), equipped with secondary electron detector, backscatter electron detector. The samples were placed on an aluminum stub covered with a carbon adhesive tab (Electron Microscopy Sciences). IR measurements were performed with an FTIR spectrophotometer (BRUKER, TENSILE model 27) equipped with an ATR experimental configuration (SPECAC, model MKII Golden Gate). The samples (in solid form) were prepared in the same way as in the preparation of the modified electrodes.

Cyclic voltammetry (CV) and chronoamperometry experiments were performed using an electrochemical analyzer Autolab 20 (Eco Chemie, The Netherlands) and an LC-4C amperometric detector (BAS) connected to a personal computer with GPES software.

The measurements were carried with a typical cell of 10 mL at room temperature (25 °C), using a three electrodes configuration. A platinum electrode and Ag/AgCl were used as counter and reference electrode, respectively. Glassy carbon (GC) unmodified electrode and GC modified electrode, using a MWCNTs + THF + PVC + GA mixture (MWCNTs-TPG/GC), were used as working electrodes. MWCNTs-TPG/GC electrode was prepared in our laboratory according to the procedure described below. A magnetic stirrer provided the convective transport during the amperometric measurements.

2.3. Preparation and Modification of GC Electrode Surface

CNTs were purified prior to use by a 2 M nitric acid solution. The GC electrode (3 mm in diameter, CH Instrument) was first polished with alumina paper (polishing strips 301044-001, Orion, Spain) and then washed with THF and water (5:5 v/v).

A mixture of MWCNTs + THF + PVC was prepared via dispersing 1.4 mg MWCNTs and 4 mg PVC into a 750 μL of THF by ultrasonication agitation for about 10 min. The GC electrode was coated with 4 μL of the MWCNTs + THF + PVC mixture and finally incubated during 30 seconds in a GA solution (50% aqueous solution), washed with few redistilled water and dried at 40 °C for about 30 min, obtaining a MWCNTs-TPG film onto the GC electrode surface. After the modification, the surface of the MWCNTs-TPG/GC was washed carefully with double distilled water. In brief, it was used as working electrode.

2.4. Electrochemical Measurements

Cyclic voltammetry (CV) and chronoamperometry studies were performed using an electrochemical analyzer Autolab 20 (Eco Chemie, The Netherlands). A Pt wire and Ag/AgCl electrode were used as the auxiliary and reference electrodes, respectively, and the MWCNTs-TPG/GC was used as the working electrode. The amperometric responses to NADH were measured in aliquots of 10 mL of a 0.1 M phosphate buffer solution pH 7.0 where various additions of NADH were then applied onto the reaction cell. The applied potential to the working electrode for NADH determination was +0.70 V for MWCNTs-TPG/GC electrode. The background current was allowed to decay to a constant level before aliquots of NADH sample were added to the stirred buffer solution.

3. Results and Discussion

3.1. Characterization of MWCNTs Dispersed in Different Systems

Before application into a biosensor system the CNTs must be first modified so as to be transformed to a soluble product. The preparation of homogeneous dispersions of CNTs suitable for processing into thin films or for other applications is of a great importance. Various methods can be used for this purpose. Different solubilization procedures have been checked also at our laboratories [21]. End [22] and/or sidewall functionalization [23], use of surfactants with sonication [24], use of polysaccharide solutions [25], protonation by superacids [26] have been reported. CNTs solubilization by covalent modification is also reported by Luong et al. [27]. They solubilized MWCNTs in a mixture of 3-aminopropyltriethoxysilane (APTES) and Nafion-perfluorinated ion-exchange resin in ethanol obtaining a uniformly dispersed MWCNTs suspension for sensor applications.

Although these methods are quite successful, they often indicate cutting the CNTs into smaller pieces (after sonication) or changing the CNTs chemistry (after functionalization), thus partly losing sometime the electrochemical properties of CNTs. The use of polymers for wrapping of carbon nanotubes [28–30] is another simpler alternative.

Tetrahydrofuran and its mixture with poly(vinyl chloride) were firstly used to solubilize the MWCNTs. Figure 1 (A, B) show images of the prepared suspension. While both the above solutions seemed to have a well homogenized aspect a 'floculate' like aspect was observed in the case of the use of the THF mixed with PVC and a GA solution (Fig. 1C). Moreover the above suspension seemed to better adhere onto the electrode surface.

The MWCNTs suspension prepared in the three different mediums were characterized using scanning electron microscopy (SEM), and in addition the above samples were analyzed by using the IR spectroscopy.

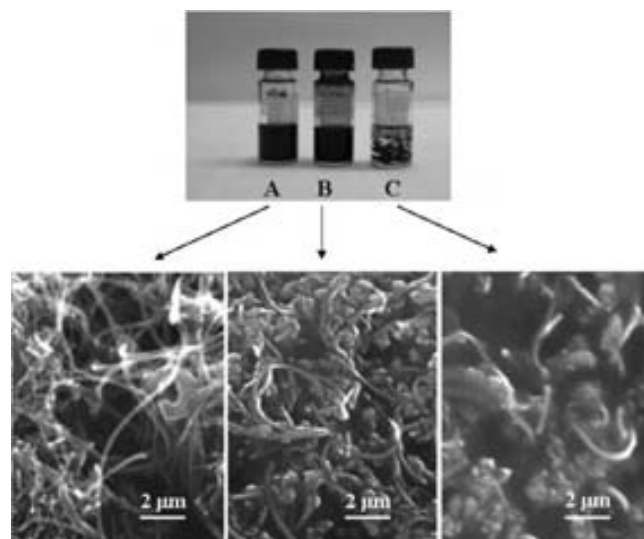


Fig. 1. Upper part: Images of the MWCNTs in THF (A), THF + PVC (B), and in THF + PVC + GA solution (C). Lower part: SEM images of the same solutions as in the upper images. The same acceleration voltage (15 kV) and resolution are used. Others experimental details as explained in the text.

Figure 1 (lower images) displays the SEM images of MWCNTs in: A) tetrahydrofuran; B) THF mixed with poly(vinyl chloride) and C) THF mixed with PVC and a glutaraldehyde solution. The MWCNTs are clearly visualized (Fig. 1A) in the case of THF. Figure 1B shows a SEM image of the MWCNTs mixed with the THF and PVC solution. In difference from the previous 1A image the MWCNTs are now 'loaded' with small aggregates of the PVC. The PVC seems to be attached onto the MWCNTs ensuring by this way a well homogenization of the whole mixture. Figure 1C is the SEM of a similar mixture as 1B but in the presence of glutaraldehyde. The comparison of Figure 1B with Figure 1C reveals (additionally to the upper solution image) that some chemical interactions might have occurred between MWCNTs, PVC and GA. The former, functionalized with carboxylic groups (MWCNT-COOH), might have formed hydrogen bonds (through OH groups) with both, GA and PVC. The hydrogen bonds formed around the nanotubes (case of THF + PVC + GA) seem to have filled the empty voids between individual carbon nanotubes and PVC, thus achieving a better entrapment of MWCNTs-COOH within the THF + PVC + GA matrix compared to the THF + PVC one.

Furthermore, the surface of the GC electrode modified with THF + PVC + GA mixture seemed to be better covered/modified, ensuring a more compact layer and apparently with a higher retention capacity than the one without GA.

The results obtained by SEM images are further supported by the corresponding ATR-IR spectra (see Figure 2) of GC electrodes modified with MWCNTs-COOH in THF (A), THF mixed with PVC (B), and THF mixed with PVC and a GA solution (C). The appearance of peaks at 1730 cm^{-1} corresponding to C=O stretching of carboxylic

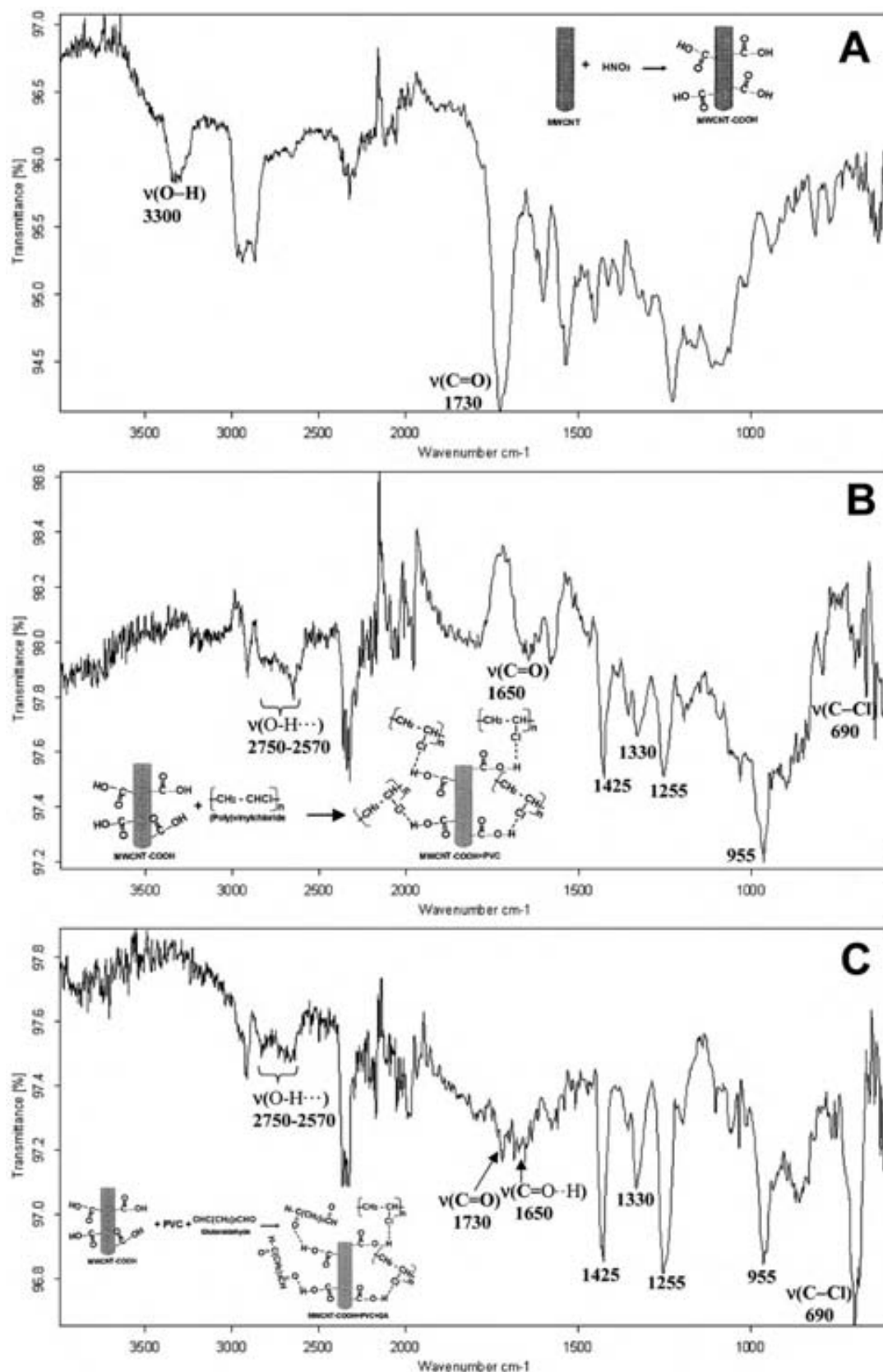


Fig. 2. ATR-IR spectra of GC electrodes modified with MWCNTs-COOH in THF (A), THF + PVC (B), and of this latter incubated in a glutaraldehyde aqueous solution (C). Inset: Scheme proposed to approach interactions in the system (see text). Absorptions between 2000 and 2400 cm^{-1} correspond to atmospheric CO_2 .

groups, and at 3300 cm^{-1} corresponding to hydroxyl groups (Fig. 2A) clearly indicates that $-\text{COOH}$ groups are present on the surface of MWCNTs. While the IR spectrum of Figure 2B shows new signals at 1425 , 1330 , 1255 , 955 , and 690 [$\nu(\text{C}-\text{Cl})$] cm^{-1} corresponding to the PVC matrix, $\nu(\text{O}-\text{H})$ and $\nu(\text{C}=\text{O})$ are shown very broadened, absorbing from 2750 down to 2570 cm^{-1} , and around 1650 respectively, both being downshifted compared to their corresponding values in absence of PVC (spectrum 2A). This can be associated to MWCNT-COO-H \cdots Cl(PVC) hydrogen bonding probably promoting the wrapping of carbon nanotubes by the PVC matrix (Figure 2B).

The spectrum of Figure 2C, closely resembling that of 2B, indicates that upon incubation in GA CNTs are still forming CNT-COO-H \cdots Cl hydrogen bonds with PVC. However, the additional band at 1730 cm^{-1} in 2C can be assigned to the presence in the matrix of GA molecules with a free carbonyl group at one end, but with their second carbonyl at the other end involved in CNT-COO-H \cdots O=C(GA) hydrogen bonding interactions. This would contribute, together with $\nu(\text{C}=\text{O})$ of CNT-COOH (spectrum 2B), to the broad and downshifted band around 1650 cm^{-1} in spectrum 2C. Therefore, once glutaraldehyde is introduced into the matrix (CNT+PVC), it seems to compete with PVC for the same OH groups of CNT but probably without a total displacement of the previously attached PVC. This phenomenon is still unclear and needs further studies but, according to our ATR-IR results, might have likely occurred due to intermolecular hydrogen bonds, as reported in the case of polyethyleneglycol (PEG)/chitosan (CS) where a cross-linked blend is formed [29].

The presence of PVC and GA would of course provoke an opposite effect on the sensor response. Nevertheless a compromise between the advantages of having a binding matrix (PVC for mechanical / stability improvements and glutaraldehyde for future crosslinking with enzymes) and the risks of blocking of CNT ends / extremes exists. The results in the coming section will show that part of the CNT ends should have been still available and probably responsible for the observed improvements.

The composition of the MWCNTs-TPG matrix has been optimized and the values reported (as given in Sec. 2.3) have been chosen as a compromise between the CNT solubility in THF and the corresponding current responses (see following sections).

3.2. Electrochemical Behaviors

3.2.1. Cyclic Voltammetry of NADH at GC Electrodes

Cyclic voltammetries were performed using an electrochemical analyzer Autolab 20 (Eco Chemie, The Netherlands) connected to a personal computer with GPEs software. Figure 3 shows the CVs of a 0.1 M phosphate buffer pH 7 (blank solution) using a bare (a), a MWCNTs + THF + PVC + GA modified (MWCNTs-TPG) (b), and a MWCNTs + THF + PVC modified (c) GC electrode at

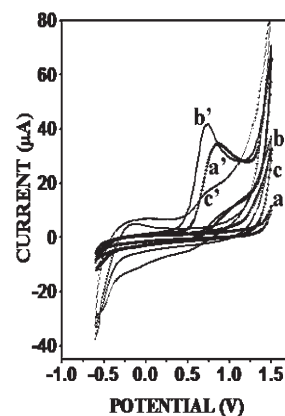


Fig. 3. Cyclic voltammograms (CV) of 0.1 M phosphate buffer pH 7 using a bare (a) and a MWCNTs+THF+PVC+GA modified (b), and a MWCNTs+THF+PVC modified (c) GC electrode. The CV responses (a' for bare, b' and c' for the modified electrodes) toward a 5 mM NADH solution are also shown using the same electrodes. The scan rate was 100 mV/s , potential range: -0.6 to $+1.5\text{ V}$. The composition of the modifying solution was: 1.4 mg MWCNTs, 4.0 mg PVC, $750\text{ }\mu\text{L}$ THF and GA solution. Other experimental details as explained in the text.

100 mV/s , at room temperature (25°C), using a three electrode configuration as it is described previously, as well as the corresponding CVs at the unmodified (a'), MWCNTs-TPG modified (b'), and MWCNTs+THF+PVC (c') GC electrode for a 5 mM NADH solution using the same experimental conditions. Irreversible oxidation processes of NADH for the three electrodes are observed. A significant current coming from NADH oxidation at the MWCNTs-TPG/GC starts to be generated at $+0.5\text{ V}$ with a peak at around $+0.7\text{ V}$. This represents a negative shift of the oxidation potential of around $+0.15\text{ V}$ with respect to bare GC electrode (a'). Moreover a higher current (around $5\text{ }\mu\text{A}$ higher) for the MWCNTs-TPG modified electrode compared to the bare electrode can be observed.

The observed potential shift attained with the use of MWCNTs/PVC/GA matrix will bring advantages providing relatively lower working potentials in future biosensors. This novel MWCNTs/PVC/GA matrix might have future interesting applications in connection to enzyme immobilization by cross-linking these and the glutaraldehyde within the matrix [30]. Moreover this MWCNTs/PVC/GA system may avoid the use of redox mediators that beside their advantages foul the electrode surface [31]. Further, is quite homogenous, ensures good adhesion onto the GC electrode surface and is simple to be applied.

3.2.2. Catalytic Activity of the MWCNTs-TPG/GC Electrode

Evaluate the catalytic activity of the MWCNTs-TPG/GC electrode toward NADH oxidation is of considerable interest. Direct oxidation of NADH is the most common electrochemical approach to NADH detection. However, the electrochemical methods possess some drawbacks due

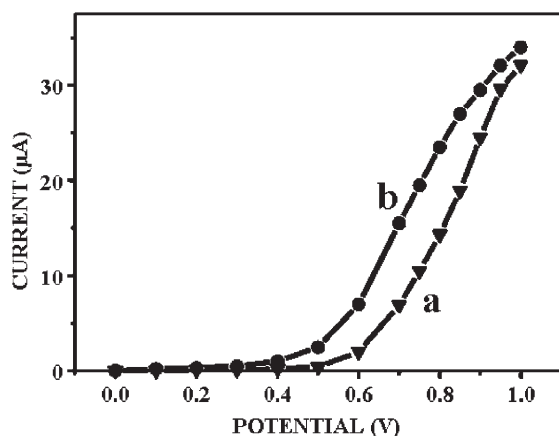


Fig. 4. Hydrodynamic voltammograms for a solution containing 5 mM NADH in 0.1 M phosphate buffer pH 7 using a bare (a) and a modified (b) GC electrode. Other experimental details as explained at Figure 3.

to the high overpotential, interfering side reactions, and electrode fouling. Thus, in the last decade, various strategies have been used to modify electrodes for minimizing these problems [32, 33]. In the case of MWCNTs-TPG/GC, as it was already reported, there is a catalytic effect on the oxidation of NADH, making a higher sensitive detection of this compound compared to the bare GC electrode.

Figure 4 shows the influence of applied potentials from 0 to +1.0 V at the bare (a) and a MWCNTs-TPG modified (b) GC electrode. These hydrodynamic voltammograms show the response of each electrode in the presence of 5 mM NADH in 0.1 M phosphate buffer pH 7 under constant agitation. The oxidation of NADH starts at potential +0.40 V for the modified electrode (b) while for the bare GC the NADH oxidation starts at +0.50 V. Moreover, the current signal for MWCNTs-TPG/GC electrode is higher than for the bare electrode. A potential shift of around $\Delta E = +100$ mV is clearly observed. The MWCNTs + THF + PVC + GA film onto the GC electrode significantly promotes its electronic transference and facilitates the amperometric determination of NADH.

3.2.3. Amperometric Detection of NADH at Modified Electrode

3.2.3.1. Responses to Lower NADH Concentrations

Figure 5 compares the chronoamperograms of the MWCNTs-TPG/GC electrode for successive additions of 0.1 mM NADH at three different potentials: +0.5 V (a), +0.6 V (b), and +0.7 V (c) in 0.1 M phosphate buffer pH 7. At potential +0.5 V, a detectable but small current response was observed toward the direct detection of 0.1 mM NADH. The catalysis of NADH at potential +0.6 V and consequently the current response toward NADH was also relatively small. However, at potential +0.7 V the modified electrode responded more sensitively in comparison to lower working potentials. Corresponding calibration plots (see insets at Fig. 5) are also shown. For the three working

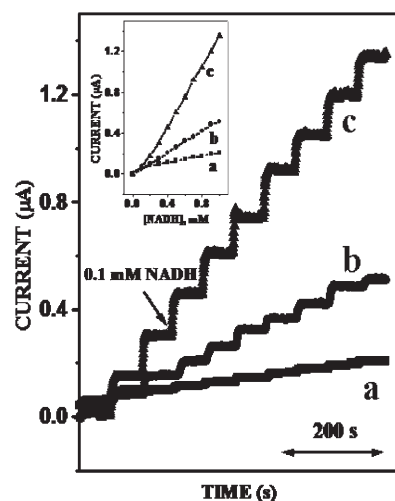


Fig. 5. Current-time recordings obtained from amperometric experiments at GC modified electrode for successive additions of 0.1 mM NADH. Working potential: +0.5 V (a), +0.6 V (b) and +0.7 V (c) in 0.1 M phosphate buffer pH 7. Inset: Corresponding calibration plots.

potentials used the MWCNTs-TPG/GC electrode exhibits a linear response range of 0.1 to 1.0 mM with correlation coefficients of 0.978, 0.999, 0.998, respectively.

3.2.3.2. Responses to Higher NADH Concentrations

The amperometric responses of the bare GC and MWCNTs-TPG/GC electrodes to NADH at ten times higher concentration ranges (comparing the previous results) are shown at Figure 6. The steps correspond to the responses of bare (a) and modified (b) GC electrode for successive additions of 1.0 mM NADH to stirring 0.1 M phosphate buffer solution at pH 7.0. The resulting calibration plots (insets) are also shown. It can be observed that MWCNTs-TPG/GC electrode offers substantially higher signal compared to bare electrode using a working potential of +0.70 V. The sensitivity of the modified GC electrode for NADH determination, found to be approximately 2 times larger than for the bare electrode, is clearly visualized in the Figure 6.

In the calibration curves (insets) the plots of current vs. NADH concentration has a linear concentration range of 1.0–10 mM for both the bare (a) and the modified (b) GC electrode. The correlation coefficients were 0.999 (both a and b) and the corresponding detection limits of 0.088 mM and 0.085 mM respectively. The corresponding calibration plots show sensitivities of $5 \mu\text{A mM}^{-1}\text{cm}^{-2}$ for bare electrode and $13 \mu\text{A mM}^{-1}\text{cm}^{-2}$ for MWCNTs-TPG/GC electrode. In addition, for the MWCNTs-TPG/GC electrode, a set of 3 different amperometric measurements for 1 mM NADH with a single electrode yielded a relative standard deviation of 5%, indicating a good repeatability of the measurements. However, for the unmodified GC electrode the RSD is of 14% which might be related also with a possible fouling of the bare GC electrode.

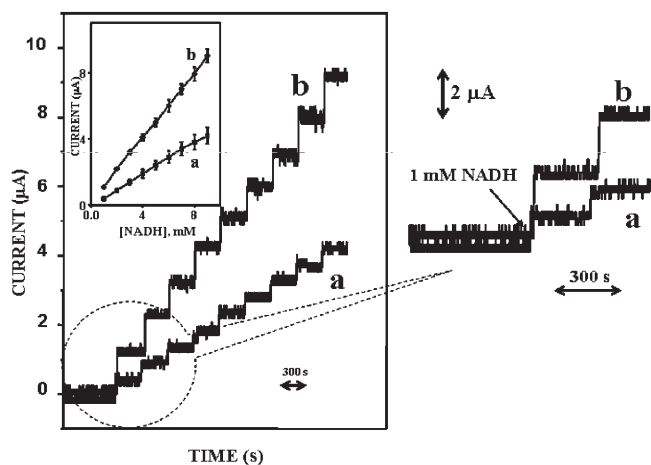


Fig. 6. Current–time recordings including (as inset) the corresponding calibration plots obtained from amperometric experiments at unmodified (a) and at modified (b) GC electrode for successive additions of 1 mM NADH in 0.1 M phosphate buffer pH 7. Working potential: +0.7 V. The stability of the response (as zoom of the left recordings) is shown for each electrode used. Experimental conditions as in Figure 3.

3.2.3.3. Stability Test

The response stability during the chronoamperometric measurements is a very important issue. For that reason the stability of the MWCNTs-TPG/GC electrode during the chronoamperometric detection of NADH was studied using the same conditions as those applied for NADH detection explained previously. The response stability was checked during each step of the amperometric response of 1 mM NADH at MWCNTs-TPG/GC electrode at operating potential of +0.7 V. The right steps are a zoom of the two current time responses (Fig. 6) showing the stability of the MWCNTs-TPG/GC electrode toward NADH over around 20 seconds of response time. It can be observed that the current obviously increases after the addition of NADH maintaining then a steady state response thereafter.

4. Conclusions

A new alternative for the integration of CNTs onto a glassy carbon electrode with interest for NADH detection have been shown. We found differences in the electrochemical activity between the CNTs-modified electrode and the unmodified electrode (GC treated in the same way but without the polymeric matrix). Some authors attributed this difference to surface chemistries (primarily to defect densities) of the corresponding CNTs layers, associated with the different production and dispersion protocols [34].

This work demonstrates that the modification of GC electrode with a mixture of MWCNTs + PVC + THF + GA represents an interesting alternative for NADH based amperometric biosensors. MWCNTs-TPG/GC electrode shows a higher detection sensitivity (approximately 2 times)

compared to the bare GC electrode; promotes electronic transference and facilitates the amperometric determination of NADH starting in a potential +0.40 V. In addition, reports a standard deviation of 5%, indicating a good repeatability of the measurements. The potential shift gained due to the use of a polymeric matrix with MWCNTs will bring advantages providing relatively lower working potentials in future biosensor applications.

The biosensor fabrication based on the MWCNTs-TPG matrix would be easier and the obtained membrane more stable from mechanical point of view compared to other modifications using CNT. It will allow an easier detection of NADH without the use of any redox mediator. The proposed matrix can be easily coupled in the future to suitable dehydrogenases enzymes by means of a cross-linking with biomolecules (i.e. enzymes) that can be easily performed using glutaraldehyde.

5. Acknowledgements

A. M. thanks the Spanish Foundation “Ramón Areces” (Project ‘Bionanosensores’) and MEC (Madrid) for the Projects MAT2005-03553 and Consolider Nanobiomed.

6. References

- [1] M. Valcárcel, C. Bartolomé, S. S. Cárdenas, C. B. Suárez, *Anal. Bioanal. Chem.* **2005**, *382*, 1783.
- [2] H. Luo, Z. Shi, N. Li, Z. Gu, Q. Zhuang, *Anal. Chem.* **2001**, *73*, 915.
- [3] M. Musameh, J. Wang, A. Merkoci, Y. Lin, *Electrochem. Commun.* **2002**, *4*, 743.
- [4] R. R. Moore, C. E. Banks, R. G. Compton, *Anal. Chem.* **2004**, *76*, 2677.
- [5] J. Wang, M. Musameh, *Anal. Chem.* **2003**, *75*, 2075.
- [6] S. Hrapovic, Y. Liu, K. B. Male, J. H. T. Luong, *Anal. Chem.* **2004**, *76*, 1083.
- [7] Z. H. Wang, J. Liu, Q. L. Liang, T. M. Wang, G. Luo, *Analyst* **2002**, *127*, 653.
- [8] J. Wang, M. Li, Z. Shi, N. Li, *Anal. Chem.* **2002**, *74*, 1993.
- [9] Y. Zhao, W. D. Zhang, H. Chen, Q. M. Luo, *Talanta* **2002**, *58*, 529.
- [10] N. Lawrence, R. P. Deo, J. Wang, *Anal. Chim. Acta* **2004**, *517*, 131.
- [11] J. X. Wang, M. X. Li, Z. J. Shi, N. Q. Li, Z. N. Gu, *Electroanalysis* **2004**, *16*, 140.
- [12] M. L. Pedano, G. A. Rivas, *Electrochem. Commun.* **2004**, *6*, 10.
- [13] C. Lau, G. U. Flechsig, P. Gründler, J. Wang, *Anal. Chim. Acta* **2005**, *554*, 74.
- [14] M. Musameh, J. Wang, A. Merkoci, Y. Lin, *Electrochem. Commun.* **2002**, *4*, 743.
- [15] M. Zhang, W. Gorski, *Anal. Chem.* **2005**, *77*, 3960.
- [16] J. Wang, M. Musameh, *Anal. Chem.* **2003**, *75*, 2075.
- [17] M. Pumera, A. Merkoci, S. Alegret, *Sens. Actuators B, Chem.* **2006**, *113*, 617.
- [18] N. S. Lawrence, J. Wang, *Electrochem. Commun.* **2006**, *8*, 71.
- [19] F. Valentini, A. Salis, A. Curulli, G. Palleschi, *Anal. Chem.* **2004**, *76*, 3244.

- [20] M. Badea, A. Curulli, G. Palleschi, *Biosens. Bioelectron.* **2003**, *18*, 689.
- [21] A. Merkoci, *Microchim. Acta.* **2006**, *152*, 157.
- [22] J. Chen, M. A. Hamon, H. Hu, Y. Chen, A. M. Rao, *Science* **1998**, *282*, 95.
- [23] D. Tasis, N. Tagmatarchis, V. Georgakilas, M. Prato, *Chem. Eur. J.* **2003**, *9*, 4000.
- [24] M. F. Islam, E. Rojas, D. M. Bergey, A. T. Johnson, A. G. Yodh, *Nano Lett.* **2003**, *3*, 269.
- [25] M. Zhang, A. Smith, W. Gorski, *Anal. Chem.* **2004**, *76*, 5045.
- [26] S. Ramesh, L. M. Ericson, V. A. Davis, R. K. Saini, C. Kittrell, M. Pasquali, W. E. Billups, W. Adams, R. H. Hauge, R. E. Smalley, *J. Phys. Chem. B* **2004**, *108*, 8794.
- [27] J. H. T. Luong, S. Hrapovic, D. Wang, F. Bensebaa, B. Simard, *Electroanalysis* **2004**, *16*, 132.
- [28] A. Star, J. F. Stoddart, D. Steurman, M. Diehl, A. Boukai, E. W. Wong, X. Yang, S. W. Chung, H. Choi, J. R. Heath, *Angew. Chem. Int. Ed.* **2001**, *40*, 1721.
- [29] W. H. Jiang, S. J. Han, *J. Polym. Sci., Part B: Polym. Phys.* **1998**, *36*, 1275.
- [30] M. In het Panhuis, V. N. Paunov, *Chem. Commun.* **2005**, 1726.
- [31] C. R. Raj, S. Behera, *Biosens. Bioelectron.* **2005**, *21*, 949.
- [32] C. X. Cai, X. Ju, H. Y. Chen, *Anal. Chim. Acta* **1995**, *310*, 145.
- [33] L. Gorton, G. Bremle, E. Csöregi, G. Jönsson-Pettersson, B. Persson, *Anal. Chim. Acta* **1991**, *249*, 43.
- [34] A. Merkoçi, M. Pumera, X. Llopis, B. Pérez, M. del Valle, S. Alegret, *Trends Anal. Chem.* **2005**, *24*, 9.



The Second Edition!

Elements and their Compounds in the Environment

Occurrence, Analysis and Biological Relevance

2nd completely revised and enlarged edition
3 Volume Set

Edited by E. MERIAN, M. ANKE, M. IHNAT
and M. STOEPLER

- The "Merian" is the established standard reference on this topic.
- This new edition is more clearly and concisely structured, with more emphasis on nutritional aspects.
- All contributions are revised and updated to present the current state of knowledge.
- Further elements, including some non-metals of nutritional importance, have been added.
- Essential information for chemists, biologists, geologists, food scientists, toxicologists and physiologists involved in environmental research and remediation, risk assessment, food research and industrial hygiene.

Wiley-VCH,
Customer Service Department,
Fax: +49 (0) 6201 606-184,
E-Mail: service@wiley-vch.de,
www.wiley-vch.de

John Wiley & Sons, Ltd., Customer Services
Department, Fax: +44 (0) 1243-843-296,
E-Mail: cs-books@wiley.co.uk,
www.wiley.com

John Wiley & Sons, Inc., Customer Care,
Fax: +1 800-597-3299,
E-Mail: custserv@wiley.com,
www.wiley.com

 WILEY-VCH

 WILEY

 WILEY
1807-2007 KNOWLEDGE FOR GENERATIONS

For your order:

ISBN 978-3527-30459-2
2004
1774pp with 97 figs and 377 tabs
Hbk
€ 629.00 / £ 400.00 / US\$ 760.00

Enhanced host–guest electrochemical recognition of dopamine using cyclodextrin in the presence of carbon nanotubes

G. Alarcón-Angeles, **B. Pérez-López**, M. Palomar-Pardave, M.T. Ramírez-Silva, S. Alegret and A. Merkoçi

Carbon

2008, **46**, 898-906



available at www.sciencedirect.comjournal homepage: www.elsevier.com/locate/carbon

Enhanced host–guest electrochemical recognition of dopamine using cyclodextrin in the presence of carbon nanotubes

G. Alarcón-Angeles^{a,b}, B. Pérez-López^{a,c}, M. Palomar-Pardave^d, M.T. Ramírez-Silva^{b,*}, S. Alegret^c, A. Merkoçi^{a,*}

^aInstitut Català de Nanotecnologia, Campus UAB, 08193 Bellaterra, Barcelona, Catalonia, Spain

^bUniversidad Autónoma Metropolitana-Iztapalapa, Área de Química Analítica, Laboratorio R-105, San Rafael Atlixco #186, Col. Vicentina, C.P. 09340 México, D.F., Mexico

^cUniversitat Autònoma de Barcelona, Grup de Sensors i Biosensors, Departament de Química, E-08193 Bellaterra, Barcelona, Spain

^dUniversidad Autónoma Metropolitana-Azcapotzalco, Departamento de Materiales, Laboratorio de Electroquímica y Corrosión, Edificio 3P. Av. San Pablo 180, Col. Reynosa-Tamaulipas, C.P. 02200 México, D.F., Mexico

ARTICLE INFO

Article history:

Received 25 March 2007

Accepted 21 February 2008

Available online 4 March 2008

ABSTRACT

A novel application of multiwall carbon nanotubes (MWCNT) for biosensor use is presented. β -Cyclodextrin (β -CD) as molecular receptor and MWCNT as enhancer of electron transfer are integrated in a dopamine (DA) electrochemical sensor system. The proposed molecular host–guest recognition based sensor has a high electrochemical sensitivity for the determination of DA. The electrochemical behaviour of DA is investigated by cyclic voltammetry (CV). The response mechanism of the MWCNT/ β -CD modified electrode for DA is based on the combination of electrostatic and inclusion interaction of β -CD with DA which is distinguished from the response mechanism of non-modified electrode. The proposed integrated sensor showed improved analytical performance characteristics in catalytic oxidation of DA compared with non-modified electrode: excellent sensitivity, repeatability, stability, selectivity and recovery for the determination of DA. Under optimized conditions linear calibration plots were obtained for amperometric detection of DA over the range 0.01–0.08 mM.

© 2008 Elsevier Ltd. All rights reserved.

1. Introduction

The various forms of carbon are being used, beside several other applications, as building blocks for sensors and biosensors with interest for (bio) analytical applications. The research in the field of carbon material applications for sensors is still a hot topic due not only to the new exciting forms of carbons (tubes, fibers, single graphene layers) but also to the great demands for sensing analytes with clinical, environmental or industrial interest. Some of the carbon

properties with great importance in sensor applications are being discovered in connection to other modifying materials that can bring additional advantages to these carbon materials. The combination of a carbon material such as carbon nanotubes (CNT) with cyclodextrin represents a novel matrix for dopamine detection sensors. This novel hybrid material matrix can be used as model that can be extended to other analytes.

Usually glassy carbon electrodes (GCE) have been mostly reported in view of their electrochemical properties, basically

* Corresponding authors: Fax: +34 935812379 (A. Merkoçi); fax: +52 55 58044666 (M.T. Ramírez-Silva).

E-mail addresses: mtrs218@xanum.uam.mx (M.T. Ramírez-Silva), arben.merkoci.icn@uab.es (A. Merkoçi).

0008-6223/\$ - see front matter © 2008 Elsevier Ltd. All rights reserved.

doi:10.1016/j.carbon.2008.02.025

because they are chemically inert, display a wide potential range and a low current in the blank being such a way appropriate devices for detecting various analytes [1–5]. The use of modified electrodes may allow avoiding interferences from other analytes while satisfying other basic requirements such as the low chemical and ohmic resistance coupled to a wide potential range, high sensitivity, selectivity and reproducibility. The search for an improvement of electrochemical properties has led to the design and development of diverse surface-modified electrodes such as those based on Nafion or polyaniline [3,6]. However, these electrodes have shown slow responses due to the analyte's diffusion coefficient on the surface film [7,8].

Since 1991, when Iijima reported on the existence of carbon nanotubes (CNT) various electrodes have been currently modified with this material because of its particular physical, chemical and electrochemical features [9–12]. When used as electrode or electrode modifier CNT are known for their ability to mediate electron-transfer reactions with electroactive species present in solution [13–22]. Therefore the integration of CNT into detection biosystems seems to be with special interest.

The efforts have been considerable to improve significantly the analytic determinations of dopamine (DA). DA is a neurotransmitter that in a similar way as adrenaline serves as chemical messenger. It affects the brain processes that control movement, emotional response, and the capacity to feel pleasure and pain. DA is vital for performing balanced and controlled movements having an important role within the biological context. Measurements of abnormal concentrations have been associated with neurological illnesses such as Parkinson's or schizophrenia [15].

Several analytic methods such as chromatography [16–19] or electrochemical methods [20,21] have been used to determine this neurotransmitter. Electrochemical techniques have been considered very attractive in view of their high sensitivity and selectivity. In addition the measurements can be carried out directly because the electrodes employed may be designed in the form that allow the *in situ* determinations.

The interference due to the presence of ascorbic acid (AA) is one of the problems faced while determining DA [22]. AA has a similar oxidation potential and is usually present *in vivo* at concentrations 10^2 – 10^3 times higher than DA. Therefore, it is essential to establish simple and rapid methods for selective determination of DA in routine analysis.

Wu and Hu [23], studied the electrochemical behaviour for DA by using a glassy carbon electrode (GCE) modified with a homogeneous and stable suspension of MWCNTs in ethanol solution of Nafion. MWCNTs-Nafion modified GCE not only improves the redox peak currents but also makes the redox reaction of DA more reversible [24].

The combination of the CNTs electrocatalytic activity with the known advantages of other compounds seems to be a very important alternative for new electroanalytical challenges. Molecules as cyclodextrin (CD) are used to stabilize, dissolve, retain and liberate in a controlled way, a large number of organic or inorganic chemicals through the formation of inclusion complexes. Moreover CD has been studied in relation to different compounds where used as recognition

agents and to study the adsorption phenomena related to electrode interactions.

Taking into consideration the electrochemical properties of CNTs as well as the reported properties of CD this work proposes a novel strategy based on the simultaneous modification of a glassy carbon electrode with a novel CNT cyclodextrin matrix. The chemical recognition of DA by the use of CD is combined with the added advantage of a faster electron transfer process due to the CNT present at the electrode interface.

In this work the DA oxidation in the surface of the electrode is enhanced by its diffusion through the CD cavities and the easy contact with the dispersed MWCNTs that facilitate the electron transfer. The operability of this system is compared with the DA detection using glassy carbon electrode without modifications (presence of CD or MWCNT) so as to verify the contribution of CD and MWCNT in the electrochemical detection.

2. Experimental

2.1. Reagents and equipment

2.1.1. Reagents

All reagents were of analytical grade: the dopamine (DA) and β -cyclodextrin (β -CD) used were from Sigma, while the KH_2PO_4 and K_2HPO_4 were from Fluka. The multiwall carbon nanotubes (MWCNT) (0.5–200 μm) were from Aldrich (Stenheim, Germany) and contains 95% MWCNT. All solutions were prepared with deionized water type 1 with 18.2 M Ω resistivity, free from organic matter, obtained from a US Filter PURE-LAB Plus UV, deaerated with nitrogen and freshly prepared prior to each determination.

2.1.2. Equipment

The electrochemical studies were carried out using a conventional three-electrode cell with Pt as counter electrode and Ag/AgCl as reference. Glassy carbon electrodes (GCE) (from CH Instrument, Texas, USA) modified or not with MWCNT-CD were used as working electrodes. All electrochemical measurements, such as cyclic voltammetry and amperometry were carried out with the aid of an electrochemical analyzer Autolab 20 and a PC for experimental parameter control and data acquisition. All measurements were conducted under the presence of a nitrogen atmosphere at a 25 ± 1 °C temperature. The scanning electronic microscopy images from the MWCNT-CD films were obtained with the aid of a Hitachi S_3200N SEM.

2.2. Electrode modification with MWCNT- β -CD film

In order to eliminate metal impurities the carbon nanotubes were dispersed in 2 M nitric acid solution during 24 h at 25 °C, and washed afterwards with deionized water to neutrality and finally dried in accordance with the procedure outlined by Pérez et al. [25].

The MWCNT were checked by scanning electron microscopy JEOL JSM-6300 (SEM, JEOL LTD, Tokyo, Japan) with microanalysis equipped by an X-ray energy dispersive spectrometer (EDS) (Link ISIS-200, England) in order to evaluate the amount

of impurities (remained from their synthesis) before and after washings with HNO_3 .

A quantity of 1 mg of MWCNT was ultrasound-dissolved then in 1 mL of β -CD at 10%. Ten microliters of this solution was introduced over the GCE, the surface of which have been previously prepared by applying the polishing procedures recommended (CH Instrument, Texas, USA). The electrode was left during 30 min to be dried at 60 °C and after that washed carefully with small portion of deionized water before used. The modified electrode was kept at room temperature when it is not used.

3. Results and discussion

3.1. Purification of MWCNT

The study by SEM and the corresponding microanalysis show that the traces of iron (Fe), nickel (Ni) and potassium (K) from

0.5%, 1.6% and 1.5% were decreased to 0.1%, 0.9% and 0.4% after treatment with nitric acid as described in Section 2.2.

3.2. Characterization of materials by SEM

Fig. 1 shows the SEM images of MWCNT, β -CD and MWCNT/ β -CD. It is possible to observe the tube morphology of MWCNT (A) and the small sheets/layers of β -CD (B). The MWCNT/ β -CD agglomerates (C) is also shown. The β -CD sheets, not observed now, should have been covered by CNTs due to electrostatic interactions [23].

The immobilization capability of CNT is combined with the β -CD adsorption property, a well known phenomena occurring onto carbon [26]. Additionally the host-guest interaction ability of CD is combined now with its facility to disperse MWCNTs that additionally enhance the electrochemical detection of DA.

Fig. 2 is a schematic (not in scale) of the sensor used. Although β -CD is water soluble and the quantity added onto

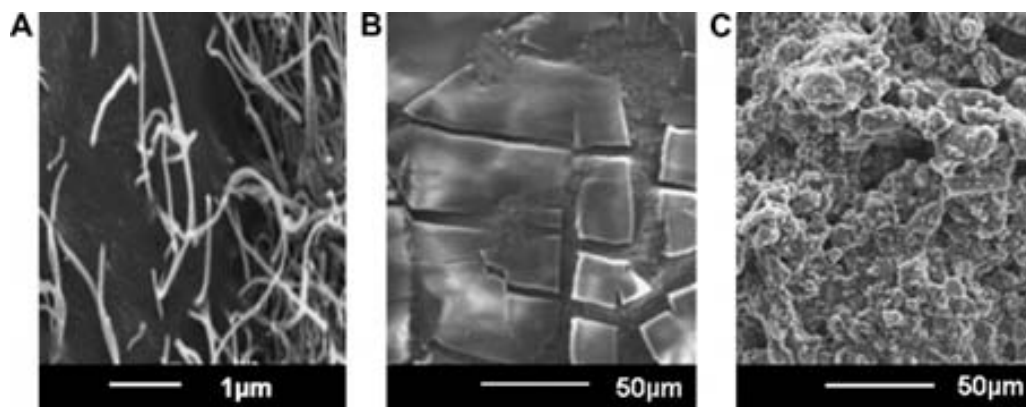


Fig. 1 – SEM images of (A) MWCNT, (B) β -CD and (C) MWCNT/ β -CD.

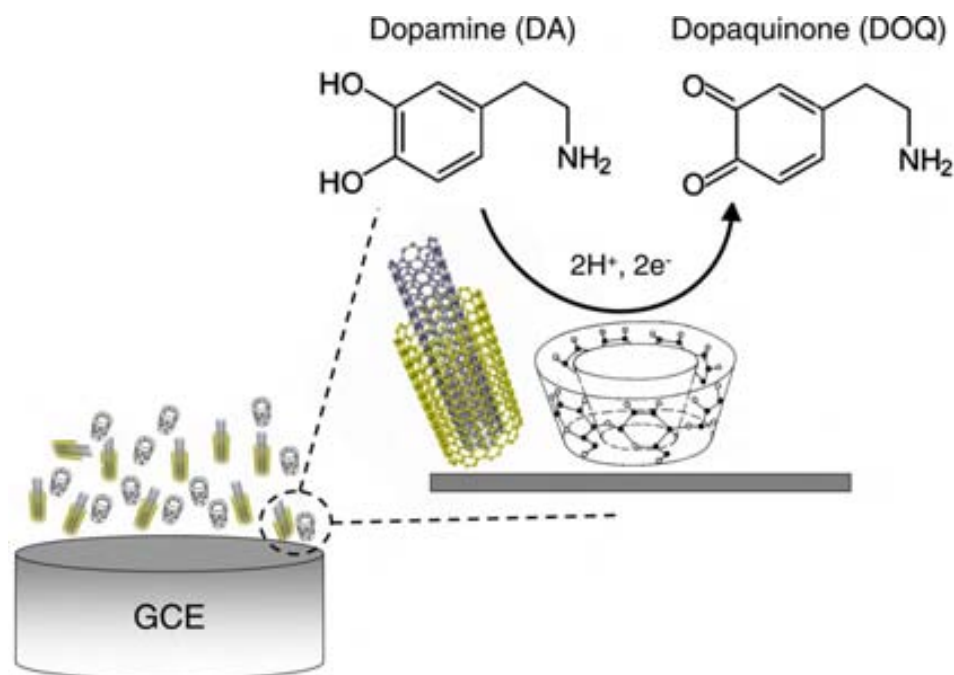


Fig. 2 – Schematic (not in scale) of the electrochemical sensor modified with the MWCNT/ β -CD matrix. The dopamine oxidation reaction is also shown.

the electrode surface was in excess enough, an important part still remained after electrode washing prior the use. CNT net created also facilitates the β -CD entrapment/adsorption. Moreover the presence of β -CD even after using the modified electrode was easily detected even by naked eyes (a white grey colour appears) compared with a glassy carbon modified electrode with CNT via sulphuric acid reported earlier [27].

Fig. 2 is a schematic representation of the electrode construction. MWCNTs dispersed into the β -CD solution are used as modifier of the glassy carbon electrode. The DA oxidation in the surface of the electrode is enhanced by its diffusion through the β -CD cavities and the easy contact with the dispersed MWCNTs that facilitate the electron transfer. Shown is also the SEM image of the MWCNT/ β -CD mixture (percentage as in the text) used to modify the GCE.

3.3. Glassy carbon electrode without modifications

3.3.1. Voltammetric behaviour and pH effect

The electrochemical behaviour of the DA at different pH values was studied. Fig. 3 shows the CV of dopamine (DA) in the presence of a 0.01 M phosphate buffer at pH 3.4 and 7.4 by

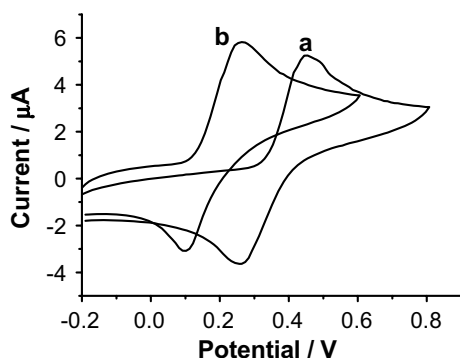


Fig. 3 – Cyclic voltammograms recorded in 0.2 mM DA and 0.01 M phosphate buffer. (a) pH 3.4 and (b) pH 7.4. Working electrode, GCE. The GCE was pretreated by performing several scans on the blank (until receiving a stable CV) and then the DA was added.

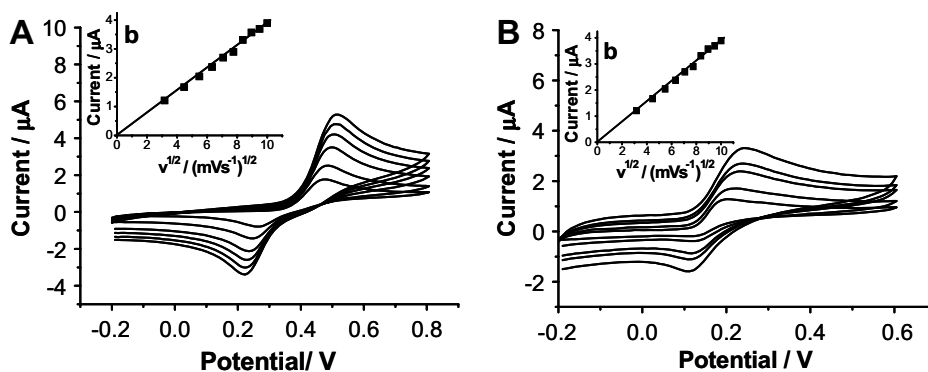


Fig. 4 – Cyclic voltammograms of DA 0.1 mM in 0.01 M phosphate buffer at (A) pH 3.4 and (B) pH 7.4, at different potential scan rates: 0.01, 0.02, 0.04, 0.06, 0.08, and 0.1 V s⁻¹. The insets show the corresponding calibration plots of anodic current as a function of scan rate using a GCE.

using a glassy carbon electrode (GCE) without any modification. In both cases the DA exhibits a quasi-reversible behaviour. The difference between the anodic peak potential E_{pa} and that of the cathodic peak E_{pc} at pH 3.4 is given as $\Delta E_p = 262$ mV while at pH 7.4 the $\Delta E_p = 151$ mV, both obtained at a potential scan rate of 0.1 V s⁻¹. Therefore, the process appears more reversible at the higher pH. Moreover the electron transfer process at pH 7.4 is faster because the oxidation peak appeared at more negative potential than at pH 3.4.

The electrochemical behaviour of the DA at both pH 3.4 and 7.4 reveals that the anodic peak potential is shifted to more negative values as the pH increases, which is thought to be due to the fact that deprotonation favours the oxidation process. Thus, given that the first deprotonation [28] exhibits a pK_a 9.05, then at pH 7.4 the oxidation process seems to occur easier than at pH 3.4. This leads to suggest that it should be appropriate to undertake further electrochemical characterization of the DA as a function of the potential scan rate.

3.3.2. Scan rate study

Fig. 4 shows the voltammograms recorded as a function of the scan rate in the 0.1 mM DA solution at pH 3.4 and 7.4. It can be observed that the scan rate affects the position of the oxidation peaks. E_{pa} shifts toward more positive potentials as the rate increased, whereas the reduction peak E_{pc} shifts toward more negative potentials. The peak differences for E_{pa} and E_{pc} are 30 mV and 170 mV, respectively, with increasing scan rate from 0.01 to 0.1 V s⁻¹. Further analysis of the results indicate that the anodic peak current increases linearly with the square root of the rate, with a linear correlation coefficient of 0.992 at pH 3.4, thus implying that the DA oxidation at GCE is a diffusion-controlled process.

The hydrodynamic voltammogram (HDV) data are very important for selecting the operational potential for amperometric measurements. In order to obtain HDV, the currents at various potentials are determined after stepping the voltage from some initial value, where the reaction does not occur, to potentials where the current remains constant. The obtained currents were then plotted vs. the applied potential (see Fig. 5). Considering the results of the hydrodynamic voltammetry of the 0.1 M DA at pH 3.4 (see Fig. 5a) and at pH 7.4 (see Fig. 5b) using the glassy carbon electrode, it becomes apparent that at potentials smaller than 200 mV (pH 3.4)

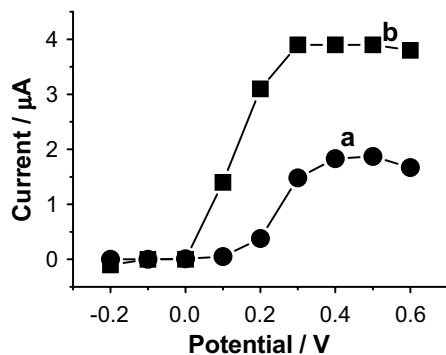


Fig. 5 – Hydrodynamic voltammograms of 0.1 mM DA with GCE at (a) pH 3.4 and (b) pH 7.4 in 0.1 mM phosphate buffer.

and 100 mV (pH 7.4) there is no redox activity. However at greater potentials there appears a gradual increase in the response thus suggesting that the glassy carbon electrode responds to the oxidation of the DA within the 200–400 mV potential range (reaching the maximum at 400 mV) at pH 3.4 and within the 100–300 mV potential range (reaching the maximum at 300 mV) at pH 7.4, which is in agreement with the cyclic voltammetry behaviour. Therefore, according to the hydrodynamic voltammetry results the condition to be used for the amperometric detection seems to be 0.3 V (pH 7.4) and 0.5 V (pH 3.4) after which the electrode responses reach maximums and remain stable.

3.3.3. Amperometric detection of DA with GCE

In order to proceed with the DA determination at pH 3.4 and 7.4, it was appropriate to study the DA's oxidation response. Fig. 6 shows a typical current–concentration plot for successive additions of DA in the 0.1 mM to 1 mM range under stirring conditions. It is noted that at pH 7.4 the response decreases rapidly after the DA reaches the concentration of 0.4 mM, whereas at pH 3.4 the response keeps increasing until the concentration of DA of 0.8 mM and remaining then almost constant.

There was no linear correlation between both pH values in the concentration range used in this work, which means that

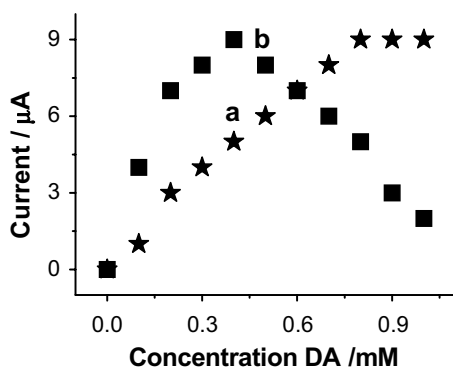


Fig. 6 – Amperometric calibration plots with GCE at (a) pH 3.4 with an applied potential of 0.5 V and (b) pH 7.4 with an applied potential of 0.3 V for successive additions of 0.01 mM DA, in 0.01 M phosphate buffer.

DA detection becomes difficult. However, in the concentration range below 0.5 mM, the linear correlation coefficient improves attaining the value of 0.99 for both pH values.

3.4. MWCNT/ β -CD modified electrode

3.4.1. Cyclic voltammetry

With the aim to improve the response toward DA, it became necessary to modify the surface of a GCE with a film of CNTs and β -cyclodextrin obtaining a modified electrode: GCE/MWCNT/ β -CD. Fig. 7A and B shows the voltammograms recorded for 0.1 mM DA in phosphate buffer at pH values of 3.4 and 7.4, respectively, using a potential scan rate of 0.1 V s⁻¹.

The oxidation peak of DA using the GCE/MWCNT/ β -CD (see Fig. 7) appears at potentials more negative than non-modified GCE (see Fig. 3 and Table 1 for comparison data). The potential differences between E_{pa} and E_{pc} , for the GCE/MWCNT/ β -CD are $\Delta E_p = 83$ mV at pH 3.4 and $\Delta E_p = 63$ mV at pH 7.4. This means that the MWCNT/ β -CD surface film deposited onto the GCE electrode surface increases the electron transfer process compared to the bare GCE. The ratio of the currents was $I_a/I_c = 0.75$ and 1 at pH 3.4 and pH 7.4, respectively. Furthermore, it is relevant to underline that the current increases 10 times as compared to the GCE, and the behaviour as a function of pH appeared to be maintained; that is, the greater the pH, the E_{pa} value appears at the more negative potentials. Higher pH values shift the observed oxidation potential to less positive values because hydrogen ions are produced in the DA oxidation process. The significant increase of the current for the GCE/MWCNT/ β -CD compared to the bare GCE is probably due to the increase of the electrostatic interaction between DA and CD modified electrode. Nevertheless the current increase might be also caused by the electron transfer enhancement due to the presence of MWCNTs to the surface of which might be adsorbed the CD by van der Waals forces [29].

A drastic enhancement of the voltammetric background current at the GCE/MWCNT/ β -CD (Fig. 7) compared to the GCE (Fig. 3) was also observed. This large background current should be caused by the complex impedance of the modified electrode/electrolyte interface compared to the non-modified electrode.

3.4.2. Effect of the scan rate

Fig. 8 shows the DA voltammograms for GCE/MWCNT/ β -CD at different scan rates at pH 3.4 (Fig. 8A) and 7.4 (Fig. 8B), respectively; the E_{pa} and E_{pc} values change slightly while the scan rate increase. When the rate increased 10 times, the ΔE_p values for pH 3.4 and 7.4 were 60 mV and 90 mV and the current ratio between the peaks was 0.7 and 0.4, respectively. These results demonstrate that the oxidation process of DA at the GCE/MWCNT/ β -CD can be considered quasi-reversible.

The peak current increased linearly with the scan rate's root and the corresponding linear equation is $i(\mu A) = 8.623v^{1/2} + 0.354$ with a linear correlation coefficient of 0.997 at pH 3.4. In the case of pH 7.4 the corresponding linear equation is $i(\mu A) = 6.95v^{1/2} + 8.315$ with a linear correlation coefficient of 0.995. Therefore, the oxidation process of DA at the GCE/MWCNT/ β -CD is diffusion controlled in both values of pH.

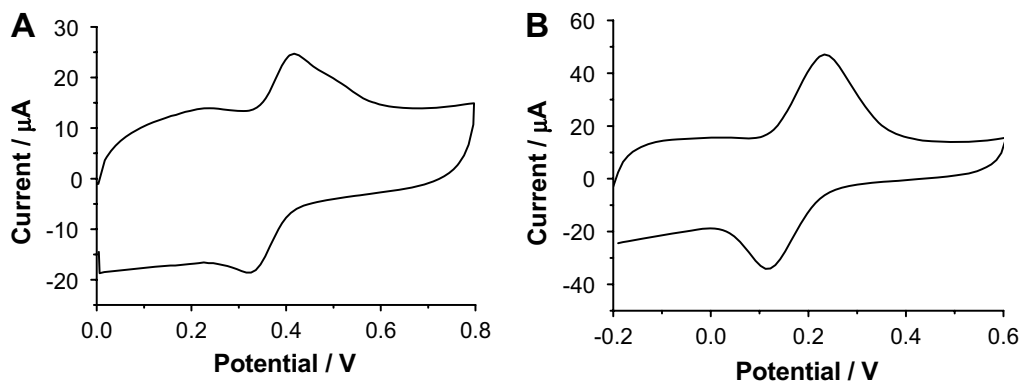


Fig. 7 – Cyclic voltammetry of 0.1 mM DA at (A) pH 3.4 and (B) pH 7.4, in 0.01 M phosphate buffer with a potential scan rate of 0.1 V s^{-1} . Working electrode: GCE/MWCNT/ β -CD.

Table 1 – Values obtained for the anodic (E_{pa}) and cathodic (E_{pc}) peak potentials, the anodic peak current (I_{pa}), the potential difference between the anodic and cathodic peaks (ΔE), using cyclic voltammetry of the 0.1 mM DA solution at pH 3.4 and pH 7.4 in 0.01 M phosphate buffer, with GCE/MWCNT/ β -CD

pH	Working electrode	E_{pa} (mV)	E_{pc} (mV)	ΔE (mV)	I_{pa} (μA)	I_{pc}/I_{pa}
3.4	GCE	495.0	233.0	262.0	3.5	0.98
	GCE/MWCNT/ β -CD	417.0	336.0	83.0	15.7	0.75
7.4	GCE	253.0	102.0	151.0	8.6	0.78
	GCE/MWCNT/ β -CD	185.0	122.0	63.0	17.5	0.54

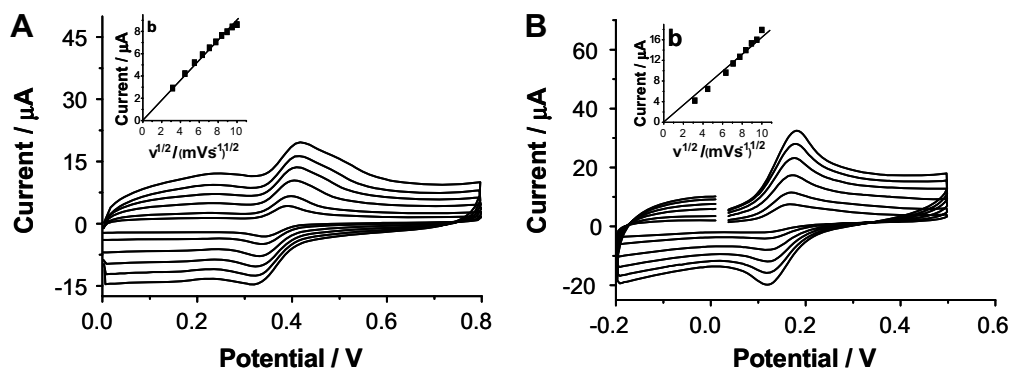


Fig. 8 – Cyclic voltammograms of DA 0.1 mM in 0.01 M phosphate buffer at (A) pH 3.4 and (B) pH 7.4, at different potential scan rates: 0.01, 0.02, 0.04, 0.06, 0.08, 0.09 and 0.1 V s^{-1} . The insets show the corresponding calibration plots of anodic current as a function of scan rate. Working electrode: GCE/MWCNT/ β -CD.

Hydrodynamic voltammetry was carried out to enable selection of the working potentials for the amperometric detection of DA. Fig. 9 shows the current values attained when the potential is varied within the -0.2 V to 0.6 V . The curves obtained show that the GCE/MWCNT/ β -CD responds to DA's oxidation at potentials higher than 0.2 V when the pH is 7.4, whereas at pH 3.4 oxidation occurs at potentials higher than 0.3 V while the current signal increases rapidly between 0.1 and 0.2 V . Further, it is shown that the response with GCE/MWCNT/ β -CD is greater at pH 7.4 compared to that observed at pH 3.4; this allows the amperometric determination of dopamine at lower potentials. These potentials are consistent with those obtained via CV. Therefore, the working

potentials to be applied for the detection of DA should be 0.5 and 0.3 V for pH 3.4 and 7.4, respectively, lower in the case of pH 3.4 compared to the bare GCE.

3.4.3. Amperometric detection of DA using the GCE/MWCNT/ β -CD

The amperometric responses to DA obtained with the GCE/MWCNT/ β -CD for pH 7.4 and 3.4 are compared in Fig. 10; the current response shows that for the oxidation at pH 3.4 the I_{pa} is directly proportional to concentration within the 0.02 mM to 0.1 mM concentration range. The linear equation describing the behaviour was j ($\mu\text{A}/\text{cm}^2$) = $117.91[\text{DA}] + 2529$, with a correlation coefficient of 0.995. At pH 7.4 the current

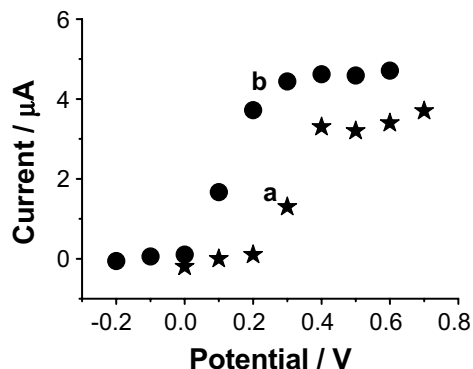


Fig. 9 – Hydrodynamic voltammograms of 0.1 mM DA with GCE/MWCNT- β -CD at (a) pH 3.4 and (b) pH 7.4 in 0.1 mM phosphate buffer.

response for the oxidation (I_{pa}) of DA is directly proportional to the concentration within the 0.01–0.08 mM concentration range. The linear equation describing this behaviour was j ($\mu\text{A}/\text{cm}^2$) = 116.63[DA] + 0.8024, with a correlation coefficient of 0.9905. However, in the concentration range below 0.03 mM, the linear correlation coefficient improves attaining the value of 0.999. The linear equation describing the behaviour was j ($\mu\text{A}/\text{cm}^2$) = 145.25[DA] + 0.3546, for pH 7.4 that means that the sensibility of the GCE/MWCNT/ β -CD is better at pH 7.4 (see Table 2 for comparison data).

The results obtained show that in the case of GCE/MWCNT/ β -CD the DA detection interval is broader and the sensitivity is increased. Moreover the electron transfer process is faster and becomes more reversible.

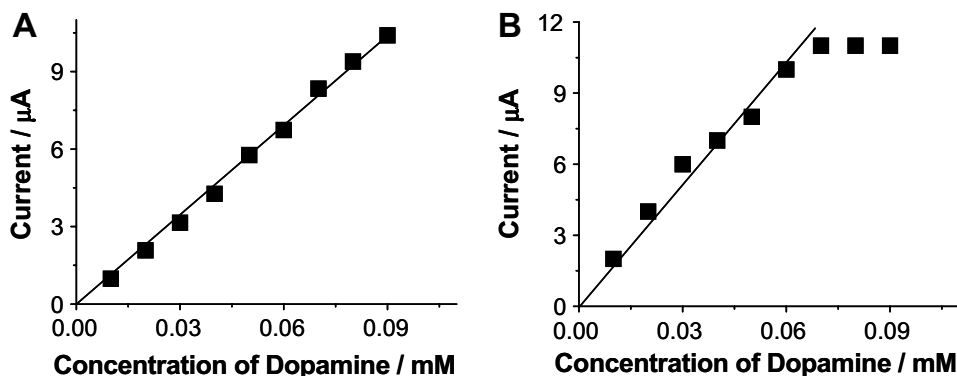


Fig. 10 – Amperometric calibration plots obtained with GCE/MWCNT- β -CD at (A) pH 3.4 and 0.5 V as working potential and (B) pH 7.4 and 0.3 V as working potential for successive additions of 0.01 mM DA, in 0.01 M phosphate buffer.

To compare the response between the MWCNT/ β -CD and the MWCNT modified GCE, a modified GCE with a suspension prepared by dissolving MWCNT in the same phosphate buffer was used. 1 mg MWCNT were dispersed in 10 ml phosphate buffer (0.1 M at pH 7) solution and sonicated during 1 h. Twenty microliters of the above solution were introduced onto the GCE and dried at 60 °C during 30 min. The obtained modified electrode did not show a good stability. The appeared distorted cyclic voltammetry of DA (results not shown) might be related to the absence of β -CD that assist the MWCNT immobilization. The DA behaviour onto the MWCNT

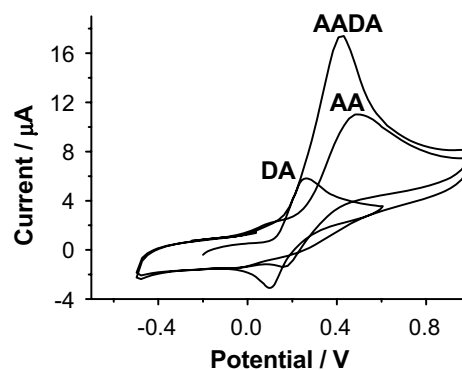


Fig. 11 – Cyclic voltammograms of DA (0.1 mM), AA (0.8 mM) and a mixture of DA + AA solutions at concentration of 0.8 mM (M/M = 1/8) in PBS 0.01 M and pH 7.4 using a GCE without modification.

Table 2 – Parameters obtained from the amperometric detection in 0.1 mM DA at pH 3.4 and pH 7.4 in 0.01 M phosphate buffer, using CV with the electrodes: GCE, GCE/MWCNT/ β -CD

pH	E_a (mV)	Working electrode	Sensitivity ($\mu\text{A}/\text{mM}$)	r^2	Concentration range (μM)	Detection limit (μM)
3.4	500	GCE	35.14	0.993	0–40	–
		GCE/MWCNT/ β -CD	117.91	0.995	20–100	–
7.4	300	GCE	22.2	0.915	0–40	25
		GCE/MWCNT/ β -CD	116.63	0.990	0–80	6.7
			145.25	0.999	0–30	

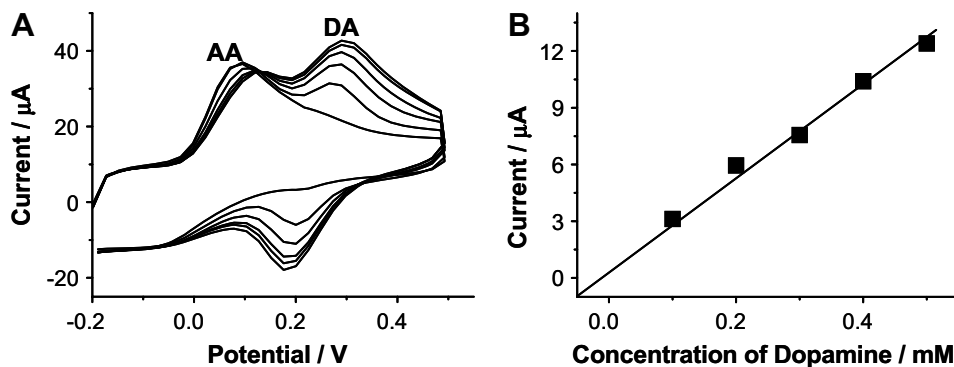


Fig. 12 – (A) Cyclic voltammetry of AA 0.8 mM and CVs obtained after 10 consecutive additions of a 0.01 mM DA solution, (B) calibration plot for successive additions of 0.01 mM DA in 0.01 M phosphate buffer. Working electrode: GCE/MWCNT/ β -CD.

only modified electrode represented an increased irreversibility probably as the results of DA adsorption onto MWCNT that were not surrounded by β -CD.

3.5. Selectivity in dopamine sensing

The analysis of DA is normally affected by the presence of other electro active species especially ascorbic acid (AA) present in physiological fluid. Therefore we investigated the DA sensing in the presence of AA. The study of AA interference was performed by using the non-modified GCE as well as the MWCNT/ β -CD/GCE.

Cyclic voltammograms of a 0.1 mM DA, 0.8 mM AA and 0.8 mM DA + AA ($M/M = 1/8$) solutions were performed first by using a GCE without any modification. The results obtained are shown at Fig. 11. The oxidation peak (E_a) of the 0.8 mM AA appears at $E_a = 504$ mV while for 0.1 mM DA the $E_a = 273$ mV. The CV of DA in the presence of AA at a molar ratio AA/DA of 8/1 shows a unique peak at $E_a = 431$ mV. The results obtained show that the presence of AA makes DA detection impossible, using a non-modified GC electrode.

The detection of DA in the presence of AA 0.8 mM pH 7.4 was analyzed by VC (Fig. 12A), the signal located around 0.1 V is the corresponding to ascorbic acid, the signal of the dopamine is observed in the potential of 0.3 V, the height and amplitude of the peak corresponding to DA increases proportionally with the concentration.

Fig. 12B shows the behaviour of the current peak vs. concentration of DA, it is possible to observe that the response is proportional to the DA concentration in the interval of concentration of 0–0.5 mM, the linear equation in this interval of concentration is i (μA) = 451.29[DA] + 0.53 the coefficient of linear correlation is of 0.992.

The detection limit (LOD) for the MWCNT/ β -CD modified electrode is 37 μM DA (calculated as the 3σ from the calibration curve obtained by plotting the DA oxidation peak at the concentration range of 0–0.5 mM in the presence of AA).

4. Conclusions

A novel strategy to selectively detect dopamine (DA) using a doubly-modified glassy carbon electrode (GCE) using β -cyclodextrin (β -CD) as molecular receptor and multiwall carbon

nanotubes (MWCNT) as enhancer of electron transfer is presented. The guest DA molecule inside the immobilized β -CD host acts as a mediator that ensures a better electrical contact between the GCE and the bulk DA solution. Moreover the MWCNT adjacent to the β -CD enhances the electron transfer improving the overall electrochemical response of the DA detection system.

The proposed β -CD/MWCNT/GCE increases the rate of electron transfer of dopamine that is corroborated by the oxidation potential shift toward more negative potentials and the fact that the DA redox process is more reversible. The DA response improves comparing to other reported systems. The developed matrix, which is applied as a modified electrode improves also the selectivity toward AA. The response of the developed system toward DA in the presence of higher concentrations of ascorbic acid show no alterations.

From the results mentioned above, we can conclude that the β -CD/MWCNT/GCE exhibits highly electrocatalytic activity toward DA oxidation. The modified electrode provides a higher selectivity in voltammetric measurements of DA. The verification of this enhanced response of the MWCNT in the presence of β -CD may point the way toward the use of other supramolecules for the chemical manipulation and processing of MWCNTs for sensor applications. As a result, it is essential to achieve a true understanding of the response enhancement as well as of the nature of such interactions linked with the unique properties of MWCNTs in the presence of the a molecular host like β -CD.

The use of a combination of host–guest electrostatic interactions with an electron enhancer is a novel aspect allowing a more rational design of analytical strategies that could find application in neuroscience. Studies in this direction are currently underway.

Acknowledgments

The authors thank the Red ALFA II for the Bio Sen Intg Clave:II-0486-FCFA-FCD-FI project and CONACyT for the support through the scholarship #184930 given to G.A.A. The Spanish “Ramón Areces” foundation (project ‘Bionanosensores’) and MEC (Madrid) (Projects MAT2005-03553, and Consolider-Ingenio 2010, Proyecto GSD2006-00012) are also acknowledged.

REFERENCES

- [1] Wang J, Li M, Shi Z, Li N, Gu Z. Electrocatalytic oxidation of norepinephrine at a glassy carbon electrode modified with single wall carbon. *Electroanalysis* 2002;14(3):225–30.
- [2] González R, Sánchez A, Chicharro M, Rubianes MD, Rivas GR. Dopamine and glucose sensors based on glassy carbon electrodes with melanic polymers. *Electroanalysis* 2004;16(15):1244–53.
- [3] Giz MJ, Duong B, Tao NJ. In situ STM study of self-assembled mercaptopropionic acid monolayers for electrochemical detection of dopamine. *J Electroanal Chem* 1999;465:72–9.
- [4] Kawage TK, Wightman RM. Characterization of amperometry for in vivo measurement of dopamine dynamics in the rat brain. *Talanta* 1994;41(6):865–74.
- [5] Gerhardt GA, Oke AF, Nagy G. Nafion-coated electrodes with high selectivity for CNS electrochemistry. *Brain Res* 1984;290(2):390–5.
- [6] Yuzhong Z, Guiying J, Zhousheng Y, Hong Z. Determination of dopamine in the presence of ascorbic acid using a poly(amidosulfonic acid) modified glassy carbon electrode. *Chem Mater Sci* 2004;147(4):225–30.
- [7] Wang J, Peng TZ. Selectivity and sensitivity improvements at perfluorinated ionomer/cellulose acetate bilayer electrodes. *Anal Chem* 1986;58:3257–61.
- [8] Guadalupe AR. Voltammetric determination of nonelectroactive ions at a modified electrode. *Anal Chem* 1985;57:142–9.
- [9] Iijima S. Helical microtubules of graphitic carbon. *Nature* 1991;354:56–8.
- [10] Iijima Ichihashi. Single-shell carbon nanotubes of 1-nm diameter. *Nature* 1993;363:603–5.
- [11] Bethune DS, Kiang CH, DeVries MS, Gorman G. Cobalt-catalysed growth of carbon nanotubes with single-atomic-layer walls. *Nature* 1993;363:605–7.
- [12] Saito Y, Yoshihawa T. Carbon nanocapsules encaging metals and carbides. *J Phys Chem Solids* 1993;54(12):1849–60.
- [13] Merkoçi A, Pumera M, Llopis X, Perez B, Del Valle M, Alegret S. New materials for electrochemical sensing VI carbon nanotubes. *Trends Anal Chem* 2005;24(9):826–38.
- [14] Merkoçi A. Carbon nanotubes: exciting new materials for microanalysis and sensing. *Microchim Acta* 2006;152:156–7.
- [15] Asanuma M, Miyazaki I, Ogawa N. Dopamine- or L-DOPA-induced neurotoxicity: the role of dopamine quinone formation and tyrosinase in a model of Parkinson's disease. *Neurotox Res* 2003;5(3):165–76.
- [16] Yoshitake T, Kehr J, Yoshitake S, Fujino K, Nohta H, Yamaguchi M. Determination of serotonin, noradrenaline, dopamine and their metabolites in rat brain extracts and microdialysis samples by column liquid chromatography with fluorescence detection following derivatization with benzylamine and 1,2-diphenylethylenediamine. *J Chromatogr B* 2004;807(2):177–83.
- [17] Heidbreder CA, Lacroix L, Atkins AR, Organ AJ, Murray S, West A, et al. Development and application of a sensitive high performance ion-exchange chromatography method for the simultaneous measurement of dopamine, 5-hydroxytryptamine and norepinephrine in microdialysates from the rat brain. *J Neurosci Meth* 2001;112(2):135–44.
- [18] Chi JD, Odontiadis J, Franklin M. Simultaneous determination of catecholamines in rat brain tissue by high-performance liquid chromatography. *J Chromatogr B* 1999;731(2):361–7.
- [19] Parsons LH, Kerr TM, Weiss F. Simple microbore high-performance liquid chromatographic method for the determination of dopamine and cocaine from a single in vivo brain microdialysis sample. *J Chromatogr B Biomed Sci Appl* 1998;709(1):35–45.
- [20] Li N, Duan J, Chen G. Determination of trace procaine hydrochloride by differential pulse adsorptive stripping voltammetry with a Nafion modified glassy carbon electrode. *Anal Sci* 2003;19(12):1587–92.
- [21] Doménech A, García H, Doménech-Carbó MT, Galletero MS. 2,4,6-Triphenylpyrylium ion encapsulated into zeolite Y as a selective electrode for the electrochemical determination of dopamine in the presence of ascorbic acid. *Anal Chem* 2002;74(3):562–9.
- [22] Falat L, Cheng HY. Voltammetric differentiation of ascorbic acid and dopamine at an electrochemically treated graphite/epoxy electrode. *Anal Chem* 1982;54:2108–11.
- [23] Wu K, Hu S. Electrochemical study and selective determination of dopamine at a multi-wall carbon nanotube-nafion film coated glassy carbon electrode. *Microchim Acta* 2004;144(1–3):131–7.
- [24] Britto PJ, Santhanam KSV, Ajayan PM. Carbon nanotube electrode for oxidation of dopamine. *Bioelectrochem Bioeng* 1996;41(1):121–5.
- [25] Pérez B, Pumera M, Del Valle M, Merkoçi A, Alegret S. Glucose biosensor based on carbon nanotube epoxy composites. *J Nanosci Nanotechnol* 2005;5(10):1694–8.
- [26] Abe I, Fukuhara T, Kawasaki N, Hitomi M, Kera Y. Characteristics of cyclodextrin adsorption onto activated carbons. *J Colloid Interface Sci* 2000;229:615–9.
- [27] Musameh M, Wang J, Merkoçi A, Lin Y. Low-potential stable NADH detection at carbon-nanotube-modified glassy carbon electrodes. *Electrochem Commun* 2002;4:743–6.
- [28] Sanchez-Rivera AE, Corona-Avendano S, Alarcon-Angeles G, Rojas-Hernandez A, Ramirez-Silva MT, Romero-Romo MA. Spectrophotometric study on the stability of dopamine and the determination of its acidity constants. *Spectrochim Acta A Mol Biomol Spectrosc* 2003;59(13):3193–203.
- [29] Chambers G, Carroll C, Farrell GF, Dalton AB, McNamara M, In het Panhuis M, et al. Characterization of the interaction of gamma cyclodextrin with single-walled carbon nanotubes. *Nano Lett* 2003;3(6):843–6.

Carbon nanofiber vs. carbon microparticles as modifiers of glassy carbon and gold electrodes applied in electrochemical sensing of NADH

B. Pérez, M. del Valle, S. Alegret and A. Merkoçi

Talanta

2007, **74**, 398-404



Carbon nanofiber vs. carbon microparticles as modifiers of glassy carbon and gold electrodes applied in electrochemical sensing of NADH

Briza Pérez^{a,b}, Manel del Valle^b, Salvador Alegret^b, Arben Merkoçi^{a,b,*}

^a *Nanobioelectronics & Biosensors Group, Institut Català de Nanotecnologia, Campus Universitat Autònoma de Barcelona, 08193 Bellaterra, Catalonia, Spain*

^b *Grup de Sensors & Biosensors, Departament de Química, Universitat Autònoma de Barcelona, 08193 Bellaterra, Catalonia, Spain*

Received 10 September 2007; received in revised form 3 October 2007; accepted 4 October 2007
Available online 22 October 2007

Published in honour of Professor Joseph Wang's 60th birthday.

Abstract

Carbon materials (CMs), such as carbon nanotubes (CNTs), carbon nanofibers (CNFs), and carbon microparticles (CMPs) are used as doping materials for electrochemical sensors. The efficiency of these materials (either before or after acidic treatments) while being used as electrocatalysts in electrochemical sensors is discussed for β -nicotinamide adenine dinucleotide (NADH) detection using cyclic voltammetry (CV). The sensitivity of the electrodes (glassy carbon (GC) and gold (Au)) modified with both treated and untreated materials have been deeply studied. The response efficiencies of the GC and Au electrodes modified with CNF and CMP, using dimethylformamide (DMF) as dispersing agent are significantly different due to the peculiar physical and chemical characteristics of each doping material. Several differences between the electrocatalytic activities of CMs modified electrodes upon NADH oxidation have been observed. The CNF film promotes better the electron transfer of NADH minimizing the oxidation potential at +0.352 V. Moreover higher currents for the NADH oxidation peak have been observed for these electrodes. The shown differences in the electrochemical reactivities of CNF and CMP modified electrodes should be with interest for future applications in biosensors.

© 2007 Elsevier B.V. All rights reserved.

Keywords: Carbon nanofibers; Carbon microparticles; NADH; Electrochemical sensing; Cyclic voltammetry

1. Introduction

Carbon materials (CMs), such as graphite/carbon microparticles (CMPs), carbon nanotubes (CNTs), and carbon nanofibers (CNFs) have shown significant improvements in the development of novel sensors and biosensors [1–5]. High-surface area of CMs may also lead to new signal transduction processes [6,7] and to increased sensitivity in sensing applications [8–10].

Various processes used to be involved within a (bio)sensor system. These ranges from the analyte recognition, catalytic conversion, oxidation–reduction processes, mediation of electron

transfer, and finally the signal transduction and data display. To achieve a smooth running of the above processes a careful evaluation of the properties of the materials, ensuring an efficiency of their electrochemical properties, while incorporating them into the biosensor membranes must be considered. A better interaction and communication between the biomolecule and the transducer is also aimed to be achieved while using these materials. Only under these conditions a biosensor device will provide analytically useful information.

In recent years, with the great progress made in nanoscience and nanotechnology, interest is increasing in exploring the unique properties and potential technological applications of various nanostructures [11,12]. Many nanomaterials, such as peptide nanotubes [11], poly(1,2-diaminobenzene) nanotubules [13], and TiO₂ nanostructured films [14], particularly carbon nanotubes (CNT) [15–17], have been devoted to decreasing the high-overpotential for β -nicotinamide adenine dinucleotide

* Corresponding author at: Nanobioelectronics & Biosensors Group, Institut Català de Nanotecnologia, Campus Universitat Autònoma de Barcelona, 08193 Bellaterra, Catalonia, Spain.

E-mail address: arben.merkoci.icn@uab.es (A. Merkoçi).

(NADH) oxidation, minimizing surface fouling, and improving electron-transfer kinetics. Depending on the size, shape, and internal structure, nanoparticles frequently display unique physical and chemical properties [18].

CMP represents a highly ordered form of carbon. It is a solid that possesses delocalized π electrons on the basal planes, and this property imparts a weak basic character to the material in which the polarity can be manipulated by selected chemical treatments [19]. Carbon nanofibers (CNFs) represent carbon fibers with a nanometer-size diameter and no hollow core, but with many edge sites on the outer wall [20]. It has been recognized as one of the very promising materials based on its nanostructure and particular properties [21] and is expected to be used in various applications such as catalysts or catalyst supports [22], probe tips [23], and fuel cells [24].

Although there is a large amount of size overlap between CNT and CNF, there are significant structural differences. CNF consist of graphitic layers that stack either at an angle, perpendicular or parallel to the tube axis [25–28] while the CNT represent two single-walled and multi-walled structures. Single-wall CNTs (SWCNTs) comprise of a cylindrical graphite sheet of nanoscale diameter capped by hemispherical ends. The multi-wall CNTs (MWCNTs) comprise several to tens of incommensurate concentric cylinders of these graphitic shells with a layer spacing of 0.3–0.4 nm. MWCNTs tend to have diameters in the range 2–100 nm. The MWCNT can be considered as a mesoscale graphite system, whereas the SWCNT is truly a single large molecule [5].

Due to the unique characteristics of CNF there is a wide range of applications. The thermal and chemical stability, high-surface area, low-ohmic resistance, and the surface properties are the unique qualities that are exploited when CNF are used as catalytic support materials [25–30]. The surface at the tip of a CNF possesses a large amount of exposed edges due to the arrangement of the graphitic layers [31].

Recently, Wu et al. [32] studied the excellent catalytic activity of soluble CNF with good dispersion, to the oxidation of NADH for biosensing application. They show as the edge plane sites and oxygen-rich groups presented on the CNF surface could be partially responsible for its electrocatalytic behavior, which induced a substantial decrease by 573 mV in the overpotential of NADH oxidation reaction (compared to a bare glassy carbon electrode).

CNFs lead to more facile electron transfer [33] compared to CMPs. The solubility of CNF in dimethylformamide (DMF) facilitates its manipulation, including the coating on electrode surfaces for electrochemical biosensing applications, because the insolubility of carbon materials in most solvents is a major obstacle in implementing their widespread use [34].

In this work, chemically treated and untreated carbon materials (CNF and CMP) were used as modifiers of glassy carbon and gold electrode surfaces. The objective was to compare their efficiencies for electrochemical oxidation of NADH while using cyclic voltammetry (CV). Interesting results with interest for future biosensing applications will be shown.

2. Experimental

2.1. Materials and reagents

Herringbone graphite nanofibers, CNFs (100 nm in width and up to 10 μ in length) were purchased from catalytic materials. Graphite powder (carbon microparticle, CMPs, size 50 μ m) was obtained from BDH, UK. Further purification of carbon material was accomplished by stirring the CMs in 2 M nitric acid (PanReac, Spain) at 25 °C for 24 h [35]. A 0.7 mg of carbon material (CMP or CNF) was dispersed in 700 μ L of dimethylformamide (DMF, from Sigma–Aldrich). β -Nicotinamide adenine dinucleotide reduced form (NADH), potassium dihydrogen phosphate, potassium hydrogen phosphate, and sodium hydroxide were obtained from Sigma–Aldrich (Spain). The working solutions (NADH) were prepared daily by dilution in 0.1 M phosphate buffer at pH 7.0 with ultra pure water from a Millipore-MilliQ system.

2.2. Apparatus

Scanning electron microscopy (SEM, Hitachi S-570, Tokyo, Japan) was used to study the morphology of the electrode surfaces. Transmission electron microscope (TEM) images of the carbon materials were obtained using a Hitachi H-7000 (Hitachi Ltd., Tokyo, Japan). Scanning electron microscopy JEOL JSM-6300 (SEM, JEOL Ltd., Tokyo, Japan) with microanalysis equipped by an X-ray energy dispersive spectrometer (EDS) (Link ISIS-200, England) was used in order to evaluate the amount of chemical impurities (remained from their synthesis) and of oxygen groups introduced during the treatment of CMs with HNO₃.

The electrochemical measurements were performed with an electrochemical analyzer CHI 630B (CH Instruments) connected to a personal computer. The measurements were carried with a typical cell of 10 mL at room temperature (25 °C), using a three-electrode configuration. A platinum electrode and Ag/AgCl were used as counter and reference electrode, respectively. The glassy carbon (GC) and gold (Au) electrodes, with diameter of 2 mm, were from CH Instruments (Austin, TX, USA). The GC or Au modified electrodes using CNFs or CMPs suspended in DMF were also used as working electrodes. Modified electrodes were prepared in our laboratory according to the procedure described below.

2.3. Modification of GC and Au electrode surfaces

CNF and CMP were purified prior to use by a 2 M nitric acid solution. The bare electrodes (GC and Au electrodes) were polished with alumina paper (polishing strips 301044-001, Orion, Spain) and washed with water. These electrodes were then used for further modifications with CMs dispersed into DMF. Usually 0.7 mg CMs (treated or untreated) were mixed/dispersed into 700 μ L of DMF by ultrasonic agitation for about 1 h. After, 10 μ L of CMs–DMF solution were dropped directly onto of GC and Au electrode surfaces and allowed to dry at 40 °C for 45 min. Finally the electrodes were washed with water, and were ready

for use. For comparison experiments, bare GC and Au electrodes was prepared, following exactly the same experimental procedure.

2.4. Electrochemical measurements

Electrochemical experiments were performed using a three-electrode system with an Ag/AgCl reference electrode, a Pt wire auxiliary electrode and CNF/GC, CMP/GC or CNF/Au, CMP/Au as working electrodes.

The measurements were performed with an electrochemical analyzer CHI 630B (CH Instruments) connected to a personal computer. Cyclic voltammograms using electrodes modified with treated and untreated CMs were performed in 2.5 mM NADH solution. The response to NADH was measured in 10 mL of a 0.1 M phosphate buffer solution (PBS) pH 7.0.

The potential range used for NADH determination was -0.6 to $+1.2$ V for CNF–DMF/GC, CMP–DMF/GC, CNF–DMF/Au, and CMP–DMF/Au. The background current was allowed to decay to a constant level before aliquots of NADH sample were added to the buffer solution.

3. Results and discussion

3.1. Characteristics of the carbon materials and the corresponding films

The dispersion of the CNF–DMF or CMP–DMF onto the electrode surfaces (GC and Au) is an important issue in producing carbon films onto the electrode surfaces. Scanning electron microscopy was used to analyze the carbon films on GC and Au electrode surfaces. Fig. 1 compares SEM images of treated CNF and CMP and untreated CNF and CMP films deposited onto the surfaces of GC and Au electrodes. It can be appreciated that the treated CMPs produce a more uniform carbon film over the electrode surfaces (GC and Au) compared to untreated CMPs. The CMPs are more scattered over the gold electrode surface than in the GC electrode. However, untreated CNF create a better uniform/homogeneous film and even more coverage over the surface of GC and Au electrodes, while treated CNF creates more scattered and even thinner layer onto the GC and Au surfaces. Fig. 1 shows that in all the cases, the surfaces of the electrodes are covered (although not in the same level) with either the treated or with untreated CMs which seem to be available to act as an electrochemical sensing surface for NADH detection.

TEM images reveal the structure of the CMs, both CMPs and CNFs (Fig. 2). CMPs structures consists of carbon layers (in which the carbon atoms are arranged in an open honeycomb network) situated ones over others and the electrical conductivity between them is very poor [36]. The impurity species may occupy some interstitial position between the graphene layer planes, which are bonded by a weak van der Waals force. These weak interplanar bonds at graphite allow dopant atoms or molecules to be intercalated between the carbon layers to form intercalation compounds [36]. The TEM of CNFs are also presented. A clear difference of TEMs between CMPs and CNFs

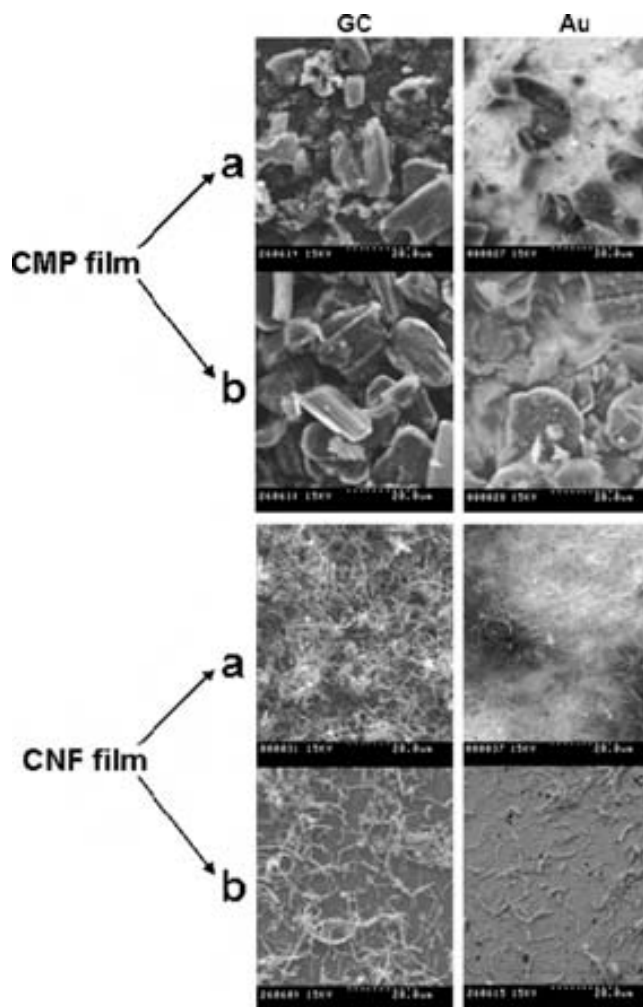


Fig. 1. SEM images for CMP and CNF films on GC and Au electrode surfaces; without treatment (a) and with treatment (b) in HNO_3 . The same acceleration voltage (5 kV) and resolution are used.

can be observed while the differences between the treated and untreated CMs are not visible except of a kind of structure rupture after treatment with HNO_3 of both materials. In addition we can observe a slight growth of the surface area covered with treated CNFs.

The measured surface area can be regarded as the external surface area of the fibers.

Apparently, with the process of oxidation in $\text{HNO}_3/\text{H}_2\text{SO}_4$ or KMnO_4/H^+ , the macrostructure of the fibers becomes somewhat less dense, and a slightly higher pore volume (space between the fibers). As a result of the oxidation, the fibers have a surface roughening that can explain the increase in surface area (see Fig. 2b CNF), but its pore volume and the average pore diameter are decreased [37]. Probably, as a result of this decrease, the electronic transference is smaller in treated CNF, and due to its porous structure in comparison with the structure of the CMPs that is more rigid the electrochemical response is better with untreated CNF.

Fig. 3 is a schematic of CMP and CNF structures showing the graphene layers along with several possibilities for other molecules (NADH in our case) to enter in between. CNF struc-

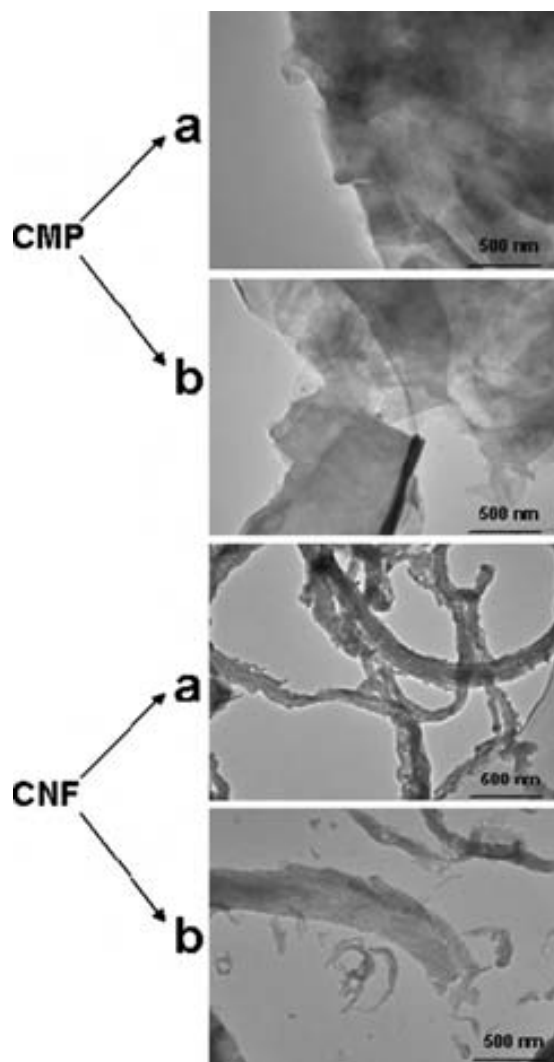


Fig. 2. TEM images of CMPs and carbon nanofibers (CNFs) untreated (a) and treated (b) with HNO_3 , and suspended using dimethylformamide (DMF) as described in the text.

ture is of the herringbone type disclosing the origin of the surface roughness. Probably, CNF due to its structure can adsorb species on their external and internal surfaces and between adjacent nanofibers. In the case of CNF, the guest species is believed to decorate the exterior of the nanofiber, and also to enter the hollow cores of the CNF.

Moreover, the two types of carbon materials have a difference in orientation of the carbon planes. Taking into consideration the textures of CMs it can be previewed how an oxidant (for example HNO_3) might introduce changes at the structures. Fig. 3 presents the possible sites of attachment that can be introduced onto the surface of the carbon materials studied.

The SEM microanalysis and X-ray energy dispersive spectrometer (EDS) results for CNFs and CMPs, comparing the CMs before and after treatment with HNO_3 (results now shown) could give also an insight of the chemical impurities and the oxygen groups present in each CMs. Table 1 represents the microanalysis data obtained by SEM of the untreated and treated carbon materials. These data show that there are variations between the

Table 1

Microanalysis data of the CMP and CNF (without any treatment and with treatment with HNO_3) obtained by SEM (the same acceleration voltage (5 kV) and resolution are used)

Carbon material		Element (%)			
		C	O	Si	S
CMP	Untreated	73.30	25.78	0.36	0.31
	Treated	77.35	31.85	–	0.37
CNF	Untreated	70.19	28.19	0.19	0.51
	Treated	62.82	35.70	0.17	0.40

untreated and treated CMPs and CNFs (introduced as DMF suspensions) in terms of oxygen percentage. It can be observed an increase of around 6% of oxygen in the treated CMPs while in the case of CNFs the oxygen percentage was increased a little bit more (8.75%). The formation of oxygen-containing surface groups occurs at defect sites on the carbon nanofibers. We could not evaluate significant changes regarding the presence of other elements (Si, S, Al, etc.).

3.2. Electrochemical characterization of CMs films on GC and Au electrode surfaces

The electrochemical properties of the CMs were examined using cyclic voltammetry (CV). The fast and reliable detection of NADH at low potential is particularly important.

The electrochemical signal transduction ability of CMs and their possible application in biosensor systems was evaluated by measuring the response of GC and Au electrode surfaces modified with treated and untreated CMPs and CNFs films.

Fig. 4 shows the cyclic voltammograms of bare Au electrode (upper CVs) and Au electrodes modified with untreated (A) and treated (B) CNFs. The same CVs for the Au electrodes modified with untreated (C) and treated (D) CMPs are also shown. A pH 7.0 PBS containing 2.5 mM NADH, a scan rate of 100 mV s^{-1} during a potential range of -0.6 to 1.2 V have been used in all cases. The CNF and CMP modified Au electrodes (CNF/Au and CMP/Au) showed two redox waves. Firstly, the NADH oxidation peaks: $+0.349 \text{ V}$ (untreated CNF); $+0.520 \text{ V}$ (treated CNF); $+0.517 \text{ V}$ (untreated CMPs) and at $+0.505 \text{ V}$ (treated CMPs). Secondly, the reduction peaks (at around 0.4 V) possibly ascribed to gold reduction appearing as a result of uncovered Au surfaces that could also be observed in the SEM images shown previously (Fig. 1).

On the other hand in the case of Au electrodes (Fig. 4) the shifts of the NADH oxidation potentials vary according to each CMs. In the case of modified Au electrode the peak of the NADH oxidation current corresponding to untreated CNF compared to the bare electrode represents a shift of around $\Delta E = +0.354 \text{ V}$. This peak represents also the highest current value comparing to the treated CNF and treated or untreated CMPs. For the Au electrodes modified with CMPs the highest oxidation potential observed ($21.04 \mu\text{A}$) corresponds to the treated CMPs. This peak (at $+0.505 \text{ V}$) represents a shift of $\Delta E = +0.198 \text{ V}$ with respect to bare Au electrode.

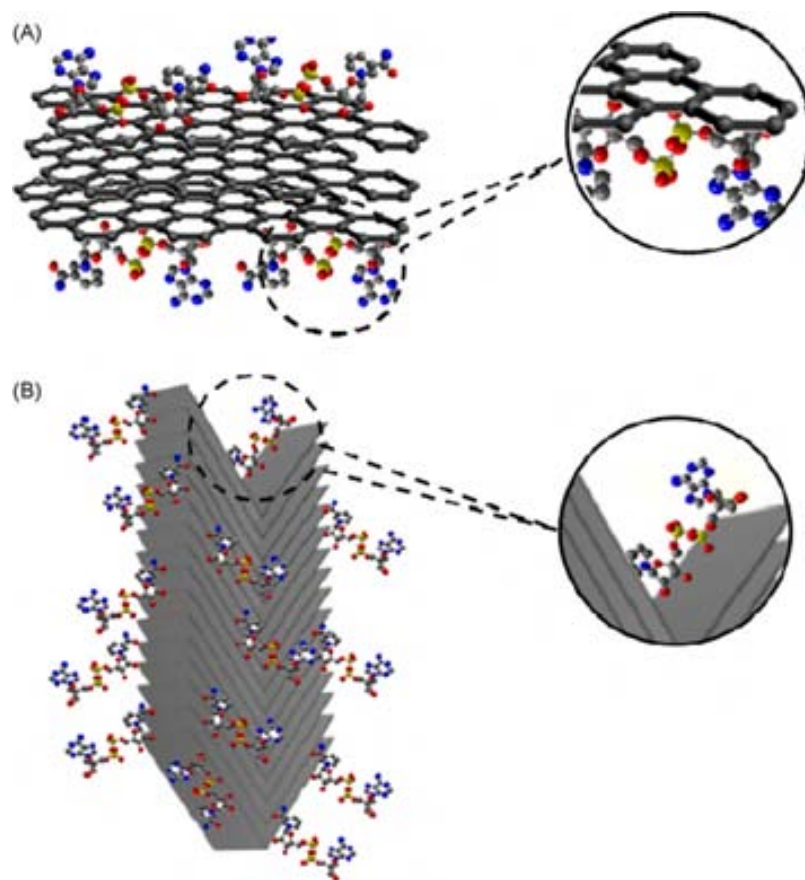


Fig. 3. Schematic representation (not in scale) of the possible interactions of the NADH molecules with: (A) graphene layers for the CMPs and (B) graphene layers for CNFs.

Fig. 5 shows the cyclic voltammograms of bare GC electrode (upper part) for a 2.5 mM NADH including the response in PBS buffer only (pH 7.0). The CVs for the GC electrodes modified with untreated (A) and treated (B) CNF are shown. The same CVs for GC electrodes modified with untreated (C) and treated (D) CMPs are also presented for the same conditions as presented for the modified Au electrodes (Fig. 4). All the CVs show clearly the NADH oxidation peaks comparing to PBS buffer. The peak currents for NADH oxidation are of a similar magnitude for each CM independently of being treated or not.

By comparing Fig. 5 (GC electrode) with Fig. 4 (Au electrode) it can be concluded that the GC electrodes utilized as substrate for deposition of carbon material films display a sig-

nificantly different responses compared to the gold electrodes (Fig. 4). The sensitivity toward NADH oxidation, in the case of electrodes modified with CMPs is higher with GC electrode (Fig. 5C and D) than with Au electrode (Fig. 4C and D) (note the differences in scale). The obtained results can be supported also by the images of Fig. 1 where better films onto GC electrode surfaces compared to those onto Au electrodes can be appreciated. Higher electrochemical responses, in both electrodes (GC and Au), have been observed for modifications using CNFs. The peak current (84.69 μA at +0.352 V) for the NADH oxidation for GC modified with untreated CNF shifted with a $\Delta E = +0.393$ V with respect to bare GC electrode. Lower sensitivity (18.21 μA) is observed for the Au electrode modified with untreated CMPs.

Table 2

Summary of responses toward a solution of NADH 2.5 mM at 0.1 M phosphate buffer pH 7 obtained by two different electrode transducers (GC and Au) modified with carbon nanofibers (CNFs) + dimethylformamide (DMF) and graphite + DMF

Modifier	Transducer	Glassy carbon (GC)			Gold (Au)		
		I_p (μA)	E_o (V)	ΔE (V)	I_p (μA)	E_o (V)	ΔE (V)
Graphite	Untreated	40.91	0.538	0.207	18.21	0.517	0.186
	Treated	52.42	0.535	0.210	21.04	0.505	0.198
Carbon nanofibers	Untreated	84.69	0.352	0.393	83.32	0.349	0.353
	Treated	71.28	0.505	0.240	25.58	0.520	0.183

I_p : the peak of the NADH oxidation current; E_o : NADH oxidation potential; ΔE : shift of the oxidation potentials between bare and modified electrodes.

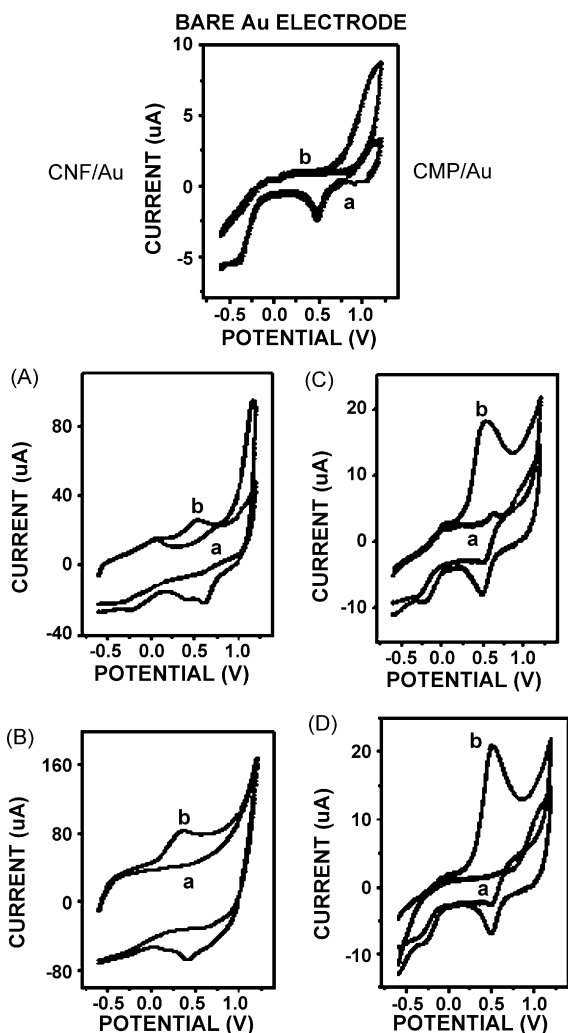


Fig. 4. Cyclic voltammograms (CV) for an 0.1 M phosphate buffer pH 7 (a) using: a bare Au electrode (upper CVs) and Au electrodes modified with untreated CNFs (A), treated CNFs (B), untreated CMPs (C), and treated (D) CMPs. The CV responses toward a 2.5 mM NADH solution (b) (at the same pH) are also shown using the same electrodes. The scan rate was 100 mV/s, potential range: -0.6 to 1.2 V. The composition of the modifying solution for all the cases was: 0.7 mg carbon material and 700 μ L DMF, respectively. Other experimental details as explained in the text.

Comparing both electrodes used (Au and GC) the sensitivity based on the current observed, increases from untreated to treated CMPs and from treated to untreated CNFs (Figs. 4 and 5).

From the obtained results, it can be concluded that the modifications with CNF brings to the electrodes higher sensitivity to the oxidation of NADH and therefore the electrochemical properties are more favourable comparing to modifications with CMPs.

Table 2 summarizes all the values (potential and currents) discussed previously for each electrode and the corresponding modifications. The shown differences can be attributed to the different structural forms of the carbon materials used. Carbon nanofibers (see Fig. 3) provide a very high-surface area and, consequently, a very high number of binding sites for NADH. This high density of binding sites may increase sensi-

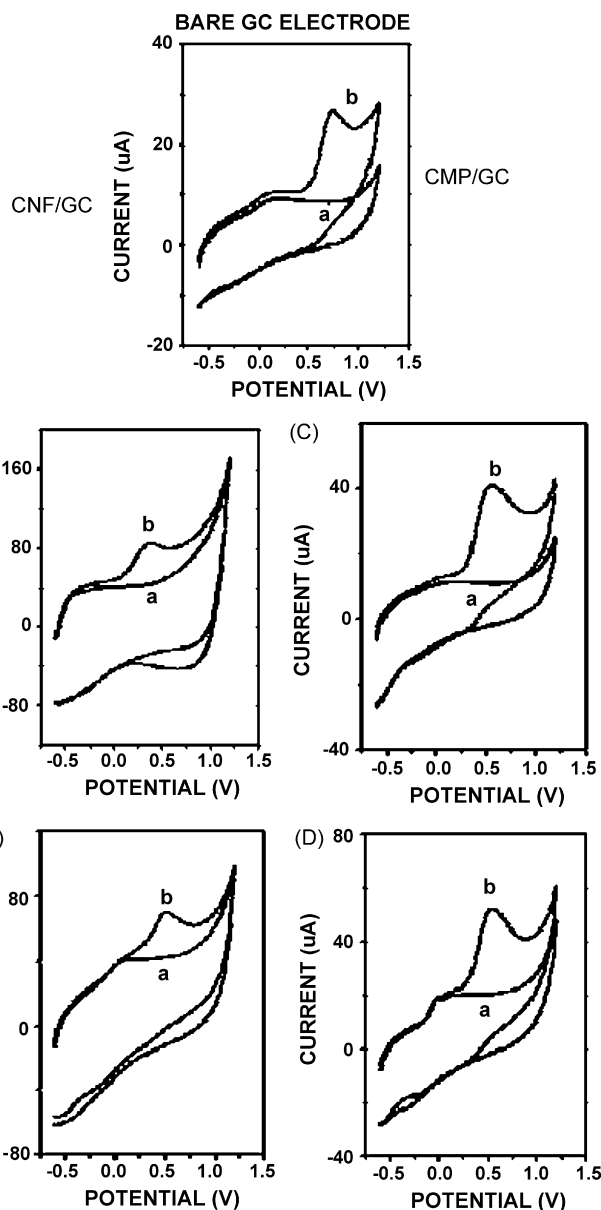


Fig. 5. Cyclic voltammograms (CV) for an 0.1 M phosphate buffer pH 7 (a) using: a bare GC electrode (upper CVs) and GC electrodes modified with untreated CNFs (A), treated CNFs (B), untreated CMPs (C), and treated (D) CMPs. The CV responses toward a 2.5 mM NADH solution (b) (at the same pH) are also shown using the same electrodes. The scan rate was 100 mV/s, potential range: -0.6 to 1.2 V. The composition of the modifying solution for all the cases was: 0.7 mg carbon material and 700 μ L DMF, respectively. Other experimental details as explained in the text.

tivity in the same manner as in porous materials [38]. Generally, electron transfer may be more facile at samples containing a higher proportion of binding sites, producing a faster electron transfer.

The principal reasons for different “electrocatalytic” properties of carbon materials on different substrates toward different analytes are still unclear and are under investigation. A possible explanation of such an effect is the different contact resistances of carbon materials (CMPs and CNFs) with the GC and Au electrode surfaces [15].

4. Conclusions

The electrochemical response for NADH oxidation is significantly different for each carbon material used as modifier as well as between GC and Au electrodes examined as substrates onto which the modifications have been performed. The results obtained show that the better substrate is the GC electrode, and the better modification is the untreated CNF film showing a peak current of 84.69 μA at +0.352 V with a shift of the oxidation potential of +0.393 V respect to bare GC electrode. The lower sensitivity is observed for the Au electrodes modified with untreated CMPs giving a peak height of 18.21 μA at +0.517 V with a shift of the oxidation potential of +0.186 V respect to bare Au electrode.

CNFs modifications show in most of the cases (except treated CNF at Au electrode) lower overpotentials and higher oxidation currents for the detection of NADH comparing to modifications performed with CMPs. The shown ability of untreated CNF to promote the electron transfer between NADH and the electrode surface suggest an attractive electrocatalytic nanomaterial for development of new amperometric biosensors. In addition to the attractive electrocatalytic properties the solubility of CNF in DMF better facilitates its manipulation for future biosensing applications.

Congratulations



A. Merkoçi

It was really a great pleasure for me (one of the authors of this article) to work during the year 2002 as scientific manager of Dr. Wang's Labchip laboratory in Las Cruces, NM. I found there a very motivated and hard working team led by a great scientist and person.

Thanks Dr. Wang for the opportunity to work with you!

I wish you all the best for this anniversary.

Acknowledgements

The Spanish "Ramón Areces" foundation (project 'Bionanosensores') and MEC (Madrid) for the Project MAT2005-03553 are acknowledged.

References

[1] Ü.A. Kirgoz, S. Timur, D. Odaci, B. Pérez, S. Alegret, A. Merkoçi, *Electroanalysis* 19 (2007) 893–898.
 [2] S. Alegret, A. Merkoçi, M.I. Pividori, M. del Valle, Chapter Encyclopedia of Sensors, vol. 3, in: A.G. Craig, C.D. Elizabeth, V.P. Michael (Eds.), The Pennsylvania State University, University Park, USA. For-

warded by Prof. R.A. Marcus, Nobel Prize Laureate, 2006, pp. 23–44, <http://www.aspbs.com/eos/>.
 [3] B. Pérez, M. Pumera, M. del Valle, A. Merkoçi, S. Alegret, *J. Nanosci. Nanotechnol.* 5 (2005) 1694–1698.
 [4] S. Alegret, A. Merkoçi, S. Alegret (Eds.), *Integrated Analytical Systems*, Elsevier, Amsterdam, 2003, pp. 377–412, ISBN: 0-444-51037-0 (NL).
 [5] A. Merkoçi, M. Pumera, X. Llopis, B. Pérez, M. del Valle, S. Alegret, *Trends Anal. Chem.* 24 (2005) 826–838.
 [6] K.-P.S. Dancil, D.P. Greiner, M.J. Sailor, *J. Am. Chem. Soc.* 121 (1999) 7925–7930.
 [7] J.M. Buriak, *Chem. Commun.* (1999) 1051–1060.
 [8] L.A. DeLouise, B.L. Miller, *Anal. Chem.* 76 (23) (2004) 6915–6920.
 [9] J. Wang, Q. Chen, C.L. Renschler, C. White, *Anal. Chem.* 66 (1994) 1988–1992.
 [10] C. Lei, Y. Shin, J. Liu, E. Ackerman, *J. Am. Chem. Soc.* 124 (2002) 11242–11243.
 [11] M. Yemini, M. Reches, E. Gazit, J. Rishpon, *Anal. Chem.* 77 (2005) 5155–5159.
 [12] S.S. Wong, E. Joselevich, A.T. Wooley, C.L. Cheung, C.M. Leiber, *Nature* 394 (1998) 52–55.
 [13] F. Valentini, A. Salis, A. Curulli, G. Palleschi, *Anal. Chem.* 76 (2004) 3244–3248.
 [14] A. Curulli, E. Valentini, G. Padeletti, A. Viticoli, D. Caschera, G. Palleschi, *Sens. Actuator B: Chem.* 111 (2005) 441–449.
 [15] M. Pumera, A. Merkoçi, S. Alegret, *Electrophoresis* 28 (2007) 1274–1280.
 [16] M. Musameh, J. Wang, A. Merkoçi, Y.H. Lin, *Electrochem. Commun.* 4 (2002) 743–746.
 [17] B. Pérez, M. Pumera, M. del Valle, A. Merkoçi, S. Alegret, *J. Nanosci. Nanotechnol.* 5 (2005) 1694–1698.
 [18] S. Hrapovic, Y. Lui, K.B. Male, J.H. Luong, *Anal. Chem.* 76 (2004) 1083–1088.
 [19] C. Park, E.S. Engel, A. Crowe, T.R. Gilbert, N.M. Rodriguez, *Langmuir* 1 (2000) 8050–8056.
 [20] S.-U. Kim, K.-H. Lee, *Chem. Phys. Lett.* 400 (2004) 253–257.
 [21] S.H. Yoon, S. Lim, Y. Song, Y. Ota, W.M. Qiao, A. Tanaka, I. Mochida, *Carbon* 42 (2004) 1723–1729.
 [22] M.K. van der Lee, A. Jos van Dillen, J.H. Bitter, K.P. de Jong, *J. Am. Chem. Soc.* 127 (2005) 13573–13582.
 [23] H. Cui, S.V. Kalinin, X. Yang, D.H. Lowndes, *Nano Lett.* 4 (2004) 2157–2161.
 [24] H. Hacker, E. Wallnofer, W. Baumgartner, T. Schaffer, J.O. Besenhard, H. Schrottner, M. Schmied, *Electrochem. Commun.* 7 (2005) 377–382.
 [25] N.M. Rodriguez, M.-S. Kim, R.T.K. Baker, *J. Phys. Chem.* 98 (1994) 13108–13111.
 [26] N.M. Rodriguez, A. Chambers, R.T.K. Baker, *Langmuir* 11 (1995) 3862–3866.
 [27] C.A. Bessel, K. Laubernds, N.M. Rodriguez, R.T.K. Baker, *J. Phys. Chem. B* 105 (2001) 1115–1118.
 [28] P. Serp, M. Corrias, P. Kalck, *Appl. Catal.* 253 (2003) 337–358.
 [29] M. Endo, Y.A. Kim, T. Hayashi, Y. Fukai, K. Oshida, M. Terrones, T. Yanagisawa, S. Higaki, M.S. Dresselhaus, *Appl. Phys. Lett.* 80 (2002) 1267–1269.
 [30] M.J. Ledoux, R. Vieira, C. Pham-Huu, N. Keller, *J. Catal.* 216 (2003) 333–342.
 [31] G.N. Patrick, Doctoral Thesis: The Use of Bipolar Electrochemistry in Nanoscience: Contact Free Methods for the Site Selective Modification of Nanostructured Carbon materials; Development of bipolar electrodeposition as a tool for nanotechnology: Part 1 from Platelets to Nanofibers (Chapter 3).
 [32] L. Wu, X. Zhang, H. Ju, *Anal. Chem.* 79 (2007) 453–458.
 [33] C.E. Banks, R.G. Compton, *Analyst* 130 (2005) 1232–1239.
 [34] L. Li, C.M. Lukehart, *Chem. Mater.* 18 (2006) 94–99.
 [35] M. Pumera, A. Merkoçi, S. Alegret, *Sens. Actuator B* 113 (2006) 617–622.
 [36] M.S. Dresselhaus, G. Dresselhaus, *Top. Appl. Phys.* 80 (2001) 11–28.
 [37] T.G. Ros, A.J. van Dillen, J.W. Geus, D.C. Koningsberger, *Chem. Eur. J.* 8 (2002) 1151–1162.
 [38] S.E. Baker, K.-Y. Tse, E. Hindin, B.M. Nichols, T.L. Clare, R.J. Hamers, *Chem. Mater.* 17 (2005) 4971–4978.

Carbon nanotube composite as novel platform for microbial biosensor

Ü.A. Kirgoz, S. Timur, D. Odaci, **B. Pérez**, S. Alegret and A. Merkoçi

Electroanalysis

2007, **19** (7-8), 893-898



Full Paper

Carbon Nanotube Composite as Novel Platform for Microbial Biosensor

Ülkü A. Kirgoz,^{a,*} Suna Timur,^b Dilek Odaci,^b Briza Pérez,^{c,d} Salvador Alegret,^d Arben Merkoçi^{c,*}

^a Mugla University, Faculty of Art and Science, Chemistry Department, 48000-Kötekli, Mugla Türkiye

*e-mail: ulkukirgoz@mu.edu.tr

^b Ege University, Faculty of Science, Biochemistry Department, 35100-Bornova, Izmir, Türkiye

^c Grup de Sensors i Biosensors, Departament de Química, Universitat Autònoma de Barcelona, 08193 Bellaterra, Catalonia, Spain

*e-mail: arben.merkoci.icn@uab.es

^d Institut Català de Nanotecnologia, Campus UAB, 08193 Bellaterra, Barcelona, Catalonia, Spain

Received: September 24, 2006

Accepted: December 8, 2006

Abstract

The presented work includes the development of a microbial biosensor based on a carbon-nanotube epoxy composite (CNTEC) platform used as supporting electrode for cell immobilization. For this purpose, cells of *Pseudomonas fluorescens* were immobilized on the surface of the CNTEC electrode by means of gelatin which was then cross linked with glutaraldehyde. After optimization of experimental parameters like cell amount, pH and temperature, the system was calibrated for glucose. From the calibration graph the linear range was estimated as 0.5–4.0 mM with a response time of 100 s. Furthermore, substrate specificity and operational stability were investigated. Finally, the results that were obtained with CNTEC electrodes were compared with conventional graphite epoxy composite electrode (GECE) and as a result, higher current values (2 to 3 folds) were observed with CNTEC microbial biosensor.

Keywords: Microbial biosensor, *Pseudomonas fluorescens*, Carbon nanotube, Graphite-epoxy composite

DOI: 10.1002/elan.200603786

1. Introduction

Since their rediscovery in 1991, carbon nanotubes (CNT) have attracted considerable interest due to their remarkable properties [1]. Besides their high surface area, ability to accumulate analyte, minimization of surface fouling and electrocatalytic activity, their high electrical conductivity allows the utilization of CNTs as an electrode material [2]. The electrocatalytic activity of CNT has been investigated for a wide range of compounds, such as neurotransmitters [3–6], NADH [1, 7–9], hydrogen peroxide [2, 3, 8, 10], ascorbic [2–5] and uric acid [2], cytochrome *c* [11], hydrazines [12], hydrogen sulfide [13], amino acids [14] and DNA [15]. The reported catalytic property of CNT is claimed to originate from the open ends and possible defects of the structure [9, 16].

Various types of CNT modified electrodes were prepared including physical adsorption of CNT onto electrode surfaces, like glassy carbon [1, 3–5, 7, 10, 11, 13, 14] and composite paste electrodes [9, 15] while in some case, it was consolidated into Teflon [8].

Recently CNT was incorporated into an epoxy polymer, forming an epoxy composite hybrid material as a new electrode with improved electrochemical sensing properties. The performance of this electrode in electrochemical and bioanalytical processes were investigated [2]. As a result, lower peak to peak separations and well defined

peaks were obtained with this electrode. On the other hand, multi wall carbon nanotube (MWCNT) biosensor was obtained by means of GOx immobilization through physical entrapment inside an epoxy resin matrix and its performance was examined for glucose determination. As a result a biosensor that has high sensitivity and good stability was fabricated [17].

Following these studies, present work contains the results obtained with a MWCNTEC modified with bacterial cells for future applications as a microbial biosensor.

Microbial biosensors are devices incorporating a biological sensing element (microorganism) that can specifically recognize species of interest, either intimately connected to or integrated within a suitable transducing system. The transducer is the responsible for the quantitative conversion of the biochemical signal into an electronic signal that can be suitably processed and outputted. In this way, analytes of interest may be measured by using the assimilation capacity of the microorganism as an index of the respiration activity or of the metabolic activity [18]. The major application of microbial biosensors is in the environmental field [19–21]. Real-time analysis, simplicity of operation, portability, sensitivity and specificity of the microbial biosensor make these tools very interesting.

In this study, the effect of CNT on microbial sensor response in terms of electron transportation was aimed to search. For this purpose, *Pseudomonas fluorescens* was used

as a biological material where the immobilization of the cell was done via gelatin membrane that was then cross-linked with glutaraldehyde. The characterization and optimization of the system were performed by using glucose as a substrate. Amperometric measurements were based on the respiratory activity of the cells which means, in the presence of glucose, oxygen consumption due to the metabolic pathway of the *P. fluorescens* was followed by means of a potentiostat. In order to investigate the contribution of CNT on the biosensor response, obtained results under the optimum conditions were compared with that of conventional GECE based bacterial sensor.

2. Experimental

2.1. Apparatus

Chronoamperometric experiments were carried out with a Radiometer electrochemical measurement unit (France). The electrodes were inserted into the cell through its Teflon cover. Ag/AgCl (including 3 M KCl with saturated AgCl as an internal solution, Radiometer Analytical, REF321) and Pt (Radiometer Analytical, M241PT) were used as reference and counter electrodes, respectively. Micrographs of the CNTEC surfaces without any modification were obtained by scanning electron microscopy (SEM) using Hitachi S-570DATA while the SEM image for the microorganism was obtained by using a Philips XL30SFEG SEM.

2.2. Reagents

Glucose was purchased from Merck AG (Darmstadt, Germany) while 300 bloom calf skin gelatin and glutaraldehyde were obtained from Sigma Chem. Co. (St. Louis, MO, USA). All other chemicals were of analytical grade.

Mineral salt medium (MSM) with the following composition was used as a growth medium for *Pseudomonas fluorescens*; 0.244% Na₂HPO₄, 0.152% KH₂PO₄, 0.050% (NH₄)₂SO₄, 0.02% MgSO₄ · 7H₂O, 0.005% CaCl₂ · 2H₂O and trace element solution (10 mL/L) [22] were prepared from reagent grade chemicals. The pH of the growth media was adjusted to 6.9.

2.3. Biological Material

Pseudomonas fluorescens (*Pseudomonas putida* DSM 6521) was obtained from DSMZ (German Collection of Microorganisms and Cell Cultures, Braunschweig, Germany) and subcultured on Nutrient Agar. Cell were inoculated into 50 mL of MSM containing 250 mg/L glucose and incubated at 28 °C on an orbital shaker at 150 rpm. After 24 h, when cells were grown, the biomass was harvested by centrifugation at 10000 rpm and suspended in MSM and then recentrifuged. The supernatant was removed and the cellular paste was used for making biosensor. Bacterial cells

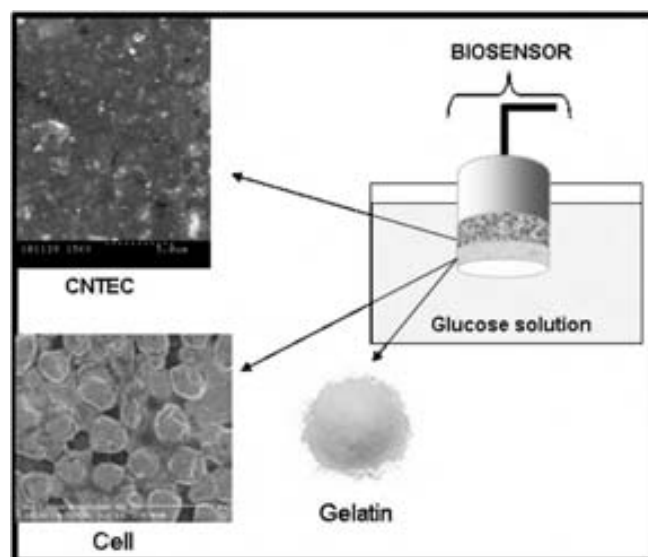


Fig. 1. Schematic diagram (not in scale) of the CNTEC based microbial biosensor including the SEM images of CNTEC and *P. fluorescens*. The acceleration voltage for CNT and CNTEC was 5.00 kV and for *P. fluorescens* it was 3.00 kV.

in logarithmic phase were used during the experiments and cell growth was followed spectrophotometrically by measuring optical density at 560 nm. The standard graph of optical density versus living cells were used to find the optimum cell amount for the preparation of biosensor [22]. Daily inoculated bacteria containing biosensors were prepared daily. Also, microbial electrodes were immersed into MSM containing glucose between the measurements.

2.4. Preparation of Biosensor

CNTEC and GECE electrodes were prepared as described previously [17]. *Pseudomonas fluorescens* cells which have 1.34×10^9 cell titer (25 μ L) and 300 bloom gelatin (10 mg) were mixed at 38 °C in phosphate buffer (50 mM, pH 7.5, 25 μ L). Mixed solution was placed onto the CNTEC working electrode surface and allowed to dry at 4 °C for 45 minutes. Finally, it was immersed in 2.5% glutaraldehyde in phosphate buffer (50 mM, pH 7.5) for 5 min. The schematic representation of biosensor preparation was given in Figure 1 with the SEM images of CNT and microorganism.

2.5. Measurements

All measurements were carried out at 30 °C under continuous and constant magnetic stirring. After each run, the electrode was washed with distilled water and kept in 50 mM phosphate buffer (pH 7.0) solution at 30 °C for 10 min. The current change that was resulted from glucose addition into the medium was recorded at 100–120th s. Since the oxygen concentration in the bioactive layer decreases related to

substrate addition, 100–120 s. is needed to reach the new steady state. The current density ($\mu\text{A}/\text{cm}^2$) changes were registered with a potentiostat at -0.7 V and the results were expressed in terms of % biosensor response. The current density that was obtained at the optimal working conditions was assumed as 100% and other measured values were calculated relative to this value.

3. Results and Discussion

Pseudomonas fluorescens is an aerobic, gram-negative bacterium which use organic compounds as their only source of carbon and energy and has shown to be an interesting model to study the biochemical impact of environmental stress on cellular metabolism [23]. The measurement was based on the respiratory activity of the cells. It is known that simple carbon sources like sugars are preferentially utilized by microorganisms. In pseudomonads, glucose utilization follows two routes: (i) the direct oxidative pathway, which converts glucose to gluconate, 2-ketogluconate and then subsequently to 6-phosphogluconate by extracellular, high affinity, glucose dehydrogenase and gluconate dehydrogenase and (ii) the intracellular, low affinity, nucleotide-dependent phosphorylative pathway where glucose is converted to 6-phosphogluconate by glucokinase and glucose 6-phosphate dehydrogenase. Depending on the physiological conditions, one or other of the pathways predominates. In the previous works, in order to elucidate the glucose metabolic pathway, O_2 uptake and enzyme activity studies were carried out [24]. In our study, oxygen consumption in the presence of glucose due to the metabolic pathway of the *P. fluorescens* was monitored amperometrically.

The carbon nanotube based biosensors combine the bioselectivity of redox enzymes with the inherent sensitivity of amperometric transductions, and have proven to be very useful for the quantification of glucose [17]. It is expected to have lower oxidation potential and higher sensitivity due to electrocatalytic properties of CNT [1–17]. In the previous work, CNTEC based glucose biosensor was developed and the results were compared with that of GECE [17]. In this work, for the first time a CNTEC based microbial sensor was developed by using *Pseudomonas fluorescens* as biological material. For this study GECE based *P. fluorescens* was utilized as control experiment for the verification of electrocatalytic benefit of CNT.

3.1. Optimization of Experimental Parameters

3.1.1. Effect of pH

According to the optimization studies, the effect of pH on the electrode response was investigated by using phosphate buffer systems (50 mM) between pH 6.0–8.2 for 2.0 mM glucose (Fig. 2). As clearly can be seen from the Figure, the response current of the electrode to glucose increases

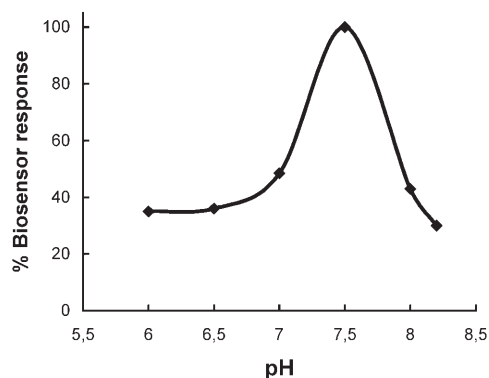


Fig. 2. Effect of pH on the biosensor response (pH 6.0–8.2; phosphate buffer (50 mM), -700 mV, 30°C).

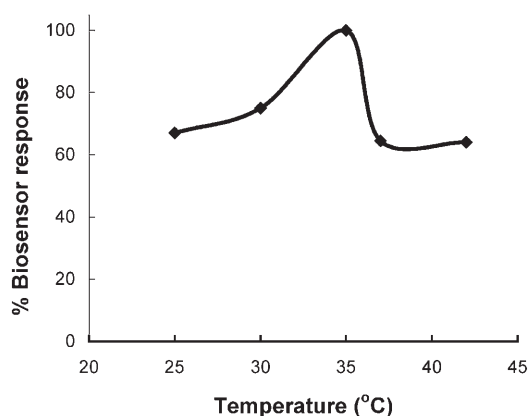


Fig. 3. Effect of temperature on the biosensor response (in phosphate buffer, 50 mM, -700 mV, pH 7.5).

significantly from pH 6.5 to 7.5, and then a sharp decrease is obtained at pH values higher than 7.5. As a result pH 7.5 was chosen as optimum pH and used for further studies.

3.1.2. Effect of Temperature

The amperometric response of the microbial electrode to 2.0 mM glucose was measured at different temperatures varying from 25 to 42°C and the results are shown in Figure 3. As best current value was observed at 35°C , further experiments were conducted at this temperature.

3.1.3. Effect of Cell Amount

For this purpose 12.5 μL , 25 μL , and 37.5 μL of bacterial cell which have the same cell titer were used to prepare three immobilization mixture. To investigate the effect of cell amount three separate calibration graphs were obtained by using each amount. The highest responses were obtained with 25 μL cell amount. As the cell activity of 12.5 μL was inadequate and 37.5 μL bacterial cells caused diffusion problem to the substrate, both amounts has tended to decrease the resulting signal. Further experiments were conducted by using 25 μL cell amount (Fig. 4).

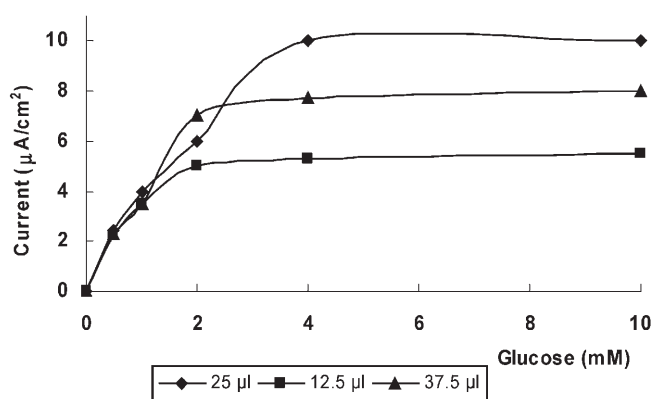


Fig. 4. Effect of cell amount (12.5 μL (■), 25 μL (◆), 37.5 μL (▲)) on the electrode response in phosphate buffer (50 mM at pH 7.5, 30 °C, -700mV).

3.1.4. Stability

The stability of cell based biosensor was investigated at working conditions (30 °C in phosphate buffer, pH 7.5) by using 2 mM glucose and a 13% decrease of activity is observed after 4 hours (data not shown). During this period approximately 16 measurements have been made and it could be possible to make more measurements in a longer time period. Moreover to be sure of the life time of bacterial cells in bioactive layer and to obtain reproducible results, the sensors including daily inoculated cells were prepared freshly for each day and utilized through the experiments.

3.1.5. Effect of Working Potential

The effect of working potential was searched by measuring the amperometric responses of two types of microbial electrode based on CNTEC and GECE to 2.0 mM glucose at different potentials vs. Ag/AgCl between -550 and -800 mV. As it is mentioned before, the measurement was based on the respiratory activity of the cells. At lower potentials (between -550 and -650 mV), CNTEC showed almost 1.5 fold higher biosensor response value than traditional GECE that was in agreement with the fact that CNTs promote electron-transfer reactions at low potentials. However maximum currents were obtained at -700 and -750 mV for both systems (Fig. 5) and for this reason -700 mV was chosen as the operating potential for further experiments.

At the previous work, glucose biosensor was fabricated by dispersing multiwall CNT inside the epoxy resin [17] and as a result, lower detection potential ($+0.55$ V) than for GOx-GECE ($+0.90$ V; difference $\Delta E = 0.35$ V) was obtained.

Due to loss of metabolic activity of microbial cell, it is inappropriate to disperse bacterial cell into composite materials like epoxy. For this reason they were immobilized onto the electrode surface by means of gelatin membrane [22]. Both gelatin membrane and the structure of bacterial cell membrane act like a diffusion barrier for electron

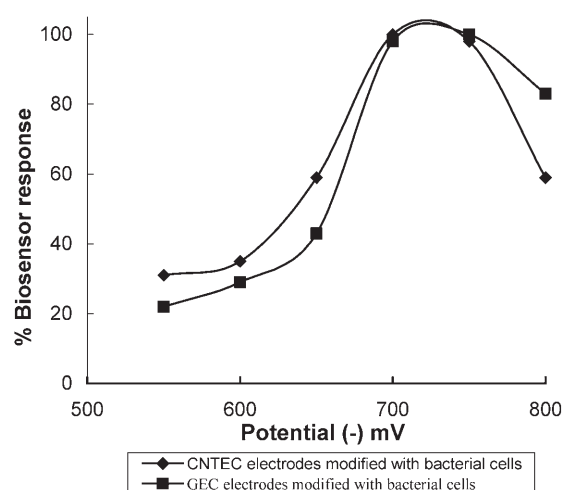


Fig. 5. Effect of working potential on the electrode response in phosphate buffer (50 mM at pH 7.5, 30 °C).

transfer and tend to slow down the reaction kinetics. Though better current values were observed with CNTEC, in our opinion, due to these complex mechanisms, significant lower values can not be obtained in terms of operating potential. The effect of CNT on electron transfer kinetics at microbial systems will be under investigation with the help of monomeric and polymeric mediators.

3.1.6. Analytical Characteristics

CNTEC electrode provides linear relationship between biosensor response (y) and substrate concentration (x) in the range of 0.5–4.0 mM glucose under the response times of 100 s with the equation of $y = 2.1x + 1.67$ ($R^2 = 0.995$, y in mM, x in $\mu\text{A}/\text{cm}^2$). At higher concentrations, standard curve showed a deviation from linearity. On the other hand, with GECE same linearity was obtained while the equation of linear graph was estimated as $y = 0.795x + 0.897$ with $R^2 = 0.983$ (y in mM, x in $\mu\text{A}/\text{cm}^2$) respectively. Besides, it was observed that CNTEC possess higher current values (2 to 3 folds) compared to GECE. This can be attributed to unique properties of CNT that promotes the electron transfer. [25, 26]. Though the electrocatalytic properties of the CNT have not been completely explained yet, it was suggested that the open ends of the nanotubes might be responsible from this attractive behavior [2].

The repeatability of the biosensor was tested for 2 mM of glucose ($n=7$) and the standard deviation (SD) and variation coefficient (cv) were calculated as ± 0.06 mM and 2.7%, respectively.

Moreover, the substrate specificities of proposed biosensor to different utilizable substrates (galactose, mannose, phenol, ethanol and methanol) were also tested and given in Table 1. No signal was obtained for phenol as well as methanol and ethanol. Since nonadapted bacterial cell were used, they didn't metabolize phenol and alcohols as expected.

Table 1. Substrate specificity of CNTEC microbial biosensor. N.D.: Not determined.

Substrate	Concentration (mM)	Current ($\mu\text{A}/\text{cm}^2$) [a]
Glucose	1 mM	3.58 ± 0.09
	2 mM	6.03 ± 0.05
Mannose	1 mM	0.56 ± 0.05
	2 mM	1.20 ± 0.05
Galactose	1 mM	1.6 ± 0.16
	2 mM	4.8 ± 0.18
Phenol	1 mM	N.D
	5 mM	N.D
Methanol	1 mM	N.D
	5 mM	N.D
Ethanol	1 mM	N.D
	5 mM	N.D

[a] Measurements were performed 4–5 times and data were given as \pm SD.

4. Conclusions

In the previous work, carbon nanotube epoxy composite (CNTEC) electrodes have been developed, characterized and compared with graphite-epoxy composite (GEC) electrodes prepared from the same epoxy resin. According to data, the CNTEC electrode has been possessed as an improved electrochemistry for ferricyanide, NADH and hydrogen peroxide. It is also stated that the resulting CNTEC electrode might offer a great promise for biosensing by incorporating biomolecules [2]. Present work represents the first example of modification of CNTEC with bacterial cells. Resulted microbial biosensor was characterized for glucose and compared with conventional GECE based microbial biosensor. As the electron transfer mechanism in the case of bacterial cells is more complicated than as it is for enzymes, lower operating potential could not be obtained with CNTEC based microbial biosensor. Although the immobilization method used in this work provides mild conditions in terms of protecting microbial activity nevertheless the usage of gelatin membrane for immobilization procedure rather than dispersing the cells into the epoxy [2] might have affected the overall response mechanism. On the other hand, higher current values (2 to 3 folds) were observed with CNTEC microbial biosensor when compared with GECE based microbial biosensor.

Microbial biosensors are good alternative to monitor some global parameters such as bioavailability and toxicity which cannot be probed with molecular recognition or chemical analysis since complex reactions including bacterial metabolic pathways can only exist in an intact functioning cell [23]. In view of the direct relevance of bioavailability and toxicity to the presence of pollutants, many of the efforts at the development of whole-cell biosensors were directed towards environmental applications. The microbial cell used in our work is well known phenol-degrading bacteria. However, adaptation process is required before using this kind of microbial cells as a specific degrader organisms. Adaptation process may be operationally defined as an increase in the ability of a microbial community to degrade a

chemical after prolonged exposure to the material. This phenomena could be due to the several alterations in structure and function of microbial species such as induction or depression of enzymes, genetic change etc. [27]. It could be also possible to use the same bacteria, as the one used in the present study, after an adaptation process to obtain microbial sensors for the environmental monitoring of other analytes [28, 29].

Design of CNT based arrays might also be promising as a good platform for the bacteria and such arrays can serve for high-throughput screening of chemicals and drugs. Utility of different immobilization matrices, as well as electron transfer mediators to overcome the possible diffusion problems and to get more efficient biosensor systems are under investigation.

5. Acknowledgements

Spanish Ramón Areces Foundation (project 'Bionanosensores') and MEC (Madrid) (Projects MAT2005-03553, and CONSOLIDER NANOBIOMED are acknowledged.

6. References

- [1] R. R. Moore, C. E. Banks, R. G. Compton, *Anal. Chem.* **2004**, *76*, 2677.
- [2] M. Pumera, A. Merkoçi, S. Alegret, *Sens. Actuators B* **2005**, *113*, 617.
- [3] H. Luo, Z. Shi, N. Li, Z. Gu, Q. Zhuang, *Anal. Chem.* **2001**, *73*, 915.
- [4] J. Wang, M. Li, Z. Shi, N. Li, *Electroanalysis* **2002**, *14*, 225.
- [5] Z. H. Wang, J. Liu, Q. L. Liang, T. M. Wang, G. Luo, *Analyst* **2002**, *127*, 613.
- [6] M. D. Rubianes, G. A. Rivas, *Electrochem. Commun.* **2003**, *5*, 689.
- [7] M. Musameh, J. Wang, A. Merkoçi, Y. Lin, *Electrochem. Commun.* **2002**, *4*, 743.
- [8] J. Wang, M. Musameh, *Anal. Chem.* **2003**, *75*, 2075.
- [9] F. Valentini, A. Amine, S. Orlanducci, M. L. Terranova, G. Palleschi, *Anal. Chem.* **2003**, *75*, 5413.
- [10] S. Hrapovic, Y. Liu, K. B. Male, J. H.T. Luong, *Anal. Chem.* **2004**, *76*, 1083.
- [11] J. Wang, M. Li, Z. Shi, N. Li, *Anal. Chem.* **2002**, *74*, 1993.
- [12] Y. Zhao, W. D. Wang, H. Chen, Q. M. Luo, *Talanta* **2002**, *58*, 529.
- [13] N. Lawrence, R. P. Deo, J. Wang, *Anal. Chim. Acta* **2004**, *517*, 131.
- [14] J. X. Wang, M. X. Li, Z. J. Shi, N. Q. Li, Z. N. Gu, *Electroanalysis* **2004**, *16*, 131.
- [15] M. L. Pedano, G. A. Rivas, *Electrochem. Commun.* **2004**, *6*, 10.
- [16] M. Zhang, A. Smith, W. Gorski, *Anal. Chem.* **2004**, *76*, 5045.
- [17] B. Perez, M. Pumera, A. Merkoçi, S. Alegret, *J. Nanosci. Nanotechnol.* **2005**, *5*, 1694.
- [18] K. Riedel, *Enzyme and Microbial Biosensors: Techniques and Protocols Part II* (Eds: A. Mulchandani, K. R. Rogers), Humana Press, Totowa, NJ **1998**, p. 199.
- [19] S. F. D'Souza, *Appl. Biochem. Biotechnol.* **2001**, *96*, 225.
- [20] J. Liu, B. Mattiasson, *Water Res.* **2002**, *36*, 3786.
- [21] Z. Yang, S. Sasaki, I. Karube, H. Suzuki, *Anal. Chim. Acta* **1997**, *357*, 41.

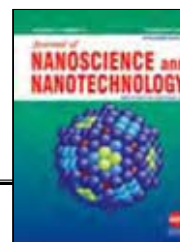
- [22] S. Timur, N. Pazarlioglu, R. Pilloton, A. Telefoncu, *Talanta* **2003**, *61*, 87.
- [23] V. D. Appanna R. D. Hamel, *Dev. Microbiol.* **1999**, *3*, 615.
- [24] A. Basu, P. S. Phale, *Microbiol. Lett.* **2006**, *259*, 311.
- [25] A. Merkoçi, M. Pumera, X. Llopsi, B. Perez, M. del Valle, S. Alegret, *Trends Anal. Chem.* **2005**, *24*, 826.
- [26] E. Banks, R. Compton, *Analyst* **2006**, *131*, 15.
- [27] R. J. Shimp, F. K. Pfaender, *Appl. Environ. Microbiol.* **1987**, *53*, 1496.
- [28] J. C. Philp, S. Balmand, E. Hajto, M. J. Bailey, S. Wiles, A. S. Whiteley, A. K. Lilley, J. Hajto, S. A. Dunbar, *Anal. Chim. Acta* **2003**, *487*, 61.
- [29] S. Belkin, *Current Opinion Microbiol.* **2003**, *6*, 206.

Glucose biosensor based on carbon nanotube epoxy composites

B. Pérez, M. Pumera, M. del Valle, A. Merkoçi and S. Alegret

Journal of Nanoscience and Nanotechnology

2005, **5**, 1694-1698





Glucose Biosensor Based on Carbon Nanotube Epoxy Composites

Briza Pérez, Martin Pumera, Manel del Valle, Arben Merkoçi,* and Salvador Alegret

Grup de Sensors i Biosensors, Departament de Química, Universitat Autònoma de Barcelona,
E-08193 Bellaterra, Barcelona, Catalonia, Spain

RESEARCH ARTICLE

A novel glucose biosensor based on a rigid and renewable carbon nanotube (CNT) based biocomposite is reported. The biosensor was based on the immobilization of glucose oxidase (GOx) within the CNT epoxy-composite matrix prepared by dispersion of multi-wall CNT inside the epoxy resin. The use of CNT, as the conductive part of the composite, ensures better incorporation of enzyme into the epoxy matrix and faster electron transfer rates between the enzyme and the transducer. Experimental results show that the CNT epoxy composite biosensor (GOx-CNTEC) offers an excellent sensitivity, reliable calibration profile, and stable electrochemical properties together with significantly lower detection potential (+0.55 V) than GOx-graphite epoxy composites (+0.90 V; difference $\Delta E = 0.35$ V). The results obtained favorably compare to those of a glucose biosensor based on a graphite epoxy composite (GOx-GEC).

Keywords: Carbon Nanotubes, Glucose Oxidase, Biosensor, Multi-Wall Carbon Nanotubes, Amperometric Detection.

1. INTRODUCTION

The combination of biological molecules and novel nanomaterial components is of great importance in the process of developing new nanoscale devices for future biological, medical, and electronic applications.^{1,2} The electrical contacting of redox enzymes with electrodes is a subject of extensive research over the last decade, with important implications for developing biosensing enzyme electrodes, biofuel cells, and bioelectronic systems.^{3,4} In this context carbon nanotubes (CNT) are particular nanomaterials that have generated a considerable interest owing to their unique structure-dependent electronic and mechanical properties.⁵

CNT can be divided into single-wall carbon nanotubes (SWCNT) and multi-wall carbon nanotubes (MWCNT). SWCNT possess a cylindrical nanostructure formed by rolling up a single graphite sheet into a tube. SWCNT can thus be viewed as molecular wires with every atom on the surface. MWCNT comprise of an array of such nanotubes that are concentrically nested like rings of a tree trunk.⁴

CNT have several characteristics that make them useful for biosensing. First, CNT have high electrical conductivity so they can act as electrodes. Second, they can be derivatized with functional groups that allow immobilization of biomolecules. Third, CNT have a high surface area-to-weight ratio (around $300 \text{ m}^2 \text{ g}^{-1}$); most of this surface area is, in principle, accessible to both electrochemistry and immobilization of biomolecules.⁶

Since their discovery in 1991, CNT⁷ have been shown to be an attractive nanomaterial with specific electronic, chemical, and mechanical properties with many applications in the field of material science, chemistry, and physics.^{8,9} As electrode materials, CNT can facilitate electron-transfer between the electroactive species and electrode, and provide a new avenue for fabricating chemical sensors or biosensors.^{10,11} Recently, the numbers of the reports on CNT-based sensors have rapidly increased.^{6,12} Biosensors based on acetylcholinesterase (AChE)¹³ immobilized through a CNTs modified thick film strip electrode for organophosphorus insecticides, horseradish peroxidase (HRP),¹⁴ attached covalently onto the ends of SWCNTs, or L-amino acid oxidase¹⁵ incorporated via an alkoxy silane sol-gel process have been used. The sol-gel process has

*Author to whom correspondence should be addressed.

been also reported to couple urease or acetylcholinesterase activity with CNT electrochemical transducing.¹⁶ The carbon nanotube based sensors promote the electrocatalytic oxidation of hydrogen peroxide and suggest great promise for oxidase-based amperometric biosensors.¹⁷ To achieve a fast electron-transfer (i.e., in the case of glucose oxidase) between the enzyme redox active site—flavin adenine dinucleotide (FAD)—and the transducing electrode, CNT modified gold electrodes have been used.^{18,19} These biosensors combine the bioselectivity of redox enzymes with the inherent sensitivity of amperometric transductions, and have proven to be very useful for the quantification of glucose.

The effective immobilization of glucose oxidase (GOx) is one of the key features for successful application of amperometric biosensors. Hence, it is pertinent to explore and develop a simple and reliable method to integrated CNT with enzymes. Many methods such as GOx incorporation into carbon paste and use of self-assembled monolayers, cross-linking, physical adsorption, and nafion have been employed to immobilize GOx. GOx have been immobilized onto CNTs via polypyrrole^{20,21} or even through CNT inks.²² However, some of these methods are relatively complicated, require unattractive reagents, and have led to biosensors with stability problems.²³

In this work, a MWCNT biosensor based on the GOx immobilization through physical entrapment inside an epoxy resin matrix, forming a rigid and renewable sensing surface, showed excellent performance for glucose determination. It has high sensitivity, good stability along with advantages such as simple in making, it is cheap in application, and easy in operating.

2. EXPERIMENTAL DETAILS

2.1. Reagents

Glucose oxidase (GOx, type VII, *Aspergillus niger* (EC 1.1.3.4), 200,000 U per gram of solid, Catalog No. G-2133) was obtained from Sigma and β -D-(+)-glucose was purchased from Sigma. The multiwalled carbon nanotubes powders (0.5–200 μ m) (MWCNT), were purchased from Aldrich (Stenheim, Germany) with \sim 95% purity. Further purification was accomplished by stirring the carbon nanotubes in 2 M nitric acid (PanReac, Spain) at 25 °C for 24 hours, according to the procedure described earlier.²⁵ Graphite powder (particle size 50 μ m) was obtained from BDH, U.K. Epoxy resin Epotek H77 A and hardener Epotek H77 B were received from Epoxy Technology. The working solutions (β -D-(+) glucose) were prepared daily by dilution in 0.1 M phosphate buffer at pH 7.0 with ultra pure water from a Millipore-MilliQ system.

2.2. Apparatus

The amperometric measurements were performed with an LC-4C amperometric detector (BAS). Electrochemical

experiments were carried out with a typical cell of 10 mL, room temperature (25 °C), using a three electrodes configuration. A platinum electrode and an Ag/AgCl were used as counter and reference electrode, respectively. A magnetic stirrer provided the convective transport during the amperometric measurements. The SEM images were conducted using a Hitachi S-3200N scanning electron microscope (SEM).

2.3. Procedures

2.3.1. Construction of the Glucose Biosensor

Carbon nanotube-epoxy composite (CNTEC) electrodes were prepared by mixing manually (using a spatula) multiwalled carbon nanotubes (MWCNT) with Epoxy resin Epotek H77 A and hardener Epotek H77 B in the ratio 20:3 (80.0% w/w). Graphite-epoxy composite (GEC) electrodes (blank electrodes) were prepared in a similar way by mixing graphite powder with Epoxy resin Epotek H77 A and hardener Epotek H77 B in the ratio 20:3 as described previously.²⁴ CNTEC and GEC electrodes containing the enzyme glucose oxidase (GOx) (GOx-CNTEC and GOx-GEC; see schematic presentation in Fig. 1), were prepared by mixing carbon nanotubes powder or graphite (18.0% w/w) with GOx (2.0% w/w), followed by the incorporation of Epoxy resin (80.0% w/w) and mixing for 30 minutes to ensure an homogeneous biocomposite paste; this paste was then introduced in a PVC tube containing an electrical connection through a copper disk and wire. The conducting biocomposite was cured at 40 °C for one week. Prior the used the hardened electrode surface was polished with different abrasive papers of decreasing grain

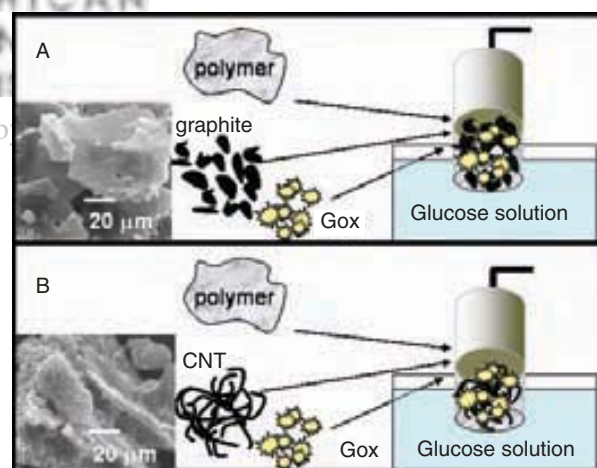


Fig. 1. Schematic of the glucose biosensors based on GEC (A) and CNTEC (B). Shown, the left side, are also the SEM images of the dried mixtures of glucose oxidase with graphite (A) and CNT (B) before mixing with the epoxy polymer to form GEC and CNTEC pastes. A better entrapment of GOx inside the sponge like structure of the CNT bundles compared to graphite particle is clearly visualized in the SEM images. Electrodes composition: Carbon, 18% (w/w); GOx, 2% (w/w); epoxy, 80% (w/w).

size, ending with alumina paper (polishing strips 301044-001, Orion, Spain).

2.3.2. Amperometric Determination of Glucose

The steady state amperometric response to glucose was measured in aliquots of 10 mL of buffer solution with differing additions of glucose applied then onto the reaction cell. The measurements were carried out in a 0.1 M phosphate buffer solution pH 7.0, employed as supporting electrolyte. The applied potential to the working electrode for glucose determination was +0.55 V and +0.90 V for GOx-CNTEC and GOx-GEC electrodes respectively. The background current was allowed to decay to a constant level before aliquots of glucose sample were added to the stirred buffer solution.

3. RESULTS AND DISCUSSION

3.1. Material and Electrode Morphologies

The mixtures of GOx with graphite or carbon nanotubes were observed using scanning electron microscopy (SEM). The inset SEM images of Figure 1 correspond to the dried mixtures of glucose oxidase with graphite (A) and CNT (B) before mixing with the epoxy polymer to form GEC and CNTEC composite pastes. A better entrapment of GOx inside the sponge like structure of the CNT bundles

compared to graphite particle is clearly visualized in the SEM images. The dispersed GOx particles (after mixing well with the conducting phase) seem to be entrapped better within the CNT wire bundles rather than to graphite particles.

The resulted electrode surfaces were also observed by SEM after mixing with epoxy resin and proper hardening as described in the experimental section so gain insight on the surface characteristics. Figure 2 represents the electrode surface without (A) and with (B) incorporated GOx for GEC (a) and CNTEC (b) electrodes. These images show that: there is difference between the CNTEC electrodes without (b, A) and with (b, B) incorporated GOx resulting into different surface morphologies, while in case of GEC electrodes without (a, A) and with incorporated (a, B) GOx the surface morphologies do not significantly vary. The CNT-epoxy matrix provides better entrapment of the GOx compared to a graphite-epoxy one. This is related to the CNT filament-like structure that homogenizes with the epoxy resin better than the graphite particles. Consequently the physical entrapment of GOx at CNT-epoxy matrix ensures a better immobilization than in the graphite-epoxy matrix. Additionally, the CNTEC electrode shows a more porous structure and consequently a larger specific surface area compared to GEC electrode.

3.2. Amperometric Detections

3.2.1. Electrocatalytic Properties of the Glucose Biosensor

For developing oxidase-based biosensors the detection of hydrogen peroxide is of considerable interest. It is widely known that the electrooxidation and electroreduction of hydrogen peroxide at different carbonaceous materials (glassy carbon, graphite paste, graphite, carbon fiber, glassy carbon paste, screen-printed electrodes), require elevated overvoltages. In the case of CNTEC, as it was already reported there is an important catalytic effect both on the reduction and oxidation of hydrogen peroxide, making a high sensitive detection of this compound possible. Figure 3 compares hydrodynamic voltammograms for a 4 mM glucose solution at GOx-GEC (a) and at GOx-CNTEC (b) electrodes. The oxidation current for the hydrogen peroxide enzymatically generated by glucose oxidase incorporated into the epoxy composite matrix starts at potential +0.55 V at GOx-CNTEC, while at GOx-GEC electrode it starts at +0.90 V. A potential shift of around $\Delta E = 0.35$ V is clearly observed. Moreover, at GOx-CNTEC the signal increases around 90% (note the different current scales at Fig. 3) indicating larger glucose signal when the GOx-CNTEC electrode was employed. CNT significantly promote the electron transfer between hydrogen peroxide and GOx-CNTEC facilitates the low-potential amperometric determination of glucose.

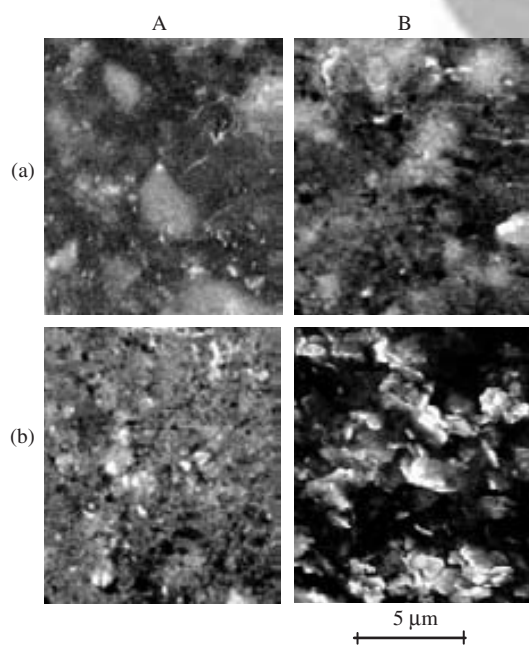


Fig. 2. SEM images of the biosensor surfaces without (A) and with (B) glucose oxidase incorporated. Shown are GEC (a) and CNTEC (b) based biosensors. All electrode surfaces have been polished in the same way as explained in the text. The same acceleration voltage (5 kV) and resolution are used. Electrodes composition: (A) Carbon, 18% (w/w); epoxy, 82% (w/w); (B) Carbon, 18% (w/w); GOx, 2% (w/w); epoxy, 80% (w/w).

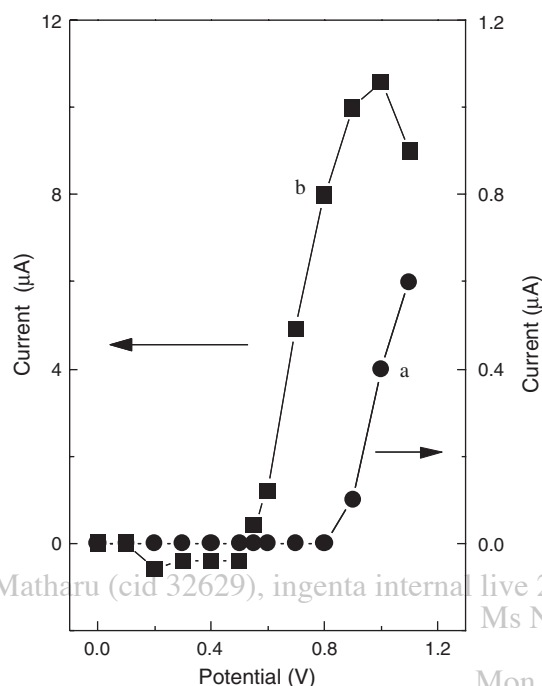


Fig. 3. Hydrodynamic voltammogram for 4 mM glucose for GOx-GEC (a) and at GOx-CNTEC (b) in 0.1 M phosphate buffer pH 7.0. Electrodes composition: as described in the Figure 1.

3.2.2. Calibration of Biosensor to Glucose

The amperometric responses of GOx-GEC and GOx-CNTEC electrodes to glucose are compared in Figure 4. The steps correspond to the responses of GOx-GEC (a) and GOx-CNTEC (b) for successive additions of 0.5 mM glucose in 0.1 M pH 7.0 phosphate buffer solution and using operating potentials of +0.90 (A) and +0.55 (B). The resulting calibration plots (insets) are also shown. It can be observed that GOx-CNTEC electrodes offers substantially higher signals for both operating potentials (+0.55 and +0.90 V) compared to GOx-GEC electrode.

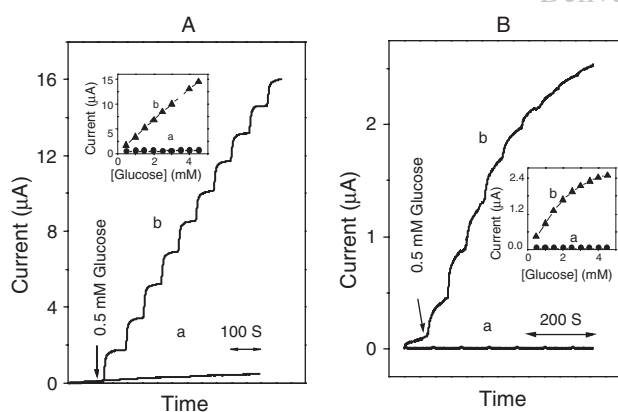


Fig. 4. Current-time recordings obtained from amperometric experiments at GOx-GEC (a) and at GOx-CNTEC (b) for successive additions of 0.5 mM glucose. Working potential: (A) +0.90 V and (B) +0.55 V in 0.1 M phosphate buffer pH 7.0. The insets show the corresponding calibration plots. Electrodes composition: as described in the Figure 1.

The electrocatalytic activity of carbon nanotubes is even more pronounced from comparison of the response at +0.55 V, where the conventional GOx-GEC electrode is not responding (see Fig. 4B, curve a). The sensitivity of detection at an applied potential of +0.90 V for glucose determination, based in the amount of hydrogen peroxide produced by enzyme reaction, was found to be more than 6 times larger than that when an applied potential +0.55 V was employed. As expected from the HDV (Fig. 3), higher sensitivity is observed at +0.90 V (note the different scales). In Figure 4A the plot of current vs glucose concentration was linear over a wide concentration range of 0.5–4.5 mM for GOx-CNTEC electrode (A, b), had a correlation coefficient of 0.999, a linear concentration range of GOx-GEC (A, a), the electrode was 0.5–2.5 mM, a correlation coefficient of 0.999 (in this range), and detection limits of 0.09 mM and 0.10 mM respectively. The corresponding calibration plots show sensitivities of $0.10 \mu\text{A} \cdot \text{mM}^{-1}$ for GOx-GEC electrode and $3.21 \mu\text{A} \cdot \text{mM}^{-1}$ for GOx-CNTEC electrode.

3.3. Stability Measurements

The functioning principle of the glucose biosensor is based on the amperometric detection of H_2O_2 , which is generated during the course of the enzyme-catalyzed oxidation of glucose by dissolved oxygen. In this work, amperometric measurements were carried out in 0.1 M phosphate buffer solution pH 7.0 under magnetic stirring. Figure 5 presents the stability of the response for 4 mM glucose at the GOx-CNTEC electrode at operating potential of +0.90 V.

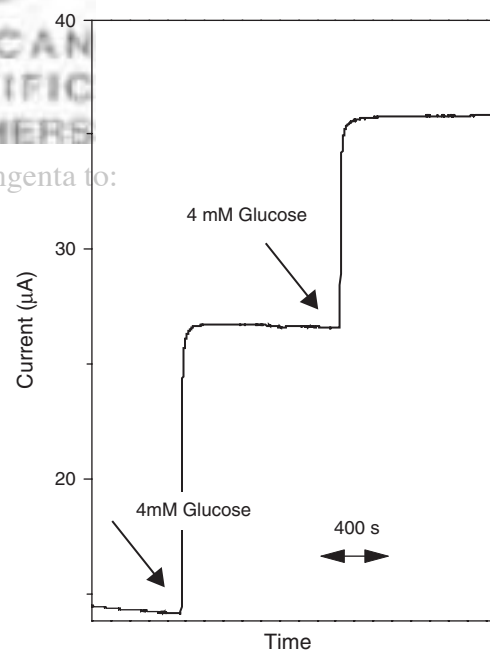


Fig. 5. Stability of the response of the GOx-CNTEC biosensor to additions of 4 mM glucose. Conditions: +0.9 V in 0.1 M phosphate buffer solution pH 7.0. Electrodes composition: as described in the Figure 1.

It can be observed that the current increases obviously after the addition of glucose maintaining then a steady state response thereafter. Additionally, a response time of about 30 seconds can be observed from Figure 5.

4. CONCLUSIONS

The emergence of nanotechnology opens new horizons for electrochemical sensors. Recent years have sparked the development of a variety of nanomaterial based bioelectronic devices exhibiting novel functions. The integration of carbon nanotubes in designing novel biosensors is just an example of the advantages offered by nanotechnology products.

A biosensor for glucose detection based on immobilization of glucose oxidase within a rigid carbon nanotube epoxy composite matrix was demonstrated. The results presented above reveal the ability of CNTEC to promote the electron transfer between the glucose oxidase and the hydrogen peroxide produced by the enzymatic reaction. The observed results were rationalized by the following explanations: (i) The CNTs dispersed in the epoxy resin ensure an electrical contact with GOx better than the graphite particles do. This is due to the sponge-like structure of the CNT that probably achieves improved electrical contacts with GOx. (ii) The CNT structure ensure better microelectrode arrays compared to graphite particles. This may also enhance the signal to noise ratio that has been reported also for graphite based composites.²⁵ The CNT biocomposite based biosensor exhibited excellent sensitivity and stability for the determination of glucose. Moreover, it is simple, it has a fast and reproducible response, and low cost. Nevertheless a future interdisciplinary research, which is under exploitation in our laboratory, could lead to a new generation of electrochemical biosensors based on robust biosensor with better electron transfer including for other enzymes.

Acknowledgments: This work was financially supported by MEC (Madrid) (Projects BIO2004-02776, MAT2004-05164), by the Spanish "Ramón Areces" foundation (project 'Bionanosensors') and the "Ramón y Cajal" program of the Ministry of Science and Technology

(Madrid) that supports A. Merkoçi. M. Pumera is grateful for the support from the Marie Curie Intra-European Fellowship from European Community under 6thFP (project 005738).

References and Notes

1. I. Willner, *Science* 298, 2407 (2002).
2. J. Wang, M. Musameh, A. Merkoçi, and Y. Lin, *Electrochem. Comm.* 4, 743 (2002).
3. F. A. Armstrong and G. S. Wilson, *Electrochim. Acta* 45, 2623 (2000).
4. A. Heller, *J. Phys. Chem. Res.* 96, 3579 (1992).
5. Y. Degani and A. Heller, *J. Phys. Chem.* 91, 1285 (1987).
6. A. Merkoçi, M. Pumera, X. Llopis, B. Pérez, M. del Valle, and S. Alegret, *Trends in Anal. Chem.* (2005), in press: doi:10.1016/j.trac.2005.03.019.
7. S. Iijima, *Nature* 354, 56 (1991).
8. P. M. Ajayan, *Chem. Rev.* 99, 1787 (1999).
9. R. H. Baughman, A. A. Zakhidov, and W. A. de Heer, *Science* 297, 787 (2002).
10. Q. Zhao, Z. Gan, and Q. Zhuang, *Electroanalysis* 14, 1609, (2002).
11. N. Li, J. Wang, and M. Li, *Rev. Anal. Chem.* 22, 19 (2003).
12. Q. Zhao, L. Guan, Z. Gu, and Q. Zhuang, *Electroanalysis* 17, 85 (2005).
13. K. A. Joshi, J. Tang, R. Haddon, J. Wang, W. Chen, and A. Mulchandani, *Electroanalysis* 17, 54 (2005).
14. X. Yu, D. Chattopadhyay, I. Galeska, F. Papadimitrakopoulos, and J. F. Rusling, *Electrochem. Comm.* 5, 408 (2003).
15. V. G. Gavalas, S. A. Law, J. C. Ball, R. Andrews, and L. G. Bachas, *Anal. Biochem.* 329, 247 (2004).
16. Z. Xu, X. Chen, X. Qu, J. Jia, and S. Dong, *Biosensors Bioelectronics* 20, 579 (2004).
17. J. Wang and M. Musameh, *Anal. Chem.* 75, 2075 (2003).
18. F. Patolsky, Y. Weizmann, and I. Willner, *Angew. Chem. Int.* 43, 2113 (2004).
19. J. Liu, A. Chou, W. Rahmat, M. N. Paddon-Row, and J. J. Gooding, *Electroanalysis* 17, 38 (2005).
20. M. Gao, L. Dai, and G. Wallace, *Synth. Met.* 137, 1393 (2003).
21. K. P. Loh, S. L. Zhao, and W. D. Zhang, *Diamond Rel. Mater.* 13, 1075 (2004).
22. J. Wang and M. Musameh, *Anal.* 129, 1 (2004).
23. A. Salimi, R. Compton, and R. Hallaj, *Anal. Biochem.* 333, 49 (2004).
24. (a) M. Pumera, M. Aldavert, C. Mills, A. Merkoçi, and S. Alegret, *Electrochimica Acta* 50, 3702 (2005); (b) M. Pumera, A. Merkoçi, and S. Alegret, *Sensors and Actuators B* (2005), in press.
25. S. Alegret and A. Merkoçi, Composite and biocomposite materials for electrochemical sensing. *Integrated Analytical Systems*, edited by S. Alegret, Amsterdam, Elsevier (2003), p. 377.

Received: 12 May 2005. Revised/Accepted: 20 May 2005.

New materials for electrochemical sensing. VI. Carbon nanotubes

A. Merkoçi, M. Pumera, X. Llopis, **B. Pérez**, M. del Valle and S. Alegret

Trends in Analytical Chemistry

2005, **24**, 826-838



New materials for electrochemical sensing VI: Carbon nanotubes

Arben Merkoçi, Martin Pumera, Xavier Llopis, Briza Pérez, Manel del Valle, Salvador Alegret

Carbon nanotubes (CNTs) combine in a unique way high electrical conductivity, high chemical stability and extremely high mechanical strength. These special properties of both single-wall (SW) and multi-wall (MW) CNTs have attracted the interest of many researchers in the field of electrochemical sensors. This article demonstrates the latest advances and future trends in producing, modifying, characterizing and integrating CNTs into electrochemical sensing systems.

CNTs can be either used as single probes after formation *in situ* or even individually attached onto a proper transducing surface after synthesis. Both SWCNTs and MWCNTs can be used to modify several electrode surfaces in either vertically oriented “nanotube forests” or even a non-oriented way. They can be also used in sensors after mixing them with a polymer matrix to form CNT composites.

We discuss novel applications of CNTs in electrochemical sensors, including enzyme-based biosensors, DNA sensors and immunosensors, and propose future challenges and applications.

© 2005 Elsevier Ltd. All rights reserved.

Keywords: Amperometry; Carbon nanotube; CNT; DNA sensor; Electrochemical sensing; Electrochemical stripping; Enzyme biosensor; Multi-wall carbon nanotube; MWCNT; Single-wall carbon nanotube; SWCNT

Arben Merkoçi*,

Martin Pumera, Xavier Llopis,
Briza Pérez, Manel del Valle,
Salvador Alegret

Grup de Sensors & Biosensors,
Departament de Química,
Universitat Autònoma de
Barcelona, E-08193 Bellaterra,
Catalonia, Spain

1. Introduction

The trend of using novel materials in electrochemical sensing systems is constant, with their success largely due to the continuous design and development that meets the needs of modern electrochemical (bio)sensor technology. Materials ranging from carbon composites (Parts I and II of this series) [1,2], beads or microspheres (Part III) [3], molecular imprinted polymers (MIP) (Part IV) [4] or quantum dots (Part V) [5] are playing an important role in these sensing systems.

Since their discovery in 1991 [6], carbon nanotubes (CNTs) have generated great interest in future applications based on their field emission and electronic transport properties [7], their high mechanical strength [8] and their

chemical properties. There is increasing potential for CNTs to be used as field emission devices [9], nanoscale transistors [10], tips for scanning microscopy [11] or components for composite materials [12].

CNTs are one of the most commonly used building blocks of nanotechnology. With 100 times the tensile strength of steel, thermal conductivity better than all but the purest diamond, and electrical conductivity similar to copper, but with the ability to carry much higher currents, they are very interesting.

CNTs include both single-walled and multi-walled structures (Fig. 1). Single-wall CNTs (SWCNTs) (Fig. 1A) comprise of a cylindrical graphite sheet of nanoscale diameter capped by hemispherical ends. The closure of the cylinder is result of pentagon inclusion in the hexagonal carbon network of the nanotube walls during the growth process. SWCNTs have diameters typically ~1 nm with the smallest diameter reported to date of 0.4 nm. This corresponds to the theoretically predicted lower limit for stable SWCNT formation based on consideration of the stress energy built into the cylindrical structure of the SWCNT.

The multi-wall CNTs (MWCNTs) (Fig. 1B) comprise several to tens of incommensurate concentric cylinders of these graphitic shells with a layer spacing of 0.3–0.4 nm. MWCNTs tend to have diameters in the range 2–100 nm. The MWCNT can be considered as a mesoscale graphite system, whereas the SWCNT is truly a single large molecule.

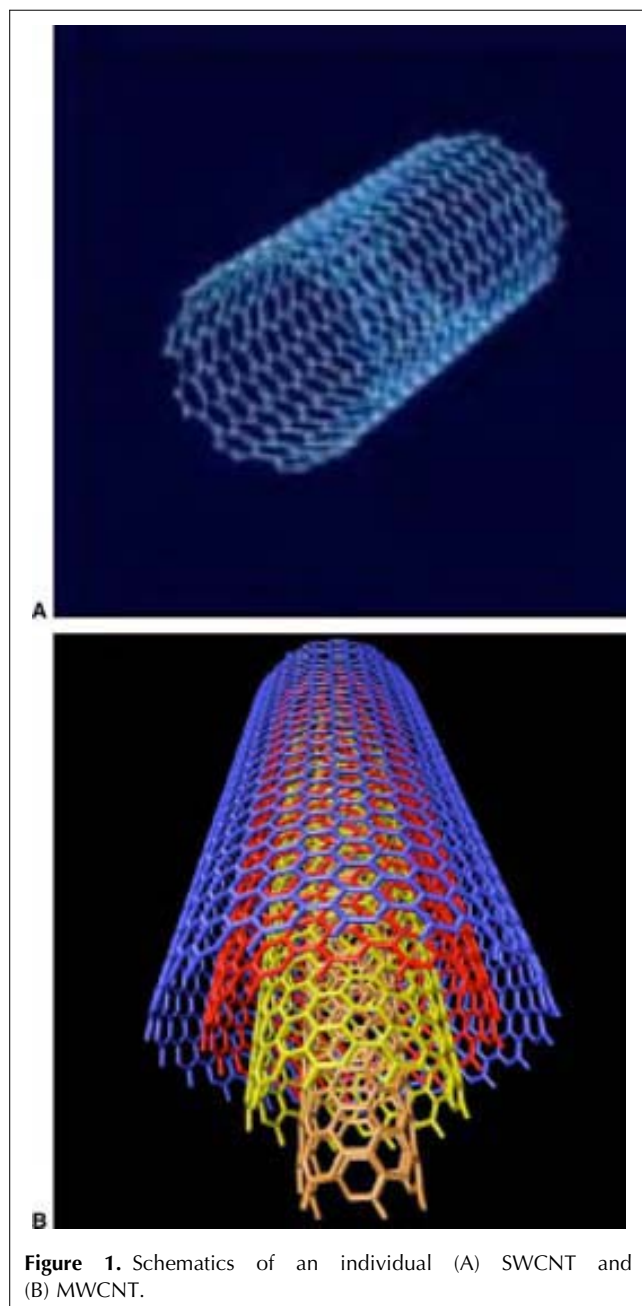
CNT metal–insulator–semiconductor capacitors were examined theoretically by Guo et al. [13]. CNTs can have metallic or semiconducting properties. Because of the small diameter of CNTs,

*Corresponding author.

Tel.: +34 93 581 1976/2118;

Fax: +34 93 581 2379;

E-mail: arben.merkoci@uab.es



quantum-mechanical effects determine their electronic structure. This means that the quantization conditions along the nanotube perimeter determine whether a nanotube acts as a metal or a semiconductor. These properties are being considered as the basis of future nanoelectronics, which represent one of the most important applications of CNTs.

The aim of this part of the “New materials for electrochemical sensing” series is to cover only particular aspects related to integrating CNTs into electrochemical sensing systems. We will describe the different methods of preparing CNTs, the possible ways of modifying and solubilizing CNTs, with the major part devoted to describing how CNTs are integrated into sensors and

biosensors. We will also set out novel ideas on using and integrating CNTs in electrochemical sensors.

2. Synthesis of carbon nanotubes

2.1. Arc-discharge method

There are several ways of preparing CNTs, the arc-discharge method [14,15] being the first. This method creates MWCNTs through arc-vaporization of two graphite rods placed end to end, separated by approximately 1 mm, in an enclosure usually filled with inert gas (helium, argon) at low pressure (between 50 and 700 mbar). After applying a dc arc voltage between two separated graphite rods by modifying apparatus for producing SiC powder, the evaporated anode generates fullerenes in the form of soot in the chamber, and part of the evaporated anode is deposited on the cathode. When a graphite rod containing a metal catalyst (e.g., Fe and Co) is used as the anode and the cathode is pure graphite, SWCNTs [16] are generated instead of MWCNTs.

Large-scale synthesis of MWCNTs by arc-discharge was achieved [13,17] in a helium atmosphere. The arc-discharge evaporation of pure graphite rods has been carried out in not only ambient gases, such as helium or argon, but also methane [18]. It was found that methane is the best gas for the synthesis of MWCNTs. This is due to the thermal decomposition of methane producing hydrogen ($2\text{CH}_4 \rightarrow \text{C}_2\text{H}_2 + 3\text{H}_2$) that achieves higher temperature and activity compared to inert gases, such as He or Ar. The effectiveness of hydrogen in the synthesis of MWCNTs has been reported [19].

The drawback of arc-discharge method is purification of CNTs. Removal of non-nanotube carbon and metal catalyst material is much more expensive than production itself.

2.2. Laser-furnace method

The laser-furnace method or laser ablation [20] was originally used as a source of metal clusters [21] and ultrafine particles [22]. It was then developed for fullerene and CNT production. The laser-vaporization method is widely used for the production of SWCNTs. The laser is suitable for materials with a high boiling temperature, such as carbon, as the energy density of lasers is much higher than that of other vaporization devices.

The basic principle of this method is as follows:

- a CO_2 laser beam is introduced onto the target (carbon composite doped with catalytic metals) located in the center of a quartz tube furnace;
- the target is vaporized in a high-temperature argon atmosphere and SWCNTs are formed; and,
- the SWCNTs produced are conveyed by the gas to a special collector.

The method has several advantages, such as the high quality of the diameter and controlled growth of the SWCNTs. The change of the furnace temperature, catalytic metals and flow rate directly affect the SWCNT diameter [23].

2.3. Chemical-vapor deposition

The first two methods, arc-discharge and laser furnace, have the drawback that they do not allow control of the location and the alignment of the synthesized CNTs. This can be avoided by chemical-vapor deposition (CVD). This popular method uses hydrocarbon vapor (e.g., methane) that is thermally decomposed in the presence of a metal catalyst. The method is also known as thermal or catalytic CVD.

CVD is a versatile process in which gas-phase molecules are decomposed to reactive species, leading to film or particle growth [24]. CVD is a simple, economic technique for synthesizing CNTs at low temperature and ambient pressure, at the cost of crystallinity [25]. CVD has been used for producing carbon filaments and fibers since 1959 [26]. The process involves passing a hydrocarbon vapor through a tube furnace in which a catalyst material is present at sufficiently high temperature to decompose the hydrocarbon. CNTs grow over the catalyst and are collected on cooling the system to room temperature. CNTs have also been successfully synthesized using organometallic catalyst precursors [27]. The three main parameters for CNT growth in CVD are type of hydrocarbon, type of catalyst and growth temperature.

Apart from large-scale production [28], CVD also offers the possibility of producing single CNTs for use as probe tips in atomic force microscopy (AFM) [29]. The tips produced are smaller than mechanically assembled ones, thus significantly improving the resolution of AFM.

3. Modifying carbon nanotubes

3.1. Boron and nitrogen doping

The electronic, chemical and mechanical properties of CNTs can be tailored by replacing some of the carbon (C) atoms with either boron (B) or nitrogen (N). If B (with one electron less than C) or N (one electron more than C) replaces some C atoms, *p* or *n* type conductors can be formed, respectively. From the chemical point of view, these doped structures would be more likely to react with donor or acceptor molecules, depending on the doping.

B- or N-doped CNTs can be obtained by the arc method by arching either B- or N-graphite electrodes in an inert atmosphere, as described above. Laser [30] and CVD [31] methods have been also used. Although not so far reported in electrochemical sensing systems, these B- or N-doped CNTs should merit future attention.

3.2. Metal filling

Metal-filled CNTs are promising nanowires with excellent protection against oxidation. They can be produced by the CVD method. Nanoparticles containing a transition metal are essential in the nanotube growth. This is because the nanoparticles do not only catalyze nanotube growth but also affect the structural properties. The syntheses of Fe-, Ni- and Co-filled CNTs using the CVD method have been reported [32]. CNTs filled with ferromagnetic metals (i.e., Fe, Ni, and Co) yield fascinating new materials. These carbon-covered ferromagnetic nanowires have significant potential in data-storage technology due to their size and enhanced magnetic properties. In addition, the carbon shells provide an effective barrier against oxidation and consequently ensure long-term stability of the ferromagnetic core. Another example of metal filling is the *in situ* reaction forming cadmium sulphide crystals from cadmium oxide by treatment with hydrogen sulphide at 400°C [33]. This loaded CNT can find applications in DNA labeling, as was explained in the Part V of this series [5].

Nanoparticles containing Co and Mo, prepared by a reverse micelle method, have been applied to the catalytic growth of SWCNTs and MWCNTs [34]. Both molten media and wet chemistry solution methods have been used to introduce metals or metal oxides into hollow nanotube cavities. Chemical reactions have been carried out inside the tubes, including the reduction of encapsulated materials to metals [33].

4. Solubilization

Before application to (bio)analytical assays, CNTs (prepared as described in Section 2 above) must be first modified to be transformed to a soluble product. The preparation of homogeneous dispersions of CNTs, suitable for processing into thin films or for other applications, is of a great importance. Various methods can be used for this purpose (detailed information in Table 1 and typical examples in Fig. 2).

End [35] and/or sidewall [36] functionalization, use of surfactants with sonication [37], polymer wrapping of nanotubes [38], and protonation by superacids [39] have been reported. Although these methods are quite successful, they often indicate cutting the CNTs into smaller pieces (sonication and/or functionalization), thus partly losing the high aspect ratio of SWCNTs.

Kim et al. [40] provided an example of CNT solubilization. They developed a simple, efficient process for solubilizing CNTs with amylose in dimethyl sulphoxide-H₂O (DMSO-H₂O) mixture as well as in pure water. This process requires two important conditions, pre-sonication of CNTs in water and subsequent treatment of the fine CNT dispersion with amylose in a specified

Table 1. Approaches for solubilization of carbon nanotubes

Solubilization agent	Type of	Note	Reference
Helical amylose in DMSO–H ₂ O	SWCNT	Supramolecular encapsulation	[41]
Polyvinyl pyrrolidone and polystyrene sulphonate	SWCNT	Non-covalent association CNT with linear polymers, “polymer wrapping”	[38a]
η -Cyclodextrin	SWCNT	CNT forms inclusion complex with 12-unit η -cyclodextrin	[81]
Nafion	MWCNT	CNT/Nafion association does not impair the electrocatalytic properties of CNT	[82]
Tetrahydrofuran/Li ⁺	SWCNT	Negatively charged CNT forms with Li ⁺ conducting polyelectrolyte salts	[83]
Diamine-terminated oligomeric poly(ethylene glycol)	SWCNT	Reaction between amino group of polymer and carboxy group of oxidized CNT	[84]
2-Aminomethyl-18-crown-6 ether	SWCNT	Reaction between amino group of crown ether and carboxy group of oxidized CNT	[85]
Glucosamine	SWCNT	Reaction between amino group of glucosamine and carboxy group of oxidized CNT	[86]
3-Aminopropyltriethoxysilane	MWCNT	Nanoscale dendrites of CNTs modified by 3-aminopropyltriethoxysilane that forms a conducting network, promoting electrode reaction	[42]
Diamine-terminated oligomeric poly(ethylene glycol), poly(propionylethylenimine-co-ethylenimine) and poly(vinyl alcohol)	SWCNT	Reaction between amino (or hydroxy) group of polymer and carboxy group of oxidized CNT	[87]
Tris-triphenylphosphine rhodium(I) chloride (RhCl(pph ₃) ₃ – Wilkinson’s compound)	SWCNT	Rh metal coordinates to oxidized nanotubes through the increased number of oxygen atoms, forming a hexacoordinate structure around the Rh atom	[88]
Poly(propionylethylenimine-co-ethylenimine)	MWCNT	Sonication-assisted reaction between imido group of polymer and carboxy group of oxidized CNT	[89]

DMSO–H₂O mixture, followed by a post-sonication. The former step disaggregates the CNT bundles, and the latter step maximizes cooperative interactions between CNTs and amylose, leading to immediate and complete solubilization. The best solvent composition was found to be 10–20% DMSO, in which amylose assumes an interrupted loose helix. The resulting colloidal solution was stable and exhibited no precipitation over several weeks.

CNT solubilization by covalent modification was reported by Luong et al. [41]. MWCNTs were solubilized in a mixture of 3-aminopropyltriethoxysilane (APTES) and Nafion-perfluorinated ion-exchange resin and ethanol. Uniformly dispersed MWCNTs were obtained after 20 min sonication and used for sensor applications. The interactions between CNTs and amino-terminated organic species are complex and depend on the conditions of the functionalization reaction.

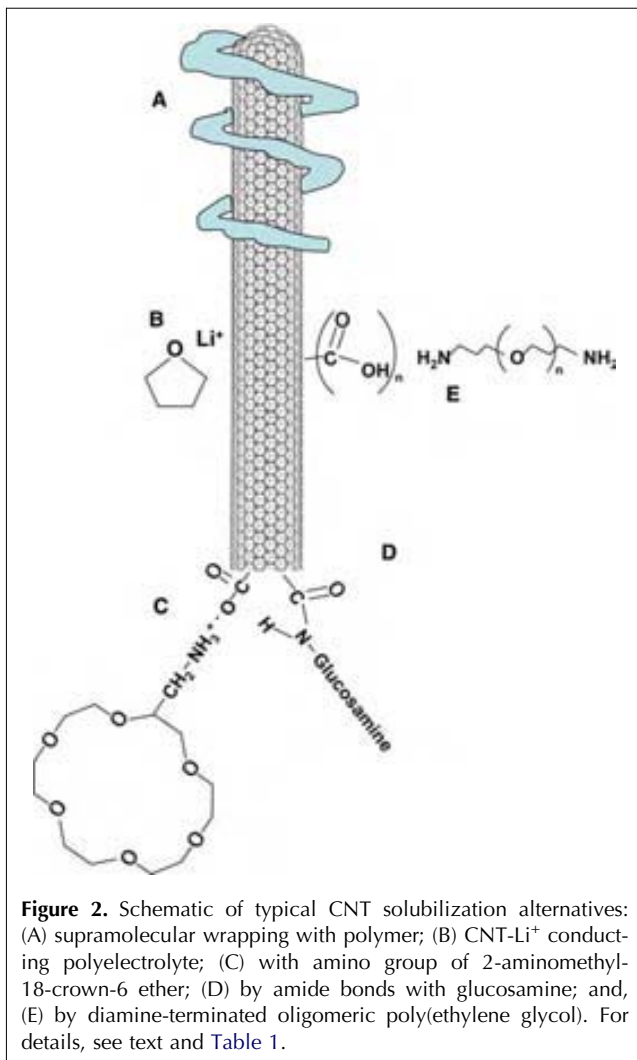
5. Integration of carbon nanotubes

CNTs can be integrated into a variety of configurations to perform electrochemical detections. The current formats (Fig. 3) can be classified in groups:

- individual CNT configurations;
- conventional electrodes that are modified with CNTs, in both oriented or non-oriented configurations; and,
- CNTs integrated into a polymer matrix, creating a CNT composite.

5.1. Individual CNTs

With extremely small size, high conductivity, high mechanical strength and flexibility (ability to easily bend elastically), nanotubes may ultimately become indispensable in their use as nanoprobe. One could think of such probes being used in a variety of applications, such as high-resolution imaging, nanolithography, nanoelectrodes, drug delivery, sensors and field emitters. Experimental results show that SWCNTs can carry currents up to 10⁹ A/cm², whereas the maximum current densities for normal metals are ~10⁵ A/cm² [42]. Unfortunately, the large current-carrying capability is less useful for sensor applications because of the necessarily large contact resistances. An electronic circuit involving electrical leads to and from a SWCNT will have a resistance of at least 6.5 k Ω



[43]. Contacting all layers in a CNT can reduce this contact resistance, but it cannot be totally eliminated [44].

The use of individual SWCNTs as nanoelectrodes for electrochemistry was reported recently by Dekker et al. [45]. SWCNTs were contacted by nanolithography and cyclic voltammetry was performed in aqueous solutions. These studies demonstrate the potential of using SWCNTs as model carbon nanoelectrodes for electrochemistry.

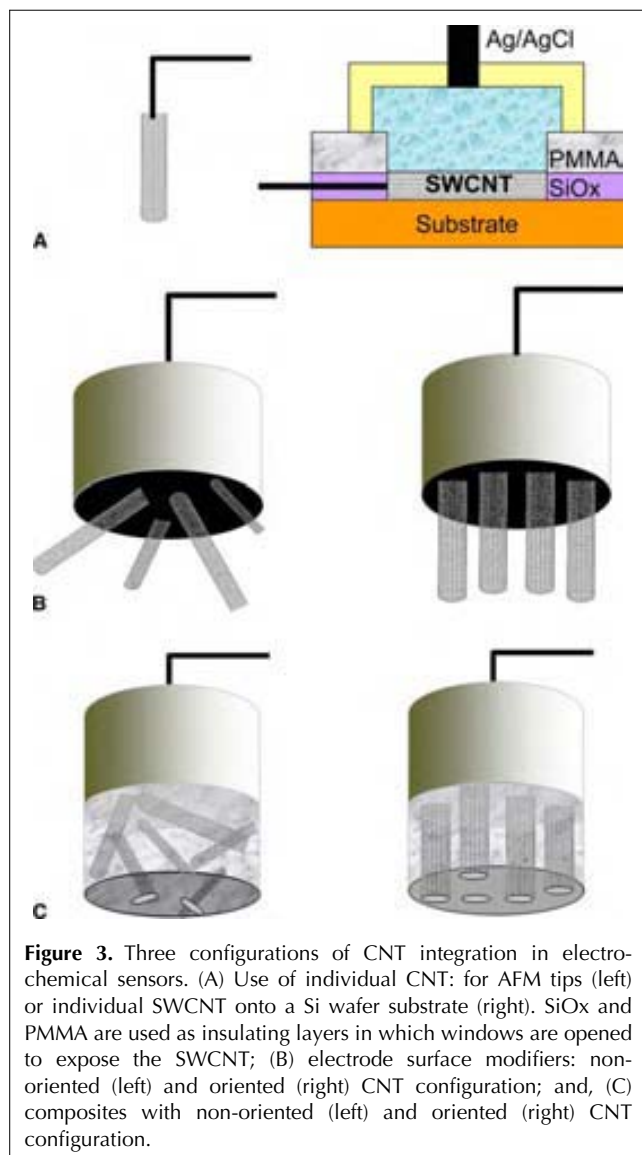
The use of CNTs attached to the end of a scanning probe microscope tip for imaging, including electrical measurements, has already been demonstrated [46].

5.2. CNTs as modifiers of electrode surfaces

CNTs – both non-oriented (random mixtures, Fig. 3B, left) and oriented (vertically aligned, Fig. 3B, right) – have been used to modify several conventional electrode surfaces, glassy carbon being the most reported.

5.2.1. Oriented modifications. The open end of an MWCNT has a fast electron transfer rate (ETR) similar to a graphite edge-plane electrode, while the SWCNT presents a very slow ETR and low specific capacitance, similar to the graphite basal plane [47]. Based on that idea, Li et al. [48] believed that the proper construction and orientation of the electrode is critical for its electrochemical properties. For that reason, they used a bottom-up approach, which is compatible with Si-microfabrication processes. They combined microlithography and nanolithography with catalytic CNT-growth techniques. A forest-like vertically aligned MWCNT array was grown on Ni-catalyst film using plasma-enhanced CVD. A dielectric encapsulation was then applied, leaving only the very end of CNTs exposed to form inlaid nanoelectrode arrays. The electrical and electrochemical properties of this oriented MWCNT array for small redox molecules have been characterized (by cyclic voltammetry and electrochemical impedance spectroscopy), showing well-defined quasi-reversible nanoelectrode behavior and ultrasensitive detection. Palleschi et al. [49] fabricated tungsten microelectrodes coated with homogeneous layers of SWCNTs. The coating of the tungsten wires by SWCNTs was accomplished in a CVD reactor. The electrodes prepared demonstrated excellent reproducibility, good stability in various chemical media, and very high sensitivity to a series of inorganic and organic compounds. The authors attributed the good performance of these SWCNT-modified tungsten electrodes to several factors, including the intrinsic physico-chemical and electrical properties of SWCNTs, as well as the effective method for their deposition as perpendicularly oriented bundles on wire microelectrodes.

5.2.2. Non-oriented modifications. CNTs have been used to modify the surface of a conventional glassy-carbon electrode (GCE). The first use of CNTs was based on modifying GCEs with CNTs dispersed in sulphuric acid [50]. Prior to the surface modification, the GCE polished with alumina slurries and washed was cast with 10 μ L of a concentrated solution of CNT in sulphuric acid (1 mg CNT/mL). The coated electrode was dried at 200°C for 3 h and it was then ready to be used after careful washing. GCEs were also modified with CNTs using three other dispersing agents: dimethylformamide (DMF), concentrated nitric acid or a Nafion/water mixture [51]. In all cases, the CNTs were purified prior to use by nitric acid solution for 20 h to ensure complete removal of metal catalysts from the CNTs. The CNT-casting solutions were dropped directly onto the glassy carbon surface and allowed to dry. The electrode was then ready for use. The authors found differences in the electrochemical reactivity between the CNT-modified electrodes and the control electrodes (glassy carbon treated in the same way but without CNTs). They attributed this difference to surface chemistries (primarily to defect densities) of



the corresponding CNT layers, associated with the different production and dispersion protocols. Another interesting conclusion by the same authors, regarding the differences in the electrocatalytic activities between electrodes modified with CNTs produced by arc or CVD method, was that it was independent of the casting mode.

CNT-CHIT (chitosan) film electrodes were prepared by casting a CNT-CHIT solution (0.50 wt% CHIT, 0.50 mg of CNT/mL, pH 3.5) on the surface of a glassy carbon (GC) electrode [52]. The oxidation of NADH at the GC/CHIT control electrode and at the GC/CNT-CHIT electrode yielded peak currents at 0.60 and 0.34 V, respectively. The authors assumed that such a large decrease in the overpotential for the oxidation of NADH at a CNT-based electrode was attributable to the high local density of electronic states in CNT, related to their helicity and possible topological defects.

Compton et al. [53,54] compared the response for the graphite powder, nanotube-modified and fullerene (C₆₀)-modified, highly oriented pyrolytic graphite (HOPG) electrodes in order to provide evidence that CNTs have an electrocatalytic effect. He suggested that the CNTs act as effective electrocatalysts, but the graphite powder produced similar effect. (We will return to this issue in detail in Section 7 below).

A two-dimensional network of SWCNTs formed by CVD on an insulating support (SiO₂) and its application in electrochemical measurements was also reported [55].

5.3. Pastes and composites

Carbon-paste (CP) and composite electrodes have been used in electrochemical sensors for several years. By analogy, similar matrices that involve CNTs have recently been one of the focuses of research in the field of electrochemical sensors. CNTs inside the polymer matrix can be distributed oriented either randomly (Fig. 3C left) or vertically (Fig. 3C, right). A variety of binders (e.g., mineral oil, Teflon or epoxy resins) to produce CNT pastes or composites were reported, with rigid epoxy-based CNT composites being the least exploited.

5.3.1. Mineral oil. SWCNT paste electrodes can be obtained by mixing CNTs with a mineral oil binder [56]. The high surface area of CNTs makes possible the construction of stable, robust paste electrodes with high amounts of mineral oil (50% CNTs and 50% mineral oil). Such high mineral oil loadings are not possible when a conventional graphite-powder CP electrode (CPE) is prepared, since it results in the CPE leaking into the solution. The electrochemistry of CNT paste electrodes (CNTPEs) for ferricyanide, sodium hexachloroiridate(III) hydrate, catechol, dopamine, serotonin 5-HT, and caffeic acid was improved significantly compared to that of conventional CPEs. According to the authors, the electrochemical pretreatment and chemical oxidation of CNTPEs and CPEs by concentrated HNO₃ change their electronic properties and produced different electrocatalytic behaviors. The oxidation-activation mechanism is still uncertain, but is believed to be caused by the formation of carboxy functional groups at the CNT surface.

5.3.2. Teflon. CNT/Teflon composite electrodes were prepared in the dry state by hand-mixing the desired amounts of CNTs with granular Teflon [57]. A portion of the resulting consolidated composite was packed firmly into the electrode cavity forming the electrode. The authors did not observe redox activity for peroxide and NADH at the conventional graphite/Teflon control electrode using potentials lower than 0.6 and 0.5 V, respectively. The control graphite/Teflon electrode showed only a small gradual increase of response at higher potentials. By contrast, the CNT/Teflon electrode responded favorably to both analytes over the entire

potential range (0.0–1.0 V) with significant oxidation and reduction currents, starting around +0.20 V, for hydrogen peroxide and with an anodic signal for NADH that increased rapidly between 0.0 and 0.6 V. The substantial lowering of the detection potential observed for both analytes at the CNT-based composite was coupled to significantly larger current signals. The authors showed that the association of CNT with the Teflon binder did not decrease their strong electrocatalytic properties.

5.3.3. Rigid epoxy composites. A novel CNT epoxy-composite (CNTEC) electrode has been fabricated and characterized by our group [58]. Epoxy resin and hardener were mixed in the ratio 20:3 (w/w). CNTEC electrodes have been produced by loading the epoxy resin, before curing, with MWCNTs of different lengths (0.5–2 and 0.5–200 μm). Based on electrochemical reversibility and sensitivity studies, it was found that the electrodes containing 20% (w/w) CNT represented the optimal composition. Fig. 4 shows scanning electron microscope (SEM) micrographs of MWCNTs before and after being included in the epoxy resin. Good dispersion of CNTs in the polymer matrix with a sponge-like topography of the surface can be observed in this figure. The behavior of CNTEC electrodes has been compared with that of conventional graphite epoxy composite (GEC) electrode. It was found that long-MWCNT (0.5–200 μm)-based epoxy composite electrodes show strong electrocatalytic activity towards NADH and hydrogen peroxide, while short-MWCNT (0.5–2 μm)-based epoxy composite electrodes show oxidation potential similar to GEC electrodes for the both NADH and H_2O_2 . In both cases, CNTEC electrodes provide better reversibility, peak shape, sensitivity and stability than GEC electrodes. The CNTEC material is more robust in terms of mechanical strength

than the CNT paste or Teflon composite reported above. The new CNT composite indicates that it may become a new class of smart material with unique properties and applications. The resulting CNTEC electrode may offer great promise for biosensing by incorporating biomolecules, such as enzymes, antibodies or DNA, in the CNT/epoxy composite. Research along these lines is in progress in our laboratory.

6. Coupling with biological molecules

6.1. Enzymes

One of the key issues in biosensor design is the establishment of a fast electron-transfer between the active site of the enzyme and the electrochemical transducer. This is a significant challenge in designing enzyme-based sensors, taking into consideration the additional restrictions applied when miniaturization of the device is attempted.

The majority of reported articles (see Section 5) have demonstrated that CNTs promote electron-transfer reactions at low overpotentials (see Table 2). This advantage has inspired increased research in coupling CNT-based sensors with enzymes.

Glucose is one of the most reported analytes detected *via* enzyme–CNT electrodes. Several strategies were used to immobilize the necessary enzymes. Glucose oxidase (GOx) has been immobilized onto CNTs *via* polypyrrole [59,60] or even through CNT inks [61].

Glucose dehydrogenase (GDH) has been covalently immobilized in the CNT–CHIT (Chitosan) films using glutaric dialdehyde (GDI) [51]. The stability and the sensitivity of the GC electrode modified with CNT–CHIT–GDI–GDH biosensor allowed interference-free determination of glucose in the physiological matrix.

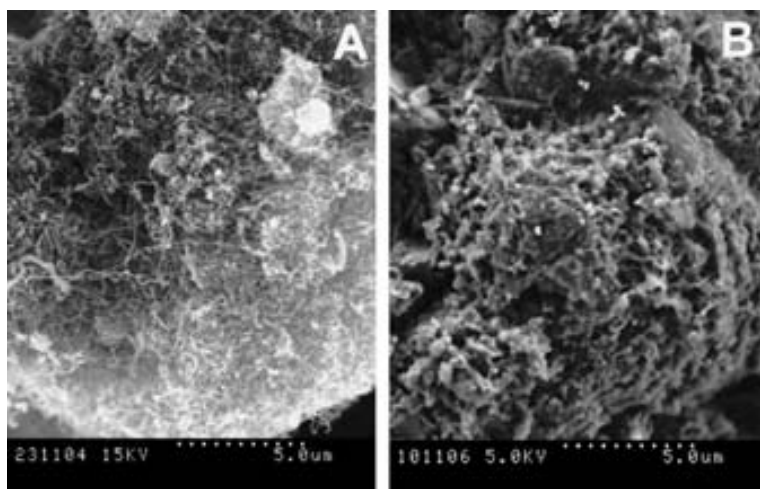


Figure 4. SEM images of MWCNT (0.5–200 μm) powder (A) and the corresponding CNT epoxy composite (20% (w/w) CNT) (B). Conditions: Purified MWCNT powder was sputtered with gold for 2 min at 25 mA. The same acceleration voltage and resolution were used.

Table 2. Reported cyclic voltammetric peak-to-peak separations and oxidative peak potentials for CNT-based electrodes

CNT/length/source	CNT solubilization solvent/immobilization matrix	Control electrode	Analyte	Oxidation potential/peak-to-peak separation ^{a,b}		Potential shift (V)	Reference
				CNT electrode (V)	Control electrode (V)		
SWCNTs deposited by CVD onto tungsten wire	–	Glassy carbon	Fe(CN) ₆ ^{3-/4-}	0.31 ^a	0.32 ^a	0.01	[49]
SWCNT/-/CVD Nanolab	H ₂ SO ₄ /film	Glassy carbon	NADH	0.32 ^a	0.82 ^a	0.50	[50]
MWCNT/-/CVD Nanolab			NADH	0.33 ^a	0.82 ^a	0.49	
MWCNT/1–5 μm/CVD Nanolab	DMF/film	Glassy carbon	Fe(CN) ₆ ^{3-/4-}	0.43 ^a	0.70 ^a	0.27	[51]
			H ₂ O ₂	0.40 ^a	0.65 ^a	0.25	
			NADH	0.43 ^a	0.70 ^a	0.27	
MWCNT/1–5 μm/CVD Nanolab	Nitric acid/film	Glassy carbon	Fe(CN) ₆ ^{3-/4-}	0.43 ^a	1.00 ^a	0.57	[51]
MWCNT/5–20 μm/CVD Nanolab			H ₂ O ₂	0.48 ^a	0.75 ^a	0.27	
MWCNT/1–5 μm/CVD Nanolab			NADH	0.43 ^a	1.00 ^a	0.57	
MWCNT/1–5 μm/CVD Nanolab	Nafion/film	Glassy carbon	H ₂ O ₂	0.37 ^a	0.54 ^a	0.17	[51]
MWCNT/-/Nanolab	Chitosan/film	Glassy carbon/chitosan	NADH	0.34 ^a	0.60 ^a	0.26	[52]
CNT formed <i>in situ</i> onto Au substrate	Polypyrrole/film	Au/PPy	H ₂ O ₂	0.20 ^a	0.65 ^a	0.45	[59]
MWCNT/1–5 μm/CVD Nanolab	DMF/film	Glassy carbon	H ₂ S	–0.30 ^a	0.10 ^a	0.40	[90]
MWCNT/Arc method produced			H ₂ S	0.00 ^a	0.10 ^a	0.10	
MWCNT	Acetonitrile/film	Glassy carbon and graphite powder	Fe(CN) ₆ ^{3-/4-}	0.146 ^b	0.167 ^b	–	[53]
			Norepinephrine	0.30 ^a	0.29 ^a	–0.01	
			NADH	0.52 ^a	0.56 ^a	0.04	
			Epinephrine	0.44 ^a	0.48 ^a	0.04	
SWCNT/Sigma	Mineral oil/paste	Carbon paste	Fe(CN) ₆ ^{3-/4-}	0.090 ^b	0.209 ^b	–	[56]
			Na ₃ IrCl ₆	0.120 ^b	0.090 ^b	–	
			Ru(NH ₃) ₆	0.094 ^b	0.092 ^b	–	
			Ferrocyanic acid	0.060 ^b	0.060 ^b	–	
			Catechol	0.239 ^b	0.344 ^b	–	
			Dopamine	0.164 ^b	0.149 ^b	–	
			Caffeic acid	0.422 ^b	0.299 ^b	–	
MWCNT/-/Merck Inc	Teflon binder/paste	Graphite–Teflon composite	H ₂ O ₂	0–1.0 ^a	0.6–1.0 ^a	0–0.4	[57]
			NADH	0–1.0 ^a	0.5–1.0 ^a	0–0.5	
MWCNT/0.5–2 μm/Sigma	Epoxy/composite	Graphite–epoxy composite	Fe(CN) ₆ ^{3-/4-}	0.302 ^b	0.369 ^b	–	[58]
MWCNT/0.5–200 μm/Sigma			Fe(CN) ₆ ^{3-/4-}	0.211 ^b	0.369 ^b	–	
MWCNT/0.5–2 μm/Sigma			NADH	0.72 ^a	0.74 ^a	0.02	
MWCNT/0.5–200 μm/Sigma			NADH	0.45 ^a	0.74 ^a	0.29	
MWCNT/0.5–2 μm/Sigma			H ₂ O ₂	0.60 ^a	No clear peak	–	
MWCNT/0.5–200 μm/Sigma			H ₂ O ₂	0.50 ^a	No clear peak	–	

^{a,b} – values marked with “a” correspond to the oxidation potential, while values marked with “b” correspond to CV peak-to-peak separation.

To achieve a fast electron-transfer (i.e., in the case of glucose oxidase) between the redox active site of the enzyme – flavin adenine dinucleotide (FAD) – and the transducing electrode, CNT-modified gold electrodes have been used [62,63] (see Fig. 5). Gold electrodes were first modified with a self-assembled monolayer of cysteamine and then short SWCNTs were aligned normal to the electrode surface by self-assembly. The CNTs were plugged into the enzymes in two ways:

- native glucose oxidase was covalently attached to the ends of the aligned tubes which allowed close approach to FAD and direct electron transfer was observed with a rate constant of 0.3/s; and,
- FAD was attached to the ends of the tubes and the enzyme reconstituted around the surface immobilized FAD. This latter approach allowed more efficient electron transfer to the FAD with a rate constant of 9/s.

According to Gooding [63], advantages of these electrode arrays are:

- the electroactive ends of the nanotubes are readily accessible to species in solution; and,
- the rigidity of the tubes allows them to be plugged into biomolecules, so enabling electrical connection to the redox centers of the biomolecules.

Biosensors have been based on other enzymes, such as acetylcholinesterase (AChE) [64] immobilized through a CNT-modified thick-film strip electrode for organophosphorus insecticides, horseradish peroxidase (HRP) [65] attached covalently onto the ends of SWCNTs, or L-amino acid oxidase [66] incorporated *via* an alkoxy silane sol-gel process. The sol-gel process has been also reported for coupling urease or acetylcholinesterase activity with CNT electrochemical transduction [67].

6.2. DNA

The use of CNT as a novel platform for DNA immobilization has recently attracted various researchers. Aminated or carboxylated DNA oligonucleotides were covalently linked, respectively, to carboxylated or aminated SWCNT-multilayer films, through appropriate coupling chemistries. The resulting DNA-functionalized SWCNT-multilayer films exhibit excellent specificity and

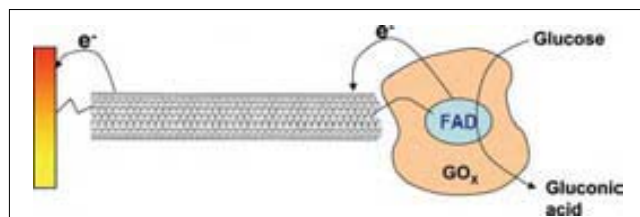


Figure 5. Schematic of direct electron transfer through the transducer and the redox center (FAD) of GOx *via* CNT. (Adapted from Refs. [63,64].)

chemical stability under the DNA-hybridization conditions. This modified layer provides a way of developing DNA-hybridization sensors in which the exquisite binding specificity of biomolecular recognition is directly coupled to SWCNTs [68].

Functionalized MWCNT-COOH was used for covalent DNA-probe immobilization and for enhancing sequence-specific DNA-detection sensitivity (see Fig. 6A). The electro-active daunomycin was used as the marker (intercalator) of this electrochemical DNA-sensing assay [69]. Compared to previous DNA sensors with oligonucleotides directly incorporated on carbon electrodes, this assay based on MWCNT-COOH increased the rate of heterogeneous electron transfer between the electrode and the redox active daunomycin.

CNTs may even play a dual-amplification role in both recognition and transduction events. This is demonstrated in high-sensitivity DNA detection, where CNTs have been loaded with numerous enzyme tags and used as DNA labels during hybridization detection (see Fig. 6B) [70]. Beside enzyme loading, the CNTs participate in accumulating the product of the enzymatic reaction, enhancing the DNA signal. These novel support and preconcentration functions of CNTs reflect their large specific surface area and are illustrated using the alkaline phosphatase (ALP) enzyme tracer. Such coupling of several CNT-derived amplification processes leads to the lowest detection limit reported for electrical DNA detection. A similar loading effect was also demonstrated earlier with quantum dots as electroactive labels for DNA-hybridization detection (Fig. 6C) [71].

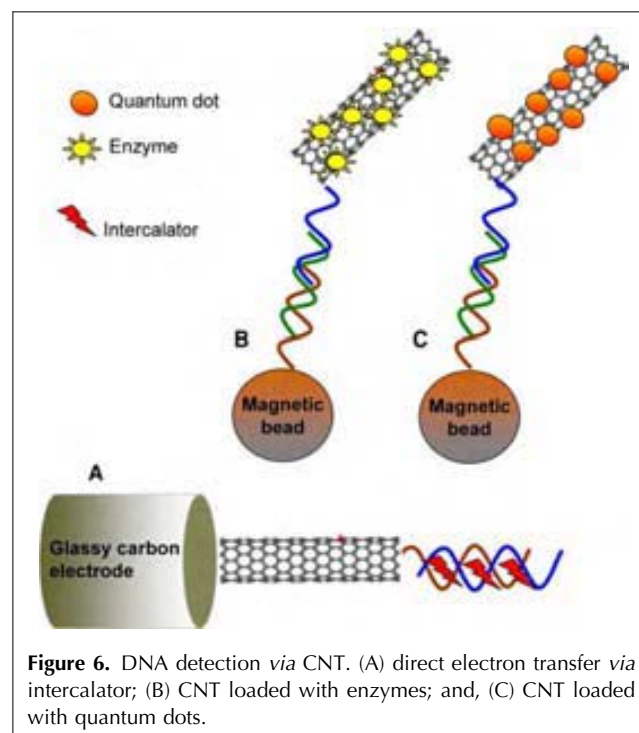


Figure 6. DNA detection *via* CNT. (A) direct electron transfer *via* intercalator; (B) CNT loaded with enzymes; and, (C) CNT loaded with quantum dots.

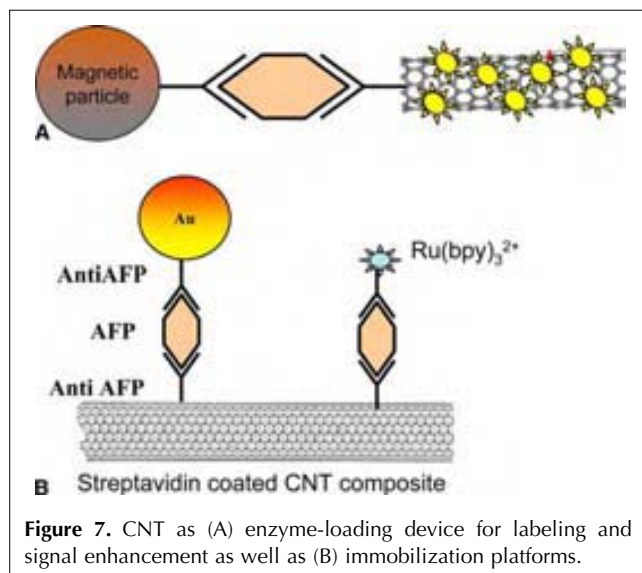


Figure 7. CNT as (A) enzyme-loading device for labeling and signal enhancement as well as (B) immobilization platforms.

6.3. Proteins

Following the same strategy as for DNA (see Section 6.2), it was also possible to detect proteins [69] by using CNTs as reservoirs of enzyme molecules and at the same time to accumulate the products coming from the enzymatic reaction during a complete sandwich-detection scheme (see Fig. 7A).

Wohlstader et al. [72] immobilized biotinylated anti-AFP (alpha-feto protein) antibodies on the surface of a streptavidin-coated CNT composite using poly(ethylene)-vinylacetate as binder and they exposed this derivatized composite to a sample containing AFP and anti-AFP antibodies conjugated with colloidal gold or $\text{Ru}(\text{bpy})_3^{2+}$ (Fig. 7B). The sandwich immunoassay was biospecific, and this was verified by SEM and electrochemical-luminescence (ECL) measurements. The ECL signal was found to be linearly dependent on AFP concentration up to concentrations of 30 nM. This work shows that CNTs can be used as immobilization platform and working electrode at the same time. The CNT-modification procedure (based on covalent coupling of streptavidin) can be extended to electrochemical-detection procedures based on voltammetric measurements, including those involving enzymes as markers.

7. Conclusions and future prospects

We have described several possible applications of CNTs, with emphasis on material science-based applications of interest to sensor design. We have remarked on electrochemical applications of CNTs.

The main message that we would like to convey is that the unique structure, topology and dimensions, along with electrochemical properties of CNTs, have created a

new material, which can be considered suitable for a variety of interesting possibilities in the design of sensors. The remarkable physical properties of CNTs create a host of application possibilities. Some of these are derived as an extension of traditional carbon, carbon fiber or bead applications, but many are new possibilities, based on the novel electronic and mechanical behavior of CNTs. The excitement in this field arises from the versatility of CNT material and the possibility of predicting novel properties and applications.

There are various advantages that CNTs bring to electrochemical-sensor design. Perhaps the most attractive feature of the CNT enzyme-based biosensor found to date is improved operational stability. Nevertheless, to assess the feasibility and the advantages of using CNTs in designing sensors, there needs to be thorough examination and resolution of issues, such as how CNTs are produced and dispersed, surface chemistry and morphology, effective surface area and presence of metal impurities.

Works reported to date have tried to provide evidence of the electrochemical activity of CNT-based electrochemical sensors, including potential shifts compared to the corresponding non-modified sensors (see Table 2). The majority of the authors agree that the presence of oxidants, such as strong acids, can open the ends of CNTs or introduce defects in their sidewalls [55,73]. Acid treatment (purification and/or casting) also introduces oxygen-containing surface groups (e.g., carboxyl or quinone), which are believed to improve the electrocatalytic properties of CNTs. The extent to which different factors affect the electrochemical behavior depends on the mechanisms of the particular redox systems.

Contrary to this widespread opinion, Musameh et al. [74] demonstrated that introducing oxygen functionalities at the end of the caps or the walls does not enhance the electrocatalytic ability of CNTs. Oxidation phenomena of CNTs need to be examined carefully in the future.

The open ends of CNTs have been linked to edge planes of HOPG with the nanotube walls suggested to have properties similar to those of basal planes of HOPG electrodes [75,76]. Compton recently demonstrated evidence that electrocatalytic properties of MWCNTs originate from their ends [52,53]. He showed that MWCNTs have an electrocatalytic effect similar to edge planes of HOPG and carbon powder, while fullerene (fullerene "ball-like" molecule does not contain any "open edges")-modified electrodes showed behavior similar to basal-plane HOPG electrodes. This discovery is consistent with Wang's explanation of the electrocatalytic effect of CNTs and his description of the electrochemical activation of MWCNTs [73]. He compared two different types of MWCNT:

- one produced by the arc method, which creates CNTs with closed (fullerene-like) ends; and,
- the other produced by the CVD method, which creates MWCNTs with open ends [50,73].

The open-ended, CVD-produced MWCNTs showed higher electrocatalytic activity than the end-capped, arc-produced MWCNTs. Anodic pretreatment of the arc-produced MWCNTs resulted in dramatic improvement in their electrochemical activity, while anodic pretreatment of CVD-produced MWCNTs did not show any significant difference. The authors suggested that anodization of arc-produced CNTs produces stress on the CNTs and this effectively breaks their end-caps.

The exploitation of CNTs in the design of electrochemical sensors is still in its infancy. Future efforts should aim at better understanding the structural-electrochemical reactivity of CNT-modified electrodes and the factors that govern the electron-transfer kinetics of these attractive devices, so as to avoid precipitate conclusions in attributing electrocatalytic properties to nanotubes without conducting the appropriate control experiments. It was shown that, in some cases, the electrocatalytic effect of carbon powder is similar to that of CNTs [52,53], while, in other cases, there is a huge difference between carbon powder and CNTs [56,57]. Interesting information on electrochemical properties of CNTs can be also obtained from studies (i.e., impedance spectroscopy [77]) for other applications.

The research in the applications of CNTs to sensors can also take advantage of a variety of CNT applications in materials science. Other configurations of CNTs can be foreseen in future applications of electrochemical sensors. For example, small-diameter zigzag SWCNTs, produced by cross linking of side walls of short CNTs, should show novel physical, chemical, and electronic properties [78].

DNA-directed self-assembly of CNTs [79] can also bring new possibilities for CNT configurations to sensor applications. The combination of the electronic properties and the dimensions of CNTs make them ideal building blocks for molecular electronics. The reported technology based on the use of a DNA-scaffold molecule, which provides the address for precise localization of a semiconducting SWCNT [80] as well as the template for the extended metallic wires contacting it, may open new possibilities for designing individual CNT sensors.

The possibility of producing an SWCNT nanoelectrode may also open the way to electrochemical studies of single redox molecules [44].

Acknowledgments

This work was financially supported by:

- (1) the Ministry of Education and Culture (MEC), Spain (Projects BIO2004-02776 and MAT2004-05164, and Grant MEC 2003-022, given to M. Pumera);

- (2) the Spanish foundation Ramón Areces (Project 'Bionanosensores'); and,
- (3) the "Ramón y Cajal" program of MEC, Spain, that supports A. Merkoçi.

References

- [1] F. Céspedes, E. Martínez-Fàbregas, S. Alegret, *Trends Anal. Chem.* 15 (1996) 296.
- [2] F. Céspedes, S. Alegret, *Trends Anal. Chem.* 19 (2000) 276.
- [3] S. Solé, A. Merkoçi, S. Alegret, *Trends Anal. Chem.* 20 (2001) 102.
- [4] A. Merkoçi, S. Alegret, *Trends Anal. Chem.* 21 (2002) 717.
- [5] A. Merkoçi, S. Alegret, *Trends Anal. Chem.* 24 (2005) 341.
- [6] S. Iijima, *Nature (London)* 354 (1991) 56.
- [7] (a) M.S. Dresselhaus, G. Dresselhaus, P.C. Eklund, *Science of Fullerenes and Carbon Nanotubes*, Academic Press, New York, USA, 1996;
(b) W.Z. Li, S.S. Xie, L.X. Qian, B.H. Chang, B.S. Zou, W.Y. Zhou, R.A. Zhao, G. Wang, *Science (Washington, DC)* 274 (1996) 1701;
(c) Z.F. Ren, Z.P. Huang, J.W. Xu, J.H. Wang, P. Bush, M.P. Siegal, P.N. Provencio, *Science (Washington, DC)* 282 (1998) 1105;
(d) H. Murakami, M. Hirakawa, C. Tanaka, H. Yamakawa, *Appl. Phys. Lett.* 76 (2000) 1776;
(e) T.W. Ebbesen, H.J. Lezec, H. Hiura, J.W. Bennet, H.F. Ghaemi, T. Thio, *Nature (London)* 382 (1996) 54.
- [8] M.M. Treachy, T.W. Ebbesen, J.M. Gibson, *Nature (London)* 381 (1996) 678.
- [9] (a) W.A. de Heer, A. Chatelaine, D. Ugarte, *Science (Washington, DC)* 270 (1995) 1179;
(b) W.B. Choi, D.S. Chung, J.H. Kang, H.Y. Kim, Y.W. Jin, I.T. Han, Y.H. Lee, J.E. Jung, N.S. Lee, G.S. Park, J.M. Kim, *Appl. Phys. Lett.* 75 (1999) 3129;
(c) J.M. Bonard, *Solid State Electron.* 45 (2001) 893.
- [10] (a) S.J. Tans, A.R.M. Verschueren, C. Dekker, *Nature (London)* 393 (1998) 49;
(b) R. Martel, T. Schmidt, H.R. Shea, T. Hertel, P. Avouris, *Appl. Phys. Lett.* 73 (1998) 2447.
- [11] H. Dai, J.H. Hafner, A.G. Rinzler, D.T. Colbert, R.E. Smalley, *Nature (London)* 384 (1996) 147.
- [12] M.S. Shaffer, X. Fan, A.-H. Windle, *Carbon* 36 (1998) 1603.
- [13] J. Guo, S. Goasguen, M. Lundstrom, S. Datta, *Appl. Phys. Lett.* 81 (2002) 1486.
- [14] T.W. Ebbesen, P.M. Ajayan, *Nature (London)* 358 (1992) 220.
- [15] Y. Ando, S. Iijima, *Jpn. J. Appl. Phys.* 32 (1993) 107.
- [16] S. Iijima, T. Ichihashi, *Nature (London)* 363 (1993) 603.
- [17] D.T. Colbert, J. Zhang, S.M. McClure, P. Nikolaev, Z. Chen, J.H. Hafner, D.W. Owens, P.G. Kotula, C.B. Carter, J.H. Weaver, A.G. Rinzler, R.E. Smalley, *Science (Washington, DC)* 266 (1994) 1218.
- [18] Y. Ando, *Fullerene Sci. Technol.* 2 (1994) 173.
- [19] X. Zhao, M. Ohkohchi, M. Wang, S. Iijima, T. Ichihashi, Y. Ando, *Carbon* 35 (1997) 775.
- [20] T. Guo, P. Nikolaev, A. Thess, D.T. Colbert, R.E. Smalley, *Chem. Phys. Lett.* 243 (1995) 49.
- [21] D.E. Powers, S.G. Hansen, M.E. Geusic, A.C. Puiiu, J.B. Hopkins, T.G. Dietz, M.A. Duncan, P.R.R. Langridgesmith, R.E. Smalley, *J. Chem. Phys.* 86 (1982) 2556.

- [22] E.R. Bernstein (Editor), *Atomic and Molecular Clusters*, Elsevier Science B.V., New York, USA, 1990.
- [23] R. Sen, Y. Ohtsuka, T. Ishigaki, D. Kasuya, S. Suzuki, H. Kataura, Y. Achiba, *Chem. Phys. Lett.* 332 (2000) 467.
- [24] G. Che, B.B. Lakshmi, C.R. Martin, E.R. Fisher, *Chem. Mater.* 10 (1998) 260.
- [25] V. Ivanov, J.B. Nagy, P. Lambin, A. Lucas, X.B. Zhang, X.F. Zhang, D. Bernaerts, G. Van Tendeloo, S. Amelinckx, J. Van Landuyt, *Chem. Phys. Lett.* 223 (1994) 329.
- [26] P.L. Walker Jr., J.F. Rakszawski, G.R. Imperial, *J. Phys. Chem.* 63 (1959) 133.
- [27] C.N.R. Rao, R. Sen, B.C. Satishkumar, A. Govindaraj, *Chem. Commun.* 15 (1998) 1525.
- [28] E. Couteau, K. Hernadi, J.W. Seo, L. Thien-Nga, C. Miko, R. Gaal, L. Forro, *Chem. Phys. Lett.* 378 (2003) 9.
- [29] J.H. Hafner, C.L. Cheung, C.M. Lieber, *J. Am. Chem. Soc.* 398 (1999) 9750.
- [30] Y. Zhang, H. Gu, K. Suenaga, S. Iijima, *Chem. Phys. Lett.* 279 (1997) 264.
- [31] M. Terrones, N. Grobert, J. Olivares, J.P. Zhang, H. Terrones, K. Kordatos, W.K. Hsu, J.P. Hare, P.D. Townsend, K. Prassides, A.K. Cheetham, H.W. Kroto, D.R.M. Walton, *Nature (London)* 388 (1997) 52.
- [32] A. Leonhardt, M. Ritschel, R. Kozhuharova, A. Graff, T. Muhl, R. Huhle, I. Monch, D. Elefant, C.M. Schneider, *Diamond Relat. Mater.* 12 (2003) 790.
- [33] Y.K. Chen, A. Chu, J. Cook, M.L.H. Green, P.J.F. Harris, R. Heesom, M. Humphries, J. Sloan, S.C. Tsang, J.F.C. Turner, *J. Mater. Chem.* 7 (1997) 545.
- [34] H. Agoa, S. Ohshima, K. Uchida, T. Komatsu, *Physica B (Amsterdam)* 323 (2002) 306.
- [35] J. Chen, M.A. Hamon, H. Hu, Y. Chen, A.M. Rao, P.C. Eklund, R.C. Haddon, *Science (Washington, DC)* 282 (1998) 95.
- [36] D. Tasis, N. Tagmatarchis, V. Georgakilas, M. Prato, *Chem. Eur. J.* 9 (2003) 4000.
- [37] M.F. Islam, E. Rojas, D.M. Bergey, A.T. Johnson, A.G. Yodh, *Nano Lett.* 3 (2003) 269.
- [38] (a) A. Star, J.F. Stoddart, D. Steuerman, M. Diehl, A. Boukai, E.W. Wong, X. Yang, S.W. Chung, H. Choi, J.R. Heath, *Angew. Chem. Int. Ed.* 40 (2001) 1721;
(b) M.J. O'Connell, P. Boul, L.M. Ericson, C. Huffman, Y. Wang, E. Haroz, C. Kuper, J. Tour, K.D. Ausman, R.E. Smalley, *Chem. Phys. Lett.* 342 (2001) 265;
(c) J. Chen, H. Liu, W.A. Weimer, M.D. Halls, M.D.H. Waldeck, G.C. Walker, *J. Am. Chem. Soc.* 124 (2002) 9034.
- [39] S. Ramesh, L.M. Ericson, V.A. Davis, R.K. Saini, C. Kittrell, M. Pasquali, W.E. Billups, W. Adams, R.H. Hauge, R.E. Smalley, *J. Phys. Chem. B* 108 (2004) 8794.
- [40] O.K. Kim, J. Je, J.W. Baldwin, S. Kooi, P.E. Pehrsson, L.J. Buckley, *J. Am. Chem. Soc.* 125 (2003) 4426.
- [41] J.H.T. Luong, S. Hrapovic, D. Wang, F. Bensebaa, B. Simard, *Electroanalysis (NY)* 16 (2004) 132.
- [42] Z. Yao, C.L. Kane, C. Dekker, *Phys. Rev. Lett.* 84 (2000) 2941.
- [43] Z. Yao, C. Dekker, Ph. Avouris, *Top. Appl. Phys.* 80 (2001) 147.
- [44] R.H. Baughman, A. Anvar, A. Zakhidov, W.A. de Heer, *Science (Washington, DC)* 297 (2002) 787.
- [45] I. Heller, J. Kong, H.A. Heering, K.A. Williams, S.G. Lemay, C. Dekker, *Nano Lett.* 5 (2005) 137.
- [46] M.A. Poggi, L.A. Bottomley, P.T. Lillehei, *Anal. Chem.* 74 (2002) 2851.
- [47] L. McCreery, in: A.J. Bard (Editor), *Electroanalytical Chemistry*, vol. 17, Marcel Dekker, New York, USA, 1991, p. 221.
- [48] J. Li, J.E. Koehne, A.M. Cassell, H. Chen, H. Tee Ng, Q. Ye, W. Fan, J. Han, M. Meyyappan, *Electroanalysis (NY)* 17 (2005) 15.
- [49] F. Valentini, S. Orlanducci, E. Tamburri, M.L. Terranova, A. Curulli, G. Palleschi, *Electroanalysis (NY)* 17 (2005) 28.
- [50] M. Musameh, J. Wang, A. Merkoçi, Y. Lin, *Electrochem. Commun.* 4 (2002) 743.
- [51] N.S. Lawrence, R.P. Deo, J. Wang, *Electroanalysis (NY)* 17 (2005) 65.
- [52] M. Zhang, A. Smith, W. Gorski, *Anal. Chem.* 76 (2004) 5045.
- [53] R.R. Moore, C.E. Banks, R.G. Compton, *Anal. Chem.* 76 (2004) 2677.
- [54] C.E. Banks, R.R. Moore, T.J. Davies, R.G. Compton, *Chem. Commun.* (2004) 1804.
- [55] T.M. Day, N. Wilson, J.V. Macpherson, *J. Am. Chem. Soc.* 126 (2004) 16724.
- [56] F. Valentini, A. Amine, S. Orlanducci, M.L. Terranova, G. Palleschi, *Anal. Chem.* 75 (2003) 5413.
- [57] J. Wang, M. Musameh, *Anal. Chem.* 75 (2003) 2075.
- [58] M. Pumera, A. Merkoçi, S. Alegret, *Sensors & Actuators B*, (2005), submitted.
- [59] M. Gao, L. Dai, G. Wallace, *Synth. Met.* 137 (2003) 1393.
- [60] K.P. Loh, S.L. Zhao, W.D. Zhang, *Diamond Relat. Mater.* 13 (2004) 1075.
- [61] J. Wang, M. Musameh, *Analyst (Cambridge, UK)* 129 (2004) 1.
- [62] F. Patolsky, Y. Weizmann, I. Willner, *Angew. Chem. Int. Ed.* 43 (2004) 2113.
- [63] J. Liu, A. Chou, W. Rahmat, M.N. Paddon-Row, J.J. Gooding, *Electroanalysis (NY)* 17 (2005) 38.
- [64] K.A. Joshi, J. Tang, R. Haddon, J. Wang, W. Chen, A. Mulchandani, *Electroanalysis (NY)* 17 (2005) 54.
- [65] X. Yu, D. Chattopadhyay, I. Galeska, F. Papadimitrakopoulos, J.F. Rusling, *Electrochem. Commun.* 5 (2003) 408.
- [66] V.G. Gavalas, S.A. Law, J.C. Ball, R. Andrews, L.G. Bachas, *Anal. Biochem.* 329 (2004) 247.
- [67] Z. Xu, X. Chen, X. Qu, J. Jia, S. Dong, *Biosens. Bioelectron.* 20 (2004) 579.
- [68] D.H. Jung, B.H. Kim, Y.K. Ko, M.S. Jung, S. Jung, S.Y. Lee, H.T. Jung, *Langmuir* 20 (2004) 8886.
- [69] H. Cai, X. Cao, Y. Jiang, P. He, Y. Fang, *Anal. Bioanal. Chem.* 375 (2003) 287.
- [70] J. Wang, G. Liu, M.R. Jan, *J. Am. Chem. Soc.* 126 (2004) 3010.
- [71] J. Wang, G. Liu, M.R. Jan, Q. Zhu, *Electrochem. Commun.* 5 (2003) 1000.
- [72] J.N. Wohlstadter, J.L. Wilbur, G.B. Sigal, H.A. Biebuyck, M.A. Billadeau, L.W. Dong, A.B. Fischer, S.R. Gudiband, S.H. Jamieson, J.H. Kenten, J. Leguin, J.K. Leland, R.J. Massey, S.J. Wohlstadter, *Adv. Mater.* 15 (2003) 1186.
- [73] C.N. Rao, B.C. Satishkumar, A. Govindaraj, M. Nath, *Chem. Phys. Chem.* 2 (2001) 78.
- [74] M. Musameh, N.S. Lawrence, J. Wang, *Electrochem. Commun.* 7 (2005) 14.
- [75] J.J. Gooding, R. Wibowo, J. Liu, W. Yang, D. Losic, S. Orbons, F.J. Mearns, J.G. Shapter, D.B. Hibbert, *J. Am. Chem. Soc.* 125 (2003) 9006.
- [76] J.M. Nugent, K.S.V. Santhanam, A. Rubio, P.M. Ajayan, *Nano Lett.* 1 (2001) 87.
- [77] Z. Yang, H. Wu, *Chem. Phys. Lett.* 343 (2001) 235.
- [78] H. Cheng, G.P. Pez, A.C. Cooper, *Nano Lett.* 3 (2003) 585.
- [79] S. Li, P. He, J. Dong, Z. Guo, L. Dai, *J. Am. Chem. Soc.* 127 (2005) 14.
- [80] K. Keren, R.S. Berman, E. Buchstab, U. Sivan, E. Braun, *Science (Washington, DC)* 302 (2003) 1380.
- [81] H. Dodziuk, A. Ejchart, W. Anczewski, H. Ueda, E. Krinichnaya, G. Dolgonosa, W. Kutner, *Chem. Commun.* (2003) 986.
- [82] J. Wang, M. Musameh, Y. Lin, *J. Am. Chem. Soc.* 125 (2003) 2408.
- [83] A. Penicaud, P. Poulin, A. Derre, E. Anglaret, P. Petit, *J. Am. Chem. Soc.* 127 (2005) 8.
- [84] W. Huang, S. Fernando, L.F. Allard, Y.-P. Sun, *Nano Lett.* 3 (2003) 565.
- [85] M.G.C. Kahn, S. Banerjee, S.S. Wong, *Nano Lett.* 2 (2002) 1215.

- [86] F. Pompeo, D.E. Resasco, *Nano Lett.* 2 (2002) 369.
[87] K.A.S. Fernando, Y. Lin, Y.-P. Sun, *Langmuir* 20 (2004) 4777.
[88] S. Banerjee, S.S. Wong, *J. Am. Chem. Soc.* 124 (2002) 8940.
[89] W. Huang, Y. Lin, S. Taylor, J. Gaillard, A.M. Rao, Y.-P. Sun, *Nano Lett.* 2 (2002) 231.
[90] N.S. Lawrence, R.P. Deo, J. Wang, *Anal. Chim. Acta* 517 (2004) 131.

Arben Merkoçi was awarded his PhD in chemistry from the University of Tirana, Albania, in 1991 and then did post-doctoral researches in Greece, Hungary, Italy, Spain and USA. His main interest has been electroanalytical methods for several applications in sensors and biosensors. Currently, he is "Ramon y Cajal" researcher and professor at the Sensor & Biosensor Group, Chemistry Department, Autonomous University of Barcelona (AUB), Spain. His main research interests concern the design of composites, biocomposites and nanobioconjugate materials for enzyme-, immuno- and DNA-based electrochemical sensors.

Martin Pumera received his PhD in Analytical Chemistry from Charles University, Prague, The Czech Republic, in 2001. Shortly after that he became post-doctoral researcher at Prof. Joseph Wang's Sensor-Chip Laboratory at NMSU, USA, where he developed new concepts of electrochemical detection on Lab-on-a-Chip devices for space (JPL/NASA) and security/forensic applications (US Navy). Currently, he conducts research focused on integration of nanobiotechnology (CNTs, quantum dots, DNA-gold nanoparticle conjugates) on the Lab-on-a-Chip platform at Sensor and Biosensor Group at the AUB.

Xavier Llopis obtained chemistry and food technology diplomas at the AUB, in 1998 and 2000, respectively. Since 2000, he has been a PhD

student at Sensor & Biosensor Group in the Chemistry Department of the AUB. His research activity is focused on developing novel flow-through injection and Lab-on-a-Chip biosystems with electrochemical detection based on magnetic particles, biocomposites and lastly on CNTs.

Briza Pérez got her diploma in chemistry in Mexico in 2000 and her master's degree in chemistry at Polytechnical University of Catalonia, Spain, in 2003. In 2004, she joined the Sensor & Biosensor Group at the AUB to carry out her PhD thesis. Her research is focused on the study of electrochemistry of CNTs and their integration into biosensing systems.

Manuel del Valle got his PhD thesis at AUB in 1992. He was made Associate Professor at the AUB in 1997. His research lines include chemical sensors (including those for non-ionic or anionic surfactants), biosensors, ISEs, ISFETs, computer-based instrumentation, sensor arrays, electronic tongues, automated analytical systems (flow-injection analysis, sequential injection analysis), conducting polymers, nano-structured materials, and impedance spectroscopy.

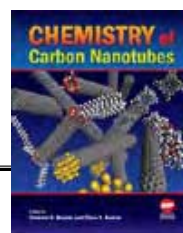
Salvador Alegret was made professor of Analytical Chemistry at the AUB in 1991. He is head of the Sensor & Biosensor Group in the Chemistry Department. Currently, he is devoted to the development of electrochemical chemo- and biosensors based on amperometric, potentiometric and ISFET transducers in chemical, enzymatic, immunological and DNA-recognition systems. The resulting sensor devices are being applied in automated analytical systems based on bio- or biomimetic instrumentation concepts for monitoring and process control in different fields, such as biomedicine, the environment and the chemical industry.

Application of carbon nanotubes in analytical chemistry

B. Pérez and A. Merkoçi

American Scientific Publishers

2008, **2**, 337-353



CHAPTER 13

Applications of Carbon Nanotubes in Analytical Chemistry

Briza Pérez,^{1,2} Arben Merkoçi¹

¹*Nanobioelectronics and Biosensors Group, Institut Català de Nanotecnologia*

²*Grup de Sensors and Biosensors, Departament de Química, Universitat Autònoma de Barcelona, 08193 Bellaterra, Catalonia, Spain*

CONTENTS

1. General Characteristics of Carbon Nanotubes	337
1.1. What do they Present?	337
1.2. Production Methods	338
1.3. Purification	338
1.4. Solubilization	339
1.5. Emerging Analytical Applications	339
2. Applications in Electrochemical (Bio)Sensors	339
2.1. Sensors	340
2.2. Enzyme-Based Sensors	347
2.3. Immunosensors	349
2.4. Genosensors	350
3. Applications in Liquid Chromatography	351
4. Applications in Optical Sensors	352
5. Conclusions	352
References	353

1. GENERAL CHARACTERISTICS OF CARBON NANOTUBES

1.1. What do they Present?

Carbon is an important element in chemistry. There are about sixteen million compounds of carbon, more than for any other element. There are three allotropes of carbon: diamond, which is a semiconductor, graphite, and carbon nanotubes (CNTs), which can be conductors or semiconductors. They were given the name nanotubes because it appeared that they were made up of a perfect network of hexagonal graphite rolled up onto itself to form hollow tubes with armchair, zigzag, and chiral

configurations [Figure 1]. The history of CNTs began with the discovery of buckminsterfullerene in 1985 that opened a new era for the chemistry of carbon and for novel materials. The Japanese scientist Sumi Iijima discovered CNTs in 1991 [1]. Since their discovery the CNTs have generated great interest for various applications based on their field emission and electronic transport properties, their high mechanical strength, and their chemical properties [2]. From this arises an increasing potential for their use as field emission devices [3], nanoscale transistors [4], tips for scanning microscopy [5], or components for composite materials [6].

CNTs are one of the most commonly used building blocks of nanotechnology. With one hundred times the

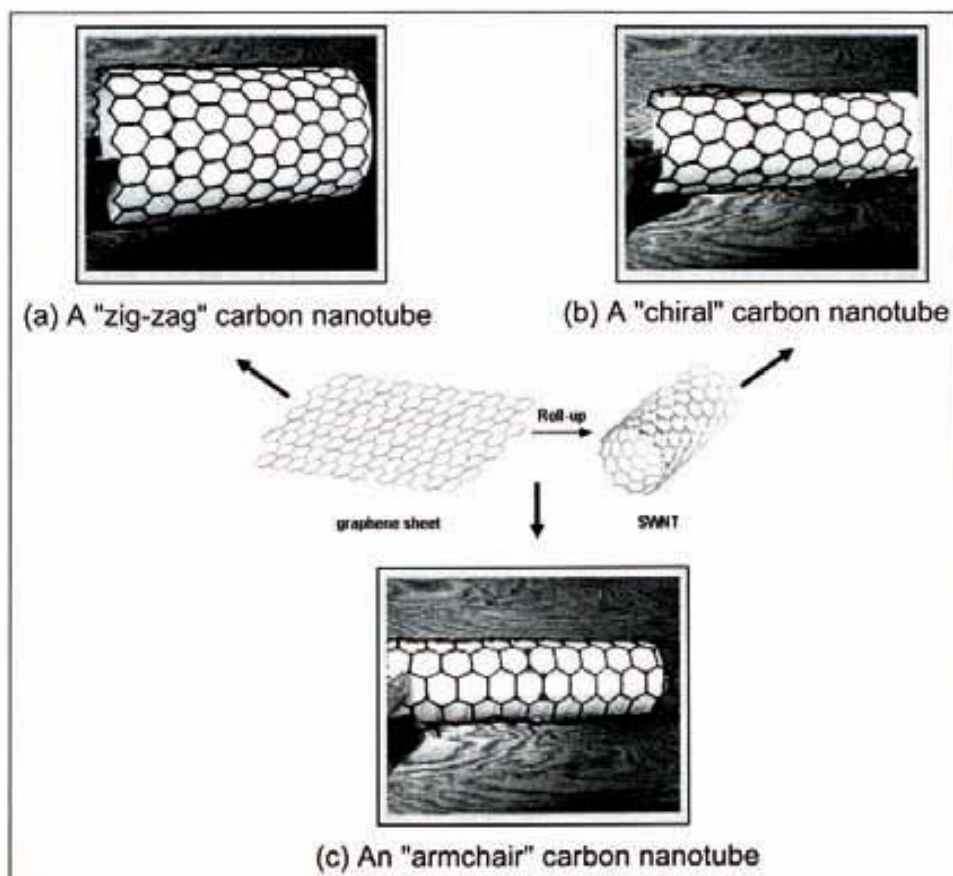


Figure 1. Nanotubes (a) zig-zag (b) chiral and (c) armchair.

tensile strength of steel, a thermal conductivity comparable to diamond crystal, and an electrical conductivity similar to copper but with the ability to carry much higher currents, CNTs seem to be a wonder material.

CNTs can exist as single- and multi-walled nanotubes. Single-walled carbon nanotubes (SWNTs) are comprised of a cylindrical graphite sheet of nanoscale diameter capped by hemispherical ends. The closure of the cylinder is the result of a pentagon inclusion in the hexagonal carbon network of the nanotube walls during the growth process. SWNTs typically have diameters ~ 1 nm with the smallest diameter reported to date of 40 Å. This corresponds to the theoretically predicted lower limit for stable SWNT formation based on consideration of the stress energy built into the SWNT's cylindrical structure. Multi-walled carbon nanotubes (MWNTs) comprise several to tens of incommensurate concentric cylinders of these graphitic shells with a layer spacing of 3–4 Å. MWNTs tend to have diameters in the range of 2–100 nm. The MWNTs can be considered as a mesoscale graphite system, whereas a SWNT is truly a single large molecule.

1.2. Production Methods

There are several methods presently used to form CNTs. The first is a slightly modified version of the method used for fullerene production, an *arc discharge* between graphite electrodes, allowing a nanotube deposit to accumulate on the cathode. One can form nanotubes of a single rolled up graphene shell (SWNTs) of diameter in the 1 nm range; and

multi-walled nanotubes consisting of several concentrically arranged single-wall carbon nanotubes nested into each other like a Russian doll. These multi-shell nanotubes are referred to as multi-walled carbon nanotubes (MWNTs). Historically SWNTs were discovered later, after an efficient production method was discovered by Smalley and colleagues [7], using laser ablation of graphite in the presence of catalytic particles. The SWNTs found in the resulting soot are organized into bundles of various diameters.

However, in order to use CNTs in novel devices, it is necessary to produce these materials with a high crystallinity on a large scale economically. In this context, the catalytic chemical vapor deposition (CVD) method is considered to be the optimum for producing large amounts of CNTs, particularly with the use of a floating-catalyst method [8]. This technique is more controllable and cost-efficient when compared with arc discharge and others methods.

1.3. Purification

Even though synthetic techniques have been improved to obtain high-purity CNTs, the formation of by-products containing impurities such as metal particles in the tip of a CNT, and amorphous carbon has been an unavoidable phenomenon because the metal nanoparticles are essential for the nanotube growth. Thus, extensive research has been dedicated to the purification of CNTs in order to remove foreign nanoparticles that modify the physico-chemical properties of CNTs.

Chemical methods have been applied for purifying SWNTs. A generalized method for SWNT purification developed by Smalley and co-workers [9] consists of refluxing as-grown SWNTs in nitric acid solutions. Subsequently, more-effective purification techniques have been developed with minor physical damage to the tubes [10–12]. Chattopadhyay et al. [13] reported the complete removal of metallic impurities through a sonication-mediated treatment of as-grown SWNTs in a mixture of hydrofluoric and nitric acids. Also, Martinez et al. [14] reported a combined technique of high-temperature air oxidation in conjunction with microwave acid treatments, thus removing a high portion of metal particles in relatively short periods of time.

For MWNTs, high-temperature treatments in an inert atmosphere are the most effective methods for removing structural defects or impurities such as metallic compounds [15–17].

Another alternative is the treatment of MWNTs with a UV-ozone (UVO) generator under ambient conditions having a dramatic effect on the nature of the surface oxidation [18]. This solvent-free UVO treatment has the potential for producing a solvent-dispersible CNT powder with minimal morphological defects. This offers a great opportunity for producing versatile CNT solutions that could be used as a solution mixture with polymers for a wide range of technological applications.

1.4. Solubilization

Before application to analytical assays, CNTs must be first modified to be transformed into a soluble product. The preparation of homogeneous dispersions of CNTs, suitable for processing into thin films or for other applications, is of a great importance. Various methods can be used for this purpose.

End [19] and/or sidewall [20] functionalization, use of surfactants with sonication [21], polymer wrapping of nanotubes [22–24], and protonation by superacids [25] have been reported. Although these methods are quite successful, they often indicate cutting the CNTs into smaller pieces (sonication and/or functionalization), thus partly losing the high aspect ratio of SWNTs.

Kim et al. [26] provided an example of CNT solubilization. They developed a simple, efficient process for solubilizing CNTs with amylose in a dimethyl sulphoxide–H₂O (DMSO–H₂O) mixture, as well as in pure water. This process required two important conditions; pre-sonication of CNTs in water and subsequent treatment of the fine CNT dispersion with amylose in a specified DMSO–H₂O mixture, followed by post-sonication. The former step disaggregates the CNT bundles, and the latter step maximizes cooperative interactions between CNTs and amylose, leading to immediate and complete solubilization. The best solvent composition was found to be 10–20% DMSO, in which amylose assumes an interrupted loose helix. The resulting colloidal solution was stable and exhibited no precipitation over several weeks.

CNT solubilization by covalent modification was reported by Luong et al. [27]. MWNTs were solubilized in a mixture of 3-aminopropyltriethoxysilane (APTES), Nafion-perfluorinated ion-exchange resin, and ethanol. Uniformly-dispersed MWNTs were obtained after 20-min sonication

and used for sensor applications. The interactions between CNTs and amino-terminated organic species are complex and depend on the conditions of the functionalization reaction.

1.5. Emerging Analytical Applications

CNTs offer significant advantages over many existing materials due to their exceptional mechanical, electronic, and chemical properties such as a high surface area, accumulation, branched conductivity, minimization of surface fouling, and electrocatalytic activity. Particularly, the CNTs are offering new opportunities to analytical chemistry. The integration of nanotechnology-based materials such as CNTs with biology and analytical chemistry is an important trend in current analytical chemistry.

CNTs have features that make them very attractive in electrochemical studies and consequently in several analytical applications. For example, the structural and electronic properties of CNTs endow them with distinct electrocatalytic activities and capabilities for facilitating direct electrochemistry of proteins and enzymes from other kinds of carbon materials. Moreover recent studies have demonstrated that CNTs exhibit strong electrocatalytic activity for a wide range of compounds, such as neurotransmitters [28, 29], NADH [44, 30], hydrogen peroxide [28, 31], ascorbic [32, 33] and uric acid [28], cytochrome c [34], hydrazines [35], hydrogen sulphide [36], amino acids [37], and DNA [38] (details will be given in the following sections). It has been suggested that electrocatalytic properties originate from the ends of CNTs [39]. These striking electrochemical properties of CNTs pave the way to CNT-based bioelectrochemistry and to bioelectronic nanodevices such as electrochemical sensors and biosensors. The electrochemistry and bioelectrochemistry, along with other interesting features of CNTs coupled to several analytical procedures are summarized and discussed in detail in the following sections.

2. APPLICATIONS IN ELECTROCHEMICAL (BIO)SENSORS

The rapid development of new nanomaterials and nanotechnologies has provided many new opportunities for electroanalysis. In particular, the unique properties of CNTs make them extremely attractive for the fabrication of electrochemical (bio)sensors. Recent studies have demonstrated that CNTs can enhance the electrochemical reactivity of biomolecules and promote the electron-transfer reactions of proteins. The high conductivity of CNTs permits their use as highly sensitive nanoscale sensors.

Different configurations of CNT-based (bio)sensors have been reported. CNTs have been (a) aligned onto a conductor platform, (b) randomly distributed onto a conducting platform, (c) mixed with polymer-forming CNT composites, and (d) single CNTs have been used as sensors.

SWNTs and MWNTs have been vertically aligned onto a gold electrode [40]. In this case the CNTs act as molecular wires, allowing electrical communication between the underlying electrode and the redox enzyme or biomaterial. The direct electron transfer between the biomaterial and

Table 1. Solubilization/immobilization strategies used for CNT integration into sensor formats.

CNT	Platform	Solubilization	Ref.
MWNT	Glassy carbon	Nafion/film 2 mg:1 mL (1% Nafion)	[104]
SWNT	Gold	DMF 0.2 mg:1 mL (in 0.5 mg of dicyclohexyl carbodiimide)	[40]
MWNT	Glassy carbon	Nitric acid/film 2 mg:1 mL	[104]
MWNT	Glassy carbon/chitosan	Chitosan/film 0.50–3.0 mg:0.50% (0.05 M HCl)	[105]
SWNT	Carbon paste	Mineral oil/paste 60%:40%	[106]
MWNT	Glassy carbon	H ₂ SO ₄ /film	[44]
SWNT		1 mg:1 mL	

the electron surface obviates the need for redox mediators and is thus extremely useful in sensing devices. Another way for confining CNTs onto electrochemical (bio)sensors is accomplished by their random distribution/casting onto conventional electrodes. One barrier for developing these CNT film-based biosensing devices is the insolubility of CNTs in most solvents. Earlier reported CNT-modified electrodes have thus commonly relied on casting a CNT/sulfuric acid solution onto a glassy carbon surface [41]. The use of CNT composite electrodes, prepared by dispersion of CNTs inside the epoxy resin, has been another strategy. [42] The use of CNTs as the conductive part of the composite ensures better incorporation of biomaterial into the epoxy matrix and faster electron transfer rates between the biomaterial and the transducer.

In a recent paper, Dekker and coworkers [43] described the use of a SWNT as an electrode for electrochemistry studies. This work constitutes an important advance in the development of electrodes with nanometer dimensions with interest in biological studies. The analytical potential of this electrode will probably be extended even further with the use of functionalized CNTs, which will permit the detection of single biomolecules in local cellular compartments.

Various strategies for CNT solubilization so as to be introduced/immobilized later onto electrode surfaces have been reported. [2] Some selected examples are summarized in Table 1.

CNTs are an efficient material for use in a wide range of electrochemical sensors as well as biosensors, ranging from enzyme electrodes to immune and DNA biosensors. Some interesting applications of CNTs for each of the mentioned (bio)sensors are presented in the following sections.

2.1. Sensors

Chemical sensors have become an increasingly attractive tool for monitoring noxious substances, for quality control, and in medicinal and environmental chemistry. The tremendous importance of CNTs for sensor applications has led to wide research activities in this area. One of the advantages of these sensors is that they can be used as "one shot"-sensors that can be disposed of after usage.

Voltammetric or potentiometric methods for the determination of inorganic and biologically relevant compounds in various samples (biological, environmental, human) have been used. It has been demonstrated that CNTs have a

stable electrochemical behavior and catalyze the electrochemical reactions for several compounds. The application of CNT-based sensors for organic compounds (e.g., NADH and dopamine), metals, and for other species will be shown.

2.1.1. Organic Compounds and Biomolecules

2.1.1.1. NADH β -Nicotinamide adenine dinucleotide (NADH) is involved as a cofactor in several hundred enzymatic reactions of NAD⁺/NADH-dependent dehydrogenases. The electrochemical oxidation of NADH has thus been the subject of numerous studies related to the development of amperometric biosensors. Problems inherent to anodic detection are the large overvoltage encountered for NADH oxidation at ordinary electrodes and surface fouling associated with the accumulation of reaction products. For these reasons considerable effort has been devoted to identifying new electrode materials that will reduce the overpotential for NADH oxidation and minimize surface passivation effects.

The catalytic oxidation of NADH and highly stable amperometric NADH response at glassy carbon electrodes modified with CNT coatings have been reported. [44] The CNT-coating offers a marked (490 mV) decrease in the overvoltage for the NADH oxidation and eliminates surface fouling effects. Figure 2 (left) compares the amperometric response to 5×10^{-3} M NADH, as recorded over a continuous 60-min period, at the unmodified (A) and MWNT-modified (B) glassy carbon electrodes held at +0.60 V. A more stable response for the CNT-modified sensor can be observed. The electrocatalytic action facilitates low-potential amperometric measurements of NADH. Figure 2 (right) compares the amperometric response (at +0.30 V) of the bare (A) and MWNT-coated (B) electrodes to successive 1×10^{-4} M additions of NADH. It was observed that the CNT-modified electrode responds very rapidly to these changes in the NADH concentration.

Gorski et al. [45] reported an electrochemical sensing platform based on the integration of redox mediators and CNTs in a polymeric matrix. To demonstrate the concept, a redox mediator, Azure dye (AZU), was covalently attached to polysaccharide chains of chitosan (CHIT) and dispersed with CNTs to form composite films for the amperometric determination of NADH. The incorporation of CNTs into

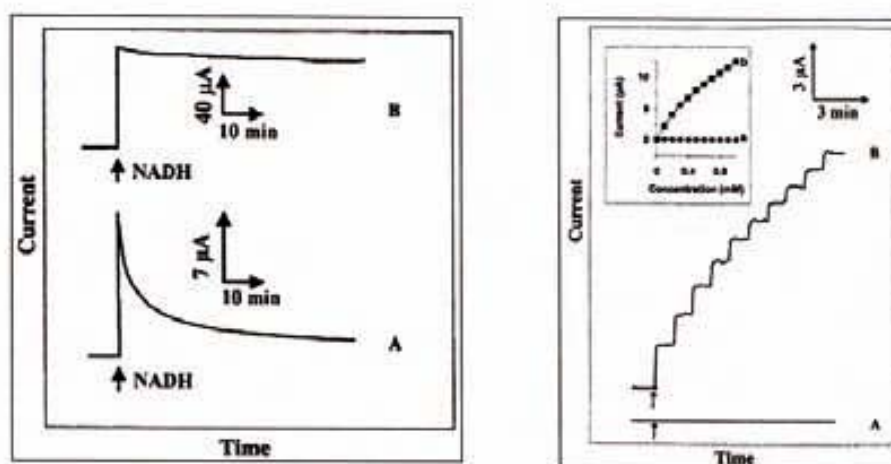


Figure 2. (Left) Stability of the response to 5×10^{-3} M NADH using unmodified (A) and MWNT-modified (B) glassy carbon electrodes. Operating potential, +0.60 V; stirring rate, 500 rpm; electrolyte, phosphate buffer (0.05 M, pH 7.4). (Right) Current–time recordings obtained on increasing the NADH concentration in 1×10^{-2} M steps at unmodified (A) and MWNT-coated (B) glassy carbon electrodes. Operating potential, +0.3 V; other conditions, as in the left figure. Reprinted with permission from [44]. M. Musameh et al., *Electrochem. Commun.* 4, 743 (2002). © 2002, Elsevier.

the CHIT-AZU matrix facilitated the AZU-mediated electrooxidation of NADH. In particular, CNTs decreased the overpotential for the mediated process by an extra 0.30 V and amplified the NADH current by ~ 35 times (at -0.10 V) while reducing the response time from ~ 70 s for CHIT-AZU to ~ 5 s for CHIT-AZU/CNT films.

Although most of the CNT-based electrodes for NADH detection applications are based on physical adsorption of CNTs onto electrode surfaces (usually glassy carbon), it is important to note that CNTs have also been mixed with Teflon [46] or dispersed inside an epoxy resin.

An example of carbon nanotube-epoxy composite (CNTEC) electrodes is reported by our group [47]. CNTECs were constructed from two kinds of MWNTs differing in length ($0.5\text{--}2$ μ m and $0.5\text{--}200$ μ m) mixed with epoxy resin. The behavior toward NADH of CNTEC electrodes prepared with different percentages of CNTs has

been compared with that of graphite-epoxy composite (GEC) electrodes. In all cases CNTEC electrodes provide better reversibility, peak shape, sensitivity, and stability compared with GEC electrodes. The obtained experimental results demonstrate remarkable electrochemical and mechanical advantages of CNT composites compared to graphite composites for electrochemical sensing of NADH [Figure 3].

The CNT electrodes allow highly sensitive, low-potential, stable amperometric sensing. Such ability of CNTs to promote the NADH electron-transfer reaction suggests great promise for dehydrogenase-based amperometric biosensors.

2.1.1.2. Dopamine Since its discovery in the 1950s, dopamine (DA) has been of interest to neuroscientists and chemists as an important neurotransmitter in the mammalian

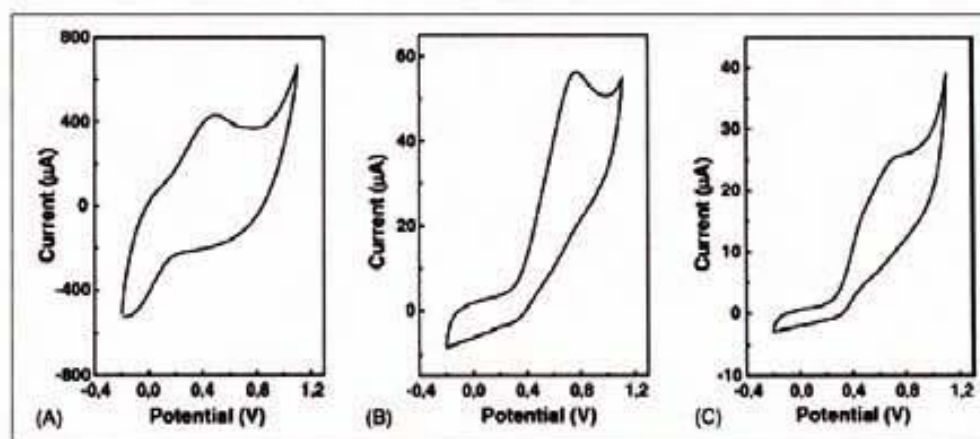


Figure 3. Cyclic voltammograms for 1 mM NADH of the (A) CNTs-200-EC, (B) CNTs-2-EC and (C) GEC electrodes. Conditions: 50 mM phosphate buffer, pH 7.4; scan rate 0.1 V s $^{-1}$; carbon/epoxy ratios, 20:80 (w/w). Reprinted with permission from [47]. M. Pumera et al., *Sens. Actuators B Chem.* 113, 617 (2006). © 2006, Elsevier.

central nervous system [48]. Disturbances in physiological dopamine levels are with interest to be monitored in the case of Parkinson's disease and other similar diseases. Thus, various commonly usable analytical methods for dopamine and its analogs have been developed in the past. Some examples of these methods are the rapid liquid chromatography/tandem mass spectrometry (LC-MS/MS), the chromatography method, and capillary electrophoresis mass spectrometry. All these methods are very sensitive, however, and require sophisticated temperature control systems for separation followed by spectrophotometric or electric detection systems. Recently, there has been an increasing demand for more sensitive and simpler analytical methods. Square-wave voltammetry techniques are very useful and popular for trace analysis since these techniques are compact, efficient, and sensitive [49]. Various voltammetry techniques, depending on the working electrode material, have been found to have a low detection limit required for neurotransmitter dopamine analysis.

Young Ly et al. [49] presented a simply prepared sensor. They immobilized DNA onto the surface of a CNT paste electrode (CNTPE). The CNTPE was prepared by mixing 40% CNTs and 40% DNA (double-stranded and prepared from calf thymus) with 20% mineral oil. The developed sensor was utilized to monitor DA ion concentration using the cyclic voltammetry (CV) and square-wave (SW) stripping voltammetry methods. The result obtained was a very low detection limit of DA ($2.1 \times 10^{-11} \text{ mol}\cdot\text{L}^{-1}$) compared with other common voltammetric methods being the relative standard deviation for a $0.05 \mu\text{g DA L}^{-1}$ of about 0.02% ($n = 15$) at the optimum conditions [Figure 4].

Ascorbic acid (AA) is one of the most important interfering elements while determining DA concentration [50]. AA has a similar oxidation potential and is usually present in vivo at concentrations 102–103 times higher than DA. Therefore, it is essential to establish simple and rapid methods for selective determination of DA concentrations in routine analysis. A conventional way is to coat the working electrode surface with an anionic film such as Nafion to protect the surface from the interference of the negatively-charged DA.

Wu and Hu [51], reported a glassy carbon electrode (GCE) modified with a homogeneous and stable suspension

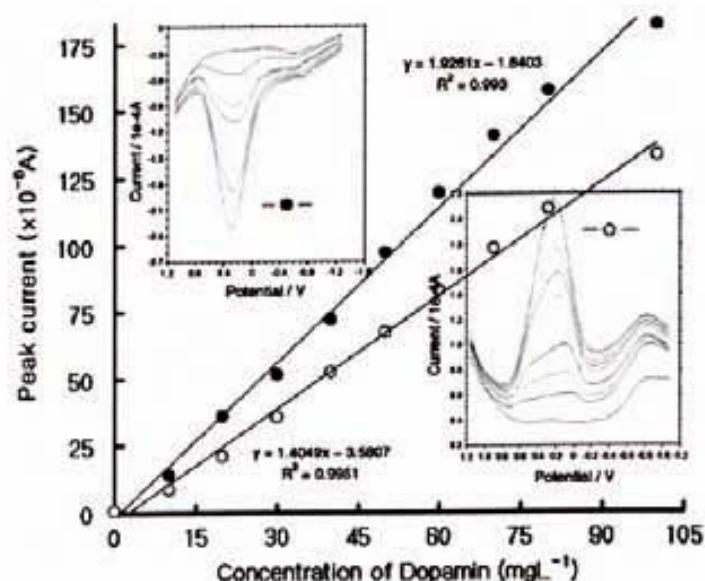


Figure 4. Square-wave stripping voltammograms of dopamine at various concentrations: 0, 10, 20, 30, 40, 50, 60, 70, 80, and 100 $\text{mg}\cdot\text{L}^{-1}$ at optimum conditions, in a 0.1 M $\text{NH}_4\text{H}_2\text{PO}_4$ solution with a pH of 3.5, a deposition time of 5 s at -1.3 V anodic and 1.2 V cathodic potentials, a frequency of 75 Hz, an increment potential of 35 mV, an amplitude of 0.5 V, and the calibration curve with the results of regression. Reprinted with permission from [49], S. Y. Ly, *Bioelectrochem.* 68, 227 (2006). © 2006, Elsevier,

of MWNTs in an ethanol solution of Nafion (0.1%). A uniform MWNT-Nafion cast film was obtained over the GCE after the solvent evaporation. Figure 5(A) shows the TEM images of the MWNTs (a) and the MWNT-Nafion suspension (b). Many CNTs with diameters ranging from 20–30 nm were observed. In photograph a, they twist together heavily and have different lengths. It can also be seen that the morphological properties of the MWNTs are very uniform. Apart from that, negligible carbon particle impurities were observed. From photograph b it is apparent that the twisted MWNTs have been untwisted and homogeneously dispersed into Nafion solution. The SEM images of the Nafion film (a) and MWNTs-Nafion film (b) on the

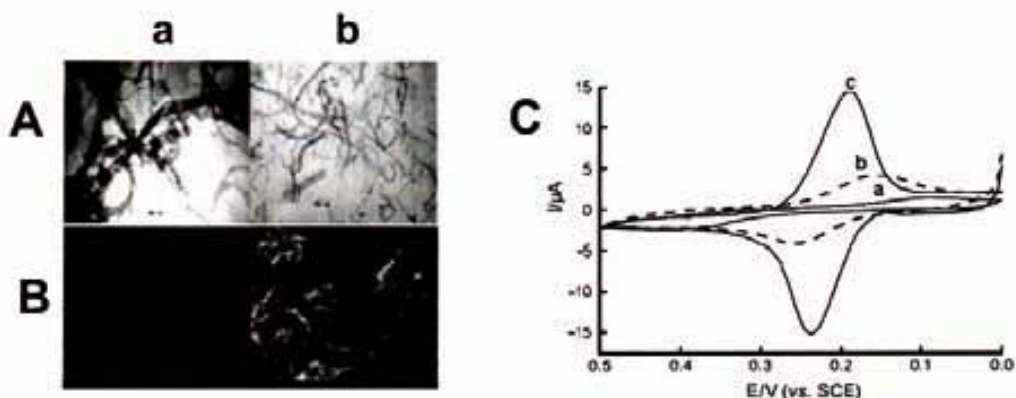


Figure 5. (A) TEM images of MWNTs (a) and MWNTs-Nafion dispersion (b). (B) SEM image of the Nafion film (a) and MWNT-Nafion film (b) on a GC disk magnified by a factor of 25,000. (C) Cyclic voltammograms of $1 \times 10^{-5} \text{ mol}\cdot\text{L}^{-1}$ DA in $0.1 \text{ mol}\cdot\text{L}^{-1}$ phosphate buffer (pH 6.0). Curve (a): at bare GCE, curve (b): Nafion-modified GCE, and curve (c): MWNT-Nafion-modified GCE. The scan rate is $0.1 \text{ V}\cdot\text{s}^{-1}$. Reprinted with permission from [51], K. Wu and S. Hu, *Microchim. Acta* 144, 131 (2004). © 2004, Springer-Verlag.

pretreated glassy carbon electrode disk are depicted in Figure 5(B). The comparison of these two images clearly shows that the GCE surface is coated with a homogeneous MWNTs film.

The electrochemical behavior of DA was also examined using cyclic voltammetry (CV). At the bare GCE, a couple of quasi-reversible redox peaks were observed for $1 \times 10^{-5} \text{ mol}\cdot\text{L}^{-1}$ DA [Figure 5(C) curve a]. The Nafion-modified GCE significantly enhanced the redox peak currents of DA compared with the bare GCE [Figure 5(C) curve a]. This enhancement is undoubtedly attributed to the cation exchange properties of Nafion film. It can also be seen that the peak current of DA increases further at the MWNT-Nafion modified GCE [Figure 5(C) curve c]; meanwhile, the oxidation peak potential (E_{pa}) shifts negatively to 0.235 V, and the reduction peak potential (E_{pc}) shifts positively to 0.201 V. The separation between peak potentials (δE_p) was 34 mV, indicating that two electrons are involved in the redox process of DA, which is in good agreement with the reported [52]. As can be seen, MWNT-Nafion modified GCE not only improves the redox peak currents but also makes the redox reaction of DA more reversible.

Chicharro et al. [53] have also reported on the successful use of CNTPEs as detectors in flow systems such as flow injection analysis (FIA) and capillary electrophoresis (CE) with a new electrochemical cell adapted to a commercial instrument. The usefulness of CNTPEs in flow systems was evaluated by using FIA in connection with the amperometric response of $1.0 \times 10^{-6} \text{ M}$ DA at 0.400 V. CNTPEs prepared with short (1–5- μm length) and long CNTs (5–20- μm -length) of 20–50-nm diameter have demonstrated to be highly useful as detectors in FIA and CE using a new electrochemical cell for the detection that allows an easier handling and more reproducible responses. Therefore, the combination of the CNT's electrocatalytic activity with the known advantages of composite materials, the efficiency of the new electrochemical cell, and the excellent separative properties of capillary electrophoresis represents a very important alternative for new electroanalytical challenges.

2.1.1.3. Hemoglobin and Cholesterol An interesting research field in biological systems using CNTs is the study of the direct electrochemistry of hemoglobin (Hb). Didodecylmethylammonium bromide (DDAB) film on the SWNT-modified electrode was used to prepare a SWNT/DDAB film-modified glassy carbon electrode [54]. This modified electrode was used to study the electrochemical behavior of Hb. Cyclic voltammetry of Hb showed two pairs of well-defined and nearly reversible peaks. The results obtained show that the electrochemical reaction of Hb on the SWNT/DDAB film-modified electrode was controlled by absorption.

Figure 6 illustrates the cyclic voltammograms of Hb at four types of electrodes in a $0.1\text{-mol}\cdot\text{L}^{-1}$ $\text{KH}_2\text{PO}_4\text{--Na}_2\text{HPO}_4$ buffer solution (pH 7.0). On the bare glassy carbon electrode, a pair of very small redox peaks appeared at about -0.2 V [Figure 6(a)], and on the SWNT-film modified glassy electrode the current increases, but the electrochemical behavior of Hb changed slightly [Figure 6(c)]. On DDAB film-modified glassy carbon electrode, Hb showed two pairs of redox peaks at -0.2 V and -1.1 V , respectively, which were assigned to the Fe(III)/Fe(II) and Fe(II)/Fe(I) heme center redox processes [Figure 6(b)]. However, on the SWNTs/DDAB-film modified glassy carbon electrode, cyclic voltammetry of Hb showed two pairs of well defined and nearly reversible peaks [Figure 6(d)], and the currents of redox peaks increased significantly.

The square wave voltammograms of Hb on SWNTs/DDAB film-modified GC electrode also showed two pairs of well-defined and nearly reversible peaks [Figure (6)]. The above experiments showed that SWNTs and DDAB could facilitate the electron transfer of Hb and enhance the electrochemical signal. The reason is that SWNTs have a large surface area and good electrical conductivity. DDAB can provide an environment compatible to biomolecules because of forming a similar biomembrane structure. The DDAB film lets the Hb maintain its suitable conformation and activity, which make the electron transfer between hemoglobin and the SWNT-modified electrode easy.

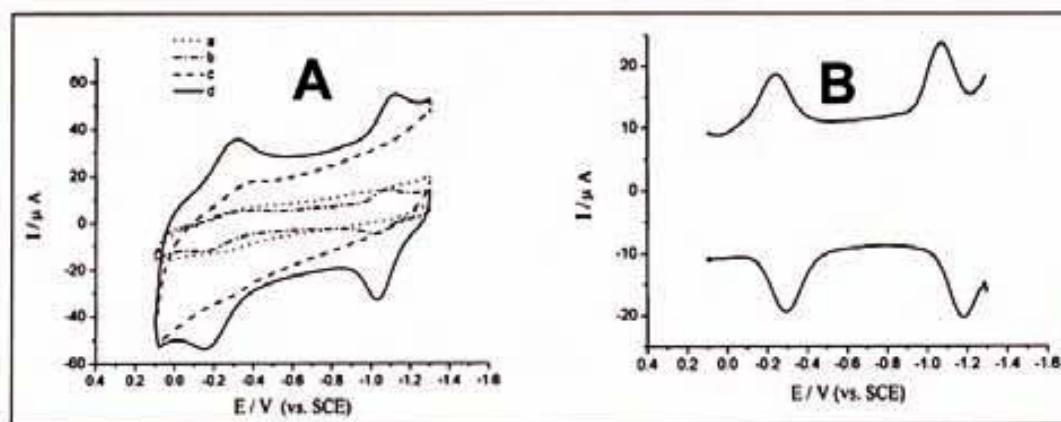


Figure 6. (A) Cyclic voltammograms for hemoglobin ($5.0 \times 10^{-5} \text{ M}$) in 0.1 M $\text{Na}_2\text{HPO}_4\text{--KH}_2\text{PO}_4$ buffer solution (pH 7.0) on a bare GCE (a), DDAB film-modified GC electrode (b), SWNT film-modified GCE (c), and SWNT/DDAB film-modified electrode (d) with the scan rate 0.5 V/s . [54] (B) Square-wave voltammograms of $5.0 \times 10^{-5} \text{ M}$ Hb in 0.1 M $\text{Na}_2\text{HPO}_4\text{--KH}_2\text{PO}_4$ buffer solution (pH 7.0) on the SWNT/DDAB film-modified GCE. Frequency: 100 Hz ., pulse height: 100 mV . Reprinted with permission from [54], P. Yang et al., *Electroanal.* 16, 97 (2004). © 2004, Wiley-VCH.

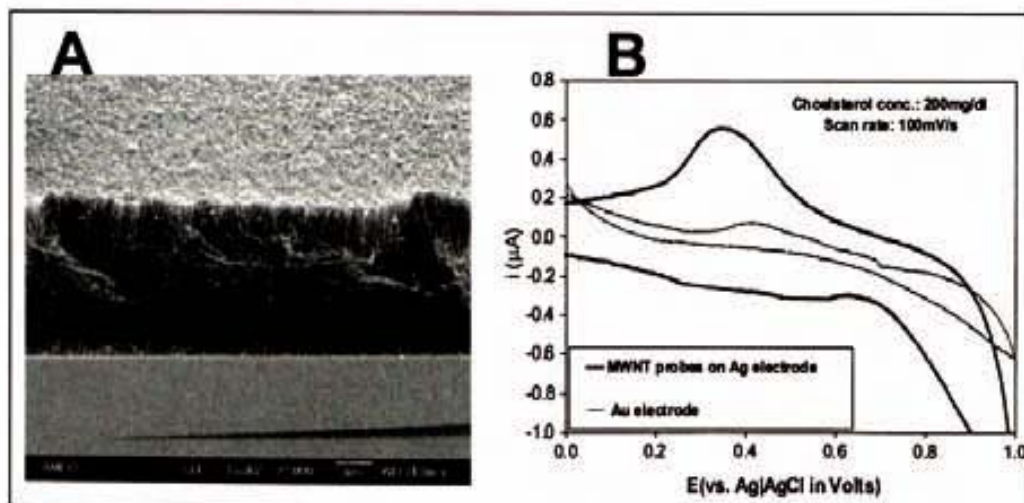


Figure 7. (A) Scanning electron microscope image of the vertically aligned thin MWNTs in the Si platform. (B) Enhancement of electron transfer in the presence of CNTs. Cyclic voltammograms of the Au working electrode with and without CNTs (identical enzyme immobilization procedure in both cases) in $200 \text{ mg}\cdot\text{dL}^{-1}$ of cholesterol in PBS solution (0.1 M, pH 7.0). Reprinted with permission from [56], S. Roy et al., *Nanotech.* 17, S14 (2006). © 2006, IOP Publishing.

Another interesting application includes the use of CNTs in the detection of blood cholesterol that it is of great clinical significance. CNTs have been shown to promote electron transfer reactions for important biomolecules such as ascorbic acid, dopamine, cytochrome *c* and NADH. Lia et al. [55] reported modification of screen-printed carbon electrodes (on a polycarbonate substrate) with CNT solution for the detection of total cholesterol. According to another recent strategy S. Roy et al. [56] reported the fabrication of vertically aligned CNT bioprobes on silicon substrates for enzymatic assay of cholesterol. Due to its compatibility with the standard Si micro-fabrication technology, the proposed scheme has the potentiality to integrate an array of sensors for lab-on-a-chip systems. The platform for the set of bioprobes was Si substrate ($2 \text{ mm} \times 5 \text{ mm}$) on which a layer of SiO_2 ($\sim 300 \text{ nm}$ thick) was grown by thermal oxidation. The substrate was then placed in a quartz tube CVD reactor, where MWNTs were grown on the defined region. The average diameter of these thin MWNTs was $\sim 10 \text{ nm}$ and the length was in the range of $30\text{--}35 \mu\text{m}$ Figure 7(A). After CNT growth, the chip was cleaned in diluted HNO_3 solution that caused purification of the CNTs as well as removal of the loose carbon particles from the chip. Electrical contact was made in the bonding pad region followed by coating the entire chip by an insulated film except for the active region ($1 \text{ mm} \times 1 \text{ mm}$) through which the CNT bioprobes were exposed [56]. Figure 7(B) represents a comparison of the cyclic voltammograms for the Au working electrode (on SiO_2/Si) with and without CNT probes. Surface functionalization with polyvinyl alcohol (PVA)-entrapped enzymes was identical in both cases. It is evident that the presence of CNTs certainly causes an increase in the sensor signal as well as the signal-to-noise ratio.

2.1.2. Stripping-Based Metal Sensors

Stripping analysis is the most sensitive electroanalytical technique and is highly suitable for the monitoring of toxic

metals. Approximately 30 metals can thus be determined by using electrolytic (reductive) deposition or adsorptive accumulation of a suitable complex onto the electrode surface [57]. Voltammetric stripping analysis has the capability of simultaneous determination of multiple elements, and relatively cheaper instrumentation compared with spectroscopic techniques used for trace metal analysis. In addition, its low operating power makes them attractive as portable and compact instruments for onsite monitoring of trace metals. [58] The growing demand for reliable and real-time monitoring of trace metal contaminants in natural waters has prompted the development of new methods and appropriate sensors to perform in situ measurements [59].

In a recent study by A. Profumo et al. [60], a CNT chemically-modified gold electrode (CNTs-CME) has been developed bearing SH groups for trace determination of As(III) and Bi(III) in natural and high-salinity waters. The preparation of this MWNT chemically modified electrode consisted of putting MWNTs to reflux in SOCl_2 for 12 h. A solution of mercaptoethanol and of triethylamine in CH_2Cl_2 was added, and the mixture was refluxed for 24 h. The suspension was centrifuged and the solid repeatedly washed with methanol to give derivatized MWNTs.

The MWNT-CME was prepared by dipping the cleaned gold electrode in a sonicated suspension of 3 mg of derivatized nanotubes in 1 mL of DMSO for 48 h. It demonstrated to be effective for trace determination of As(III) and Bi(III) in acetic buffer.

An ultrasensitive voltammetric detection of trace heavy metal ions, using nanoelectrode arrays (NEA) that are based on low-site density CNTs was also reported [61]. The nanoelectrode showed an increased mass-transport rate, a decreased influence of the solution resistance, and a higher signal-to-noise ratio leading to a much lower background current. A CNT-NEA sensing platform was used in connection to bismuth film, which was prepared in situ together with target metals. This novel platform represents a promising replacement for the common toxic mercury electrode.

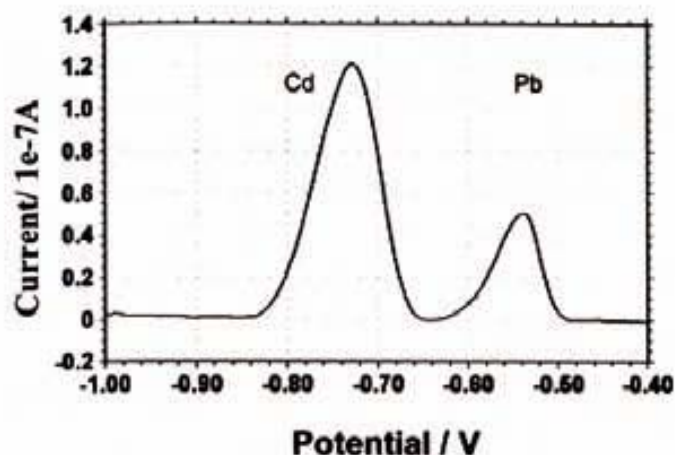


Figure 8. Typical square-wave voltammogram of $5 \mu\text{g}\cdot\text{L}^{-1}$ cadmium and lead on the CNT-NEA in 0.1 M acetate buffer (pH 4.5) in the presence of $500 \mu\text{g}\cdot\text{L}^{-1}$ bismuth. Other conditions include in situ plated bismuth-coated CNT-NEA with 1 min pretreatment at 0.3 V; 2 min accumulation at 21.2 V; 10-s rest period (without stirring); square-wave voltammetric scan with a step potential of 5 mV; amplitude, 20 mV; frequency, 25 Hz. Reprinted with permission from [61], G. Liu, *Analyst* 130, 1098 (2005). © 2005, The Royal Society of Chemistry.

The new CNT-NEA sensing platform shows the potential to detect very low concentrations of heavy metal ions compared with a traditional bulk and macroelectrode-sensing platform. Additionally the CNT-NEA coated with a bismuth film was used successfully for voltammetric detection of trace cadmium (II) and lead(II) at the sub-ppb level, obtaining a detection limit of $0.04 \mu\text{g}\cdot\text{L}^{-1}$. Figure 8 represents a typical square voltammogram for a mixture containing $5 \mu\text{g}\cdot\text{L}^{-1}$ cadmium and lead ions in the presence of $500 \mu\text{g}\cdot\text{L}^{-1}$ bismuth in connection to a 2-min deposition. A well-defined, undistorted, sharp signal with a favorable resolution was obtained. The peak potentials of cadmium and lead are -0.75 V and -0.55 V , respectively. The stripping signal for the selected target metals is surrounded with low background contributions, indicating effective sealing on the sidewall of CNTs in the preparation of the CNT-NEA.

Another interesting study for electroanalytical sensor applications was demonstrated by Tsai et al. [62]. They prepared a composite film of MWNTs with Nafion by cast deposition on glassy carbon electrodes, obtaining an anodic stripping response for Cd metal from a solution of $1\text{--}4 \mu\text{M}$ in aqueous 0.1 M acetate buffer solution; the limit of detection under these conditions can be estimated as $\sim 76 \text{ nM Cd}^{2+}$. The used electrode was based on uniformly casting a dispersion of 40–60-nm MWNTs in 0.5 wt% Nafion onto the surface of a glassy carbon electrode. This mercury-free thin film electrode can be employed to accumulate and detect cadmium in aqueous solution. The stripping peak current varies proportionally to the concentration of cadmium. The success of this strategy suggests that MWNT/Nafion film will have significant electroanalytical utility in metal detection in the future.

2.1.3. Nanoparticle Detection

The remarkable properties of CNTs also suggest their use in developing (bio)sensing systems where other nanoparticles have been involved. The simultaneous determination of the

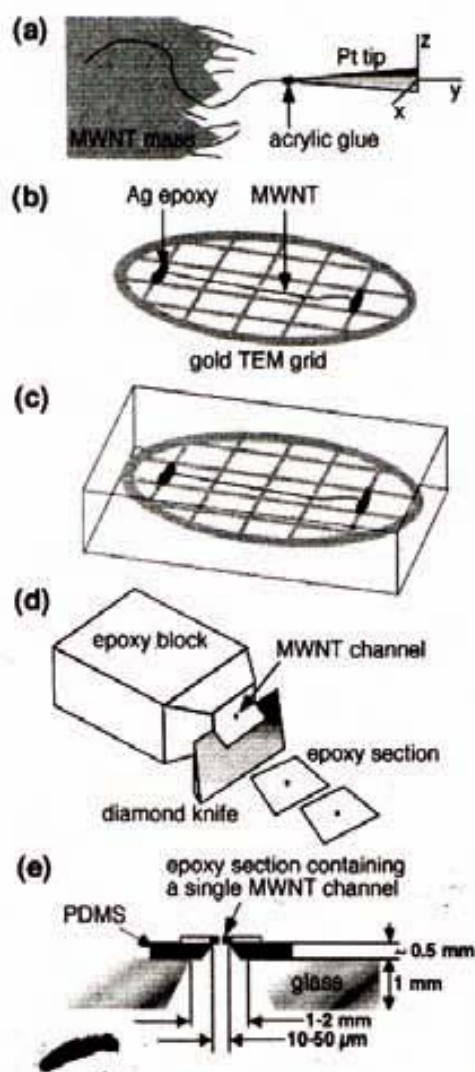


Figure 9. Fabrication of membranes containing a single MWNT channel used as a resistive pulse counter (Coulter counter). Reprinted with permission from [63], T. Ito et al., *Anal. Chem.* 75, 2399 (2003), © 2003, American Chemical Society.

size and surface charge of individual acid-functionalized nanoparticles using a resistive-pulse counter based on a single 130-nm diameter pore defined by a MWNT has been reported by Ito et al. [63]. A resistive-pulse Coulter counter based on a membrane containing a single MWNT channel was used to simultaneously determine the size and surface charge of carboxy-terminated polystyrene nanoparticles. The membrane was prepared from an epoxy section containing a MWNT channel mounted on a poly-(dimethylsiloxane) (PDMS) support structure; it was immobilized on a glass substrate ($\sim 12 \text{ mm} \times 12 \text{ mm}$) containing a cylindrical, sand-blasted hole ($\sim 2 \text{ mm}$ diameter), as shown in Figure 9.

Coulter particle counters have been used to count and analyze many different types of particles, ranging from biological cells to colloidal particles [64]. A typical Coulter counter consists of a single small pore (typically $5 \mu\text{m}\text{--}2 \text{ mm}$ in diameter) that separates two electrolyte solutions. A constant potential is applied across the sensing pore, and the resulting ion current is continuously monitored. Transport of analyte particles through the pore results in an increase in the pore

resistance, and the corresponding decrease in the ion current can be detected. The magnitude of the current decrease correlates to the size of the analyte particles, and its duration is related to the residence time of the analyte in the pore. The number of such current pulses can be related to the analyte concentration. The principles governing this detection strategy predict that smaller sensing pores permit detection of smaller particles. The width of the current pulses is a measure of the nanoparticle transport time, and it permits calculation of the electrokinetic surface charge. Different types of polystyrene nanoparticles having nearly the same size, but different electrokinetic surface charge, could be resolved on the basis of the difference in their transport time.

This new research shows a greatly improved signal-to-noise ratio and better time resolution as compared to their previous report of a MWNT-based Coulter counter [65]. Accordingly, it is now possible to accurately measure the true height and width of pulse signals corresponding to transport of individual particles through a MWNT channel.

2.1.4. Electrical Sensors for Gases

Gas sensor devices have attracted widespread attention in the past decades due to their potential applications in environmental pollution monitoring, flammable and toxic gas detection, and food quality control.

The most important problem in gas sensors is their selectivity, i.e., the capability to provide different responses while exposed to different gaseous species. The efforts to improve the selectivity of gas sensors have also been focused on searching for new sensing materials and more recently on using sensor arrays [66].

CNT-based gas sensors have received great attention beside other applications [67]. Changes in the resistance of the CNT layer have been used for detection of nitrogen dioxide [68], ammonia [69], hydrogen [69], and inorganic vapor [70]. Different interaction mechanisms between the analytes and CNTs, as well as different modes of preparing CNT-based sensors have been reported. Various groups have explored the potential of CNTs for gas sensing based on the electrical conductance changes.

A novel microelectronic gas sensor utilizing CNTs in a thin-layered Pd/CNTs/n⁺-Si structure for hydrogen detection was reported by Wong et al. [71]. Due to their hollow center, nanometer-size and large surface area, CNTs are ideal for fast gas adsorption and hence detection. The sensor is fabricated on an n-type silicon wafer, which is needed as an ohmic supporting substrate. MWNTs were grown selectively on the substrate via catalytic activation with microwave plasma-enhanced chemical vapor deposition (MPECVD). A thin film of palladium, acting as a nanocluster catalytic center for CNT nucleation, was selectively sputtered on the surface of the silicon substrate with a patterning mask. The sputtered sample was then transferred in air to the CVD chamber for CNT deposition. The deposition was carried out under a working pressure of 10 Torr and substrate temperature of 700°C. The sensor was tested for current versus applied voltage (I-V) characteristics in open air and in the presence of hydrogen at several operating temperatures. The results demonstrated that CNTs in thin-layered Pd/CNTs/n⁺-Si configuration are good hydrogen gas sensors with high sensitivity over a wide operating temperature range in an open environment.

A novel electrochemical sensor based on MWNTs for the determination of carbon monoxide (CO) has been developed by He [72]. The catalytic activation of MWNT microelectrodes (MWNTME) with Pt micro-disk as a substrate was investigated. The MWNTME was fabricated according to literature [73]. In brief, a 80- μm diameter Pt disk microelectrode was first chemically etched in heat aqua regia to form a cavity $\sim 100\ \mu\text{m}$ deep at the tip of the Pt disk microelectrode and the etched tip was then grounded on a flat plate (such as a glass slide) with MWNTs until the microcavity was filled with MWNTs [72]. The results showed that MWNTME represents a catalytic effect toward the electrochemical oxidation of CO in $0.5\ \text{mol}\cdot\text{L}^{-1}\ \text{HClO}_4$. As compared with the bare Pt disk electrode, MWNTMEs can greatly decrease the over potential and obviously increase the current of CO oxidation [Figure 10(a)]. The current-time curve recorded under conditions of constant potential and various CO concentrations suggests that current response

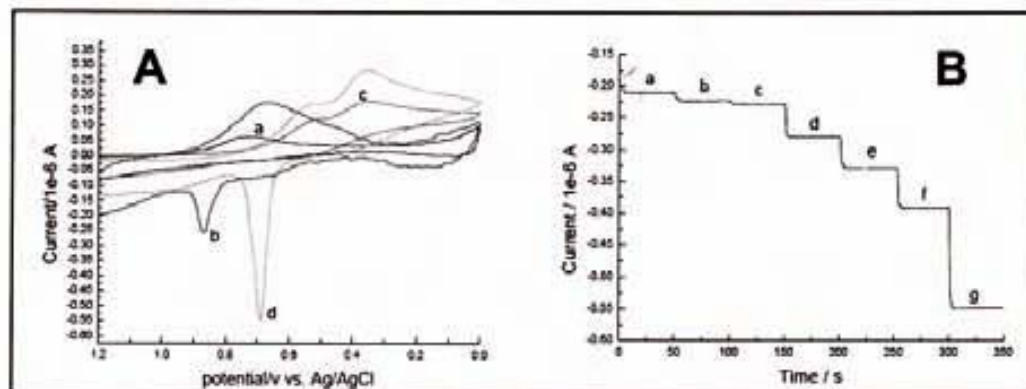


Figure 10. (A) Cyclic voltammograms with a bare Pt electrode in (a) air; (b) CO in N₂ stream and with MWNTME in (c) air; and (d) CO in N₂ stream with $0.5\ \text{mol}\ \text{l}^{-1}\ \text{HClO}_4$ as supporting electrolyte solution. The potential scan rate is $100\ \text{mVs}^{-1}$. (B) The current responses of the MWNTME toward CO in the presence of different concentrations (a) $0.6\ \text{gml}^{-1}$, (b) $0.72\ \text{gml}^{-1}$, (c) $1.44\ \text{gml}^{-1}$, (d) $6.55\ \text{gml}^{-1}$, (e) $13\ \text{gml}^{-1}$, (f) $26\ \text{gml}^{-1}$, and (g) $52\ \text{gml}^{-1}$ in N₂ stream, with $0.5\ \text{mol}\ \text{l}^{-1}\ \text{HClO}_4$ as supporting electrolyte solution. The potential is 700 mV. Reprinted with permission from [72], J. B. He et al., *Sens. Actuators B Chem.* 99, 1 (2004). © 2004, Elsevier.

depends linearly on CO concentration [Figure 10(b)] with a correlation coefficient of 0.9957, detection limit of $0.60 \mu\text{g mL}^{-1}$, and a relative standard deviation of 4.8% ($n = 5$) at room temperature.

On the other hand, polymers have been used to impart high sensitivity and selectivity in the gas electrodes. Hyeok et al. [74] fabricated a gas sensor from a nanocomposite by polymerizing pyrrole monomer with SWNTs. Polypyrrole (Ppy) was prepared by a simple and straightforward in situ chemical polymerization of pyrrole mixed with SWNTs, and the sensor electrodes were formed by spin-casting SWNTs/Ppy onto pre-patterned electrodes. Ppy was uniformly coated on the wall of the SWNTs to increase the specific surface area. The measured resistivity was greatly reduced due to the presence of the conductive SWNT network, whereas the specific surface area was increased about threefold. The sensitivity of the gas sensor fabricated with the SWNT/Ppy nanocomposite towards NO_2 gas as measured by a direct voltage divider at room temperature was very high and similar to that of the fabricated SWNT alone. The reported literature shows that CNTs are expected to serve as an economically viable material for use in gas detection. The successful utilization of CNTs in gas sensors may open a new door for the development of novel nano-structured gas-sensing devices.

Other work was designed by Philip et al. [75] for the development of composite thin films of polymethylmethacrylate (PMMA) with MWNTs and surface-modified MWNTs (f-CNTs) for gas-sensing applications. The responses of these composites for different organic vapors were evaluated by monitoring the change in the resistance of thin films of composite when exposed to gases like dichloromethane, chloroform, acetone, methanol, ethyl acetate, toluene, and hexane. It was observed that the f-CNT/PMMA composite showed a higher response. There was an increase in resistance on the order of 10^2 – 10^3 due to surface modification when exposed to dichloromethane, chloroform, and acetone. The composites were prepared by ultrasonication of 20 mg of CNTs or f-CNTs and 80 mg of PMMA for 2 h in dichloromethane. The composite thin films were fabricated on a printed circuit board (PCB) and the change in electrical resistance due to the presence of various organic vapors was evaluated. The surface of CNTs were used to study the interaction of polar groups with gas molecules [Figure 11].

An interesting application of MWNTs is the fabrication of a carbon dioxide (CO_2) sensor built by a thin layer of a

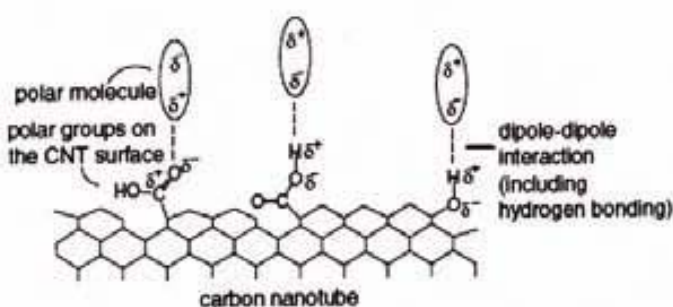


Figure 11. Interaction of gas molecules with the surface of a CNT. Reprinted with permission from [75], B. Philip et al., *Smart Mater. Struct.* 12, 935 (2003). © 2003, IOP Publishing.

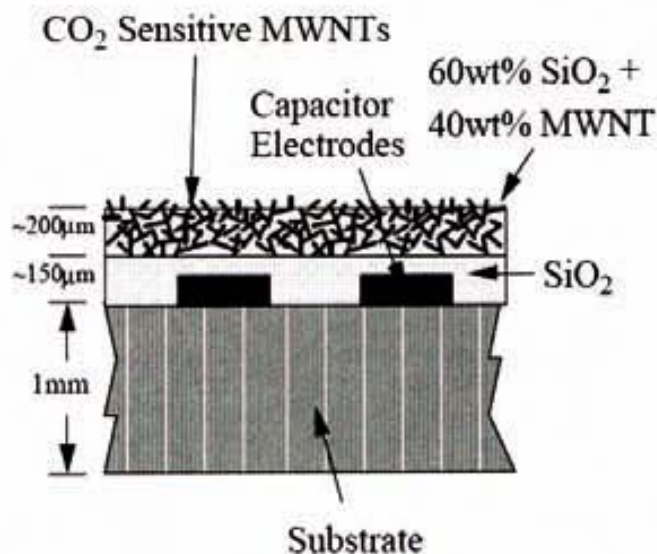


Figure 12. Sensor fabrication, cross sectional view of the interdigital capacitor. An electrically insulating $150 \mu\text{m}$ thick SiO_2 layer is first applied to protect the sensor, followed by a $200 \mu\text{m}$ MWNTs- SiO_2 gas sensing layer. Reprinted with permission from [76], K. G. Ong and C. A. Grimes, *Sensors* 1, 193 (2001). © 2001, Molecular Diversity Preservation International.

MWNT-silicon dioxide (SiO_2) composite upon a planar inductor capacitor resonant circuit [76]. A 2 cm square sensor was fabricated by photolithographically patterning a square spiral inductor and an interdigital capacitor on a printed circuit board (PCB). An $\sim 150\text{-}\mu\text{m}$ thick layer of SiO_2 followed by an $\sim 200\text{-}\mu\text{m}$ thick layer of the MWNT- SiO_2 mixture were then coated onto the capacitor of the sensor, with a resulting sensor cross-section as shown schematically in Figure 12. Experimental results show the response of the sensor is linear, reversible with no hysteresis observed between the cycles of CO_2 and dry air ($\sim 20\% \text{ O}_2 + 80\% \text{ N}_2$), and has a response time of $\sim 45 \text{ s}$.

2.2. Enzyme-Based Sensors

Several studies on redox enzymes have promoted the electron transfer with electrodes in various ways [77]. In recent years, it has aroused great interest in modifying electrode surfaces on the molecular scale with novel nanomaterials for the direct electron transfer of redox enzymes and retention of bioactivity [78]. This advantage has inspired increased research in coupling CNT-based sensors with enzymes [2].

Integration of biomaterials such as proteins, enzymes, antigens, antibodies, or DNA with the CNTs essentially provides new hybrid systems that combine the conductive or semiconductive properties of the CNTs with the recognition or catalytic properties of the biomaterials. Superior to other kinds of carbon-based materials, the internal cavities or external sides of CNT walls provide the platform for the accommodation of the biomolecules.

2.2.1. Glucose

Glucose is one of the most reported analytes detected via enzyme-CNT electrodes. Several strategies were used to immobilize the necessary enzyme. Glucose oxidase (GOx)

has been immobilized onto CNTs via polypyrrole. Wang et al. [79] prepared a glucose biosensor based on incorporating a CNT dopant and the biocatalyst within an electropolymerized polypyrrole film.

The electrode fabrication consisted of dispersing the desired amount of the functionalized nanotubes in distilled water (pH 6.4) by sonication for 15 min. The selected amount of GOx (usually 0.5 mg/mL) was then added to the CNT solution. Polypyrrole (PPy) was then added to the GOx-MWNTs mixture and the electropolymerization proceeded at a fixed potential and time (usually +0.70 V for 10 min). The electrode was then rinsed with double distilled water and stored at 4°C.

The amperometric response of the PPy/CNTs/GOx biosensor to successive 4 mM increments in the glucose concentration responds favorably and rapidly (~15 s) to these changes in the glucose concentration. Such entrapment of the CNTs dopant facilitates a highly sensitive biosensing of glucose, and represents a simple and effective route for preparing amperometric enzyme electrodes. The resulting calibration plots indicated that the PPy/CNTs/GOx biosensor was sensitive enough to detect a wide linear range (0–50 mM) with a detection limit of 0.2 mM for glucose.

Another strategy used to immobilize GOx with CNTs was developed by our group [42]. This strategy is based on CNT/epoxy composites. The biosensor was based on the immobilization of GOx within the CNT/epoxy-composite matrix prepared by dispersion of MWNTs inside the epoxy resin. The use of CNTs as the conductive part of the composite ensures better incorporation of enzyme into the epoxy matrix and faster electron transfer rates between the enzyme and the transducer. Experimental results show that the CNT/epoxy composite biosensor (GOx-CNTEC) offers an excellent sensitivity, reliable calibration profile, and stable electrochemical properties together with significantly lower detection potential (+0.55 V) than GOx-graphite epoxy composites (+0.90 V; difference $\delta E = +0.35$ V). The results obtained favorably compare to those of a glucose biosensor based on a graphite epoxy composite (GOx-GEC) [Figure 13].

The possibility of direct electron-transfer between CNTs and GOx paves the way for the construction of a new generation of amperometric glucose biosensors. Such electrical communication with GOx (and other oxidoreductase enzymes) would obviate the need for a co-substrate and allow efficient transduction of the biorecognition event. The redox center of glucose oxidase, like those of most oxidoreductases, is electrically insulated by a protein shell. Because of this glycoprotein shell, the enzyme cannot be oxidized or reduced at an electrode at any potential. Guiseppi-Elie et al. [80] reported the direct electron transfer between SWNTs and the redox active prosthetic group flavin adenine dinucleotide (FAD) of the adsorbed GOx enzyme. Both FAD and GOx were found to spontaneously adsorb to unannealed CNTs that were cast onto glassy carbon electrodes (GCE). The peak current of the electroactive FAD at SWNT/GCEs was almost 22 times as large as that found at the bare GCE [Figure 14]. This indicates a much larger effective working electrode area of SWNT/GCEs compared with GCE alone.

In summary, the immobilization of GOx onto CNTs would appear to offer an excellent and convenient platform for a fundamental understanding of biological redox

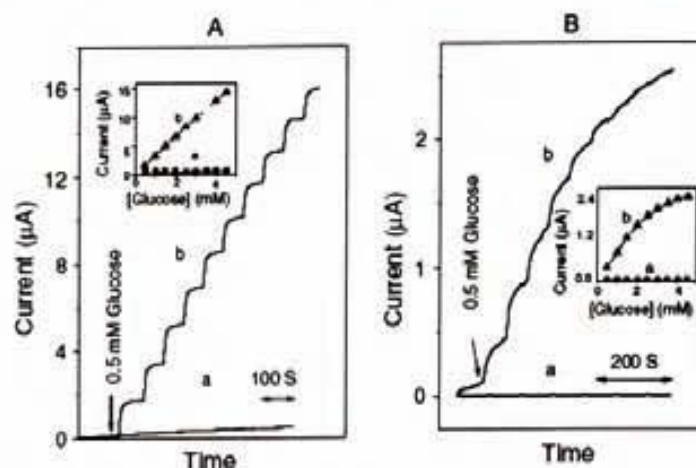


Figure 13. Current-time recordings obtained from amperometric experiments at GOx-GEC (a) and at GOx-CNTEC (b) for successive additions of 0.5 mM glucose. Working potential: (A) +0.90 V and (B) +0.55 V in 0.1 M phosphate buffer, pH 7.0. The insets show the corresponding calibration plots. Reprinted with permission from [42], B. Pérez et al., *J. Nanosci. Nanotechnol.* 5, 1694 (2005). © 2005, American Scientific Publishers.

reactions as well as the development of new glucose (nano)biosensors.

2.2.2. Hydrogen Peroxide

A number of electrochemical sensors for the detection of H_2O_2 have been reported in the literature using either horseradish peroxidase (HRP) in solution, covalently

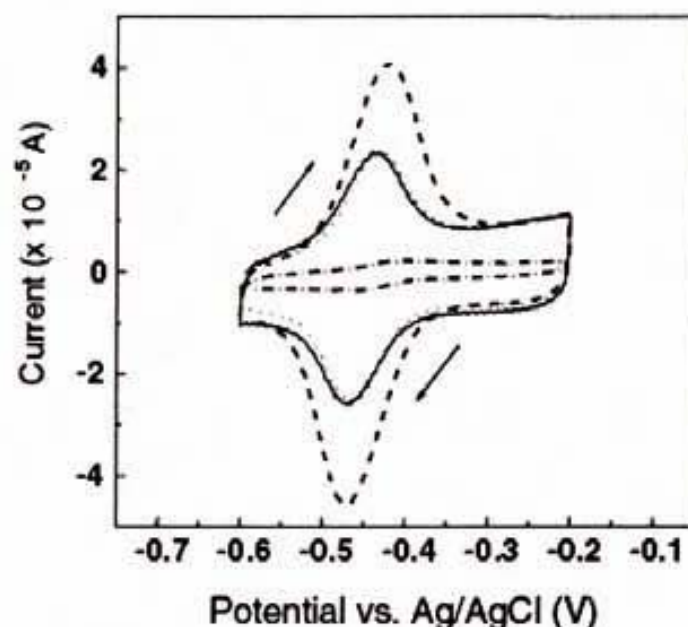


Figure 14. CV of FAD and GOx adsorbed on SWNTs/GCE. GCE in pH 7.0 phosphate buffer/0.1M KCl containing 0.1 mM FAD (dot/dash mixed curve); SWNTs/GCE in pH 7.0 phosphate buffer/0.1M KCl containing 0.1 mM FAD (dashed curve); FAD/SWNTs/GCE in pH 7.0 phosphate buffer/0.1M KCl (dotted curve); FAD/SWNTs/GCE in pH 7.0 phosphate buffer/0.1M KCl after leaving overnight (solid curve). Scan rate: 50 mV s⁻¹. Reprinted with permission from [80], A. Guiseppi-Elie et al., *Nanotech.* 13, 559 (2002). © 2002, IOP Publishing.

immobilized, or cross-linked. HRP is an important enzyme catalyzing the oxidation of a number of electron donors using H_2O_2 as the electron acceptor. [81] The enzyme, when coupled with an oxidase system or in an immunoenzyme marker, can be used for various assays with high specificity.

A hydrogen peroxide biosensor was developed based on HRP cross-linked by glutaraldehyde with MWNT/chitosan composite film on a GCE [82]. MWNTs were dissolved in a chitosan solution and then that solution was dropped onto the surface of a GCE. The enzyme electrode exhibited excellent electrocatalytic activity and rapid response for H_2O_2 in the absence of a mediator. The linear range of detection towards H_2O_2 was from 1.67×10^{-5} to 7.40×10^{-4} M with an applied potential of -0.2 V.

In recent years, the fabrication of polyaniline (PANI)/CNT composites has received great interest since the incorporation of CNTs into PANI can result in new composite materials with enhanced properties.

As both PANI and CNTs are excellent materials for the construction of electrochemical sensors and biosensors, the combination of these two materials is also expected to be an excellent platform for electrochemical sensing applications [83]. Luo et al. [84] studied the catalysis mechanism of H_2O_2 with the MWNT-HRP chemically modified electrode through the immobilization of HRP onto electropolymerized PANI films doped with CNTs. CNTs were dispersed in DMF and the resultant CNT suspension was dropped onto the GCE surface. After the evaporation of DMF in air, the resulting CNT-modified electrodes were used for electropolymerization of aniline.

The excellent conductivity and electroactivity of PANI are of special interest for applications in electrochemical biosensing systems. [85, 86]. Additionally PANI can provide a suitable environment for the immobilization of biomolecules, and the PANI-modified electrodes have several advantages such as impressive signal amplification and elimination of electrode fouling. Compared with the biosensor without CNTs, the proposed biosensor exhibited enhanced stability

and approximately eight-fold sensitivity. A linear range from 0.2–19 μ M for the detection of H_2O_2 was observed for the proposed biosensor, with a detection limit of 68 nM. The presence of CNTs in the PANI film could effectively increase the amount of immobilized HRP and enhance the stability of the immobilized enzyme as well as the biosensor performance. The responses of different modified electrodes toward the reduction of H_2O_2 are shown in Figure 15.

2.2.3. Ethanol

A rapid measurement of ethanol is very important in clinical and forensic applications as well as in the food and beverages industry [87]. Many analytical methods such as titrations, and colorimetric, spectrometric, and chromatographic methods have been developed during past years for the detection of ethanol. The mentioned methods are precise and reliable, but need expensive instrumentation. Enzyme biosensors could provide a cost-effective, alternative method for the detection of alcohol by utilizing alcohol dehydrogenase (ADH), which catalyzes the oxidation of ethanol to acetaldehyde. A clear example of this development is the amperometric biosensor described by Santos et al. [88], based on co-immobilization of ADH and Meldola's Blue (MB) on MWNTs by the cross-linking method using glutaraldehyde and agglutination with mineral oil. The efficiency of MB as an electron mediator on the electrode surface and of CNTs as an enzyme immobilization matrix was demonstrated.

2.3. Immunosensors

Immunoassays (IAs) are analytical tests that use an antibody and an antigen as very specific recognition elements. [89] The fabrication of immuno-CNT assays, which have been shown to be capable of recognizing pathogen cells via specific antibody-antigen interactions, may contribute to expanding the detection scope of CNTs sensors.

The specific molecular recognition of antigens by antibodies in formats where CNTs have been integrated has

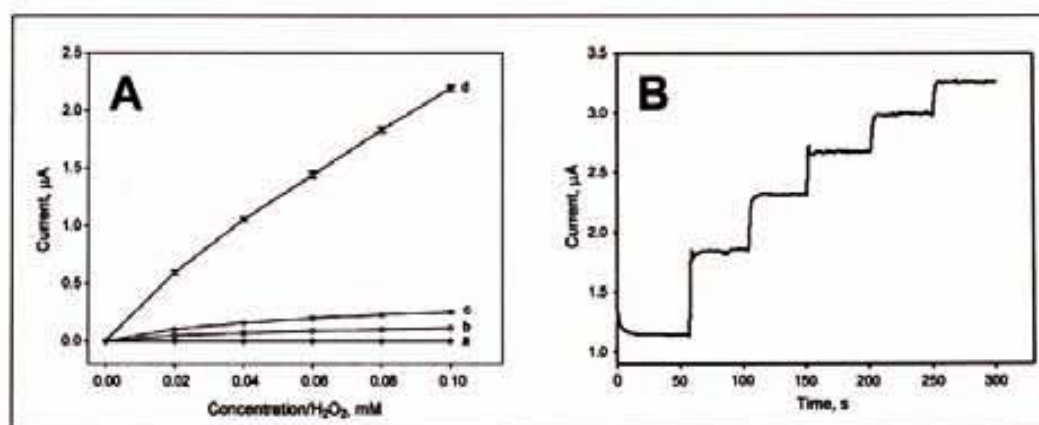


Figure 15. (A) Amperometric responses of different modified electrodes toward hydrogen peroxide at a potential of -100 mV vs Ag/AgCl. (a) PANI/GC; (b) PANI/CNTs/GC; (c) HRP/PANI/GC; (d) HRP/PANI/CNTs/GC. (B) Typical response of the CNTs-modified HRP biosensor toward the sequential injection of hydrogen peroxide at a concentration of 0.02 mM at -100 mV vs Ag/AgCl. The biosensor was prepared with 1.0 mg mL $^{-1}$ CNTs and seven electropolymerization cycles of PANI. Reprinted with permission from [84], X. Luo et al., *Anal. Chim. Acta* 575, 39 (2006). © 2006, Elsevier.

been exploited to develop highly selective detection of proteins [90]. The IA has proven to be one of the most productive technology contributions to medicine and fundamental life science research in the twentieth century for both qualitative and quantitative analysis. A great number of research papers have appeared over the last years describing the development of novel IA strategies for detecting trace amounts of chemicals in environmental and food samples.

A sensitive method for the detection of cholera toxin (CT) (causative agent for diarrhea in humans) using an electrochemical immunosensor with liposomal magnification followed by adsorptive square-wave stripping voltammetry is described by Viswanathan et al. [91]. The sensing interface consists of a monoclonal antibody against the B subunit of CT that is linked to poly(3,4-ethylenedioxythiophene) coated on Nafion-supported MWNT cast film on a GCE. The CT is detected by a "sandwich-type" assay on the electronic transducers, where the toxin is first bound to the anti-CT antibody and then to the GM1 liposomes encapsulated with an electroactive redox marker, potassium ferrocyanide. The GM1 electrochemical immunoassay can be an alternative method to enzyme-linked immunosorbent assays or other conventional assays for CT, having the advantages of sensitivity, speed, and simplicity.

MWNTs were added into 1 mL of diluted Nafion solution, forming a black suspension. Prior to this the bare GCE was activated by mechanical polishing and by electrochemical treatment, applying potentials of +1.5 and -0.2 V in 0.1 M H₂SO₄ for 5 and 3 s, respectively. The surface modification was preceded by casting a few microliters of an aliquot of MWNT-Nafion solution. The solvent was allowed to evaporate at room temperature in the air. The immunosensing layers were fabricated on the modified electrode surface by immobilizing different concentrations of CT antibody during polymerization. The electrode was then treated with 0.5% poly(vinyl alcohol) (PVA) aqueous solution followed by rinsing with PBS and stored at 4°C until use.

The calibration curve for CT had a linear range of 10^{-14} – 10^{-7} g·mL⁻¹ and the detection limit of this immunosensor was 10^{-16} g of CT (equivalent to 100 µL of 10^{-15} g·mL⁻¹).

Wohlstadter et al. [92] immobilized biotinylated anti-AFP (alpha-feto protein) antibodies on the surface of a streptavidin-coated CNT composite using poly(ethylene)-vinylacetate as a binder and exposed this derivatized composite to a sample containing AFP and anti-AFP antibodies conjugated with colloidal gold or Ru(bpy)₃²⁺. The sandwich immunoassay was biospecific and this was verified by SEM and electrochemical luminescence (ECL) measurements. The ECL signal was found to be linearly dependent from AFP concentrations up to 30 nM. This work shows that CNTs can be used as an immobilization platform and working electrode at the same time. The CNT modification procedure (based on covalent coupling of streptavidin) can be extended to electrochemical detection procedures based on voltammetric measurements including those involving enzymes as markers.

A prototype amperometric immunosensor based on the adsorption of antibodies onto SWNT forests is reported by O'Connor et al. [93]. The forests were self-assembled from oxidatively-shortened SWNTs onto Nafion/iron oxide-coated pyrolytic graphite electrodes. Anti-biotin antibody strongly

adsorbed to the SWNT forests was used with a soluble mediator to couple the majority of the enzyme label reaction to the measuring circuit. The detection limit for HRP-labeled biotin was 2.5 nM. Unlabeled biotin was detected in a competitive approach with a detection limit of 16 µM and a relative standard deviation of 12%. The immunosensor showed low non-specific adsorption of biotin-HRP (~0.1%) when blocked with bovine serum albumin.

2.4. Genosensors

Biosensors based on nucleic acid interactions are called DNA biosensors or genosensors [94] and represent a new and exciting area in analytical chemistry. The determination of nucleic acid sequences from humans, animals, bacteria, and viruses is the departure point for solving different problems; investigations into food and water contamination caused by microorganisms, detection of genetic disorders, tissue matching, and forensic applications, to name a few. DNA biosensor technologies are rapidly developing as an alternative to the classical gene assays due to several advantages such as low cost, rapid analysis, simplicity, and possibility of miniaturization.

The development of new transducing materials for DNA analysis, whose preparation is simple and suitable for mass fabrication, with a higher sensitivity and lower detection limits is a key issue in the research of electrochemical genosensing. Electrochemical genosensors are based on electrochemical transduction to detect the hybridization event. These devices can be exploited for monitoring sequence-specific hybridization events directly measuring the oxidation signal of DNA electroactive bases, DNA electroactive indicators forming complexes with DNA nitrogenous bases, or with the aid of oligonucleotides labeled with enzymes, dyes, or nanoparticles.

The integration of CNTs in genosensors has a dual amplification role: CNTs can act in both the recognition and transduction events. Their function as carrier of enzyme labels or preconcentrator of the enzymatic reaction products, for example, reflects the large specific surface area of CNTs. These advantages are illustrated using the alkaline phosphatase (ALP) enzyme tracer [95]. The use of CNTs and of enzyme labels to generate electrical signals have been extremely useful for the development of ultrasensitive electrochemical assays of DNA. Most of the CNT-sensing designs reported so far have been focused on the ability of surface-confined CNTs to promote electron-transfer reactions involved in biocatalytic devices. Wang et al. [95] developed a new CNT-based amplified bioelectronic protocol [Figure 16] that involves either a sandwich hybridization (a) or antigen-antibody (b) binding along with magnetic separation of the analyte-linked magnetic-bead/CNT assembly (A), followed by enzymatic amplification (B), and chronopotentiometric stripping detection of the product at the CNT-modified electrode (C). No such aggregation was observed in the presence of noncomplementary oligonucleotides (B). Apparently, without the recognition event, the ALP-tagged CNTs are removed by the magnetic separation, leaving the magnetic beads behind. ALP was immobilized on CNTs using a 1-ethyl-3-(3-dimethyl amino-propyl)carbodiimide linker. For electrical DNA detection, a

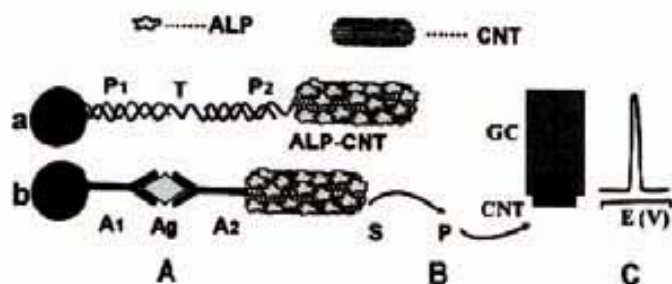


Figure 16. Schematic representation of the analytical protocol: (A) Capture of the ALP-loaded CNTs tags to the streptavidin-modified magnetic beads by a sandwich DNA hybridization (a) or Ab-Ag-Ab interaction (b). (B) Enzymatic reaction. (C) Electrochemical detection of the product of the enzymatic reaction at the CNTs-modified glassy carbon electrode; MB, Magnetic beads; P, DNA probe 1; T, DNA target; P2, DNA probe 2; Ab1, first antibody; Ag, antigen; Ab2, secondary antibody; S and P, substrate and product, respectively, of the enzymatic reaction; GC, glassy carbon electrode; CNTs, carbon nanotube layer. Reprinted with permission from [95], J. Wang et al., *J. Am. Chem. Soc.* 126, 3010 (2004). © 2004, American Chemical Society.

detection limit of 5 zmol (3000 copies) and 25 amol is reported.

The use of CNT amplifiers (loaded with numerous ALP tags) has been combined with the preconcentration feature of CNT transducers to yield a dramatic enhancement of the sensitivity. Such coupling of several CNT-derived amplification processes results in highly sensitive detection of proteins and DNA and hence indicates great promise for PCR-free DNA assays. The new CNT-derived amplification bioassays are expected to open new opportunities for medical diagnostics and protein analysis. The finding that DNA hybridization can be used for linking CNTs to particles holds promise for assembling controllable nanoscale systems.

A novel and sensitive electrochemical DNA biosensor based on MWNTs functionalized with a carboxylic acid group (MWNTs-COOH) for covalent DNA immobilization and with a favorable performance for the rapid detection of specific hybridization is described by Cai et al. [96]. The hybridization reaction was followed by using daunomycin as an electroactive intercalator indicator. When hybridization occurs, daunomycin intercalated in the DNA duplex and gave an increased electrochemical response compared to single-stranded DNA; the increase in the height of the daunomycin redox peak is used to detect the presence and the amount of the complementary sequence.

The MWNT-COOH-modified GCE was fabricated and oligonucleotides with the 5'-amino group were covalently bonded to the carboxyl group of CNTs. A schematic representation of the electrochemical DNA biosensor based on the MWNT-COOH-modified GCE for covalent DNA immobilization and target-specific DNA detection (the detection limit was $1.0 \times 10^{-10} \text{ mol}\cdot\text{L}^{-1}$) is shown at Figure 17. It was observed that the voltammetric signals of daunomycin are greatly amplified when MWNT-COOH-modified GCEs are used for the fabrication of the DNA hybridization detection assay.

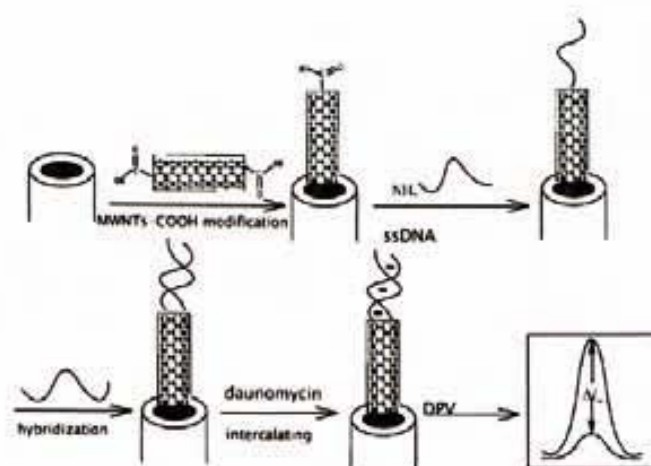


Figure 17. Schematic representation of the enhanced electrochemical detection of DNA hybridization based on the MWNTs-COOH constructed DNA biosensor. Reprinted with permission from [96], H. Cai et al., *Anal. Bioanal. Chem.* 375, 287 (2003). © 2003, Springer-Verlag.

3. APPLICATIONS IN LIQUID CHROMATOGRAPHY

Chromatography is widely used for high-resolution separation and in quantitative analysis. Liquid chromatography (LC) is the most commonly employed method for biological analysis because of its small sample volume, high sensitivity, effective separation, and small injection volume [97]. Many methods, such as high-performance liquid chromatography (HPLC) with electrochemical [98], fluorometric, or ultraviolet [99, 100] detection have been used to determine an important number of interesting compounds with a single analysis. Now, electrochemical detection (ED) is gaining more acceptance in HPLC for its more sensitivity and simple operation. In order to improve the sensitivity and selectivity of HPLC-ED, chemically modified electrodes (CMEs) have received an extensive amount of interest as a HPLC electrochemical detector [101].

The fabrication and application of a novel ED method with MWNT-modified electrodes for LC are described by Zhang et al. [97] for the determination of monoamine neurotransmitters and their metabolites. The working electrode used as detector was a MWNT-COOH CME or GC electrode. Figure 18 shows the current responses of the monoamine neurotransmitters and their metabolites [dopamine (DA), norepinephrine (NE), 3-methoxy-4-hydroxyphenylglycol (MHPG), 3, 4-dihydroxyphenylacetic acid (DOPAC), 5-hydroxytryptamine (5-HT), 5-hydroxyindoleacetic acid (5-HIAA), and homovanillic acid (HVA)] at the GC electrode and at the MWNTs-COOH CME in HPLC-ED, respectively. It was found that the current responses of the monoamine neurotransmitters and their metabolites at the MWNT-COOH CME were much larger than those at the GC electrode. The detection limits were $2.5 \times 10^{-10} \text{ mol}\cdot\text{L}^{-1}$ for DA and NE, $5.0 \times 10^{-10} \text{ mol}\cdot\text{L}^{-1}$ for MHPG, $3.0 \times 10^{-10} \text{ mol}\cdot\text{L}^{-1}$ for DOPAC, $3.5 \times 10^{-10} \text{ mol}\cdot\text{L}^{-1}$ for 5-HT, $6.0 \times 10^{-10} \text{ mol}\cdot\text{L}^{-1}$ for 5-HIAA, and $1.25 \times 10^{-9} \text{ mol}\cdot\text{L}^{-1}$ for HVA.

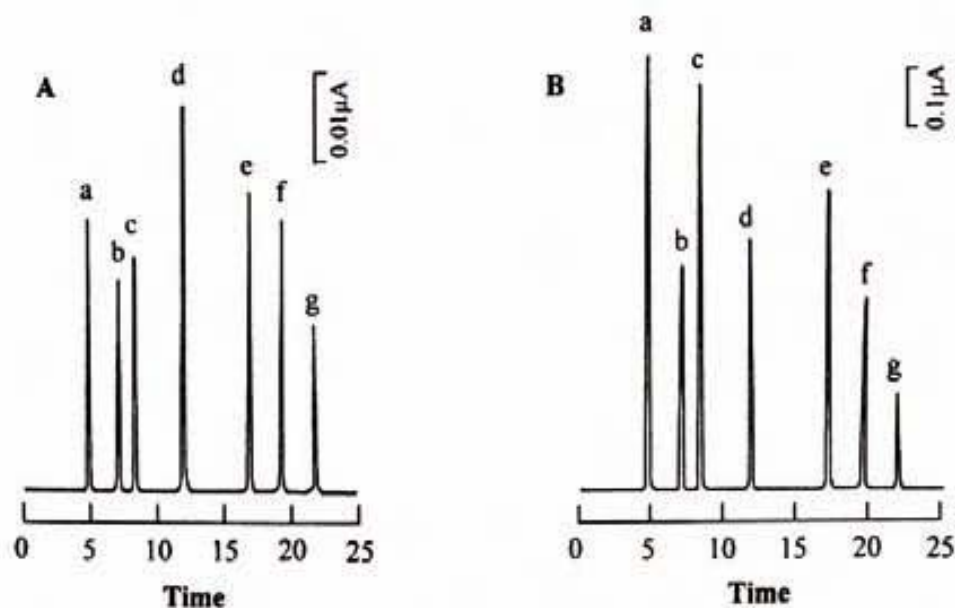


Figure 18. Chromatograms of 1.0×10^{-6} mol/l: (a) NE; (b) MHPG; (c) DA; (d) DOPAC; (e) 5-HT; (f) 5-HIAA; (g) HVA at the (A) the bare GC electrode and (B) the MWNTs-COOH CME. Applied potential: +0.70 V. Reprinted with permission from [97], W. Zhang et al., *J. Chromatogr. B* 791, 217 (2003). © 2003, Elsevier.

In LC-ED, the sensitivity for determination of these analytes was improved greatly at the MWNT-COOH CME compared to those at the GC electrode. Coupled with microdialysis sampling, the method appeared to be an appropriate analytical procedure for the routine determination of the monoamine neurotransmitters and their metabolites in real biological samples.

A new application of MWNTs is in a solid-phase extraction (SPE) system for HPLC determination of several phthalate esters (di-ethyl-phthalate, di-*n*-propyl-phthalate, di-*iso*-butyl-phthalate, and di-cyclohexyl-phthalate) from water samples [102]. The four analytes were quantitatively adsorbed on a MWNT-packed cartridge. The analytes retained on the SPE packing were then eluted with acetonitrile. Finally the acetonitrile eluate was injected into the HPLC system.

A MWNT-packed solid-phase extraction cartridge was prepared by modifying an Agilent ZORBAX SPE C18 (EC) cartridge (0.5 g, 6 mL, polypropylene) [102]. The polypropylene upper frit and lower frit remained at each end of the cartridge to hold the CNT packing in place. Next, the outlet tip of cartridge was connected to a vacuum pump and the inlet end of was connected to a PTFE suction tube whose other end was inserted into sample solution. Then, a solid-phase extraction system was ready for use. In respect to the extraction recoveries, the authors mention that the MWNTs were more effective than or as effective as some other commercially available SPE adsorbents such C18, C8, and PS-DVB for the solid-phase extraction of di-ethyl-phthalate, di-*n*-propyl-phthalate, di-*iso*-butyl-phthalate, and di-cyclohexyl-phthalate. The results show a linear correlation between the peak area and concentration of four phthalate esters from 2–100 ng·mL⁻¹ and detection limits of 0.18–0.86 ng·mL⁻¹.

4. APPLICATIONS IN OPTICAL SENSORS

The electronic and optical properties of SWNTs have inspired their incorporation into new structural, microelectronic, and sensing applications. The application of SWNTs in optical sensors is also an emerging field.

Penza et al. [103] demonstrated the integration of SWNTs onto a standard silica optical fiber (SOF) sensor for alcohol detection at room temperature. Different transducing mechanisms have been used in order to outline the sensing properties of this class of nanomaterials, in particular the attention has been focused on two key parameters in sensing applications: mass and refractive index changes due to gas absorption. Here, Langmuir-Blodgett (LB) films consisting of tangled bundles of SWNTs without surfactant molecules have been successfully transferred onto SOFs. The normalized optoelectronic signal ($\lambda = 1310$ nm) of the refractive index-sensitive SOF-SWNT sensor was found to decrease in ambient alcohols. Highly sensitive, repeatable, and reversible responses of the SOF-SWNT sensors indicate that the detection, at room temperature, in a wide mmHg vapor pressure range of alcohols and potentially other volatile organic compounds is feasible.

5. CONCLUSIONS

The applications of CNTs, with emphasis on analytical chemistry have been described. They range from electrochemical and optical sensors and biosensors to separation techniques. One of the most important applications of CNTs is without doubt the field of electrochemical (bio)sensors.

The unique structure, topology, and dimensions along with its electrochemical properties make the CNT a perfect

material with a variety of interesting possibilities in the design of sensors. The remarkable physical properties of nanotubes create a host of application possibilities, some derived as an extension of traditional carbon, carbon fibers, or bead applications, but many are new possibilities based on the novel electronic and mechanical behavior of nanotubes.

Various are the advantages that CNTs bring in the electrochemical sensor design. Perhaps the most attractive feature of CNTs enzyme based biosensor found up to date is an improved operational stability. CNTs composites represent an attractive material to be used for electrochemical sensors. Nevertheless to assess the feasibility and advantages of using CNTs in designing sensors, issues such as how the CNTs are produced and dispersed, the surface chemistry and morphology, effective surface area and presence of metal impurities need to be examined thoroughly and resolved.

The study of CNTs capabilities in electrochemical stripping of metals also a promising application that can be probably extended in the near future.

Although the increased number of reports on CNTs application in electrochemical sensors significant research is needed to figure out the mechanisms of CNTs improved electrochemical properties and avoid precipitated conclusions in attributing electrocatalytic properties to nanotubes without conducting the appropriate control experiments.

Further electrochemical study should be recommended for the future to understand better all the phenomena related with CNTs implementation in electrochemical sensors. Interesting information from electrochemical studies, i.e., impedance spectroscopy, for applications of CNTs for hydrogen storage can be obtained.

The DNA-directed self-assembling of carbon nanotubes can also bring new CNTs configuration possibilities for sensor applications. The combination of CNTs electronic properties and dimensions is making carbon nanotubes ideal building blocks for molecular electronics.

CNTs are showing to be a promising material to enhance separations in capillary electrophoresis and chromatography because of their high surface area available for chemical adsorption/interaction. The CNTs-coated capillaries allows for achievement of the separation without the use of expensive materials especially for small-molecule separations.

ACKNOWLEDGMENTS

This work was financially supported by the Spanish "Ramón Areces" foundation (project 'Bionanosensores') and Ministerio de Educación y Ciencia (Madrid) (Projects MAT2005-03553 and CONSOLIDER "NANOBIOMED").

REFERENCES

1. S. Iijima, *Nature* 354, 56 (1991).
2. A. Merkoci, M. Pumera, X. Llopis, B. Pérez, M. del Valle, and S. Alegret, *Trends Anal. Chem.* 24, 9 (2005).
3. W. B. Choi, D. S. Chung, J.H. Kang, H. Y. Kim, Y. W. Jin, I. T. Han, Y. H. Lee, et al., *Appl. Phys. Lett.* 75, 3129 (1999).
4. S. J. Tans, A. R. M. Verschueren, and C. Dekker, *Nature* 393, 49 (1998).
5. H. Dai, J. H. Hafner, A. G. Rinzler, D. T. Colbert, and R. E. Smalley, *Nature* 384, 147 (1996).
6. M. S. Shaffer, X. Fan, A.-H. Windle, *Carbon* 36, 1603 (1998).
7. S. G. Slater, *Home Health Care Management & Practice* 14, 6, 482 (2002).
8. M. Endo, T. Hayashi, Y. A. Kim, M. Terrones, M. S. Dresselhaus, *Phil. Trans. R. Soc. Lond. A* 362, 2223 (2004).
9. J. Liu, A. G. Rinzler, H. Dai, J. H. Hafner, R. K. Bradley, P. J. Boul, A. Lu, et al., *Sci.* 280, 1253 (1998).
10. S. Bandow, A. M. Rao, A. Thess, and R. E. Smalley, *J. Phys. Chem. B* 101, 8839 (1997).
11. A. G. Rinzler, J. Liu, H. Dai, P. Nikolaev, C. B. Huffman and F. J. Rodriguez-Marcias, *Appl. Phys. A* 67, 29 (1998).
12. A. C. Dillon, T. Gennett, K. M. Jones, J. L. Alleman, P. A. Parilla, and M. J. Heben, *Adv. Mater.* 11, 1354 (1999).
13. D. Chattopadhyay, I. Galeska, and F. Papadimitrakopoulos, *Carbon* 40, 985 (2002).
14. M. T. Martinez, M. A. Callejas, A. M. Benito, W. K. Maser, M. Cochet, J. M. Andres, J. Schreiber, O. Chauvet, and J. L. Fierro, *Chem. Commun.* 1000 (2002).
15. R. Andrews, D. Jacques, D. Qian, and E. C. Dickey, *Carbon* 39, 1681 (2001).
16. C. A. Grimes, E. C. Dickey, C. Mungle, K. G. Ong, and D. Qian, *J. Appl. Phys.* 90, 4134 (2001).
17. M. Endo, Y. A. Kim, Y. Fukai, T. Hayashi, M. Terrones, H. Terrones, and M. S. Dresselhaus, *Appl. Phys. Lett.* 79, 1531 (2001).
18. E. Najafi, J. Y. Kim, S. H. Han, and K. Shin, *Colloids and Surfaces A: Physicochem. Eng. Aspects* 284, 373 (2006).
19. J. Chen, M. A. Hamon, H. Hu, Y. Chen, A. M. Rao, P. C. Eklund, and R. C. Haddon, *Sci.* 282, 95 (1998).
20. D. Tasis, N. Tagmatarchis, V. Georgakilas, and M. Prato, *Chem. Eur. J* 9, 4000 (2003).
21. M. F. Islam, E. Rojas, D. M. Bergey, A. T. Johnson, and A. G. Yodh, *Nano Lett.* 3, 269 (2003).
22. A. Star, J. F. Stoddart, D. Steuerman, M. Diehl, A. Boukai, E. W. Wong, X. Yang, S. W. Chung, H. Choi, and J. R. Heath, *Angew. Chem. Int. Ed.* 40, 1721 (2001).
23. M. J. O'Connell, P. Boul, L. M. Ericson, C. Huffman, Y. Wang, E. Haroz, C. Kuper, J. Tour, K. D. Ausman, and R. E. Smalley, *Chem. Phys. Lett.* 342, 265 (2001).
24. J. Chen, H. Liu, W. A. Weimer, M. D. Halls, M. D. H. Waldeck, and G. C. Walker, *J. Am. Chem. Soc.* 124, 9034 (2002).
25. S. Ramesh, L. M. Ericson, V. A. Davis, R. K. Saini, C. Kittrell, M. Pasquali, W. E. Billups, W. Adams, R. H. Hauge, and R. E. Smalley, *J. Phys. Chem. B* 108, 8794 (2004).
26. O. K. Kim, J. Je, J. W. Baldwin, S. Kooi, P. E. Pehrsson, and L. J. Buckley, *J. Am. Chem. Soc.* 125, 4426 (2003).
27. J. H. T. Luong, S. Hrapovic, D. Wang, F. Bensebaa, and B. Simard, *Electroanal.* 16, 132 (2004).
28. H. Luo, Z. Shi, N. Li, Z. Gu, and Q. Zhuang, *Anal. Chem.* 73, 915 (2001).
29. M. D. Rubianes and G. A. Rivas, *Electrochem. Commun.* 5, 689 (2003).
30. R. R. Moore, C. E. Banks, and R. G. Compton, *Anal. Chem.* 76, 2677 (2004).
31. J. Wang and M. Musameh, *Anal. Chem.* 75, 2075 (2003).
32. J. Wang, M. Li, Z. Shi, and N. Li, *Electroanal.* 14, 225 (2002).
33. Z. H. Wang, J. Liu, Q. L. Liang, T. M. Wang, and G. Luo, *Analyst* 127, 653 (2002).
34. J. Wang, M. Li, Z. Shi, and N. Li, *Anal. Chem.* 74, 1993 (2002).
35. Y. Zhao, W. D. Zheng, H. Chen, and Q. M. Luo, *Talanta* 58 529 (2002).
36. N. Lawrence, R. P. Deo, and J. Wang, *Anal. Chim. Acta* 517, 131 (2004).

7

Annex

B. Pérez López and A. Merkoçi. Improvement of the electrochemical detection of catechol by the use of a carbon nanotube based biosensor. *Analyst*, 2009, **134**, 60.

Improvement of the electrochemical detection of catechol by the use of a carbon nanotube based biosensor

B. Pérez López and A. Merkoçi

Analyst

2009, **134**, 60-64



Improvement of the electrochemical detection of catechol by the use of a carbon nanotube based biosensor

B. Pérez López^{ab} and A. Merkoçi^{*abc}

Received 19th May 2008, Accepted 22nd August 2008

First published as an Advance Article on the web 18th October 2008

DOI: 10.1039/b808387h

Tyrosinase (Tyr) has been used frequently for the detection of phenolic compounds. The development of a biosensor based on this enzyme-integrated carbon nanotube (CNT) epoxy composite electrode (CNTECE) is described in order to perform measurements of catechol. The enzyme is immobilized into a matrix prepared by dispersion of multi-wall CNT (MWCNT) inside the epoxy resin forming a CNT epoxy-biocomposite (CNTEC-Tyr). The use of CNT improves the electronic transference between the enzyme and the electrode surface. The modified electrode was characterized electrochemically by amperometric and voltammetric techniques. An applied potential of -200 mV vs. Ag/AgCl applied to the biocomposite based electrode was found to be optimal for electrochemical reduction of the enzymatic reaction products (quinones). The biosensor modified with MWCNT is also compared with a tyrosinase biosensor based on a graphite epoxy-composite (GECE-Tyr) showing a sensitivity of $294 \mu\text{A}/\text{mM cm}^2$, a detection limit of 0.01 mM for a signal-to-noise ratio of 3 in a concentration range of 0.0 – 0.15 mM catechol with a response time of 20 s and an RSD of 8% ($n = 3$). The electrodes were stable for more than 24 h. A 90% increase of the signal indicated that the response is better with the biocomposite based on carbon nanotubes rather than with the graphite.

1. Introduction

Over the last decade, biosensors for environmental surveillance have become more prevalent in the literature with the emphasis on phenol determination and control.¹ Phenols are compounds of large scale production that cause ecologically undesirable effects.² Most phenols exhibit different toxicities and their determination is very important for evaluating the total toxicity of an environmental sample. In general phenolic compounds are subjected to chromatographic separation before detection.³ However, the separation takes time, and often requires pre-concentration. In addition, the equipment is expensive and is not generally portable. For that reason new alternative biosensor designs for phenolic compounds are being developed and investigated. Rigid conducting carbon nanotubes-polymer based composites are reported. The plastic nature of these materials makes them modifiable, permitting the incorporation of a great number of biological materials that can be immobilised by blending them with these composites to form new biocomposite materials.⁴

The use of carbon nanotubes (CNT) has become relevant due to their excellent conductivity including the improvement of electron transfer between the enzymes and the electrode surfaces⁵ and at the same time provides a very good matrix for enzyme immobilization.⁶ On the other hand, the biosensors based on nanostructured compounds^{7,8} have been demonstrated to be

simple in preparation and offer a great promise for developing amperometric biosensors.

Biosensors represent an interesting alternative for the detection of phenolic compounds. Many different approaches can be found in the literature including carbon-paste biosensors,⁹ graphite composite electrodes^{7,8}, conducting polymer modified electrodes,¹⁰ and silica sol-gel composite films.¹¹ Some of these methods are relatively complicated, require the use of several reagents and often the biosensor produced presents stability problems. Currently, there is an increasing interest to design functional membranes for biosensing application because of their possible use for analytical applications.¹² The use of enzymatic electrodes is an inherently sensitive alternative for the detection of enzyme substrate. Many biosensors have been developed in the past using the catalytic activity of the redox enzymes for phenol determination such as tyrosinase, peroxidase, laccase, *etc.*¹³ using different electrode materials, flow systems and sample pretreatment techniques.

Tyrosinase, also known as polyphenol oxidase, is a copper monooxygenase that catalyzes the oxidation of catechols to the corresponding *o*-quinones.^{14–16} The liberated quinone species can be further electrochemically reduced to phenolic substances at low potential in the absence of mediators.^{17,18} Electrochemical reduction of quinones is incomplete. This is because quinones are highly unstable in water and they easily polymerize to poly-aromatic compounds.¹⁹ In spite of this problem, sensors based on this approach have been reported using graphite electrodes and graphite-epoxy based composite electrodes.^{20,21}

Tyrosinase-based bioelectrodes^{22,23} have been reported; however, one of the most important analytical problems that appear in the case of tyrosinase-modified electrodes is their low operational stability, especially for detecting *o*-diphenols.^{24,25}

^aNanobioelectronics & Biosensors Group, Institut Català de Nanotecnologia, E-08193 Bellaterra, Barcelona, Catalonia, Spain

^bDepartament de Química, Universitat Autònoma de Barcelona, E-08193 Bellaterra, Catalonia, Spain. E-mail: arben.merkoci.icn@uab.es; Fax: +34 935868020; Tel: +34 935868014

^cICREA, E-08193 Bellaterra, Barcelona, Catalonia, Spain

This can be due to the fact that the enzyme is lost in the surrounding environment (especially when physical methods are used for enzyme immobilization), or due to its inactivation by the radical species that appear during the biocatalytic oxidation.²⁶ Thus, it is of great significance to develop new approaches to detect phenol derivatives with high sensitivity.

The main strategies for biomolecules immobilization are based on physical adsorption, cross-linking, covalent bonding, entrapment in gels or membranes, *etc.* Recent developments in the field of rigid and conducting polymer composites based on CNTs applied to electrochemistry^{7,8} have opened a new range of possibilities for the construction of electrochemical biosensors based on carbon materials. In these devices, the biocomponents are immobilised into the CNT matrix of the composite forming a biocomposite, a new material with unique properties. The main features of a biocomposite based on CNT and tyrosinase for catechol detection are described in the present work and its potential for the construction of an amperometric biosensor is also discussed.

2. Experimental

2.1. Reagents and solutions

Tyrosinase from mushroom (Tyr, 2034 U per mg, Catalog No. 93898), catechol, potassium dihydrogen phosphate and potassium hydrogen phosphate were purchased from Sigma. Epoxy resin Epotek H77 A, hardener Epotek H77 B were received from Epoxy Technology. The multiwalled carbon nanotubes powder (0.5–200 μm) (MWCNT), were purchased from Aldrich. The CNTs were purified in HNO_3 to remove impurities such as amorphous carbon, graphite particles and metal catalysts. Further purification was accomplished by stirring the CNTs in 2 M nitric acid at 25°C for 24 h. Graphite powder (particle size 50 μm) was obtained from BDH, UK. The alumina paper (polishing strips 301044–001), was obtained from Orion, Spain.

The standard catechol solutions were prepared daily by dilution in 0.1 M phosphate buffer at pH 6.5 with ultra pure water from a Millipore-MilliQ system.

2.2. Apparatus and electrodes

Cyclic voltammetry (CV) and chronoamperometry experiments were performed using an electrochemical analyzer Autolab 20 (Eco Chemie, The Netherlands) and an LC-4C amperometric detector (BAS) connected to a personal computer with GPES software.

The measurements were performed in 10 mL of a 0.1 M phosphate buffer solution (PBS) pH 6.5 without deoxygenating, at room temperature (25 °C) using three electrodes based configuration. A platinum electrode and Ag/AgCl were used as counter and reference electrode, respectively. The biosensor based on carbon nanotube (CNT) epoxy composite (CNTEC-Tyr) and the tyrosinase biosensor based on a graphite epoxy-composite (GECE-Tyr) were used as working electrodes.

2.3. Tyrosinase biosensor preparation

The carbon nanotube-epoxy biocomposite (CNTEC-Tyr) and graphite epoxy-biocomposite (GECE-Tyr) electrodes were

prepared by mixing manually during 30 minutes the tyrosinase (Tyr) (2.0% w/w), Epoxy resin (80.0% w/w) and carbon nanotubes or graphite powder (18.0% w/w), respectively; the prepared biocomposite paste was then introduced into a PVC tube containing an electrical connector completed by using a copper disk and wire. The biocomposite was cured at 40 °C for one week. Before measurements, the cured biosensor surface was polished with different abrasive papers of decreasing grain size, ending in alumina paper. The biosensors (CNTEC-Tyr and GECE-Tyr) were kept in a refrigerator while not being used.

2.4. Electrochemical measurements

Electrochemical experiments were carried out with a typical 10 mL cell, at room temperature (25°C), using the three electrodes configuration. A magnetic stirrer provided the convective transport during the amperometric measurements.

Cyclic voltammetry using modified electrodes (CNTEC-Tyr and GECE-Tyr) were performed in 0.02 mM catechol solution. The response of catechol was measured in 10 mL of a 0.1 M phosphate buffer solution (PBS) pH 6.5. The potential range used for catechol determination was -0.4 to $+0.8$ V for CNTEC-Tyr and GECE-Tyr. The surface coverage (Γ) of CNTEC-Tyr and GECE-Tyr was estimated from the area of the cyclic voltammetric peaks corresponding to the oxidation of catechol. According to the equation $\Gamma = Q/nFA$,²⁷ where Q is the area of the catechol oxidation peak, n is the number of electrons involved in the oxidation, F is the Faraday's constant, and A is the area of the electrode ($A = 0.2827 \text{ cm}^2$). Γ was found to be of $2.1 \times 10^{-8} \text{ mol/cm}^2$ for GECE-Tyr and of $2.7 \times 10^{-8} \text{ mol/cm}^2$ for CNTEC-Tyr.

The steady state amperometric response to catechol was measured in aliquots of 10 mL of buffer solution with different additions of catechol added into the reaction cell. The measurements were carried out in a 0.1 M phosphate buffer solution pH 6.5, used as supporting electrolyte. The applied potential to the working electrode for catechol determination was -0.2 V using CNTEC-Tyr and GECE-Tyr electrodes respectively. The background current was allowed to decay to a constant level before aliquots of phenolic compounds sample were added to the stirred buffer solution.

3. Results and discussion

A mushroom tyrosinase enzyme which catalyzes the oxidation of catechols to the corresponding quinone compounds is used in this carbon nanotube biocomposite based biosensor. The electrochemical reduction of o-quinone formed due to the enzymatic reaction^{17,18} (see Fig. 1) is used as an indicator reaction, by which an electrical signal proportional to the catechol concentration is obtained.

3.1. Effect of scan rate

Figs. 2A and 3A illustrate the influence of the potential scan rate ν on the cyclic voltammograms of GECE-Tyr and CNTEC-Tyr electrodes in 0.2 mM catechol solution (at 10, 20, 30, 40, 50, 60, 70, 80, 90, 100 mV/s, scanning potential range: -0.5 to 0.8 V) in 0.1 M phosphate buffer pH 6.5. It can be observed that the scan rate affects the position of the oxidation and reduction peaks.

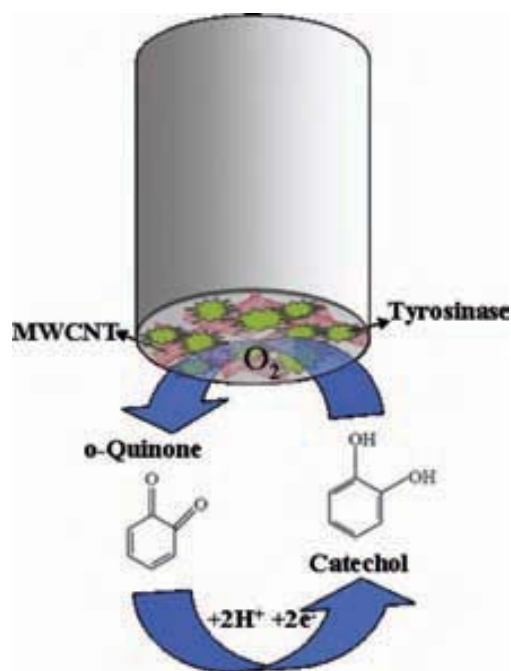


Fig. 1 Schematic representation of the reaction of catechol with tyrosinase.

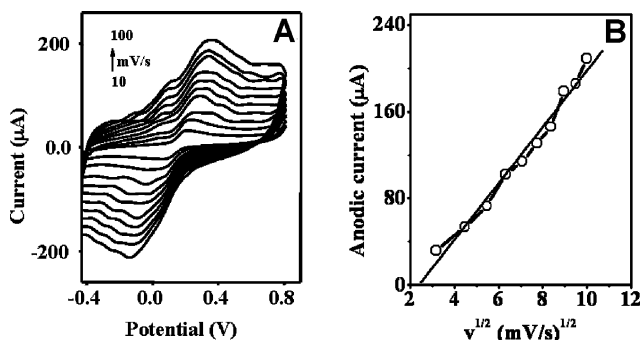


Fig. 2 (A) Cyclic voltammograms of GECE-Tyr electrode in 0.2 mM catechol solution (at 10, 20, 30, 40, 50, 60, 70, 80, 90, 100 mV/s, scanning potential range: -0.5 to 0.8 V); (B) plots of anodic peak currents versus the square root of scan rate.

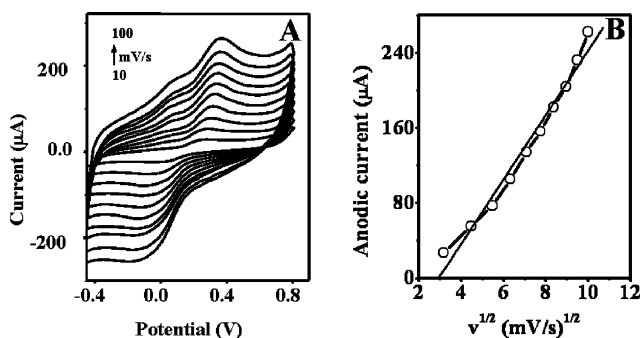


Fig. 3 (A) Cyclic voltammograms of CNTEC-Tyr electrode in 0.2 mM catechol solution (at 10, 20, 30, 40, 50, 60, 70, 80, 90, 100 mV/s, scanning potential range: -0.5 to 0.8 V); (B) plots of anodic peak currents versus the square root of scan rate.

Inspection of the curves reveals that an increase in the scan rates, v , increases the current of the oxidation of catechol and shifts the anodic peak potential (E_{pa}) toward more positive potentials as the rate increased, whereas the cathodic peak potential (E_{pc}) shifts toward more negative potentials. The differences of these potential shifts for CNTEC-Tyr are 104 mV and 131 mV, respectively.

The influence of sweep rate v ($v^{1/2}$) on anodic peak current (I_{pa}) is shown in Fig. 2B for GECE-Tyr and Fig. 3B for CNTEC-Tyr respectively. Further analysis of the results indicate that the anodic peak current increases linearly with the square root of the rate, and the corresponding linear equation is $i(\mu A) = 26.038 v^{1/2} - 62.46$ with a linear correlation coefficient of 0.9902 for GECE-Tyr and for CNTEC-Tyr the corresponding linear equation is $i(\mu A) = 34.369 v^{1/2} - 100.794$ with a linear correlation coefficient of 0.9889, both cases at pH = 6.5. The relation between I_{pa} and $v^{1/2}$ indicates that the anodic dissolution process within the potential range of peak (Fig. 2B and 3B) is a diffusion controlled process.

The difference between the E_{pa} and the E_{pc} , for the GECE-Tyr is $\Delta E_p = 214$ mV and for the CNTEC-Tyr is $\Delta E_p = 206$ mV, both obtained at a potential scan rate of $100 \text{ mV}\cdot\text{s}^{-1}$, and the current ratio between the peaks (I_a/I_c) is 0.98 and 1.14 respectively. These results demonstrate that the oxidation process of catechol in both electrodes can be considered quasi-reversible.

3.2. Amperometric behavior of tyrosinase biosensor

The hydrodynamic voltammogram (HDV) data are very important for selecting the operating potential for amperometric measurements. In the case of CNTEC-Tyr, as it was already reported, there is an important catalytic effect, on the reduction of o-quinone and oxidation of catechol, making it possible for high sensitive detection of phenolic compounds. Fig. 4 compares hydrodynamic voltammograms for 0.025 mM catechol for GECE-Tyrosinase (a) and at CNTEC-Tyrosinase (b) in 0.1 M phosphate buffer pH 6.5. The reduction current for the o-quinone enzymatically generated starts at potential -0.2 V at CNTEC-Tyr and GECE-Tyr. At CNTEC-Tyr the signal increases around 80% at the potential of -0.2 V (observe the different current scales at figure 4) indicating that the sensitivity largely increases as consequence of the type of material.

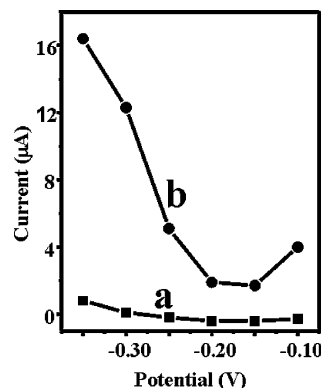


Fig. 4 Hydrodynamic voltammogram for 0.025 mM catechol for GECE-Tyr (a) and at CNTEC-Tyr (b) in 0.1 M phosphate buffer pH 6.5.

Therefore, carbon nanotubes promote in a very efficient way the electron transfer between o-quinone and CNTEC-Tyr. This electrocatalytic activity facilitates low-potential amperometric determination of catechol.

3.3. Biosensor response toward catechol

The amperometric responses for the determination of catechol on GECE-Tyr (a) and CNTEC-Tyr (b) electrodes at the scan rate of $100 \text{ mV}\cdot\text{s}^{-1}$ are compared in Fig. 5. It shows well-defined responses for each successive addition of 0.02 mM catechol at the graphite-epoxy-Tyr composite (GECE-Tyr) (a) and carbon nanotube-epoxy composite (CNTEC-Tyr) (b) electrodes using operating potential of -0.2 V in 0.1 M phosphate buffer solution pH 6.5, with their respective calibration plots (insets). The CNTEC-Tyr electrode offer substantially larger signals reflecting the electrocatalytic properties of carbon nanotubes. The sensitivity of detection for catechol determination at an applied potential of -0.2 V is based in the amount of o-quinone produced by enzymatic reaction between catechol and tyrosinase. It was of $46 \mu\text{A}/\text{mM cm}^2$ for GECE-Tyr and of $294 \mu\text{A}/\text{mM cm}^2$ for CNTEC-Tyr with a current intensity 90% higher than GECE-Tyr (note the different scales) (Fig. 5). Nevertheless, the repeatability of the method was obtained in one day by the same analyst using the same reagent solutions demonstrating to be better for GECE-Tyr than for CNTEC-Tyr with a RSD = 5% ($n = 3$) and RSD = 8% ($n = 3$), respectively. The plots of current vs catechol concentration were linear for a concentration range of $0.0\text{--}0.15 \text{ mM}$ at CNTEC-Tyr and GECE-Tyr electrodes (inset calibration plots (5a and 5b) with a correlation coefficient of 0.990 and 0.996, respectively.

The highest current response for CNTEC-Tyr due to the distinctive properties of CNTs, especially, the biocompatibility and ability to facilitate electron transfer make them suitable candidates for immobilization of biomolecules and biosensor applications.^{28,29} A variety of enzymes by using CNTs as molecule wires to facilitate the electron transfer of enzyme with electrode have been employed in the relatively new field of enzyme-based nanotube sensors.³⁰

The stability of the CNTEC-Tyr and GECE-Tyr electrodes is very important during the chronoamperometric experiments. It

was studied using the same conditions as was above mentioned. For each different addition of 0.02 mM catechol solution a response time of about 20 s was observed and thereafter a good stability is maintained at GECE-Tyr during 5 minutes and a better current increase with CNTEC-Tyr, operating at a potential of -0.2 V , the electrodes being stable for more than 24 h (results not shown).

4. Conclusions

In summary, the experiments described above illustrate an attractive construction of renewable biosensors for the catechol detection. Tyrosinase maintains its enzymatic properties in the composite matrix; furthermore, the sensing surface can be renewed by a simple polishing procedure resulting in a fresh surface. Various additives may be incorporated into the biocomposite matrix to enhance the analytical performance further.

One of the outstanding features of these conducting biomaterials is their rigidity. The proximity of the redox centres of tyrosinase and the carbon nanotubes on the sensing surface favours the transfer of electrons between electroactive species. Composites electrodes modified with carbon nanotubes show improved electrochemical properties offering important advantages: i) CNTEC-Tyr exhibit better electronic properties than GECE-Tyr due to the promotion in a very efficient way of electron transfer between o-quinone and CNTEC-Tyr electrode ii) CNTEC-Tyr shows a detection limit (0.01 mM) almost half of that obtained by GECE-Tyr iii) The CNT biocomposite offer the possibility for electrode surface renewing forming a new active layer and lastly iv) The CNTEC-Tyr and GECE-Tyr amperometric biosensors are very attractive for mass fabrication so as to obtain low cost biosensors.

Acknowledgements

The WARMER Project Reference: FP6-034472-2005-IST-5 and MAT2008-03079/NAN (From MEC, Madrid) are acknowledged.

References

- 1 K. R. Rogers, *Biosens. Bioelectron.*, 1995, **10**, 533.
- 2 J. Kulyš and R. Vidziunaite, *Biosens. Bioelectron.*, 2003, **18**, 319.
- 3 V. Carralero, M. L. Mena, A. González-Cortés, P. Yáñez-Sedeño and J. M. Pingarrón, *Biosens. and Bioelectron.*, 2006, **22**, 730.
- 4 F. Céspedes and S. Alegret, *TrAC, Trends Anal. Chem.*, 2000, **19**(4), 276.
- 5 A. Merkoçi, *Microchim. Acta.*, 2006, **152**, 157.
- 6 B. Pérez, J. Sola, S. Alegret and A. Merkoçi, *Electroanalysis*, 2008, **20**(6), 603.
- 7 B. Pérez, M. Pumera, M. Del Valle, A. Merkoçi and S. Alegret, *J. Nanosci. Nanotech.*, 2005, **5**(10), 1694.
- 8 M. Pumera, A. Merkoçi and S. Alegret, *Sens. Actuators*, **B**(113), 617.
- 9 A. Merkoçi, M. Pumera, X. Llopis, B. Perez, M. Del Valle and S. Alegret, *Trends. Anal. Chem.*, 2005, **24**, 826.
- 10 O. Adeyolu, E. J. Iwuoka, M. R. Smyth and D. Leech, *Analyst*, 1996, **121**, 1885.
- 11 Li, L. S. Chia, N. K. Goh and S. N. Tan, *Anal. Chim. Acta.*, 1998, **362**, 203.
- 12 A. Liu, H. Zhou and I. Honma, *Electrochem. Commun.* 2005, **7**, 1.
- 13 N. Duran and E. Esposito, *Appl. Catal. B Environ.*, 2000, **28**, 83.
- 14 E. I. Solomon, U. M. Sundaram and T. E. Machonkin, *Chem. Rev.*, 1996, **96**, 2563.
- 15 H. Decker and F. Tucek, *Trends Biochem. Sci.*, 2000, **25**, 392.

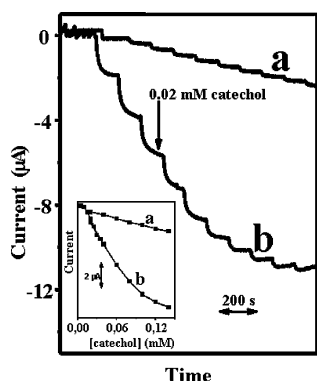


Fig. 5 Current–time recordings obtained from amperometric experiments at GECE-Tyr (a) and at CNTEC-Tyr (b) for successive additions of 0.02 mM catechol. Working potential: -0.2 V in 0.1 M phosphate buffer pH 6.5. The inset shows the corresponding calibration plots.

-
- 16 E. J. Land, C. A. Ramsden and P. A. Riley, *Acc. Chem. Res.*, 2003, **36**, 300.
 - 17 T. Toyata, S. S. Kuan and G. G. Guilbault, *Anal. Chem.*, 1985, **57**, 1925.
 - 18 A. Ghindilis, V. Gavrilova and A. Yaropolov, *Biosens. Bioelectron.*, 1992, **7**, 127.
 - 19 N. H. Horowitz, M. Fling, and G. Horn, *Methods in Enzymology*, Academic Press, New York, 1970, 120.
 - 20 F. Ortega, E. Domínguez, G. Jönsson-Pettersson and L. Gorton, *J. Biotechnol.*, 1993, **31**, 289.
 - 21 P. Önerfjord, J. Emnéus, G. Marko-Varga and L. Gorton, *Biosens. Bioelectron.*, 1995, **10**, 607.
 - 22 E. S. Forzani, G. A. Rivas and V. M. Solís, *J. Electroanal. Chem.*, 1999, **461**, 174.
 - 23 E. S. Forzani, V. M. Solís and E. J. Calvo, *Anal. Chem.*, 2000, **72**, 5300.
 - 24 A. I. Yaropolov, A. N. Kharybin, J. Emnéus, G. Marko-Varga and L. Gorton, *Anal. Chim. Acta.*, 1995, **308**, 137.
 - 25 F. Ortega, E. Domínguez, E. Burestedt, J. Emnéus, L. Gorton and G. Marko-Varga, *J. Chromatogr.*, 1994, **A675**, 65.
 - 26 C. Nistor and J. Emnéus, *Waste Manage.*, 1999, **19**, 147.
 - 27 A. J. Bard, L. R. Faulkner, *Electrochemical Methods*, Wiley, New York, 2001.
 - 28 M. Shim, N. W. Shi Kam, R. J. Chen, Y. Li and H. Dai, *Nano Lett.* **2**, 2002, 285.
 - 29 E. Katz and I. Willner, *Chem. Phys. Chem.* **5**, 2004, 1084.
 - 30 Y. Liu, X. Qu, H. Guo, H. Chen, B. Liu and S. Dong, *Biosens. and Bioelectron.* **21**, 2006, 2195.

